2017

Pablo Díaz Benito
de las Huertas Agüero

Transport of iron in plants assisted by nicotianamine and its derivatives

PhD
Thesis

Transport of iron in plants assisted by nicotianamine and its derivatives

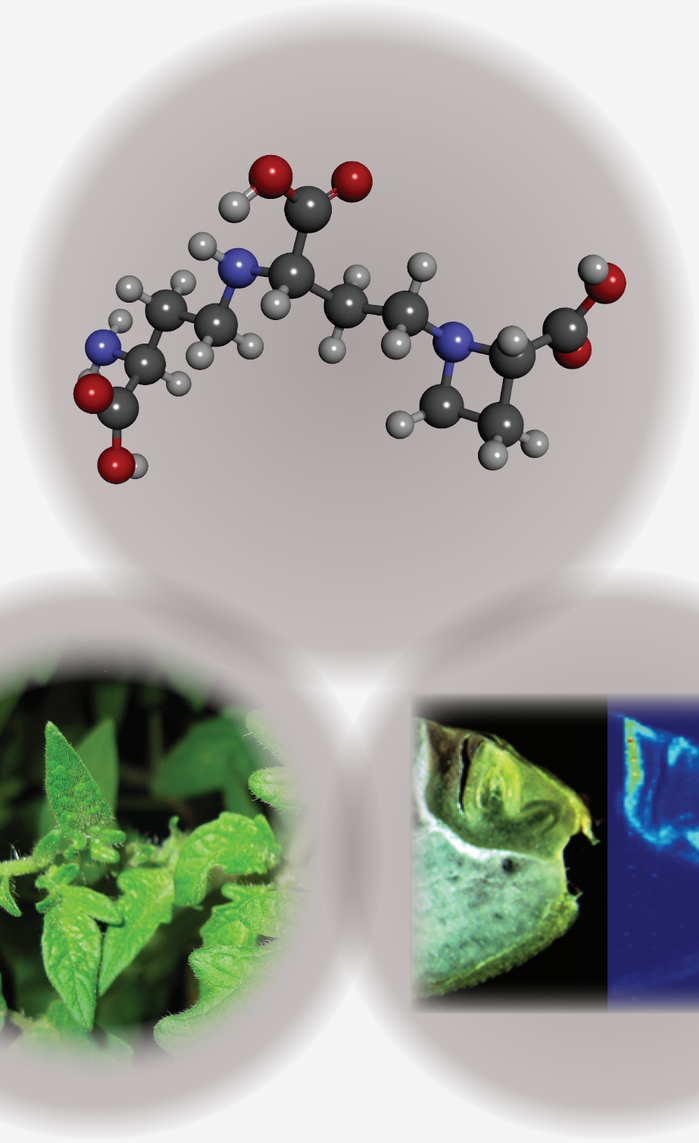

Plant Stress Physiology

CSIC

UAM UNIVERSIDAD AUTÓNOMA DE MADRID

PhD Thesis

Pablo Díaz Benito de las Huertas Agüero

Spanish National Research Council
Aula Dei Experimental Station
Plant Nutrition Department
Plant Stress Physiology Group

CSIC

Transport of iron in plants assisted by nicotianamine and its derivatives

Transporte de hierro en plantas facilitado por nicotianamina y sus derivados

Thesis submitted by **Pablo Díaz Benito de las Huertas Agüero**
for the obtention of the Doctor Degree in Biology

Dr. ANA MARÍA ÁLVAREZ FERNÁNDEZ, CSIC Scientist, and Dr. JAVIER ABADÍA BAYONA, CSIC Research Professor

AUTHORIZE

The presentation of the Doctoral Thesis entitled "Transport of iron in plants assisted by nicotianamine and its derivatives", presented by Pablo Díaz Benito de las Huertas Agüero for the obtention of the Doctor Degree in Biology by the Autonomous University of Madrid, and certify that it has been conducted under their supervision at the Aula Dei Experimental Station of the Spanish National Research Council.

Zaragoza, June 2017

Dr. Ana María Álvarez Fernández

Dr. Javier Abadía Bayona

Dr. LUIS EDUARDO HERNÁNDEZ RODRÍGUEZ, Associate Professor in the Autonomous University of Madrid

AUTHORIZE

The presentation of the Doctoral Thesis entitled "Transport of iron in plants assisted by nicotianamine and its derivatives", presented by Pablo Díaz Benito de las Huertas Agüero for the obtention of the Doctor Degree in Biology by the Autonomous University of Madrid, and certify that it has been conducted under his academic supervision and fulfilled the requeriments for the obtention of the Doctor Degree at Autonomous University of Madrid.

Zaragoza, June 2017

Dr. Luis Eduardo Hernández Rodríguez

Acknowledgements

Esta Tesis ha necesitado mucha dedicación y esfuerzo, y no habría sido tan llevadero sin la ayuda y el apoyo de mucha gente. A todos vosotros: gracias. Gracias por compartir vuestros consejos y experiencia cuando la ocasión lo requería, por compartir vuestra alegría cuando disfrutábamos y por compartir vuestro ánimo cuando era necesario.

Gracias a mis directores de tesis, Ana y Javier, por todo el trabajo que habéis realizado y todas las horas que habéis dedicado a esta Tesis. A Ana, por sus enseñanzas, esfuerzo y paciencia que han permitido desarrollarme como persona y como científico. A Javier, por su apoyo tanto en lo profesional como en lo personal, cuyos consejos me han ayudado en gran manera en ambos casos.

Gracias a mi tutor de Tesis, Luis Eduardo, que después de tantos años sigues ayudándome como si fuese mi primer día en el laboratorio de la UAM hace tantos años.

Gracias al profesor Paul Christou y su equipo de Lérida por el trabajo con el arroz, y en especial a Raviraj Banakar por todas las horas de trabajo y diversión juntos. Gracias a la Dra. Beatriz Fernández y a Sara Ródriguez de la Universidad de Oviedo por su excelente trabajo con la ablación láser y sus enseñanzas en este campo, así como su cálida acogida. Gracias al profesor Alberto Fereres y a la Dra. Elisa Garzo del Instituto de Ciencias Agrarias de Madrid por su fascinante dedicación a los pulgones.

Gracias a todos mis compañeros de laboratorio de Aula Dei. A Monona, por sus sabios consejos y poner coherencia cuando era necesario. A Ana Flor y a Fermín, por su ayuda para perfeccionar técnicas y aportar un enfoque nuevo. A Patricia, mi compañera de Tesis y confidencias; a Rubén, por iniciarme en mis primeros pasos en la metabolómica; a Jorge R., por su jovialidad y sus grandes ideas; a Elaín, por su amistad y compartir su práctica forma de ver las cosas; a Hamdi, por su coherencia y tener siempre un buen consejo bajo la manga; a Laura, por tantas horas juntos en el masas y saber cuándo necesitaba un empujón de moral; y a Adrián, por confiar en mí cuando ha necesitado ayuda. Un agradecimiento especial a Juanjo y Sandra, por su inestimable ayuda en los muestreos nocturnos y compartir tantos buenos ratos. A Aurora, por poder acudir a ella tanto para un reactivo como para un consejo; a Ade, por su eficacia y predisposición a ayudar dependiendo de lo que hiciera falta; a Gema, por su constante y contagioso buen humor en todas las situaciones; y a Marga, por escucharme en más de una ocasión. Gracias también a los demás compañeros de Aula Dei por hacer estos años en Zaragoza inolvidables. A Chus, Erica, Miquel y Ana por todas las rutas por el Pirineo. A Manu y a Jorge, por su compañerismo y los partidos que nos hemos visto juntos. A Carmen, por el cariño, fuerza y apoyo que me has brindado estos años. Y muchos más: Laura, Peñu, Manu, Ana, Pedro, Ángel, Carlos, Elena, Diego, Sergio, Giuseppe, Jorge, Leti, Cristina, Pilar, Pili, Ángela, Jorge, Brenda…

Gracias a mis amigos de Madrid, pues cuando os he necesitado habéis estado ahí.

Gracias a Dña. Carmen y a Alicia por ayudarme, siempre os estaré agradecido.

El más especial de mis agradecimientos para mis padres y mi hermana, los pilares que me sustentan en cualquier momento y situación, por todo lo que habéis hecho y todo lo que vais a hacer. Os quiero.

A Nora, por redescubrirme la fascinación por el mundo y la ilusión de aprender.

Funding

The studies included in this PhD Thesis were supported by the Spanish MINECO (AGL2010-16515, AGL2012-031988, AGL2013-42175-R and AGL2016-75226-R) and the Aragón Government (group A03). Pablo Díaz Benito de las Huertas Agüero was supported by a predoctoral FPI contract from MINECO.

UNIÓN EUROPEA
Fondo Social Europeo
Construyendo Europa desde Aragón

There is a theory that if we don't have the right words in our vocabularies, we can't even see the things that are right in front of our faces. If we can't describe our reality accurately, we can't see it […]. Our own words make us blind.

Paolo Bacigalupi, *The Water Knife*

Abbreviations

ATP	Adenosine triphosphate
BPDS	Bathophenantrolinedisulphonic acid
Chl	Chlorophyll
Cit	Citrate
c-mdh	Cytosolic malate dehydrogenase
DMA	2'-deoxymugineic acid
DTPA	Diethylenetriaminepentaacetic acid
EAR	Estimated average requeriments
EDDHA	Ethylenediamine-N,N'-bis(2-hydroxyphenylacetic acid)
EDTA	Ethylenediamine tetraacetic acid
EFSA	European Food Safety Authority
ESI	Electrospray ionization
FAAS	Flame atomic absorption spectrometry
FCR	Ferric chelate reductase
FRD	Ferric reductase deficient
FRO	Ferric reductase oxidase
FW	Fresh weight
HEDTA	Hydroxyethylenediaminetriacetic acid
HPLC	High performance liquid chromatography
ICP	Inductively coupled plasma
IRT	Iron regulated transporter
LA	Laser ablation
LOQ	Limit of quantitation
MA	Mugineic acid
Mal	Malate
MS	Mass spectrometry
MES	2-(N-morpholino)ethanesulfonic acid
NA	Nicotianamine
NAAT	Nicotianamine aminotransferase
NAD^+	Nicotinamide adenine dinucleotide (oxidized)
NADH	Nicotinamide adenine dinucleotide (reduced)
NAS	Nicotianamine synthase
NL	Nicotil lysine
PAR	Photosynthetically active radiation
PPFD	Photosynthetic photon flux density
PS	Phytosiderophore
PVDF	Polyvinylidene fluoride
RH	Relative humidity
ROS	Reactive oxigen species
RT	Retention time
SPAD	Soil-Plant Analysis Development
TOF	Time of flight
WT	Wild type
YSL	Yellow Stripe Like

Table of contents

Abstract/Resumen

With an estimated world population of 9 billion people in 2050, the production of enough food is one the biggest challenges ahead. Improving the yield and nutritional quality of agricultural produce is relevant to successfully meet this challenge. Metal micronutrient deficiency, especially that of Fe in calcareous soils, is a common reason for low crop yield and quality. This, in combination with the naturally low micronutrient concentrations in cereals, leads to metal micronutrient deficiencies in animals, including humans. In the last decades researchers have focused on crop biofortification, using different approaches to obtain new genotypes with higher Fe and Zn concentrations, but this goal has been only partially fulfilled so far. One of the key limitations in biofortification is the still incomplete knowledge of Fe homeostasis, particularly in regard to metal transport and distribution within the different plant organs. Besides proteins, several organic metal ligands, including nicotianamine (NA) and its derivative 2'-deoxymugineic acid (DMA) and carboxylates -e.g. citrate and malate-, are involved in Fe acquisition, transport and storage, but their roles and mutual relationships in these processes are still not fully understood. In this Thesis, the roles of NA and DMA in Fe transport have been studied using mass spectrometry and molecular biology approaches in two relevant crop species, tomato (*Solanum lycopersicum*; a Strategy I species) and rice (*Oryza sativa*; a Strategy II species). In tomato, the first comprehensive analysis of the changes in metal micronutrients and organic metal ligands in fluids of this plant species as affected by Fe status is presented. This study shows that in Fe-deficient tomato plants resupplied with Fe NA is involved in root Fe trafficking to reach the vasculature and in Fe remobilization from developed to young leaves via phloem sap. Also, in tomato plants citrate and malate are involved in short distance Fe transport through the apoplastic pathway in roots and leaves and in long-distance Fe transport via xylem sap. In rice, DMA and citrate are shown to play complementary roles in long-distance Fe transport via xylem sap, using the mutant Osfrdl1 and foliar citrate applications, with NA not being involved in this process. In rice seeds DMA and NA are shown to be involved in Fe loading in the endosperm and Fe/Zn loading in the embryo, respectively, using transgenic rice plants overexpressing *OsNAS1* and/or expressing *HvNAATb* and LA-ICP-MS. This Thesis has increased the knowledge on the roles and relationships between metal organic ligands in plant short- and long-distance Fe transport, provided a better understanding of plant metal homeostasis, and opened new approaches for biofortification.

Con una población mundial estimada de 9 mil millones de personas en 2050, la producción de alimentos es uno de los mayores retos del futuro. Mejorar el rendimiento y la calidad nutricional de los productos agrícolas es de especial relevancia para afrontar con éxito este desafío. La deficiencia de micronutrientes, y especialmente la de Fe en suelos calcáreos, es una causa frecuente del bajo rendimiento y calidad de los cultivos. Este aspecto, combinado con las bajas concentraciones naturales de micronutrientes en cereales, conduce a la deficiencia en animales, incluyendo humanos. En las últimas décadas la investigación se ha centrado en la biofortificación, utilizando diferentes enfoques con el fin de obtener nuevas variedades con mayores concentraciones de Fe y Zn, si bien este objetivo sólo se ha cumplido parcialmente hasta el momento. Una de las principales limitaciones de la biofortificación es el todavía incompleto conocimiento de la homeostasis del Fe, tanto en relación al transporte como a la distribución del metal dentro de los diferentes órganos de las plantas. Además de proteínas, varios ligandos orgánicos, incluyendo la nicotianamina (NA) y su derivado el ácido 2'-deoximugineico (DMA) y los carboxilatos -p. ej. citrato y malato-, están involucrados en la adquisición, transporte y almacenamiento de Fe, pero sus funciones y relaciones mutuas en estos procesos aún no se conocen por completo. En esta Tesis se han estudiado las funciones de la NA y el DMA en el transporte de Fe, utilizando enfoques de espectrometría de masas y biología molecular, en dos cultivos relevantes: tomate (*Solanum lycopersicum*, especie de Estrategia I) y arroz (*Oryza sativa*, especie de Estrategia II). En el caso de tomate se presenta el primer análisis exhaustivo de los cambios en micronutrientes metálicos y ligandos orgánicos en fluidos de esta especie en diferentes estados de nutrición de Fe. Este estudio muestra que en plantas de tomate deficientes en Fe y reabastecidas con este elemento la NA está involucrada en el tráfico de Fe en la raíz hasta alcanzar la vasculatura, así como en la removilización de Fe desde las hojas desarrolladas a las jóvenes *via* floema. Además, en las plantas de tomate el citrato y el malato están involucrados en el transporte de Fe a corta distancia a través de la ruta apoplásica en raíces y hojas, y en el transporte de Fe a larga distancia *via* xilema. En arroz se ha demostrado, utilizando para ello aplicaciones foliares de citrato a mutantes *Osfrdl1*, que el DMA y el citrato desempeñan papeles complementarios en el transporte de Fe a larga distancia *via* xilema mientras que la NA no está involucrada en esta etapa. En semillas de arroz, utilizando plantas transgénicas que sobreexpresan *OsNAS1* y/o expresan *HvNAATb* y la técnica LA-ICP-MS, se muestra que el DMA y la NA participan en la carga de Fe en el endospermo y la carga de Fe/Zn en el embrión, respectivamente. Esta Tesis ha

incrementado el conocimiento sobre las funciones y relaciones entre ligandos orgánicos de metales en el transporte de Fe a corta y larga distancia en las plantas, ha proporcionado una mejor comprensión de la homeostasis de Fe y ha abierto nuevos enfoques para la biofortificación.

Chapter 1

Introduction

1.1. Iron in nature

1.1.1. Physicochemical properties of iron

Iron (Fe, from the Latin *ferrum*) is a chemical element belonging to the transition metal class, with atomic number 26, located in group 8 and period 4 of the periodic element table. The most abundant stable Fe isotope is ^{56}Fe (91.754% of the total), with an atomic mass of 55.845 Da, and minor stable isotopes are ^{54}Fe (53.939 Da; 5.845%), ^{57}Fe (56.935 Da; 2.119%) and ^{58}Fe (57.933 Da; 0.282%) (CIAAW, 2016). Iron-56 has 26 protons and 30 neutrons in its nucleus and has in the neutral state 26 electrons ($1s^2\ 2s^2\ 2p^6\ 3s^2\ 3p^6\ 3d^6\ 4s^2$). In nature, the most common oxidation states are 2^+ (ferrous ion) and 3^+ (ferric ion). The electrons in the 3d and 4s outer orbitals are highly stable, as they are semi-full (Table 1.1), conferring these ions particular redox properties of great importance in biological systems.

Table 1.1. Distribution of electrons in the 3d and 4s orbitals of neutral (Fe), ferrous (Fe^{2+}) and ferric (Fe^{3+}) iron

	3d					4s
Fe	↑↓	↑	↑	↑	↑	↑↓
Fe^{2+}	↑	↑	↑	↑	↑	↑
Fe^{3+}	↑	↑	↑	↑	↑	

Iron is the 4th most abundant element in the earth's crust, representing 6% of its total mass. The chemical forms of Fe are strongly dependent on pH and the presence of oxidant compounds, especially molecular oxygen (O_2), since the oxidation rate of Fe^{2+} to Fe^{3+} is determined by these parameters (Stumm and Morgan, 1996; Morgan and Lahav, 2007). The current high atmospheric O_2 concentration (21%) and the alkalinity of many soils promote Fe oxidation. Although up to 16 types of Fe hydroxide minerals have been identified in soils, all these minerals are scarcely soluble and for this reason their availability for plants is limited, especially in soils with high pe+pH values (Lindsay, 1995; Fig. 1.1). Of these minerals, the amorphous *ferric hydroxide* ($Fe(OH)_3$) is the most soluble.

1.1.2. Biological relevance of Fe

All life domains (including *Archaea*, *Bacteria* and *Eukarya*) use Fe for a large number of metabolic processes. Iron is involved in multiple reactions because of the ease to give and accept electrons, being crucial for multiple cellular processes such as respiration and photosynthesis. Iron plays also roles in detoxification systems involving reactive oxygen species (ROS), in nucleotide synthesis, is able to transport oxygen in hemoglobins and leghemoglobins, and even participates in defense processes against pathogens. Iron is probably among the most important micronutrients of all required for living beings. However, when in excess, Fe can be toxic because of the production of harmful ROS and the consequent cellular damage. Therefore, the concentration of Fe in organisms must be finely regulated, with an extensive network of proteins and small organic compounds being involved in the acquisition, transport, compartimentalization and storage of this element.

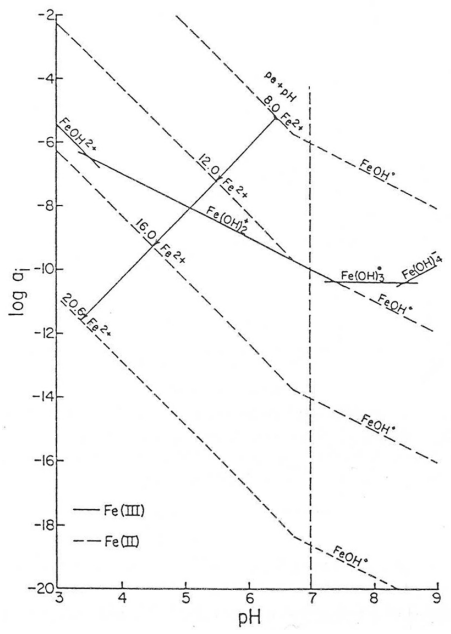

Fig. 1.1. Iron solubility (log a_i) dependency as a function of pe and pH (from Lindsay and Schwab, 1982)

In plants, Fe is involved in cellular respiration and oxygenic photosynthesis, being part of several components in both electron transport chains. It is found in iron-sulfur clusters (Fe_xS_x) and also in cytochromes, which have heme prosthetic groups. Iron-sulfur centers and cytochromes are located in all complexes of the respiratory chain and photosynthetic apparatus, with the exception of ATP synthase, underlining its fundamental role in energy-related processes. The involvement of Fe in energy metabolism is in line with the preferential localization of Fe in mitochondria and chloroplasts, although Fe is also found in other cellular compartments such as vacuoles and lysosomes and is also associated to soluble proteins in the cytosol.

Iron-deficient plants develop a number of visible symptoms, the most important being a reduced growth of the aerial part, an increased development of secondary roots and the so-called *iron chlorosis*, a yellowing of leaves that develops because of the decrease in

chlorophyll content (Abadía *et al*. 2011). In extreme deficiency situations, leaf necrosis develops and plants die.

In agricultural crops, Fe deficiency reduces crop yield and diminishes the nutritional quality of the produce (Briat *et al*., 2015). A low Fe content in plants leads to the development of Fe deficiency in humans and livestock. It is estimated that about 33% of human population suffer from *anaemia*, a reduced number of red blood cells, with approximately half of these cases being associated to low Fe diets (*ferropenic anaemia*). In many developing countries, the change from a diet rich in Fe (legumes) to a diet low in Fe (cereals, including rice) has contributed to the development of Fe deficiency in humans. This nutritional disease is present in all countries, even in those highly developed and is especially relevant in vulnerable groups of population like children (De Benoist *et al*., 2008) (Fig. 1.2). The daily recommended Fe intake for human adults (Estimated Average Requeriment, EAR) is in the range of 8 to 20 mg, from which only 10% is absorbed (Paesano *et al*., 2012; EFSA 2015).

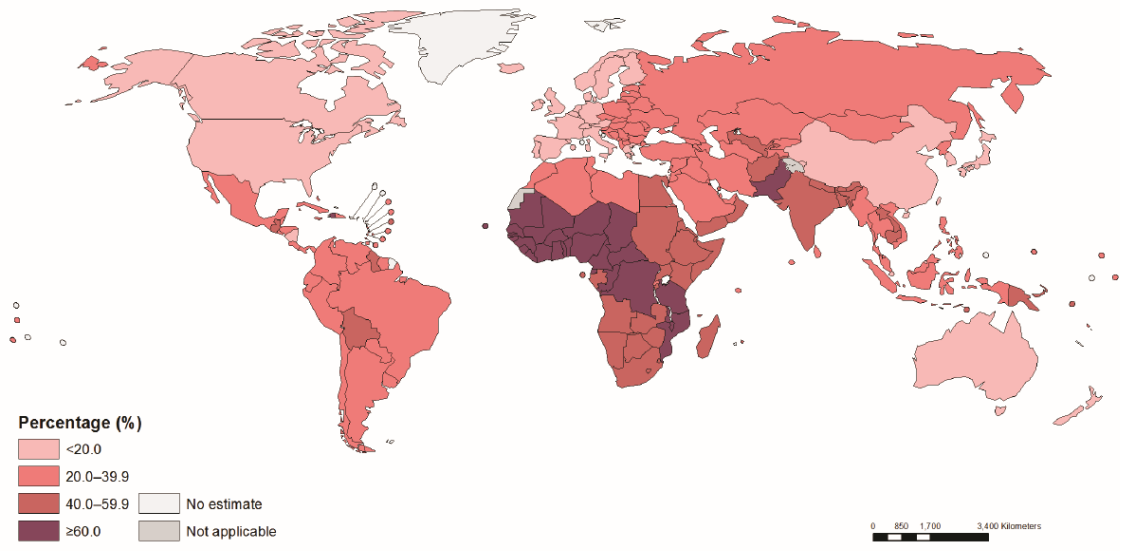

Source: WHO. The global anaemia prevalence in 2011. Geneva: World Health Organization; 2015.

Fig. 1.2. Anaemia world distribution of children younger than 5 years old (in %)

To alleviate this health problem, the most common procedures involve the administration of Fe supplements and the use of foods with higher Fe contents. Vegetable species, in the base of the trophic chain, are an important target to increase Fe concentration in their edible parts, in a process named *biofortification*. Until now, approaches targeted to induce Fe acquisition by roots and long distance transport, as well as to increase the content of Fe storage compounds and its bioavailabilty in organs of interest, such as the seed in cereals, have only obtained fairly low increases in Fe concentration (reviewed by Vasconcelos *et al*., 2017) (see section 1.2.4). This may be because the processes involved in Fe homeostasis are complex and still largely unknown. Indeed, unraveling the chemical forms of Fe in plants is one of the major challenges to better understand the Fe path from the soil to sink organs in plants. This knowledge would help producing valuable crops with increased Fe concentrations in the edible parts used for human nutrition.

1.2. Iron in plants

Plants, as sessile organisms, must cope with environmental factors by developing morphological changes and regulating metabolic processes. As indicated above, plants must acquire Fe from the environment and transport it to the sites of action.

1.2.1. Iron acquisition strategies

Plants use two different strategies for the acquisition of Fe from the growth medium: the *reduction strategy* (Strategy I) and the *chelation strategy* (Strategy II) (Marschner *et al*., 1986).

Strategy I is used by all plants with the exception of the family *Graminaceae*. In this process, Fe^{3+} must be reduced to Fe^{2+} prior to its absorption (Fig. 1.3). This reduction step is performed by the protein *Ferric Reductase Oxidase* (FRO) that uses NADH for the transfer of electrons from the cytosol to Fe forms in the substrate. The first protein of this family was found in *Arabidopsis thaliana* (Robinson *et al*., 1999) and since then members of the FRO family have been found in other plant organisms (Waters *et al*., 2002; Li *et al*., 2004). In *Arabidopsis*, 8 members of this family have been identified (FRO1-8, Jeong and Connolly, 2009), each with different cellular and subcellular locations and expression levels. After Fe reduction, Fe^{2+} is transported into the cytosol by the *Iron Regulated Transporter* (IRT, Eide *et al*., 1996). Several proteins belonging to this group have been

found so far: IRT1 and IRT2 have been found in roots, whereas IRT3 has been detected in the chloroplast envelope. These proteins have low substrate specificity, since they can transport other divalent cations such as Zn (Vert *et al*., 2002) and Cd (Eide *et al*., 1996). The acquisition process is assisted by the acidification of the rizosphere (extrusion of protons), which is carried out by an ATPase (*Arabidopsis* H^+ *ATPase2*; Santi and Schmidt, 2009). In addition, Fe availability is facilitated by the release into the rhizosphere of a wide array of small molecules, including flavins, phenolic compounds and carboxylates (Cesco *et al*., 2010; Mimmo *et al*., 2014). Recently, it has been demonstrated that several of these compounds facilitate the mining of Fe from scarcely soluble Fe forms (*e.g.*, Fe hydroxydes) in *A. thaliana* and other species (Rodríguez-Celma *et al*., 2013; Fourcroy *et al*., 2014; Sisó-Terraza *et al*., 2016a, b).

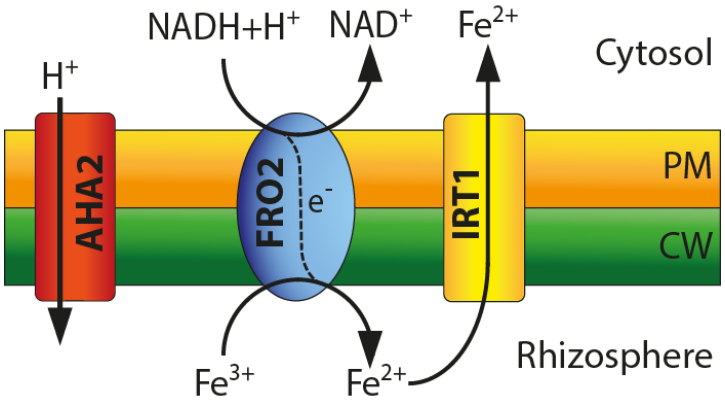

Fig. 1.3. Iron acquisition in Strategy I plants
(PM, plasma membrane; CW, cell wall)

Strategy II, also called chelation strategy, is performed by the herbaceous plants of the family *Graminaceae*, including rice (*Oryza sativa*), wheat (*Triticum sativum*) and barley (*Hordeum vulgare*), which are crop species with very high economical and nutritional importance. Iron acquisition in these plants involves the secretion to the rhizosphere of phytosiderophores [PS; members of the mugineic acids (MAs) family of compounds, which are derived from nicotianamine (NA) (Fig. 1.4)] by the protein TOM1 (Kawai *et al*., 1988; Bashir and Nishizawa, 2006; Nozoye *et al*., 2011). Secreted PS are able to form non-covalently bound Fe complexes (chelates) in the soil, which are then taken up by roots *via* specific transporters of the Yellow Stripe Like (YSL) protein family (Curie *et al*., 2009) (Fig. 1.5). This type of transporters is also involved in translocation of metal complexes with NA and/or PS including 2'-deoxymugineic acid (DMA) in different tissues, both in the vegetative and reproductive organs (Waters and Grusak, 2007; Chu *et al*., 2010; Zheng *et al*., 2012).

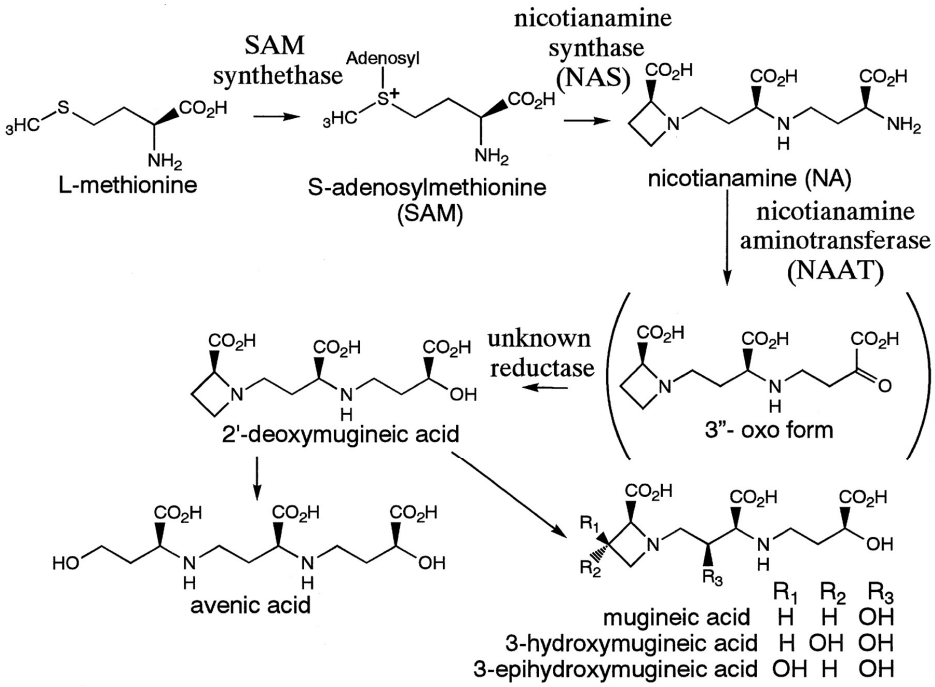

Fig. 1.4. Synthesis pathway of NA and its derivatives
(from Bashir *et al*., 2006)

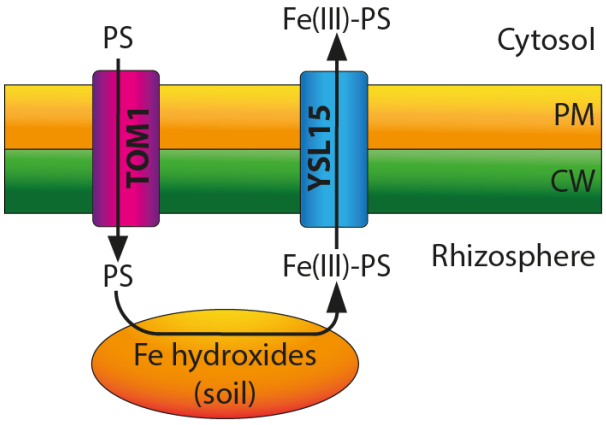

Fig. 1.5. Iron acquisition in Strategy II plants
(PM, plasma membrane; CW, cell wall)

Some Strategy II species have elements of the Strategy I and *vice versa*. For instance, rice has been found to acquire Fe^{2+} *via* an IRT transporter without any previous reduction step (Ishimaru *et al*., 2006) and is also able to take up Fe^{3+}-PS complexes *via* YSL proteins. This is likely because in the habitat in which this plant grows, flooded soils, the O_2 concentration is often low and the Fe^{2+} form occurs and is directly available for plants. In addition to its very high economical importance, this mechanistic aspect makes rice an

important plant for the study of Fe nutrition and homeostasis. Also, peanut (*Arachis hypogaea*) showed a high expression of *AhYSL1* in roots when grown intercropped with maize (*Zea mays*) (Xiong *et al*., 2013). This protein is localized in the epidermis of peanut roots and is able to take up Fe(III)-DMA, resulting in the avoidance of Fe deficiency. This indicates an important role of PS in improving the Fe nutrition status of peanut grown in intercropping systems.

1.2.2. Iron transport

After acquisition by roots and to reach their final destination within the plant (*e.g.*, organelles such as chloroplast or mitochondria), Fe and other metals taken up from the growth medium must follow a complex path through a number of different plant compartments and membrane systems (Conte and Walker, 2011; Sinclair and Krämer, 2012; Gayomba *et al*., 2015) (Fig. 1.6). During these processes metals can be adsorbed to the cell wall, sequestered in cells or transported through the symplast and/or the apoplast (Fig. 1.7). In the latter case, an active uptake of the nutrients into the symplast is required, due to the presence of the Casparian strip in the root stele that prevents the free diffusion of molecules. The general characteristics of the apoplastic and symplastic pathways are as follows:

1) Apoplastic pathway: molecules are transported through the apoplastic fluid by capillarity

2) Symplastic pathway: solutes move from cell to cell, connected by plasmodesmata, creating a network of direct connections among the cytosol of adjacent cells

Once in the root vascular parenchyma, nutrients must be loaded into the xylem sap, the fluid contained in xylem vessels that consist in dead lignified cells separated by perforated plates. The xylem sap mainly includes water and minerals, but also contains many different organic compounds (generally at concentrations ranging from µM to mM) and its composition can vary depending on the plant species, the time of the day and other factors. Its main function is the transport of water and solutes from roots to shoots using mainly hydrostatic pressure, a suction force (up to 2 MPa) produced by water transpiration in leaves.

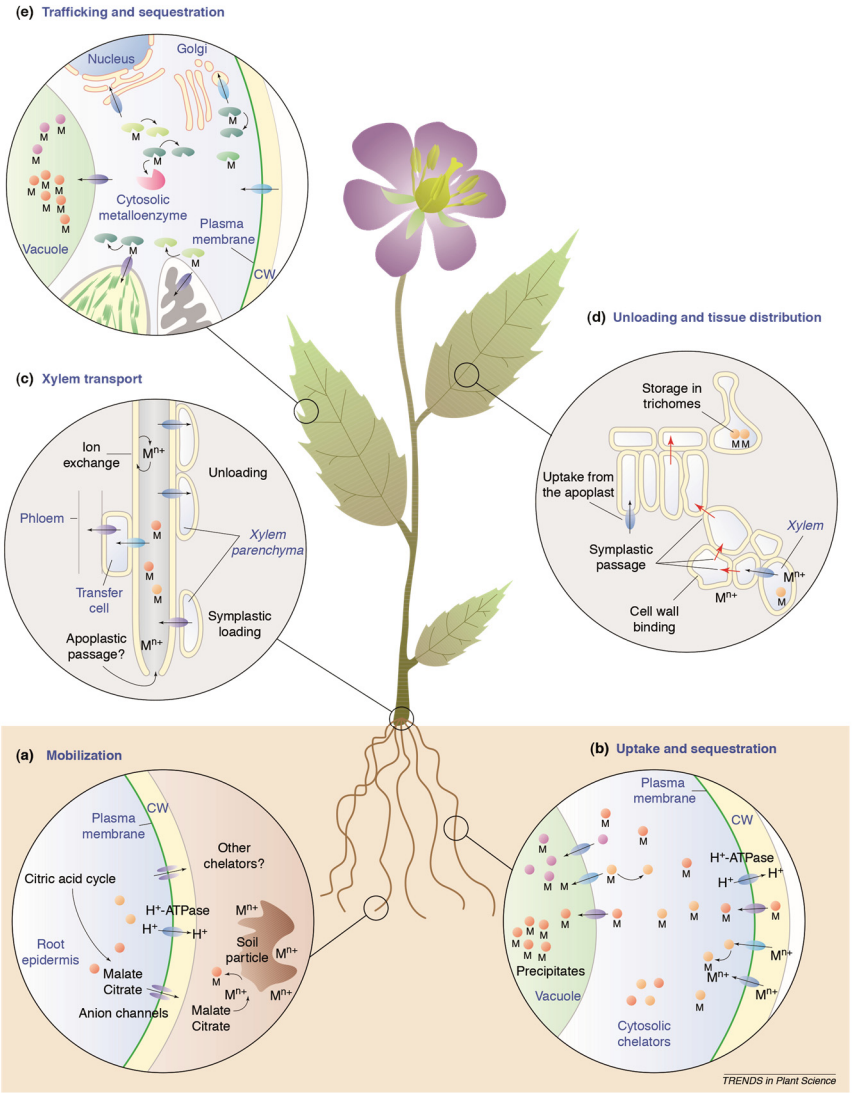

Fig. 1.6. Molecular mechanisms proposed to be involved in transition metal accumulation by plants. (a) Metal ions are mobilized by secretion of chelators and by acidification of the rhizosphere. (b) Uptake of hydrated metal ions or metal-chelate complexes is mediated by various uptake systems residing in the plasma membrane. Inside the cell, metals are chelated and excess metal is sequestered by transport into the vacuole. (c) From the roots, transition metals are transported to the shoot *via* the xylem. Presumably, the larger portion reaches the xylem *via* the root symplast. Apoplastic passage might occur at the root tip. Inside the xylem, metals are present as hydrated ions or as metal-chelate complexes. (d) After reaching the apoplast of the leaf, metals are differentially captured by different leaf cell types and move cell-to-cell through plasmodesmata. Storage appears to occur preferentially in trichomes. (e) Uptake into the leaf cells again is catalyzed by various transporters [not depicted in (e)]. Intracellular distribution of essential transition metals (= trafficking) is mediated by specific metallochaperones and transporters localized in endomembranes (please note that these processes function in every cell). Abbreviations and symbols: CW, cell wall; M, metal; filled circles, chelators; filled ovals, transporters; bean-shaped structures, metallochaperones. From Clements *et al*. (2002)

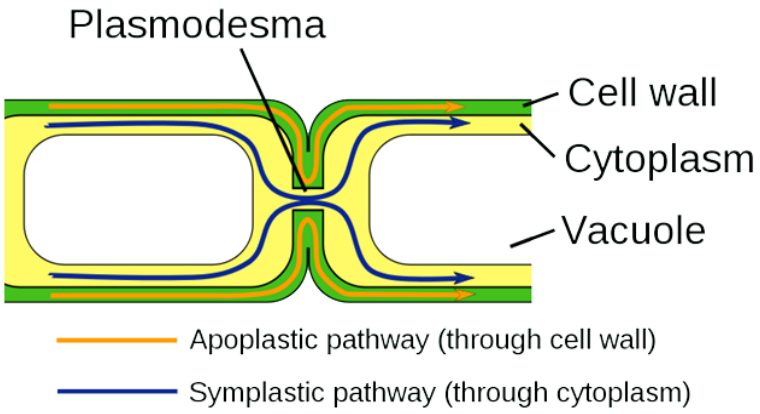

Fig. 1.7. Apoplastic and symplastic pathways for metal transport in plants (image from www.cronodon.com)

Once in leaves, metals are mobilized again *via* apoplast or symplast until they reach their final destination (Fig. 1.6). The apoplastic fluid is the space outside the plasma membrane which constitutes the aqueous interface between the symplast and the vasculature. The amount of apoplastic fluid present in leaves is small, accounting for less than 5% of total leaf volume (Steudle *et al*., 1980; Parkhurst, 1982). In this fluid there is an active exchange of compounds between the xylem sap, the phloem sap and the cells, as well as diffusion of CO_2, O_2 and other gases through the leaf stomata. Because of all these factors, the leaf apoplastic fluid composition can be highly variable.

Another component of the long-distance transport in the plant vasculature is the phloem sap. In contrast with the xylem sap, the phloem consists in living cells (sieve elements), which lack nuclei and are supported by companion cells. The sieve elements are connected at their ends by structures called sieve plates, which have a large number of enlarged plasmodesmata. The commonly accepted hypothesis for phloem sap transport is the pressure flow hypothesis ("Münch hypothesis"; see Turgeon, 2010). The phloem sap is involved in the long distance transport of nutrients from source to sink tissues, with seeds being a very important sink (see Section 1.2.4 below).

A large network of proteins is involved in metal, ligand or metal-ligand transport through all these barriers. Several families of transporters such as the YSL, the Zinc IRT-like Proteins (ZIP), the Cation Diffusion Facilitators (CDF) and the Natural Resistance-Associated Macrophage Protein (NRAMP) are involved in these processes and have been reviewed by Curie *et al*. (2009), Kambe *et al*. (2015), Kolaj-Robin *et al*. (2015) and Cellier (2012), respectively. For example, members of the YSL family (*e.g.*, AtYSL1,

OsYSL2) play roles in seed Fe loading. Also, other proteins are known to play critical roles in Fe trafficking: the *Iron Regulated 1 Ferroportin 1* protein (IREG1/FPN1) is responsible for Fe loading into the xylem sap of *Arabidopsis* (Morrissey *et al*., 2009), the Permease In Chloroplasts 1 (PIC1) is fundamental for Fe loading into chloroplasts (Duy *et al*., 2007), and the Vacuolar Iron Transporter 1 (VIT1) is responsible of Fe loading into vacuoles for storage and is especially important in seeds (Kim *et al*., 2006).

1.2.3. Transport of iron assisted by organic ligands

It has long been proposed that a significant fraction of Fe and other metals would be present in plant fluids not as free ions but in less reactive chemical forms, *e.g*., non-covalently bound to organic compounds, to prevent uncontrolled binding and also because free metals often exert some degree of toxicity. The formation of metal complexes provides both solubility and shielding during long-distance transport, since the metallic atom is enveloped by an array of bound molecules or anions (the so-called ligands), which donate one or more electron pairs to the metal to form the complex.

Indirect evidence for organic ligand-assisted transport of metals has been extensively reported. Possible ligands candidates are a range of small molecules, including organic acids (carboxylates) such as citrate (*Cit*) and malate (*Mal*), amino acids [including NA, histidine (*His*), cysteine (*Cys*) and high-affinity Fe(III) PS chelating compounds derived from NA, such as MA and DMA], as well as peptides and proteins (*e.g.*, *metallothioneins*). Detailed information about NA, DMA and carboxylates is reported below. In the case of toxic metals such as Cd, Hg, and others, plants also respond by synthesizing compounds such as the poly-glutathione peptides *phytochelatins* (PCs) that decrease the amount of free metal ions in plant fluids. Recent papers have reviewed the roles of NA (Curie *et al*., 2009; Clemens *et al*., 2013) and PCs (Pal and Rai, 2010) in plant metal homeostasis, the intra- and extra-cellular excretion of carboxylates (Meyer *et al*., 2010) and the plant metallo-chaperones (Tehseen *et al*., 2010).

During the last decade, the identification of many genes involved in plant long-distance metal transport has also been achieved, and many reviews have covered this issue in relation to either several metals (Colangelo and Guerinot, 2006; Haydon and Cobbett, 2007; Krämer *et al*., 2007; Curie *et al*., 2009; Palmer and Guerinot, 2009; Puig and Peñarrubia, 2009; Krämer, 2010; Waters and Sankaran, 2011; Komal *et al*., 2015; Yoneyama *et al*., 2015; Clemens and Ma, 2016; Culota and Scott, 2013) or to specific ones

such as Fe (Briat *et al*., 2007; Kim and Guerinot, 2007; Morrissey and Guerinot, 2009; Conte and Walker, 2011; Sperotto *et al*., 2012; Thomine and Vert, 2013; Yoneyama *et al*., 2015), Zn (Sinclair and Krämer, 2012; Yoneyama *et al*., 2015), Cu (Yruela, 2009; Pilon and Tapken, 2016), Mn (Pittman, 2005; Socha and Guerinot, 2015), and Cd (Mendoza-Cózatl *et al*., 2011).

To this date, analytical data on the actual metal complexes existing in plant fluids are still scarce. This is relevant, because the chemical forms in which a metal occurs in solution (metal speciation) affect solubility, precipitation, acid/base equilibrium, electron-transfer reactions, diffusivity, ability to undergo photolysis and others. The metal species existing in any given compartment determine biological activity, including the capability to be a substrate for membrane transport proteins involved in loading and unloading to xylem and phloem, as well as the possibility that metal toxicity can occur.

The next sections report general challenges relevant to the study of metal transport in plants such as the methodological approaches currently used to sample and analyze plant fluids, and describe the knowledge about the organic ligands relevant in Fe transport and the metal species occurring in plant fluids.

Methods for plant fluid sampling and inherent problems

Metal translocation within plants is dynamic, with the composition of plant fluids often changing with time. This mandates to establish an adequate standard sampling protocol, including sampling time and others, which must be applied to all samples so that results are fully comparable. A major limitation in the analysis of plant fluids is the need for samples of adequate purity and in sufficient volume to carry out measurements. The purity of the fluid samples must always be assessed by measuring cytosolic and/or vacuolar components associated to cell rupture. The activities of cytosolic marker enzymes, such as *malate dehydrogenase* (*c-mdh*) or others (López-Millán *et al*., 2000a), or the concentrations of K^+ as a vacuolar marker (Lohaus *et al*., 2001; Barabasz *et al*., 2012) are generally used with that purpose.

Xylem sap is relatively easy to sample (reviewed by Alexou and Peuke, 2013). The most frequently used technique is de-topping plants and letting xylem to bleed after discarding the first drops (López-Millán *et al*., 2009). Other techniques involve centrifugation of excised stems (López-Millán *et al*., 2000a) or the use of a Schölander pressure chamber (Larbi *et al*., 2003). With all these extraction techniques the xylem sap

volume sampled could reach several hundreds of µL. However, the purity of the xylem sap is still a matter of debate, since proteins of cytoplasmic origin are usually found in this fluid (for a review, see Rodríguez-Celma *et al.,* 2016)

Phloem sap has been sampled using a variety methods (reviewed by Dinant and Kehr, 2013) including those involving an incision near the inflorescence (in *Cucurbitaceae*, *Brassicaceae* and some *Lupinus* species; Lattanzio *et al*., 2013), those using aphid or leaf-hopper stylectomy (with the disadvantage of resulting in minute phloem sap volumes, ≤1µL per cut stylet; Ando *et al*., 2012), or by exudation of excised shoots maintained at >80% relative humidity in a closed chamber (the latter being only a qualitative approach; Marentes and Grusak, 1998). When using insect stylectomy, evaporation during sampling is a relevant issue; accurate determination of the phloem volume has been recently achieved by measuring the droplet diameter as it forms on the tip of the severed aphid stylet (Palmer *et al*., 2013). The purity of the phloem sap is usually assessed by measuring sugar concentrations and/or evaluating the presence of Rubisco proteins or transcripts (Giavalisco *et al*., 2006; Rodríguez-Medina *et al*., 2011; Lattanzio *et al*., 2013; Gutierrez-Carbonell *et al*., 2015). Other authors consider pH values around 8.0 indicative of phloem purity (Ando *et al*., 2012). However, phloem is a special case and there is still controversy about changes in composition induced by wounding (Atkins *et al*., 2011) and the presence of different types of phloem saps (Zhang *et al*., 2012).

Leaf apoplastic fluid has been commonly sampled by direct centrifugation of leaves without petiole (previously centrifuged at low speed to remove xylem sap from the mid vein; López-Millán *et al*., 2000a) or by using a Schölander pressure chamber (Larbi *et al*., 2003). Another method involves the infiltration of leaves with a solution under vacuum and then centrifugation to obtain a *leaf apoplastic wash fluid* (Lohaus *et al*., 2001). Since the latter procedure leads to a dilution of the apoplastic fluid, concentrations should be corrected considering estimations of apoplastic volumes occupied by water and air, using vacuum infiltration with a ^{14}C-sorbitol labeled solution and silicone oil, respectively (Lohaus *et al*., 2001). Disadvantages of these methods are the small volumes obtained as well as the risk of contamination from cell rupture. Leaf apoplastic fluid purity is also discussed in Rodríguez-Celma *et al*. (2016)

Methodological approaches used to unravel iron species in plant fluids

Until recently, researchers had to rely on indirect methods to infer the chemical forms of metals occurring in plant fluids. These methods use the measured concentrations of metals and possible ligands as well as experimentally determined metal-ligand stability constants to predict *in silico*, using chemical speciation software, the metal chemical species (Liao *et al*., 2000; Irtelli *et al*., 2009; Alves *et al*., 2011). This was always done assuming that chemical equilibrium was achieved (White *et al*., 1981b; López-Millán *et al*., 2000a; Callahan *et al*., 2006; Harris *et al*., 2012). However, chemical equilibrium is unexpected in plant fluids, since continuous changes in composition usually occur in these dynamic plant compartments.

Molecular biology approaches have provided key information on putative metal ligands and metal complexes that could play a crucial role in inter- and intra-organ metal transport (see reviews by Briat *et al*., 2007; Haydon and Cobbett, 2007; Kim and Guerinot, 2007; Milner and Kochian, 2008; Palmer and Guerinot, 2009; Pal and Rai, 2010; Waters and Sankaran, 2011; Leitenmaier and Küpper, 2013; Thomine and Vert, 2013). Genotypes with loss-of-function of genes involved in the trafficking of metals, ligands and/or their metal complexes, as well as metal hyper accumulators (*e.g.*, *Thlaspi caerulescens*) plant species have been studied. Other approaches include mutant and transgenic lines with impaired or enhanced metal ligands synthesis; a classical example of impaired ligand synthesis is the tomato mutant "*chloronerva*," which lacks NA (Pich and Scholz, 1996).

Recent advances in analytical techniques, and specifically in *Mass Spectrometry* (MS), have enabled a new insight on metal speciation. The use of highly selective and sensitive molecular and metal-specific MS techniques has allowed the identification and quantification of individual, well-defined metal species in plant tissues (including metabolites and proteins), even at sub-nM levels (Meija *et al*., 2006; Monicou *et al*., 2009). These approaches generally use hyphenated techniques based on the separation of compounds by high-resolution techniques [*e.g.*, *High Performance Liquid Chromatography* (HPLC) and *Capillary Electrophoresis* (CE)] and the determination of the metals and/or metal complexes by MS techniques [including *Inductively Coupled Plasma* MS (ICP-MS), *Electrospray Ionization* MS (ESI-MS), and others]. These new methodologies (reviewed by Monicou *et al*., 2009 and Khouzam *et al*., 2012) offer unique advantages for the *de novo* identification of metallo-metabolites occurring at low concentrations, in particular in plant materials such as plant fluids that do not require multi-

step extraction from the plant tissues. Metabolite structures can be elucidated using the empirical formulas of the parent compounds and fragment ions (data provided by high-resolution and high-accuracy MS) and the lineage of fragment ions observed in tandem MS or multistage MS (MSn). Furthermore, complexes with metals having more than one stable isotope, such as Fe, Zn, and Cu, provide metal-specific isotopic signatures that allow for identification of MS signals corresponding to metal containing molecules (see an example for metal-NA complexes in Rellán-Álvarez *et al*., 2008). In the past years, methods based on these analytical techniques have allowed the direct identification of several metal complexes with possible relevance in long distance transport, including carboxylate complexes (with Fe(III), Mn(II), Ni(II) and Zn(II)), as well as NA and PS complexes (with Fe(III), Fe(II), Ni(II), Co(II), Mn(II), Cu(II) and Zn(II)) and others (Álvarez-Fernández *et al*., 2014; Flis et al., 2016). However, only a few of these metal-ligand complexes have been directly observed in plant fluids until now.

A further approach to identify metal complexes in plant tissues -including fluids- relies on the identification of the chemical environment surrounding the metal, by means of synchrotron *X-ray absorption spectroscopy* (XAS) techniques such as *X-ray absorption near edge spectroscopy* (XANES) and *extended X-ray absorption fine structure spectroscopy* (EXAFS) (Lombi *et al*., 2011; Donner *et al*., 2012). This has been used for different metals such as Fe (Yoshimura *et al*., 2000; Terzano *et al*., 2013), Mn (Yun *et al*., 1998), Cu (Küpper *et al*., 2009; Song *et al*., 2013), Zn (Salt *et al*., 1999; Küpper *et al*., 2004; Trampczynska *et al*., 2010; Lu *et al*., 2013), Ni (McNear *et al*., 2010), Cd (Salt *et al*., 1995; Vogel-Mikuš *et al*., 2010; Huguet *et al*., 2012; Yamaguchi *et al*., 2012), Hg (Carrasco-Gil *et al*., 2011, 2013; McNear *et al*., 2012) and Pb (Tian *et al*., 2010; Chu *et al*., 2012). This technique allows direct *in situ* metal speciation in plants, without any preliminary extraction or preparation (see reviews by Lombi *et al*., 2011; Donner *et al*., 2012; Sarret *et al*., 2013). However, spectra are difficult to interpret when more than two or three species are dominant, and thus these techniques are generally used to confirm the presence of known species rather than to find new ones (Monicou *et al*., 2009). Furthermore, the applications of these techniques have been mainly restricted to tissues from metal hyper-accumulators due to the relatively low sensitivity (metal concentration should be higher than 10 μg g^{-1} dry weight).

Challenges in analyzing iron complexes in plant fluids

Several challenges are faced when studying Fe speciation in plant fluids, because of the changes in metal speciation that may occur at sampling and/or during storage, and especially during sample preparation, separation and determination (Husted *et al*., 2011). Challenges when attempting the analysis of the metal chemical form(s) existing in a plant fluid occur because:

1) dynamic metal-ligand systems such as those in plant fluids generally include labile or transient metal species
2) biochemical processes such as enzymatic activities may cause degradation and/or modification of metal complexes
3) metal species occur in plant fluids at very low concentrations (in the μM range)
4) the metal complex distribution strongly depends not only on pH, but also on the metal-to-ligand ratios

The latter is especially important in plant fluids (Weber *et al*., 2006; Xuan *et al*., 2006, 2007; Rellán-Álvarez *et al*., 2008), since unlike stable metal chelates with the hexadentate ligands NA and PSs, which always occur with 1:1 stoichiometry, many of the known metal ligands existing in the xylem and phloem saps (*e.g.*, aminoacids and carboxylates) may act as bi- and/or tri-dentate ligands, resulting in numerous metal-ligand species with different stoichiometries and charge states (see examples for Fe-*Cit* complexes in Silva *et al*. (2009) and Rellán-Álvarez *et al*. (2010a), and Fe-*Cit*-*Mal* complexes in Flis *et al*. (2016). For instance, in a solution with a 1:2 Fe:*Cit* ratio and pH 4.0, up to thirteen different Fe-*Cit* species were detected in aqueous solution by ESI-MS, whereas only two species occurred in a solution prepared at 1:100 Fe:*Cit* ratio at the same pH (Silva *et al*., 2009). Also, even for stable metal species, ligand exchange reactions may occur (altering the actual composition of the sample) at any step previous to the detection, due to the presence of competing ligands and/or redox mediators. Ligand exchanges have already been reported in the cases of Fe(III)-NA (with *Cit*; Rellán-Álvarez *et al*., 2008) and Fe(III)-DMA (with NA; Weber *et al*., 2006). Some of these challenges are especially critical in separation-based methods (*e.g*., HPLC, CE), because the separation of the free ligand does change the metal-to-ligand ratio, and also because the pH may change considerably when organic solvent modifiers are used (Rellán-Álvarez *et al*., 2008, 2010a; Köster *et al*., 2011).

Sampling and storage procedures (temperature, light, etc.) can be considered as key aspects to preserve the metal species occurring in samples during the whole analytical process (reviewed by Mesko *et al*., 2011). The temperature needs to be as low as possible to reduce metal species transformation. For this purpose, lyophilization and shock-freezing in liquid N_2 are the most common procedures used to preserve metal species in fluids. The latter is considered the safest technique to prevent metal species changes because it can be performed immediately at the sampling site and also because sample is stored in an inert gas atmosphere.

Light can cause changes in metal speciation because it can induce electron transfer reactions affecting the stability of the metal complexes and also the structural integrity of the ligands. For instance, the photochemical reduction of Fe(III) complexes with ligands such as di- and tri-carboxylic acids is known to occur (Bennett *et al*., 1982), accompanied by oxidative decarboxylation of the ligand. This issue could limit the use of irradiation with high intensity synchrotron X-rays for metal speciation (Terzano *et al*., 2013).

Finally, the accurate quantification of metal species, generally performed either on-line or off-line after separation, is currently carried out using metal (ICP-MS) or molecular (ESI-MS) detection, in combination with *isotope dilution analysis* (IDA) that requires the use of an isotopolog of the analyte. When ICP-MS is used, a stable isotope of the metal is added after the separation of the metal complexes. For instance, Rellán-Álvarez *et al*. (2010a) used ^{57}Fe post-column addition to quantify Fe-*Cit* species in tomato xylem sap. When molecular detection is used, such as in ESI-MS, the isotopolog should be either a metal complex with a stable isotope-labeled ligand, or alternatively a structural analogue of the ligand. The limited supply of stable isotope labeled ligands is an additional constraint for metal speciation.

Organic ligands relevant in iron transport in plants

Nicotianamine

Nicotianamine (NA; $C_{12}H_{21}N_3O_6$; M_W=303.31 Da) is a non-proteinogenic amino acid synthesized by all plants that occurs in all plant organs (Takahashi *et al*., 2003). Its structure has six functional groups, three carboxylic and three amino groups (Fig. 1.8), capable to act as electron donors allowing the complexation of multiple transition metals including Fe (Clemens *et al*., 2013). These structural features and the distances between the groups

facilitate the octahedral coordination with Fe by the formation of three 5-membered and two 6-membered chelate rings.

First described in 1971 (Noma *et al*., 1971), the characteristics of NA have been extensively studied *in silico*, *in vitro* and *in vivo*, mainly due to its chelating properties. Nicotianamine is able to form stable complexes with Fe(II), Mn(II), Co(II), Zn(II), Ni(II) and Cu(II) (Benes *et al*., 1983; Anderegg and Ripperger, 1989) and also has a good capacity to chelate Fe(III) (von Wirén *et al*., 1999; Weber *et al*., 2006; Rellán-Álvarez *et al*., 2008). The latter study compared *in silico* calculations and metal-NA standard solutions analysis using a MS approach, and concluded that the stability of metal-NA complexes (specially Fe-NA) is largely affected by slight changes in pH and by metal or ligand exchange reactions (for instance with Cu, Zn or *Cit*).

The roles of NA were first studied using the NA-defective *Chloronerva* tomato (*Solanum lycopersicum*) mutant. In these studies, NA was suggested to be involved in long distance transport of Cu (Pich and Scholz, 1996) and intracellular transport of Fe (Becker *et al*., 1992). Further studies with other plant species support the involvement in intracellular transport (Curie and Briat, 2003), metal transport in reproductive processes (Schuler *et al*., 2012) and heavy metal detoxification (Douchkov *et al*., 2005; Kim *et al*., 2005; Pianelli *et al*., 2005; Mari *et al*., 2006; Ouerdane *et al*., 2006; Weber *et al*., 2006; Kramër *et al*., 2007; Callahan *et al*., 2008; Cornu *et al*., 2015). The latter is also supported by a recent study showing that the secretion of NA to the rizosphere is involved in Zn tolerance in *Arabidopsis halleri* (Tsednee *et al*., 2014).

The synthesis of NA starts with the condensation of three S-adenosilmethionine molecules (Fig. 1.4), a step catalyzed by the enzyme *nicotianamine synthase* (NAS, EC 2.5.1.43) (Higuchi *et al*., 1994). This protein has been found associated to the plasma membrane in rice (Nozoye *et al*., 2014a) and *Malus xiaojinensis* (Yang *et al*., 2015). The number of NAS gene copies varies among species, with 4 copies in *A. thaliana*,

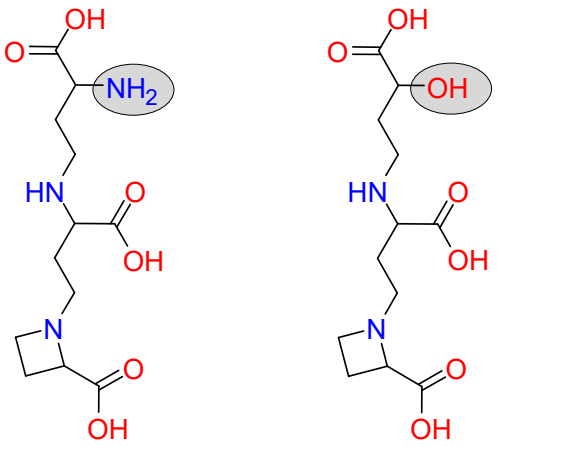

Fig. 1.8. Structure of nicotianamine and 2'-deoximugineic acid

3 in rice, 1 in tomato and 8 in barley. It is believed that different regulation and expression patterns exist between tissues and phenological states, as demonstrated by different studies (Schuler *et al*., 2012; Wang *et al*., 2013). In rice, the 3 *OsNAS* genes were up-regulated after 7 days under Fe deficiency (Kobayashi *et al*., 2014), whereas in *A. thaliana* only 2 out of the existing 4 were up-regulated under this conditions (Klatte *et al*., 2009). An overexpression of NAS genes was also found in *A. thaliana* plants grown under Zn toxicity conditions (Haydon *et al*., 2012).

2'-Deoximugineic acid

2'-Deoximugineic acid (DMA; $C_{12}H_{20}N_2O_7$; M_W=304.12 Da) is the first phytosiderophore derived from NA and is the precursor of all other members of the *mugineic acid family* (Fig. 1.4). The chemical structures of DMA and NA only differ in the occurrence of a terminal α-hydroxyl group in DMA instead of a terminal α-amino group in NA (Fig. 1.8). The first step in the DMA pathway synthesis is the deamination in the terminal C of NA by the enzyme *nicotianamine aminotransferase* (NAAT, EC 2.6.1.80), leading to an oxidized intermediate that is subsequently reduced to DMA by the enzyme *DMA synthase* (DMAS1, EC 1.1.1.285, Bashir *et al*., 2006). In rice, both *OsNAAT1* and *OsDMAS1* were upregulated after 7 days under Fe-deficiency treatment (Kobayashi *et al*., 2014).

The small differences in chemical structure of these ligands lead to important changes in affinities for metals. The metal [Zn(II), Fe(II) and Fe(III)] affinity constants of NA, DMA, mugineic acid (MA) and of three common synthetic metal chelators used in agriculture (EDTA, HEDTA and DTPA) are compared in Table 1.2. In addition, the structural differences among the phytosiderophores may play a role in substrate recognition when being transported across cell membranes through specific transporters. For instance, an amino acid sequence in HvYS1 was involved in specific Fe-phytosiderophore recognition and transport (Harada *et al*., 2007). The NA and DMA concentrations found in different plants fluids are in the range from 4 to 450 μM (Table 1.3). However, it should be noted that analytical data on NA and DMA concentrations in plant fluids are much less abundant than those on carboxylates.

Table 1.2. Comparison of the affinity constants of EDTA, HEDTA, DPTA, MA, DMA, and NA for Zn^{2+}, Fe^{2+}, and Fe^{3+} (from von Wirén *et al*., 1999)

Chelator	Log K for Metal Ion				
	Zn^{II}	Fe^{II}	Fe^{III}	Zn^{II}/Fe^{II}	Fe^{III}/Fe^{II}
EDTA[a]	16.0	14.3	25.1	1.12	1.76
HEDTA[a]	14.6	12.2	19.8	1.20	1.62
DTPA[a]	18.3	16.4	28.0	1.12	1.71
MA[b]	12.7	10.1	17.7	1.26	1.75
DMA[b]	12.8	10.4	18.4	1.23	1.77
NA[c]	15.4	12.8	n.r.[d]	1.20	n.r.

[a] Data are from Smith and Martell (1989). [b] Data are from Murakami et al. (1989). [c] Data are from Anderegg and Ripperger (1989). [d] n.r., Not reported in the literature.

Carboxylates

The term carboxylate includes in principle any compound that possesses a carboxyl group. However, in this Thesis the term *carboxylate* will refer to those pertaining to the *tricarboxylic acids* group (citric acid cycle; Figure 1.9).

Iron deficiency highly affects plant carboxylate contents, leading to a general increase in their concentrations in fluids and tissues of different organs. The first report of these increases dates back to 1939 (Schander, 1939). Increases in carboxylate root concentrations are commonly found in most plant species grown under Fe deficiency, whereas changes in leaves are different among species. Several studies have determined the changes in the carboxylate concentrations in sugar beet (*Beta vulgaris*) roots [16- and 26-fold increase in *Mal* and *Cit* concentrations, respectively, (López-Millán *et al*., 2000b)] and leaves (12- and 7-fold increase in *Mal* and *Cit* concentrations, respectively [López-Millán *et al*., 2001b]) and pear fruits (1.5-fold increase in succinate [Álvarez-Fernández *et al*., 2003] and 1.6-fold increase in *Cit* [Álvarez-Fernández *et al*., 2011]). Regarding fluids, carboxylate concentration increases were found in xylem sap and leaf apoplastic fluid of several plant species under different metal stress conditions (summarized in Table 1.3). Large increases in *Cit* have been found in xylem sap (17-fold in tomato; Rellán-Álvarez *et al*., 2010a) and leaf apoplastic fluid (20-fold in sugar beet; Larbi *et al*., 2010).

Among carboxylates, *Cit* and *Mal* have been reported to be involved in long and short distance transport of Fe. *Cit* and *Mal* were first proposed to be involved in long-distance transport of Fe in the 1960's (Lingle *et al*., 1963; Tiffin and Brown, 1961; Brown and Tiffin, 1965), but the identification of Fe-*Cit*, Fe-*Mal* and Fe-*Cit*-*Mal* complexes has been carried

out only recently (Rellán-Álvarez *et al*., 2010a; Flis *et al*., 2016). Studies with *Ferric Reductase Deficient* (FRD) mutants (i.e., *Atfrd3* and *Osfrdl1*), which lack the FRD protein responsible for the efflux of *Cit* in xylem vasculature cells, support the role of *Cit* as a major ligand responsible for Fe complexation (Durrett *et al*., 2007; Yokosho *et al.,* 2009). These mutants show leaf chlorosis and low levels of Fe in the xylem and leaves, as well as decreased *Cit* levels in the xylem sap. Taken together, all these studies support that *Cit* is responsible for the translocation of an important fraction of Fe to the shoot, and that FRD-mediated *Cit* efflux is required to sustain normal rates of root-shoot Fe delivery. More recently, it was shown that FRD is also a major player in the mobility of Fe in inter-cellular spaces lacking symplastic connections (Roschzttardtz *et al*., 2011). A summary of the *Cit* and *Mal* concentrations found in different plant fluids is shown in Table 1.3.

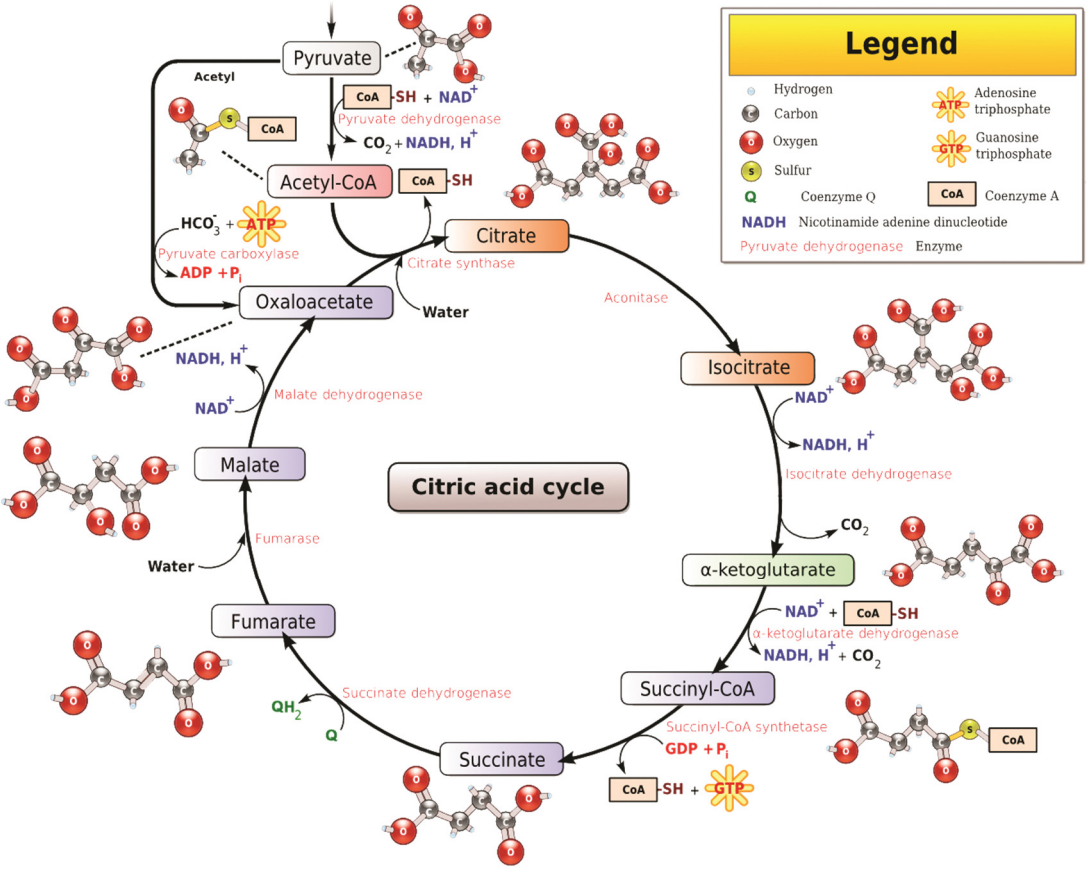

Fig. 1.9. The citric acid cycle (image from www.wikipedia.org)

Table 1.3. Metal ligand concentrations (*Mal* and *Cit* in mM, NA and DMA in µM) in the xylem sap, leaf apoplastic fluid and phloem sap of different plant species. From Álvarez-Fernández *et al*., 2014.

Species	Stress	Malate	Citrate	NA	DMA	References
XYLEM SAP						
A. serpyllifolium[H]	Ni	2[S]	0.5[S]			Alves *et al*., 2011
A. deliciosa	Fe	0.2-0.4[S]				Rombolà *et al*., 2002
A. halleri [H]	Cd	0.02[S]	0.3[S]			Ueno *et al*., 2008
A. thaliana			0.06[G]-0.09			Durrett *et al*., 2007
			0.2-0.9[G]			Schuler *et al*., 2012
B. vulgaris	Fe	2-30[S]	0.2-5[S]			López-Millán *et al*., 2000a
	Fe	2-14[S]	1-3[S]			Larbi *et al*., 2010
	Zn	0.5[C]-2[S]	0.06-0.3[S]			Sagardoy *et al*., 2011
B. carinata	Cu			64-271[S]		Irtelli *et al*., 2009
B. juncea [H]	Cd	0.02-0.23[S]	0.01[S]-0.7			Wei *et al*., 2007
B. napus	Cd	0.7-0.9[S]	0.5-0.6[S]			Nakamura *et al*., 2008
H. vulgare	Fe	0.01-0.03[S]	<0.01-0.02[S]		30-450[S]	Alam *et al*., 2001
	Fe				90[S]	Kawai *et al*., 2001
	Fe	0.8-5[S]	0.3-1.3[S]			López-Millán *et al*., 2012
G. max	Zn	0.04[S]-0.9	0.08[S]-1.5[S]			White *et al*., 1981a
O. sativa		0.15-0.18[G]	0.05[G]-0.1			Yokosho *et al*., 2009
	Fe	0.3[S]-0.4[GS]	0.1[GS]-0.2[S]			Yokosho *et al*., 2009
	Fe			10-18[S]	10-48[S]	Kakei *et al*., 2009
	Cu		0.08	28	34	Ando *et al*., 2012
P. communis	Fe	0.1-3	0.03-0.5[S]			Larbi *et al*., 2003
P. persica	Fe	0.7-2[S]	0.05-0.8[S]			Larbi *et al*., 2003
Q. suber	Cd	1-2[S]	0.5-1.2[S]			Gogorcena *et al*., 2011
S. lycopersicum	Fe	0.6-4[S]	0.04-0.6[S]			López-Millán *et al*., 2009
	Fe	0.01-0.17[S]				Rellán-Álvarez *et al*., 2010a
	Cu			nd[GS]-20[S]		Pich and Scholz, 1996
	Zn	0.06[S]-0.8[S]	<0.04[S]-0.3[S]			White *et al*., 1981a
	Cd	0.1-0.3[S]	0.01[S]-0.03-0.06[S]			Sagardoy, 2011
T. arvense	Zn	0.1-0.3[S]	nd			Lasat *et al*., 1998
T. caerulense [H]	Zn	0.1-0.2[S]	nd		nd	Lasat *et al*., 1998
LEAF APOPLASTIC FLUID						
B. vulgaris	Fe	0.7-2[S]	0.7-4[S]			López-Millán *et al*., 2000a
	Fe		0.2-4[S]			Larbi *et al*., 2010
P. communis	Fe	1.6[S]-2	0.8-1.8[S]			López-Millán *et al*., 2001b
PHLOEM SAP						
C. maxima		1.6	2.1			Fiehn, 2003
L. texensis		5.5	1.1			Lattanzio *et al*., 2013
O. sativa	Cu		>0.08	66	152	Ando *et al*., 2012
	Cd	>0.001->0.002[S]	66-83[S]	152-176[S]		Kato *et al*., 2010

[S] High or low metal supply; [G] Mutant or transgenic genotypes; and [H] Hyper-accumulator plant species. *nd*, *not detected*.

Iron species found until now in plant fluids

Xylem sap

Most of the studies exploring the chemical forms of metal complexes in plant fluids have been conducted using the xylem sap. Metals occurring in the xylem sap may be preferentially complexed by the more acidic carboxylic acids (existing at concentrations from 2 to 9 mM in the xylem) rather than the much more basic amino acids (existing at concentrations from 1 to 3 mM in the xylem) due to the relatively acidic pH of this fluid, which is generally in the pH range from 5 to 6.5 (Harris *et al*., 2012).

A Fe(III)-*Cit* complex [tri-Fe(III), tri-*Cit* complex (Fe_3Cit_3)] was found for the first time in the xylem sap of tomato, using an integrated HPLC-MS approach, consisting in *Hydrophilic Interaction Liquid Chromatography* (HILIC) coupled to both ICP-MS and ESI-MS(TOF), combined with the use of stable isotope (^{54}Fe) labeling; the identification was based on exact molecular mass, isotopic signature, Fe determination and retention time (Rellán-Álvarez *et al*., 2010a). Citrate had been considered for many years a likely candidate for Fe xylem transport, but the possible Fe-*Cit* species in the xylem sap were only predicted from the co-migration of Fe and *Cit* during paper electrophoresis of xylem sap (Tiffin, 1966) or from *in silico* calculations (von Wirén *et al*., 1999; López-Millán *et al*., 2000a, 2001b; Rellán-Álvarez *et al*., 2008). The Fe_3Cit_3 complex was only found in xylem samples with Fe concentrations above 20 μM (the limit of detection for the complex), such as those occurring in Fe-deficient plants after Fe-resupply. The complex could not be detected in Fe-deficient and control plants, which have lower xylem sap Fe concentrations. The existence of other Fe-*Cit* complexes is likely, and the complex Fe_2Cit_2 was also detected in Fe-*Cit* standards along with Fe_3Cit_3, with the allocation of Fe between the two complexes depending on the Fe:*Cit* ratio. Since in plant xylem sap a wide range of Fe to *Cit* ratios could exist, it is likely that both Fe(III)-*Cit* species could occur in different conditions (Rellán-Álvarez *et al*., 2010a). Later, other Fe-*Cit* species were found along with Fe_3Cit_3 in *H. vulgare* leaf extracts using HILIC coupled to high-resolution *Fourier Transform Ion Cyclotron Resonance* (FT-ICR) MS (Köster *et al*., 2011). Recently, a number of different Fe-*Cit* and Fe-*Cit-Mal* complexes have been found in the xylem sap of pea (*Pisum sativum*), whose composition can be described as $Fe(III)_3(Cit)_{(4-x)}(Mal)_x$ (x = 1 to 3) (Flis *et al*., 2016). The Fe speciation in tomato xylem sap was assessed for the first time using XANES on a highly brilliant synchrotron (Terzano *et al*., 2013). Although this

study confirmed the occurrence of Fe(III)-*Cit* and also found Fe(III)-acetate complexes in xylem sap, the authors indicated that the complexes found could be artifactual as a result of the high intensity radiation used.

The possible role of NA in long-distance Fe transport in the xylem is still being explored (Curie *et al*., 2009). However, this amino acid does not seem to be an absolute requirement for xylem Fe transport, since the NA-deficient tomato mutant *chloronerva* accumulates Fe in old leaves (Pich *et al*., 1994) and the *A. thaliana* NA synthase (NAS) quadruple mutant (with abolished NA synthesis) also accumulates Fe in leaves (Klatte *et al*., 2009). Until now, Fe-NA chelates have not been detected in xylem sap, and *in silico* and/or *in vitro* speciation studies tend to exclude NA as a possible xylem Fe carrier at the slightly acidic pH values typical of xylem (von Wirén *et al*., 1999; Rellán-Álvarez *et al*., 2008).

However, it has been recently suggested that NA may play a role in long distance transport of Fe when carboxylates are in short supply, as it occurs in FRD/NAS mutants (Schuler *et al*., 2012) or in plant species with less acidic xylem such in field-grown peach (*Prunus persica*) trees (where the xylem sap pH is in the range from 6.5 to 7.5, Larbi *et al*., 2003; Rellán-Álvarez *et al*., 2011a). The most accepted role of NA is in intra-organ Fe distribution, where this ligand could be crucial for xylem Fe unloading. Iron distribution within leaves is impeded in the tomato mutant *chloronerva* (Pich *et al*., 1994), and this mutant also showed a lower presence of Fe(II) ions in veins when leaves were analyzed by XANES (Yoshimura *et al*., 2000). This may suggest that the occurrence of Fe as Fe(II)-NA complex in leaf veins could be crucial for intra-organ Fe allocation (Yoshimura *et al*., 2000).

Regarding PSs, a minor peak assigned to Fe(III)-DMA was found in press sap from the roots of Fe-deficient wheat plants by HILIC-ESI-MS (Xuan *et al*., 2006), whereas Fe and DMA were found to co-elute when rice xylem sap was analyzed with CE-ICP-MS and CE-MS (Ariga *et al*., 2014).

No transporter responsible for moving Fe-complexes into the xylem sap has been conclusively identified so far, but it has been suggested that Fe-NA could be imported into the xylem by a yellow-stripe-like (YSL) transporter (Colangelo and Guerinot, 2006).

Phloem sap

The distribution of micronutrients to developing organs of plants depends to a large extent on phloem transport. Metals are sparingly soluble at the pH values typical of the phloem sap (from 7.0 to 8.0), and they are also highly reactive species, with some of them (including Fe) easily undergoing changes of valence that favor the production of highly reactive oxygen species. Therefore, metal complexation with appropriate ligands can provide solubility and shielding during phloem transport of metals to the nutrient sinks.

In the phloem sap of rice, Fe has been found predominantly (77%) associated with high molecular weight molecules (using a 3 kDa membrane filter; Nishiyama *et al*., 2012). In this study, both Fe-containing compounds or complexes of 10-30 kDa and the Fe(III)-DMA complex were detected in the phloem sap, using anion exchange HPLC separation followed by identification based on Fe determination and the comparison of the retention time with those of standards, in combination with exact molecular mass and Fe isotopic signature obtained using ESI-MS(TOF). A protein capable to bind Fe was also described in the phloem sap of *Ricinus communis* (ITP; Iron Transport Protein; Krüger *et al*., 2002) using two-dimensional gel electrophoresis protein separation (2-DE SDS-PAGE) followed by electro-blotting to PVDF membranes and staining of Fe-containing proteins with *ferene*. Recently, two more low molecular weight Fe-binding proteins were also identified in Texas lupine (*Lupinus texensis*) phloem sap using a similar approach combined with Fe affinity chromatography, although none of these proteins are considered candidates for Fe transport (Lattanzio *et al*., 2013).

The Fe(II)-NA complex has not been found so far in the phloem sap, although *in silico* and/or *in vitro* studies support that the Fe-NA complex is likely to occur at the neutral to basic pH values of this compartment (von Wirén *et al*., 1999; Rellán-Álvarez *et al*., 2008), and YSL transporters able to transport Fe-NA complexes have been described in *Arabidopsis* and *O. sativa* phloem vascular tissues (Curie *et al*., 2009). Perhaps NA is only important in Fe phloem loading (Schuler *et al*., 2012), and once in that compartment Fe may be transported in another form, for instance bound to proteins. So far, only the Zn(II)-NA complex has been determined in the phloem sap of rice plants (Nishiyama *et al*., 2012).

Other fluids

The apoplastic fluid composition is determined by the balance of import *via* xylem, uptake by cells and export to the phloem, and plays important roles in the transport and storage of mineral nutrients (Sattelmacher, 2001). However, as far as I know, there are no published reports tackling direct metal speciation on apoplastic fluids. *In silico* calculations have been carried out to speciate Fe in leaf apoplastic fluid of sugar beet (López-Millán *et al*., 2000a; Larbi *et al*., 2010) and field-grown pear trees (López-Millán *et al*., 2001b) using the concentrations of Fe, inorganic ions, carboxylates, sugars and amino acids measured in fluids isolated from Fe-sufficient and Fe-deficient plants. In both plant species, Fe was predicted to occur in the leaf apoplastic fluid as Fe-*Cit* complexes, with Fe*Cit*OH and Fe(III)Cit_2 being the major ones. The effect of Fe deficiency altered the balance between these two Fe-*Cit* species: the contribution of Fe(III)Cit_2 increased with Fe deficiency in sugar beet, whereas the contribution of Fe(III)Cit_2 was lower in Fe-deficient pear trees.

The *embryo sac liquid* (ESL) is a fluid that facilitates metal transport from the seed coat to the embryo. Iron speciation in isolated pea ESL was achieved using an integrated analytical approach, combining XANES, HILIC-ICP-MS, and HILIC-ESI-MS (Grillet *et al*., 2014). The application of XANES indicated that most of the Fe was present as Fe(III), probably associated to carboxylates (although the XANES spectra of Fe-*Cit* and Fe-*Mal* could not be distinguished) with only a minor amount of Fe(II) species being present. Most (88%) of the Fe occurring in the ESL was found as the species $Fe(III)_3Cit_2Mal_2$, $Fe(III)_3Cit_3Mal$ (both are mixed ligand species) and $Fe(III)Cit_2$; only a minor amount of Fe(II)-NA was found using HILIC separation coupled to the two cited MS detectors. Metal species were identified based on elution time, Fe determination, exact mass determination, isotopic signature, and MS^2 fragmentation pattern of the Fe species as identification tools. Recently, the presence of Fe(II)-NA and $Fe(III)_3(Cit)_{(4-x)}(Mal)_x$ (x = 1 to 3) complexes have been confirmed in the ESL of pea (Flis *et al*., 2016). On the other hand, pea embryos are capable to efflux into the ESL high amounts of ascorbate, that could chemically reduce Fe(III) from these complexes (Grillet *et al*., 2014).

Table 1.4 resumes the up to date identified metal complexes in xylem and phloem saps and embryo sac liquid of Strategy I and Strategy II plants under different metal supply conditions.

Table 1.4. Fe species found in plant fluids

Compartment	Strategy I	Strategy II
Xylem sap	Fe-*Cit*[3, 4, 5], Fe-*Mal*[5], Fe-*Cit-Mal*[5]	Fe-*Cit*[1, 2]
Phloem sap	Fe-ITP[7]	Fe-proteins[6], Fe-DMA[6], Fe-*Cit*[6]
Embryo sac liquid	Fe-*Cit*[5], Fe-*Mal*[5], Fe-*Cit-Mal*[5], Fe-NA[5]	

[1] Koster *et al*., 2011; [2] Ariga *et al*., 2014; [3] Rellán-Álvarez *et al*., 2010a; [4] Terzano *et al*., 2013; [5] Flis *et al*., 2016; [6] Nishiyama *et al*., 2012; [7] Kruger *et al*., 2002

1.2.4. Iron in seeds

Seeds are a very important sink organ for plant nutrients and are of special relevance for human nutrition and health, as addressed before. However, Fe loading and distribution mechanisms in seeds are still not completely understood.

A selective transport of nutrients is made from maternal to filial tissues (Patrick and Offler, 2001). Both the xylem and phloem sap perform nutrient delivery to seeds, with each fluid having different contributions (Waters and Grusak, 2007) even among species with the same Fe acquisition strategy (Stomph *et al*., 2009). The involvement of both vascular systems implies that Fe in seeds may have two different origins: a direct root-to-seed route *via* xylem sap and the remobilization of Fe from old and senescing leaves *via* phloem sap. Several proteins involved in micronutrient transport in seeds have been found, including members of the YSL and NRAMP families, among others (Curie *et al*., 2009; Roschzttardtz *et al*., 2009, 2013; Grillet *et al*., 2014). Mutations in some of these transporters decrease moderately Fe concentrations in seeds (*e.g.* OsYSL15, Lee *et al*., 2009a) suggesting the existence of redundant transport proteins, whereas their overexpression led to limited increases in Fe concentrations, supporting the existence of regulatory feedback loops (Banakar *et al*., 2016 and references therein). The Fe concentrations in seeds differ largely among plant species and cultivars. For instance, the analysis of 126 rice genotypes led to a Fe concentration range in whole seeds from 6.2 to 71.6 ppm (Anuradha *et al*., 2012). Also, differences in Fe concentrations among seed tissues have been found in rice, *Arabidopsis* and pea (summarized in Fig. 1.10; Grillet *et al.*, 2014).

The Fe distribution within seeds and related organs also relies on a complex system of transporters and organic ligands. In the case of rice, several YSL proteins have been found during flower and/or seed development, and those are summarized in Table 1.6. The preferential locations of these proteins in seeds are the aleurone layer and the embryo, zones

that have transport activity into the endosperm. Once in the seed, Fe may be stored in ferritins, proteins capable to store up to 4500 atoms of Fe per protein core (Vasconcelos *et al*., 2003; Briat *et al*., 2010), or sequestered into vacuoles to avoid metal toxicity (Kim *et al*., 2006). Another possible Fe ligand is phytate, a P-rich molecule preferentially located in the rice aleurone layer (Persson *et al*., 2009) that has a low bioavailability during human digestion (Guttieri *et al*., 2004, Gupta *et al*., 2015).

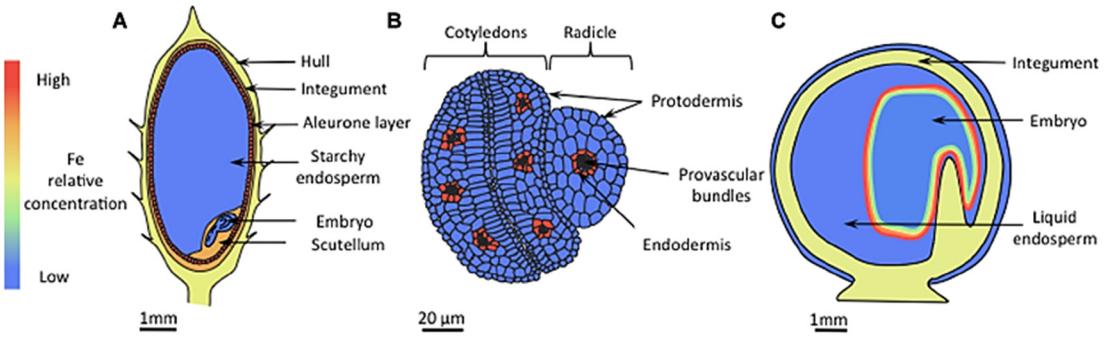

Fig. 1.10. Iron localization in seeds. (A) In rice, the concentration of Fe is highest in the aleurone layer, the integument and the scutellum. Iron levels are also high in the hull, whereas in the starchy endosperm the Fe content is low. (B) In *Arabidopsis*, Fe is mainly localized in vacuoles of endodermal cells that surround provascular tissues, whereas in other cells the Fe concentration is homogenously low. (C) In pea seeds, embryos constitute the main Fe storage pool, but unlike in *Arabidopsis*, Fe is localized in nuclei and plastids. The iron concentration is highest in the outer cell layers, progressively decreasing toward the inner layers. From Grillet *et al*. (2014)

Table 1.6. YSL proteins found in seeds and flowers of rice

Protein	Tissue	Substrate	Reference
OsYSL2	Flower	Fe(II)-NA	Koike *et al*. (2004)
	Seed	Mn(II)-NA	
OsYSL15	Flower	Fe(III)-DMA	Lee *et al*. (2009a)
	Seed	Fe(II)-DMA	
OsYSL18	Flower	Fe(III)-DMA	Aoyama *et al*. (2009)

The typical Fe concentration in polished rice seeds is about 4 µg g^{-1}, which is very low for human nutritional needs (see Section 1.1.2). The European Food Safety Authority (EFSA) has proposed 8-20 and 6-13 mg/day as the *Estimated Average Requirements* (EAR) for Fe and Zn, respectively (EFSA Journal, 2014 and 2015). Several studies have used biofortification strategies to increase the metal concentration in rice seeds (reviewed by Clemens *et al.,* 2014). These include increasing the concentrations of metal-binding chelators such as NA (see below), the overexpression of proteins involved in Fe acquisition

(Lee *et al*., 2012), transport (Nozoye *et al*., 2014b), and/or storage (Vasconcelos *et al*., 2003), decreasing the concentrations of absorption inhibitors (*e.g.*, phytate, polyphenols), increasing the concentrations of absorption promoters (*e.g.*, ascorbic acid, β-carotene), and even improving metal availability in source tissues for remobilization during seed formation (Pottier *et al*., 2014).

Increasing NA synthesis *via* overexpression of *OsNAS3* led to increases of 2.9-fold for Fe and 2.2-fold for Zn (Lee *et al.,* 2009b), whereas the overexpression of *HvNAS1* led to increases of 2.3-fold for Fe and 1.5-fold for Zn (Masuda *et al.,* 2009). The overexpression of 3 different *NAS* genes in rice led to Fe concentration increases in the range 2.4- to 3.7-fold and to Zn concentration increases in the range 1.9- to 2.5-fold (Johnson *et al.,* 2011). The simultaneous overexpression of *AtNAS1*, *PvFER* (ferritine) and *AfPHY* (phytase) increased the Fe concentration in polished grains by 4.5- to 6.3-fold and the Zn concentration by 1.5-fold (Wirth *et al.,* 2009). A large concentration increase for both elements has been recently reported with an *OsNAS2*-*Soyfer*H-1 construct, showing a 6.0-fold increase for Fe and a 3.8-fold increase for Zn, fulfilling 30% of the EAR for these metals (Trijatmiko *et al*., 2016). All these studies reflect the positive effect of increasing NA synthesis on the Fe and Zn concentrations in rice seeds. Some of these studies also reported an increase in seed DMA concentrations, but the role of this molecule in seed micronutrient loading remains unclear. Since the Fe-DMA complex has been found in the phloem sap of rice (Nishiyama *et al*., 2012), this metal ligand could be relevant in Fe translocation to seeds. The only study published so far using a combination of *NAS* and *NAAT* overexpression resulted in moderate increases (30%) in the rice seed Fe concentration (Masuda *et al.,* 2013).

Since the high metal content embryo and bran parts of the rice seed are removed during processing (polishing), the microlocalization of the metals in seeds is relevant. The microlocalization of micronutrients in seeds has been tackled using high resolution imaging techniques such as Synchrotron-based X-ray microfluorescence (μ-XRF) (Takahashi *et al.,* 2009; Lombi *et al.,* 2011; Johnson *et al.,* 2011; Lu *et al.,* 2013; Kyriacou *et al*., 2014). Elemental images obtained from plants by μ-XRF are only semi-quantitative, generally providing only relative intensities, although this technique could be quantitative in other sample types and using reference materials. In seeds, studies have shown that the accumulation of Fe and Zn occurs mainly in the embryo and that increases in the concentration of these metals occur whenever a high concentration of NA was achieved

(Johnson *et al.,* 2011). A spatial correlation between some elements was found, such as Fe with P, possibly corresponding to Fe-phytate complexes (Fig.1.11; Kyriacou *et al*., 2014).

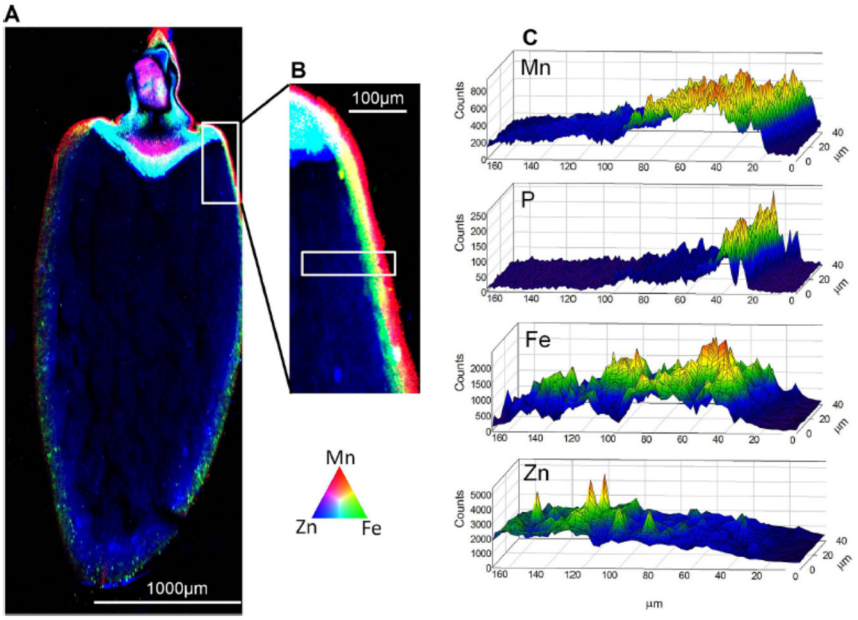

Fig. 1.10. Elemental maps for Mn (red), Fe (green) and Zn (blue) distribution obtained by XRF in a WT longitudinal rice grain section. (A) An enlarged view of the outer grain is shown in (B). The rectangle in B represents the area used to obtain elemental maps of Mn, P, Fe and Zn in C. From Kyriacou *et al*. (2014)

An alternative technique, *laser ablation inductively coupled plasma mass spectrometry* (LA-ICP-MS), has been used for studying spatial localization and quantification of elements (Konz *et al*., 2012) in a wide variety of animal tissues such as human eye sections (Konz *et al.,* 2014), whereas it has been much less applied in plant science so far (Wu and Becker, 2012). LA-ICP-MS Fe maps of plant tissues have been obtained for leaves, shoots and roots of tobacco plants (Becker *et al*., 2008) and leaves of soybean (Oliveira and Arruda, 2015). However, there is only one report on the use of LA-ICP-MS in seeds: quantitative elemental images of Zn and some toxic elements (Sb, Ar, Pb and Cd) were obtained in rice seeds from a mining area in China (Basnet *et al.,* 2014).

Chapter 2

Objectives

In the previous Chapter I have summarized the current knowledge on Fe acquisition, transport and storage in plants, focusing on the organic ligands and metal complexes involved, the analytical procedures commonly used, and the challenges inherent to these methods. During the last few years, the use of advanced analytical techniques has allowed to determine some Fe complexes in plant fluids. However, analytical data on the Fe complexes and ligands existing in plant fluids are still scarce, with nicotianamine (NA) and its derivatives being among the Fe ligands less analyzed in plant fluids and tissues. The actual knowledge on this issue also lacks comprehensive studies involving sampling of as many fluids as possible within a given plant species. The functional redundancy of Fe transport molecules (*e.g.*, NA and its derivative 2'-deoxymugineic acid -DMA- and citrate -*Cit*-) and their corresponding pathways are still poorly known.

The general objective of this Thesis is to contribute to the characterization of the roles of NA and DMA in plant Fe homeostasis, as well as to study their relationships with other organic ligands such as carboxylates and other essential metal micronutrients.

To accomplish this objective the homeostasis of Fe has been studied, using different approaches, in two crop species, tomato (*Solanum lycopersicum*) and rice (*Oryza sativa*), which have Strategy I and Strategy II for Fe acquisition, respectively. In tomato, root and leaf fluids have been obtained, and metal micronutrients, NA and carboxylates determined using mass spectrometry (MS)-based methods. In rice, molecular biology approaches have been used, in combination with MS-based methods for the determination and localization of metal micronutrients, NA and DMA in different tissues.

The specific objectives of the Thesis are as follows:

Objective 1. To study the effects of the iron status on the concentrations of metal micronutrients, nicotianamine and carboxylates in different *Solanum lycopersicum* plant fluids.

Objective 2. To study the contribution of nicotianamine, 2'-deoxymugineic acid and citrate to the long-distance iron transport in *Oryza sativa* plants.

Objective 3. To study the effects of the overexpression of genes involved in nicotianamine and 2'-deoxymugineic acid synthesis on the localization of metal and metal ligands in *Oryza sativa* seeds.

Chapter 3

Materials and methods

3.1. Plant materials

In this Thesis different plant species have been used, including tomato (*Solanum lycopersicum*), rice (*Oryza sativa*) and oilseed rape (*Brassica napus*).

The tomato cultivar FER has been often used in Fe-deficiency studies (Brown *et al*., 1971; Donnini *et al.,* 2003). In preliminary experiments, the tomato cv. "Tres Cantos" was also used, but the Fe concentration observed in fluids of this cultivar (data not shown) were found to be much lower than those in fluids of FER, and therefore it was no longer used.

Different rice genotypes were used during the Thesis. First, the mutant *Osfrdl1* and its WT "Nipponbare" were used. The OsFRDL1 protein belongs to the *Multidrug and Toxic Compound Extrusion* (MATE) family of transporters, and is involved in *Cit* loading into the xylem sap of rice (Yokosho *et al.,* 2009). This mutant shows leaf chlorosis, low levels of Fe in the leaves and precipitation of Fe in the stele. *Osfrdl1* is a OsFRDL1 (ND8025) knockout line (with a Tos-17 insertion), which was identified by Prof. J. F. Ma's group in Okayama University (Kurashiki, Japan) (Yokosho *et al*., 2009). Details on the obtention of this mutant are provided in the original paper. The *Osfrdl1* rice seeds used in this Thesis were kindly provided by Prof. Ma.

Also, rice genotypes overexpressing *OsNAS1* and/or expressing *HvNAATb* genes were obtained in the collaborating laboratory of Prof. Paul Christou in the University of Lleida, Spain. Rice plants (cv. "EYI 105") were transformed in order to obtain genotypes with high levels of NA and DMA. The details of the cloning, expression and transformation are as follows:

Cloning: The cDNAs of *OsNAS1* (GenBank ID: AB021746.2, 1,372 bp) and *HvNAATb* (GenBank ID: AB005788.1, 1,656 bp) were cloned from roots of rice (cv. "EYI 105") and barley (*H. vulgare* L. cv. "Ordalie") grown *in vitro* in Fe-deficient MS medium (Murashige and Skoog, 1962) for 2 weeks. Total RNA was extracted with RNeasy Plant Mini kit (Qiagen, Hilden, Germany) and 1 µg of RNA was used for reverse transcription using Omniscript RT Kit (Qiagen, Hilden, Germany) by RT-PCR. The cDNA obtained was amplified with the following primers:

Osnas1-BamHI-FOR 5'-AGGATCCATGGAGGCTCAGAACCAAGAGGTCG-3'
Osnas1-HindIII-REV 5'-AAAGCTTCATAATATAGTGCGCCTTTCGATCGTCCGGCTGT-3'
Hvnaatb-BamHI-FOR 5'-AGGATCCATGGCCACCGTACGGCCAGAGAGCGACG-3'
Hvnaatb-HindIII-REV 5'-AAAGCTTCTAGCAATCATCGCTCGCTCGAATTTCTC-3'

Expression: Amplification products were inserted in the expression vector pAL76 (Christensen and Quail, 1996) in sites BamHI y HindIII. This vector has the constitutive promoter *Ubiquitin-1* as well as transcription ending *nos* from *Agrobacterium tumefaciens*.

Transformation: Rice embryos at the germination state were isolated and grown as described in Sudhakar *et al.* (1998). After 7 d, embryos previously incubated for 4 h in a highly osmotic medium (0.2 M mannitol and 0.2 M sorbitol) were bombarded with Au particles carrying pAL76 plasmids. Transformed embryos were selected in an hygromicin-supplemented medium (30 mg L^{-1}) and transplanted sequentially to shoot and root development media with hygromicin.

Oilseed rape (cv. "Drakkar") plants were used for phloem isolation, because of the ease in obtaining this fluid from this plant species (Gutierrez-Carbonell *et al*., 2015).

3.2. Plant cultivation

3.2.1 Tomato

Tomato (cv. FER) plants were grown in hydroponic medium in growth chambers (Fitoclima 10.000 EHHF, Aralab) with a photosynthetic photon flux density (PPFD) photosynthetically active radiation (PAR) of 350 µmol m^{-2} s^{-1}, a 16/8 h light/dark photoperiod, at 25/18°C and 70% relative humidity (RH). Seeds were germinated in vermiculite for 11 d, transplanted to 10 L plastic buckets (34 plants per bucket) in half-strength Hoagland nutrient solution (pH 5.5, adjusted with HCl or KOH) with 45 µM Fe(III)-EDTA. The composition of the half-strength Hoagland nutrient solution is described in Table 3.1.

Table 3.1. Composition of the half-strength Hoagland nutrient solution used for tomato growth

Ion	Concentration
NO_3^{2-}	7.5 mM
PO_4^{3-}	1.0 mM
SO_4^{2-}	1.0 mM
K^+	3.4 mM
Ca^{2+}	2.5 mM
Mg^{2+}	1.0 mM
B^+	23.2 µM
Mn^{2+}	4.6 µM
Zn^{2+}	0.185 µM
Cu^{2+}	0.185 µM
Mo^{2+}	0.06 µM
Cl^-	4.6 µM
Na^+	46 µM
Fe(III)-EDTA	45 µM

Plants were pre-grown for 14 d and then transplanted to 10 L buckets (8 plants per bucket) filled with half-strength Hoagland

nutrient solution at pH 5.5, with either 45 µM Fe(III)-EDTA (Fe-sufficient plants) or 0 µM Fe(III)-EDTA (Fe-deficient plants) for 11 d. The nutrient solution was renewed two times per week. The typical phenotype of Fe-deficient tomato plants grown under these conditions for 11 d is shown in Figure 3.1.

All plant culture materials (buckets, glass tubes and pipette tips) were cleaned before use with soap and bleach, and later with 3.7% HCl to eliminate metal traces. All materials were washed with water Type I (Wasserlab).

The leaf Chl concentration was estimated daily in developed (leaves 1st to 3rd from the cotyledons) and young leaves (leaves 4th to 6th) with a portable Chl meter (SPAD-502 -Soil Plant Analysis Development- device, Minolta, Osaka, Japan).

With the final aim of obtaining plant fluids with the highest possible concentrations of Fe, the Fe acquisition mechanisms were primed in Fe-deficient tomato plants by the application of small doses of Fe(III)-EDTA (called thereafter *Fe pulses*) during the experiment, as described previously by Zouari *et al*. (2001): Fe-deficient plants were supplied with fresh nutrient solution and 0.5 µM Fe(III)-EDTA added. This was done at days 4, 8 and 10 after imposing the Fe deficiency treatment.

Eleven days after imposing the Fe deficiency treatment, a group of Fe-deficient plants having experienced the *Fe-pulses* were fully resupplied with 45 µM Fe(III)-EDTA. These plants are called thereafter Fe-resupplied plants.

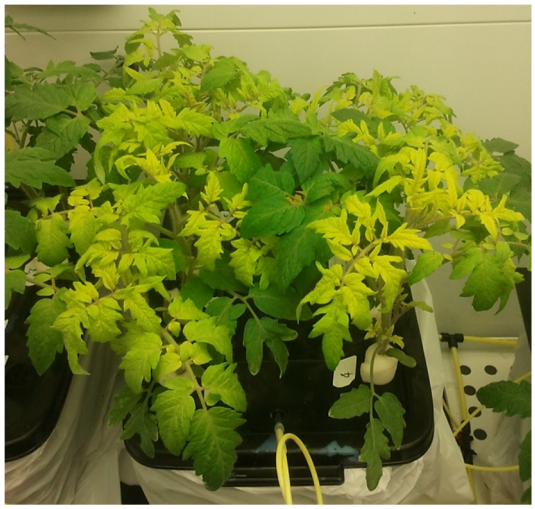

Fig. 3.1. Tomato plants showing chlorosis symptomps after 11 days of imposing the Fe-deficiency treatment

3.2.2 Rice

Cultivation of the *Osfrdl1* mutant and its WT

Osfrld1 and "Nipponbare" WT rice plants were grown hydroponically in growth chambers (Fitoclima 10.000 EHHF, Aralab, Lisbon, Portugal). Seeds were surface sterilized with 2% Ca hypochlorite solution for 30 min, rinsed with tap water for 1 h, and germinated at 25°C for 24 h in the dark between moistened towels. Germinated seeds were placed on a plastic net, floating on a 1.0 mM $CaCl_2$ solution in 4 L plastic buckets, in growth chambers and under controlled conditions (photoperiod of 12/12 h light/dark 28°C/22°C and 70% RH). Seven days later, the solution was replaced with Kimura B nutrient solution, pH 5.5, whose composition is detailed in Table 3.2, with 10 µM $FeSO_4$. Plants were grown until the length of the second leaf was about 20% of the length of the first leaf, and then transplanted in groups of 3 plants wrapped in sponge rubber to 4 L plastic buckets (12 groups per bucket) containing Kimura B nutrient solution pH 5.5 with either 10 (+Fe treatment) or 0.2 µM $FeSO_4$ (-Fe treatment). Roots were washed with deionized water before plants were transferred to the -Fe medium. Nutrient solutions were renewed every 2 days.

Table 3.2. Composition of the Kimura B nutrient solution used for rice growth

Compound	Concentration (µM)
KNO_3	90
$Ca(NO_3)_2$	180
KH_2PO_4	90
$MgSO_4$	270
$(NH_4)_2SO_4$	180
H_3BO_3	23.2
$MnSO_4 \cdot H_2O$	4.6
$ZnSO_4 \cdot 7H_2O$	0.185
$CuSO_4 \cdot 7H_2O$	0.185
$Na_2MoO_4 \cdot 2H_2O$	0.06
$FeSO_4 \cdot 7H_2O$	(+Fe) 10 (-Fe) 0.2

Fig. 3.2. WT and *Osfrdl1* rice plants

Some of the plants (in both genotypes and with both Fe treatments) were treated with foliar applications of 20 mM citric acid or 20 mM Na citrate, supplemented with the surfactant Break-Thru® OE411 (Evonik Industries, Essen, Germany) at a concentration of 1%. Applications were made with a brush every 3 days during 2 weeks and leaf Chl concentration was estimated daily in the completely developed youngest leaf of each plant

with a portable Chl meter (SPAD-502 device, Minolta). Roots and shoots were sampled at day 15 as described below (Section 3.4.6).

Cultivation of the *OsNAS1* overexpressors, *HvNAATb* expressors and their WT

Seedlings obtained as indicated above were transferred to pots filled with substrate (Traysubstract; Klasmann-Deilmann GmbH, Geeste, Germany) and grown flooded in large trays in growth chambers at 26° C, 900 µmol m^{-2} s^{-1} PPFD PAR with a 12/12 h light/dark regime and at 80% RH. Plants were watered with a 100 µM Fe solution provided as Fe(III)-EDDHA using Sequestrene 138 Fe G-100 (Syngenta Agro SA, Madrid, Spain) until flowering, and then self-pollinated. The solution in the trays (containing only water and Sequestrene 138) was replaced every week. Plants were grown and self-pollinated to obtain T4 seeds, which were harvested from the same panicle 3 weeks after polinization and then used in the experiments.

3.2.3 Oilseed rape

Oilseed rape (*B. napus* cv. Drakkar) plants were grown hydroponically in a controlled environment chamber, with a photosynthetic photon flux density at mid-plant height of 350 µmol m^{-2} PAR, 90% RH, and at a 15/9 h day/night regime and 22.5/17.5 °C (Gutierrez-Carbonell *et al*., 2015). Seeds were imbibed in water and placed in CYG germination pouches (Mega International, St Paul, MN, USA) with approximately 15 mL water for 7 d in the dark at room temperature. Seedlings were transplanted to 4 L plastic buckets (four plants per bucket) for an additional 6-week period in a nutrient solution detailed in Table 3.3. The nutrient solution was renewed weekly.

Table 3.3. Composition of the nutrient solution used for oilseed rape

Compound	Concentration
KNO_3	2.5 mM
$Ca(NO_3)_2$	2.5 mM
KH_2PO_4	1 mM
$MgSO_4$	1 mM
$CaCl_2$	25 µM
H_3BO_3	25 µM
$MnSO_4$	5 µM
$ZnSO_4$	2 µM
$CuSO_4$	0.3 µM
H_2MoO_4	0.1 µM
$NiSO_4$	0.1 µM
Fe(III)-EDTA	45 µM

3.3. *In vivo* measurement of root FCR activity in tomato

Root FCR activity was measured in intact whole tomato plants roots 2 h after the light onset and in the growth chamber as described in López-Millán *et al*. (2009). The whole root system of one plant was immersed in 250 mL of a solution containing 5 mM MES (Sigma), 300 µM BPDS (Acros Organics, Geel, Belgium) and 500 µM Fe(III)-EDTA, pH 5.5, with continuous aireation. The container was covered during the experiment with Al foil to exclude light and avoid photochemical reduction of Fe(III)-EDTA. The reaction was run for 30 min, 3 aliquots of the solution were taken and A_{535} nm measured (at the absorbance peak for the Fe(II)-$(BPDS)_3$ complex), using a UV-2450 spectrophotometer (Shimadzu, Kyoto, Japan). A molar extinction coefficient of 22.14 mM^{-1} cm^{-1} was used to determine the FCR activity. Root FCR activity values are expressed as nmol Fe(II) g root FW^{-1} min^{-1}.

3.4. Sampling of plant material

Due to the low concentration of metals present in plant fluids, all materials used for sampling were thoroughly cleaned to avoid traces of metals as described by Ando *et al*. (2012). Eppendorf tubes, micropipette tips and centrifuge tubes were washed with 0.1 M ultrapure HNO_3 for one day in agitation, then rinsed abundantly with Type I water and dried in an oven at 60 °C. After drying, the materials were stored in plastic bags and closed boxes until analysis.

3.4.1. Sampling of tomato and rice xylem sap

Xylem sap was obtained using the detopping technique (López-Millán *et al*., 2009). In tomato, shoots were cut 2 cm above the cotyledons using a carbon steel disposable scalpel (Nahita, Beriain, Spain). The cut was rinsed with Type I water and the first drops of xylem sap were discarded to avoid contamination from the cut surface. The xylem sap was collected using a micropipette tip during 20 min and kept in a test tube submerged in ice. In the case of *Osfrdl1* and WT rice, shoots were cut 2 cm above the root and xylem sampled as described above for tomato, but using a capillary tube instead of a micropipette.

In both cases (tomato and rice), cytosolic malate dehydrogenase (*c-mdh*; EC 1.1.1.37) activity, marker of cell rupture, was immediately analyzed in the collected fluids (see Section 3.4.5), and non-contaminated fluids stored at -80° C until analysis.

3.4.2. Isolation of tomato root and leaf apoplastic fluid

After collection of the tomato xylem sap, roots were separated from shoots, immersed in a solution of 1 mM EDTA for 5 min to eliminate metals adsorbed in root surface, rinsed twice for 1 min in Type I water and softly dried with tissue paper. Ten mL plastic syringes devoid of the plungers were used, with tops cut to permit fitting in the centrifugue tube. Roots were placed with the excised base towards the tip of the cut syringe and also secured with parafilm (Fig. 3.3A). This procedure allows for the collection of root apoplastic fluid with minimal tissue disruption.

Leaves, including petioles, were excised, washed in Type I water and dried with tissue paper. Leaf apoplastic fluid was obtained as described in López-Millán *et al*. (2000a) and Barabasz *et al*. (2012) with modifications. Leaves were layered on the external face of the cut syringes with their petioles facing the syringe tip and then gently secured with parafilm (Fig. 3.3B). Since tomato leaves were too fragile to stand centrifugation without collapsing, they could not be placed in the inner part of the syringes as described in the original method [López-Millán *et al*. (2000a)].

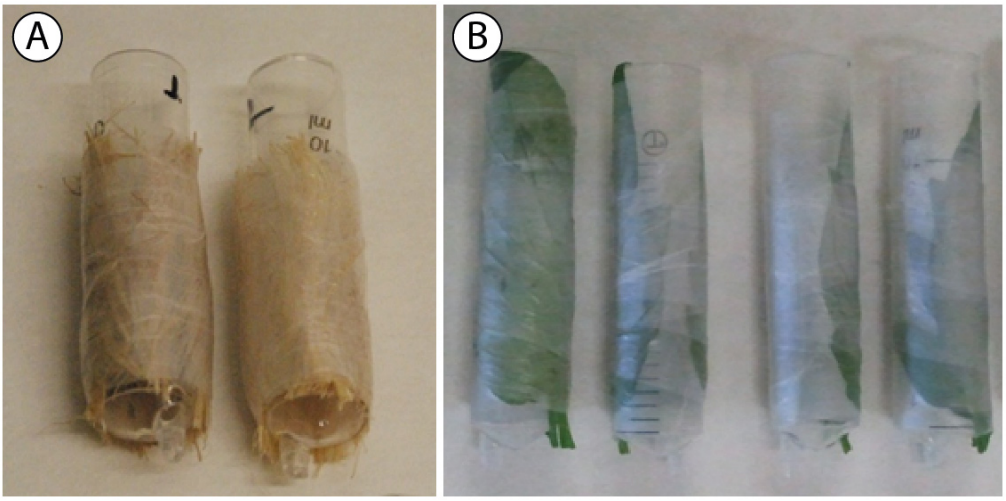

Fig. 3.3. Assembly of tomato roots (A) and leaves (B) on 10 mL cut syringes to obtain apoplastic fluid and symplastic extract

Syringes were placed into 50 mL polystyrene centrifugal tubes (Nalgene) and centrifuged in a JA 25.50 rotor (Avanti J-26XP, Beckman Coulter, California, USA). Due to the lack of a protocol for roots, different trials were made to optimize the extraction of apoplastic fluid with an adequate purity, as judged by the activity of the cytosolic marker *malate dehydrogenase* (c-*mdh*). Increasing centrifugation speeds were used until a

relatively high volume of fluid was obtained, but the *c-mdh* activity when compared with root tissue extract was only noticeable at centrifugation speeds higher than 3,000*g* (Table 3.4). Final conditions used were a first centrifugation step at 1,000*g* for 15 min to discard xylem sap fluid and adsorbed water in the external surface of the root, followed by a second centrifugation step at 2,500*g* for 15 min to obtain root apoplastic fluid. Results of the trials during this method optimization were similar to those obtained by López-Millán *et al*. (2000a) for sugar beet leaves. In the case of leaves, a first centrifugation step at 2,500*g* for 15 min was made to eliminate xylem sap from the leaf mid-vein (López-Millán *et al*., 2000a), and a second centrifugation step was made at 4,000*g* for 15 min to obtain leaf apoplastic fluid.

In all samples, the purity was assayed immediately after collection by measuring the activity of *c-mdh* (see Section 3.4.5) and the remaining fluid was frozen at -80° C until analysis.

Table 3.4. Recovered volumes and *c-mdh* activity in tomato root apoplastic fluid isolated using different centrifugation speeds. Data are means ± SD, 3 replicates were made for each speed. *n.d., not determined*.

Centrifugation speed (*g*)	Mean volume (µL)	Volume SD	*c-mdh* activity (%)	Activity SD
500	32.5	3.5	0.0	0.0
1,000	45.0	7.1	0.0	0.0
1,500	73.3	30.6	0.0	0.0
2,000	125.0	20.8	0.0	0.0
2,500	>200	n.d.	0.1	0.0
3,000	>200	n.d.	3.1	2.4
3,500	>200	n.d.	7.7	1.2
4,000	>200	n.d.	13.9	2.0

3.4.3. Isolation of tomato root and leaf symplastic fraction

After isolating the apoplastic fluid of leaves and roots, syringes with the tissues still attached were frozen in liquid N_2 and let to thaw at room temperature. After thawing, samples were centrifuged again at 4,000*g* for 15 min. The fluid obtained was recovered and considered as symplastic extract. All samples were frozen at -80° C until analysis.

3.4.4. Isolation of oilseed rape and rice phloem sap

In oilseed rape, phloem exudates (thereafter referred to as phloem sap) were collected every day for one week starting one week after treatment onset as described in Gutierrez-Carbonell *et al*. (2015). About 3 h after the beginning of the photoperiod, shallow incisions were made with a lancet device (BD, NJ, USA; using number 6 depth setting) at the base of the attached inflorescences, and droplets of phloem exudate were collected for approximately 30 min using a micropipette. The first droplets were discarded to minimize contamination with other plant fluids. The samples were kept on ice during the entire collection period, and stored at -80°C until further analysis. The full experiment was repeated three times.

In rice, a stylectomy protocol was used to obtain phloem sap. This work was made in collaboration with Dr. Elisa Garzo, from the Insect Vectors of Plant Pathogens Group, Crop Protection Department, in the Agricultural Sciences Institute (CSIC, Madrid), led by Prof. Alberto Fereres. The stylectomy protocol is as follows: an adult apterae aphid (*Sitobion avenae*) was immobilized with a silver drop in his back and a gold wire attached to a copper electrode (Fig 3.4A). The copper electrode was connected to the *Electrical Penetration Graph* recording system (EPG) and monitored with Stylet 3.0 software. Active sucking has a characteristic waveform (Fig. 3.4B). EPG records were obtained using a DC-monitor (GIGA-8, EPG-Systems, Wageningen, The Netherlands) and digitalized through a DI-710 board (Dataq Instruments, Akron, OH, USA).

Fig. 3.4. Attachment of the aphid to the copper electrode (A) and characteristic sucking waveform recorded (B)

The attached aphid was placed in the panicle of rice plants at the seed maturation stage (approximately 10 days after pollination). When an active sucking waveform was detected, the stylet of the aphid was cut with a voltage in a tungsten needle and inserted into a nanocapillar (500 nL capacity). The nanocapillar contained

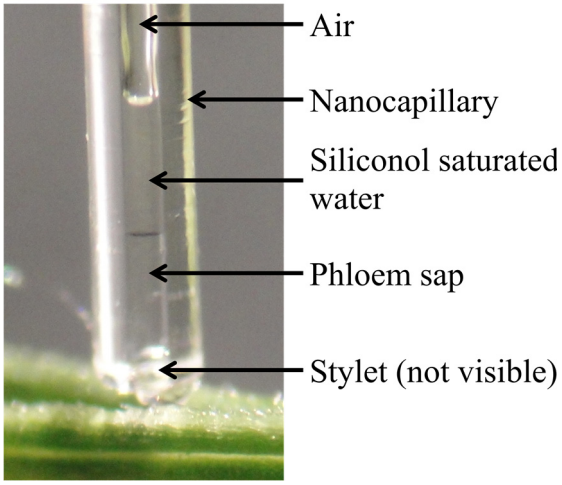

≈25 nL of siliconol-saturated water to avoid evaporation, and phloem sap flowed out passively (Fig 3.5). With this method the volume obtained was in the tenths of nL range in 1 h. Therefore, several aphids were used, and aliquots obtained were pooled to obtain volumes of a few µL.

Fig. 3.5. Obtention of phloem sap

3.4.5. Contamination assay of xylem sap, apoplastic fluid and phloem sap

The purity of the xylem sap and apoplastic fluid samples was assessed by measuring the activity of the cytosolic enzyme *c-mdh* as described in López-Millán *et al.* (2000a), based in the original method of Dannel *et al*. (1995). This enzyme catalyses the conversion of malate into oxaloacetate. The reaction is bidirectional (Fig. 3.6), so that the consumption of NADH can be monitored with an excess of oxaloacetate.

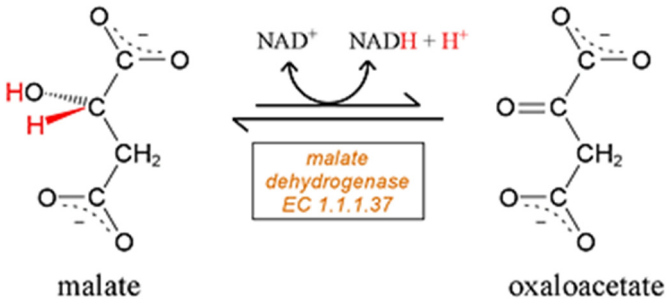

Fig. 3.6. Reaction catalyzed by *cytosolic malate dehydrogenase*

The enzyme activity in tissue homogenates (from leaves and roots) was used as a control. Fresh leaves or roots (150 mg) were milled with mortar and pestle in liquid N_2 until a fine powder was obtained. 750 µL of extraction buffer, containing 100 mM HEPES (Sigma), 30 mM sorbitol (Sigma), 1% w/w PVP (Sigma), 1% w/w BSA (Sigma), 2 mM DTT (Sigma) and 1 mM $CaCl_2$ (Panreac), pH 8.0, were added, the mixture was homogenized and the slurry transferred to an Eppendorf tube placed on ice. Another 750

µL of extraction buffer were added to the mortar, the remaining tissue was homogenized and the slurry added to that obtained in the previous step. Then, the sample was centrifuged at 10,000g for 15 min at 4°C, the supernatant was transferred to a new Eppendorf tube and the *c-mdh* activity was assayed immediately, since it decreases rapidly with time.

The reaction buffer contained 46.5 mM Tris-HCl (Merck), 400 µM oxalacetic acid (Sigma) and 150 µM NADH (Sigma), pH 9.5. The decrease in A_{340} was measured with a Shimadzu UV-2450 spectrophotometer (Shimadzu, Kyoto, Japan) for 60 seconds, using a NADH molar extinction coefficient of 6.3 mM^{-1} cm^{-1}. The NADH consumption rate was expressed as µmol NADH g FW^{-1} s^{-1} in the case of tissues and as µmol NADH mL^{-1} s^{-1} in the case of fluids. Samples were considered as contaminated, and therefore discarded, when the *c-mdh* activity in the fluid was higher than 3% of the *c-mdh* activity in the full homogenate corresponding to the same tissue and treatment.

For estimating the purity of the phloem sap, the concentrations of glucose, fructose, and sucrose in samples were measured enzymatically using a sugar assay kit (K-SUFRG, Megazyme International Ireland, Wicklow, Ireland), following the instructions provided by the manufacturer. The proportion of reducing sugars over total sugars was used to estimate purity.

3.4.6. Sampling of rice root, leaf and seed tissues

Roots and leaves of *Osfrdl1* and WT rice plants were washed in water Type I and stored in sealed plastic bags at -80°C until analysis.

In the case of the *OsNAS1* overexpressors and *HvNAATb* expressors and their WT, seed husks were removed and embryos were carefully separated from the endosperm with new stainless steel razor blades using binocular magnifying glasses. The (nutrient-rich) aleurone layer that covers the endosperm was not removed, and therefore the endosperm fractions included this tissue. The embryo samples, obtained pooling embryos from 50 to 100 seeds of the same line, were milled in liquid N_2 with mortar and pestle until a fine powder was obtained. The endosperm samples were obtained pooling endosperms without embryos from ten seeds.

3.5. Metal determination

3.5.1. Metal determination in tomato fluids

Metal determination was carried out in an External Analysis Service (Unitat d'Analysis de Metalls, UdAM-University of Barcelona, Spain). Fluid samples were filtered through 0.45 µm polyvinylidene fluoride (Durapore® PVDF) filters (Ultrafree® MC HV, Merck KGaA, Darmstadt, Germany), and 20 µL of the filtrate was digested with 120 µL of ultrapure 65% HNO_3 (Trace Select Ultra, Fluka) at 60°C for 24 h. The digests were taken to a final volume of 2 mL with Type I water. Iron, Mn, Cu and Zn were quantified using an ICP-MS Agilent 7500ce (Agilent, Santa Clara, USA), using NIST standards.

3.5.2. Metal determination in rice seeds

Fifty mg of embryos or endosperms from WT and transgenic *OsNAS1*, *HvNAATb* and *OsNAS1+HvNAATb* plants were ground in a mortar with liquid N_2. Ground tissues were digested with ultrapure 21% HNO_3 (Trace Select Ultra, Fluka) and 6% H_2O_2 (Suprapur, Merck) for 55 min at 190° C in an Ethos 1 microwave oven (Milestone Srl., Sorisole, Italy). Metal determination in the digests was made in the UdAM- University of Barcelona, with an ICP-MS Agilent 7500ce (Agilent, Santa Clara, USA) and using NIST standards.

3.5.3. Metal determination in rice tissues

Leaves and roots of *Osfrdl1* and WT rice plants were dried in an oven at 70°C for 2 d, samples were ground to a fine powder with a Retsch MM400 ball mill (Haan, Germany) using a liquid N_2-cooled sample holder and digested with 6.4 mL of ultrapure 26% HNO_3 (Trace Select Ultra, Fluka) and 1.6 mL of H_2O_2 30%. The microwave digestion programme was 5 min at 100 °C, 10 min at 170 °C and 35 min at 180 °C. Metal concentrations in the digests were determined by flame atomic absorption spectrometry (FAAS) using a Solaar 969 apparatus (Unicam Ltd., Cambridge, UK) (Carrasco-Gil *et al.*, 2016).

3.6. Carboxylate determination in plant fluids

Carboxylate determination was carried out in tomato fluids by HPLC-ESI-MS(TOF) using the method developed by Rellán-Álvarez *et al*. (2011b). An HPLC system (Alliance 2795 Separation Module, Waters) (Fig. 3.7A) with a 250 x 4.6 mm anionic exchange Supelcogel H^+ column (Sigma) was used. The matrix of the column was composed of divinylbenzene sulphonated polystyrene with a 9 µm particle diameter. The mobile phase contained 5% 2-propanol (LC-MS purity grade, Sigma) and 0.1% formic acid (LC-MS purity grade, Sigma) in Type I water. The elution program consisted in an isocratic separation at 200 µL min^{-1} for 20 min. Identification was performed using a MicroTOF (Bruker Daltonics, Bremen, Germany) mass spectrometer (Fig. 3.7B) equipped with an electrospray source (ESI).

Carboxylates were identified on the basis of retention time (RT) and mass to charge ratio (*m/z*). Standards of *cis*-aconitate, *Cit*, *Mal*, succinate and fumarate were from Sigma and the 2-oxoglutarate standard was from Fluka. The concentrations of organic acids were quantified with external calibration, using 100 µM labelled ^{13}C-*Mal* and ^{13}C-succinic acids as internal standards (Cambridge Isotopes Laboratories, Andover, USA). A typical chromatogram obtained by this method is shown in Fig. 3.8.

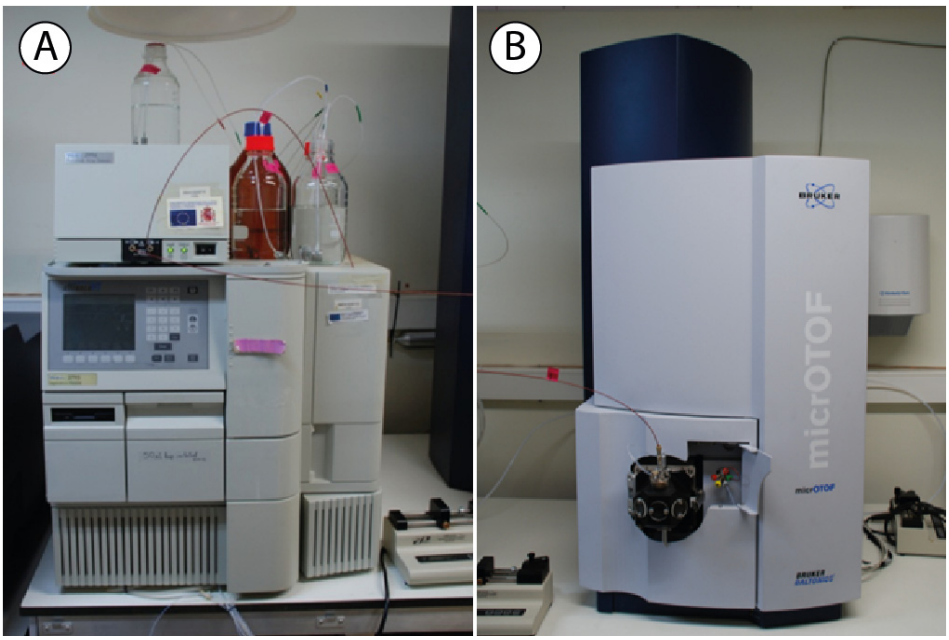

Fig. 3.7. Alliance 2795 (A) and MicroTOF mass spectrometer (B)

Before injection, all samples were filtered through 10 kDa cellulose centrifugal filters (Microcon 10 Ultracel YM-10, Millipore) and diluted appropriately. Since carboxylates can occur in the samples within a wide concentration range (from µM to mM), an initial exploration was made to find the appropriate dilution for each compound and fluid. The Limits Of Quantitation (LOQ; defined as *"the lowest concentration at which the analyte can not only be reliably detected but at which some predefined goals for bias and imprecision are met"*; Armbruster and Pry, 2008; CLSI, 2015) for this method are described in Rellán-Álvarez *et al*. (2011b). In this method, a signal to noise (*s/n*) ratio higher than 10 was used as threshold for quantitation.

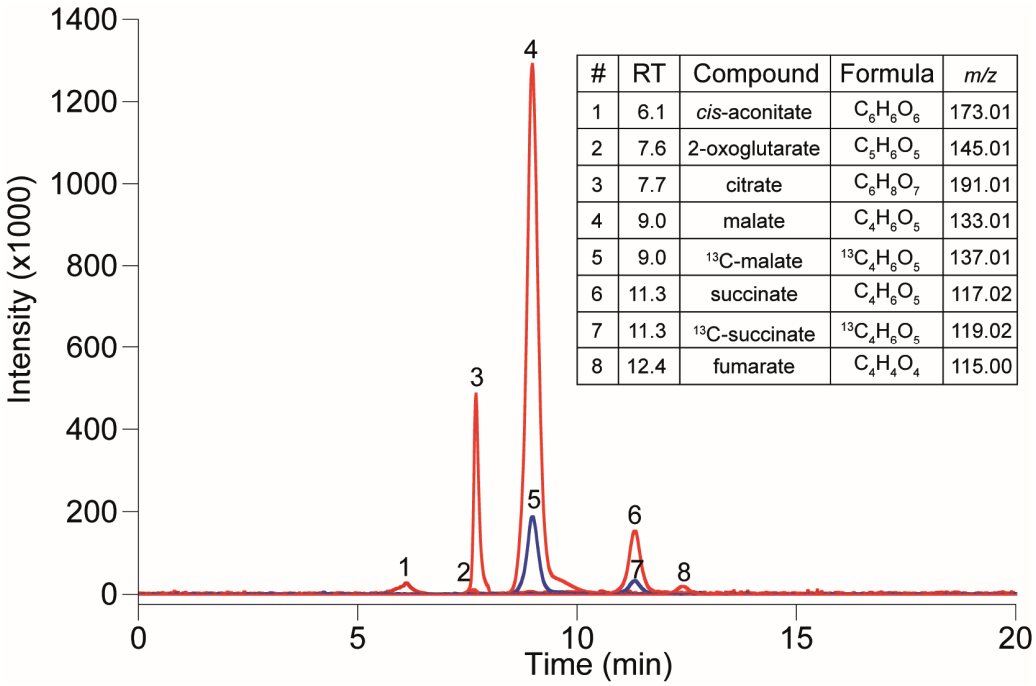

#	RT	Compound	Formula	*m/z*
1	6.1	*cis*-aconitate	$C_6H_6O_6$	173.01
2	7.6	2-oxoglutarate	$C_5H_6O_5$	145.01
3	7.7	citrate	$C_6H_8O_7$	191.01
4	9.0	malate	$C_4H_6O_5$	133.01
5	9.0	^{13}C-malate	$^{13}C_4H_6O_5$	137.01
6	11.3	succinate	$C_4H_6O_5$	117.02
7	11.3	^{13}C-succinate	$^{13}C_4H_6O_5$	119.02
8	12.4	fumarate	$C_4H_4O_4$	115.00

Fig. 3.8. HPLC-ESI-MS(TOF) chromatogram of a mixture of carboxylate standards. Concentrations were 10 µM for *cis*-aconitate (1), 2-oxoglutarate (2), succinate (6) and fumarate (8), 100 µM for *Cit* (3), 250 µM for *Mal* (4) and 100 µM for the ^{13}C-*Mal* (5) and ^{13}C-succinic acid (7) internal standards. Chromatogram traces correspond to the $[M-H]^-$ ions and were extracted with a precision of ±0.02 *m/z* units. The Table in the inset shows the RT, compound, molecular formula and theoretical *m/z* for the $[M-H]^-$ ion of each carboxylate

3.7. Determination of nicotianamine and 2'-deoxymugineic acid

Determination of NA and DMA was carried out by HPLC-ESI-MS(TOF) using the method of Xuan *et al*. (2006) with some modifications. Nicotil-lysine (NL) was used as an internal standard (Wada *et al*., 2007). Due to the formation of metal-NA complexes, dissociation of those was necessary as a prior step, and this was carried out using the synthetic metal

chelator EDTA. Stock solutions of NA (98%; Hasegawa, Kawasaki, Japan), DMA (98%; Toronto Research Chemicals Inc., Toronto, Canada) and NL (synthesized by Prof. Casarrubias, Complutense University of Madrid, Spain) were prepared at concentrations of 1 and 10 mM and stored at -80° C until use.

For the WT and transgenic (*OsNAS1* and/or *HvNAATb*) rice seeds and the leaves and roots of the WT and *Osfrdl1* mutant, extractions were made as in Wada *et al.* (2007) with some modifications. NA and DMA were extracted from 50 mg of tissue powder with 300 µL Type I water and 18 µL of 1 mM NL. The supernatant was recovered by centrifugation (15,000*g*, 4°C and 15 min) and the pellet was re-extracted twice more with 300 µL Type I water. The three supernatant fractions were pooled and the total extract was passed through a 3 kDa centrifugal filter (regenerated cellulose Amicon® Ultra filter units, Merck) at 15000*g* for 1 h. The filtrate was concentrated under vacuum until dry with a SpeedVac (RVT4104 speed-vac and SPD111V centrifugue, Thermo Fisher, Waltham, MA, USA). The residue was dissolved in 5 µL Type I water, diluted with 10 µL 50 mM EDTA, 15 µL Type I water and 30 µL mobile phase A (see below) and filtered through PVDF 0.45 µm ultrafree-MC centrifugal filter devices (Durapore, Merck) before injecting into the HPLC-ESI-MS(TOF) instrument.

In the case of the tomato plant fluids, samples were filtered through 10 kDa cellulose centrifugal filters (Microcon 10 Ultracel YM-10, Millipore). Then, 5 µL of the filtrate were diluted with 10 µL 50 mM EDTA, 6 µL Type I water, 9 µL of NL 1 mM and 30 µL mobile phase A (see below) to a final volume of 60 µL (the final concentrations of NL and EDTA were 150 µM and 8.3 mM, respectively), incubated for 24 h and filtered through PVDF 0.45 µm ultrafree-MC centrifugal filter devices (Durapore, Merck) before injection.

Chromatography was carried out using the Alliance 2795 Separation Module (Waters) equipped with a reversed phase SeQuant ZIC®-HILIC 150x1 mm column with a 5 µm particle size (Merck). The sample injection volume was 10 µL. The elution program consisted in a gradient built with solvents A (90% acetonitrile and 10 mM ammonium acetate in water, pH 7.3) and B (20% acetonitrile and 30 mM ammonium acetate in water, pH 7.3) as shown in Fig. 3.9.

The original method of Xuan *et al*. (2007), originally developed for the determination of metal ligand complexes, was modified for the quantitation of metal ligands and the total run time was decreased to 35 min. Detection was made in negative mode in the 150 to 700

m/z mass range. ESI-MS(TOF) conditions were optimized for the $[M-H]^-$ ions of NA and DMA (*m/z* values of 302.134 and 303.146, respectively) using direct injections of 100 µM standard solutions with a flow of 180 µL h^{-1} (Table 3.5). A typical chromatogram obtained by this method is shown in Figure 3.10.

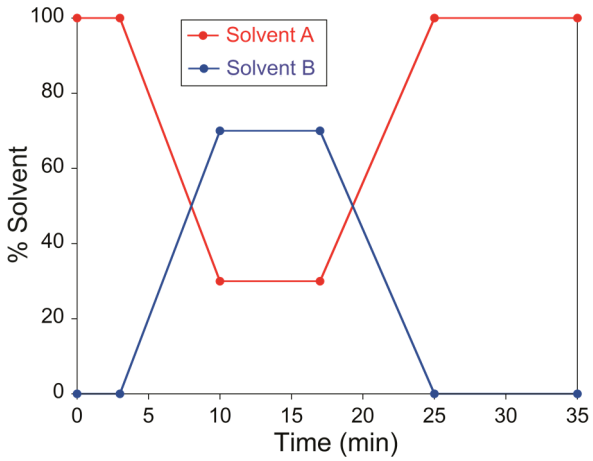

Fig. 3.9. Gradient used for the separation of NA, DMA and NL.

Solvent A: 90% acetonitrile and 10 mM ammonium acetate in water, pH 7.3
Solvent B: 20% acetonitrile and 30 mM ammonium acetate in water, pH 7.3

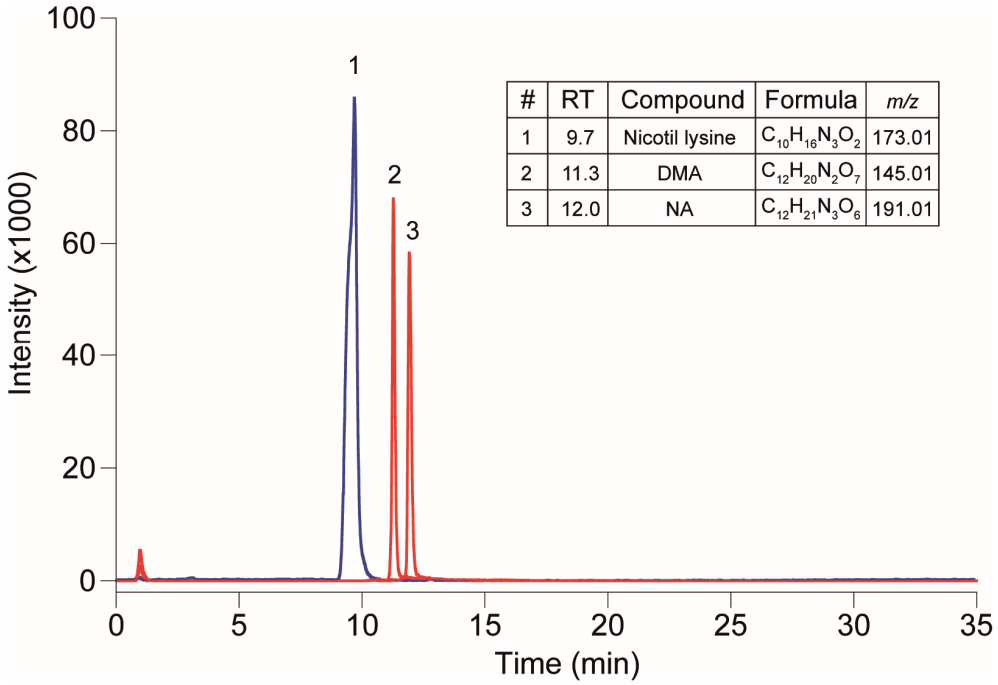

#	RT	Compound	Formula	*m/z*
1	9.7	Nicotil lysine	$C_{10}H_{16}N_3O_2$	173.01
2	11.3	DMA	$C_{12}H_{20}N_2O_7$	145.01
3	12.0	NA	$C_{12}H_{21}N_3O_6$	191.01

Fig. 3.10. HPLC-ESI-MS(TOF) chromatogram of a mixture of NL (1), DMA (2) and NA (3) standards. Concentrations were 150 µM for NL and 50 µM for NA and DMA. Chromatogram traces correspond to the $[M-H]^- \pm 0.02$ *m/z* of each analyte. The Table in the inset shows RT, compound, molecular formula and theoretical *m/z* of NL, NA and DMA

Table 3.5. Operating conditions of the time-of-flight (TOF) mass spectrometer (MS) used for NA and DMA determinations

Source	Electrospray
Polarity	Negative
Endplate voltage	-0.5 kV
Spray tip voltage	3.0 kV
Orifice voltage	107 V
Nebulizer gas	N_2
Nebulizer gas pressure	2.0 bar
Drying gas	N_2
Drying gas flow rate	8.5 L min^{-1}
Drying gas temperature	180°C

3.8. Localization of metals in rice seed sections

3.8.1. Preparation of rice seed sections

Thin sections (50-70 µm-thick) were obtained from fully developed rice seeds of the different genotypes with a vibratome VT1000S (Leica) (Fig. 3.11), following the protocol described by Johnson *et al*. (2011). Seeds were glued (with Loctite Super Glue-3, Barcelona, Spain) to a plastic support (the excised top of a 1.5 mL Eppendorf tube). The blades used were Chrome Platinum (Bic, Clichy, France). Different displacement blade speeds and vibrating frequencies were tried until optimal sections were obtained, trying to minimize as much as possible seed pulverization and/or rupture. Final parameters used were a blade movement speed of 0.2 mm s^{-1} and a vibration frequency of 70 Hz. A 100 µm-thick Kapton polyimide film (DuPont, Des Moines, USA) was used to hold the tissue section as cutting proceeded to avoid fragmentation (Johnson *et al*., 2011).

Fig. 3.11. Leica VT1000S vibratome

Sections obtained were transferred to Synchrotron Adhesive Tape (Leica) attached to glass slides and stored until laser ablation (LA) analysis. The sections were observed with a stereomicroscope (MZ16, Leica) and images were taken with the Leica Application Suite V3.5. Other sections were placed on glass slides and used to localize Fe using Perls staining (see below).

3.8.2. Quantitative elemental maps using LA-ICP-MS

Rice seed sections (*ca.* 60 µm-thick) placed in Synchrotron Adhesive Tape were analyzed by *Laser Ablation* (LA) coupled to ICP-MS at the Analytical Chemistry Department of the University of Oviedo, in collaboration with Dr. Beatriz Fernández. This technique allows the vaporization of the sample with a laser pulse (LSX-213, Cetac Technologies, Omaha, USA), with compounds being directly transported by means of a gas flow to an ICP-MS device (Element II, Thermo Fisher) to determine the elemental composition. The intensity of the signal obtained for each element was normalized using ^{13}C. Quantitative elemental maps were obtained using rice flour standards *NIST 1568b* (National Institute of Standards and Technology, USA) and *NCS ZC73028* (LGC Standards, UK) for the calibration curves. Two-dimensional images of the elemental distributions in seed sections were created using the software packages Origin® (OriginLab, Northampton, USA) and ImageJ (NIH, Bethesda, USA).

LA settings were optimized for the rice seed sections as follows: a first study was made to determine the optimal laser beam spot diameter by running two parallel lines across seed embryos, a first one with a 10 µm laser spot diameter and a second one with a 25 µm laser spot diameter, and intensities obtained for ^{56}Fe were compared. Intensities obtained for the 25 µm diameter spot were one order of magnitude larger than those obtained with the 10 µm diameter one (Fig. 3.12). Therefore, a spot diameter of 25 µm was selected, since it gave a high intensity without a major loss in spatial resolution. The final conditions used with rice seed sections (after optimization) for the LA and ICP-MS devices are summarized in Table 3.6.

When using this technique, a compromise between the area to study and the resolution to obtain is required, with higher resolutions implying slower scan speeds and longer analysis times. A full LA analysis of a whole seed surface could not be done with this method, because the time required would have been too long. For instance, with the

conditions used (a laser spot diameter of 25 µm and a 17 µm s^{-1} laser spot speed) the time required for the analysis of a 2 mm^2 area (the approximate size of the area occupied by the embryo) would be approximately 5 h. Therefore, to determine the zones with high concentration of micronutrients analyses were carried out only in two modes: a straight line crossing the whole longitudinal section, including the embryo, endosperm and aleurone seed layer, and a line crossing the only the embryo structures (Fig. 3.13). The results for the ^{56}Fe and ^{55}Mn signals in scans using the previously determined conditions of the laser (25 µm spot, scan speed 17 µm s^{-1}) are shown in Fig 3.13 for the whole longitudinal seed section (Fig. 3.13A) and the embryo structures only (Fig. 3.13B). The intensities of both Fe and Mn confirm that micronutrients have a differential spatial accumulation in the embryo and have a low concentration in the starchy endosperm. In the latter case, intensities obtained were below the limit of detection of the technique, since only a baseline signal was detected and considered as noise. Therefore, in seed metal mapping analysis only the zone of the endosperm next to the embryo was fully scanned.

3.8.3. Qualitative iron determination using Perls

Seed sections (*ca.* 60 µm-thick) obtained with the vibratome as described above were incubated with a solution containing 2% $K_4[Fe(CN)_6]$ and 2% HCl for 15 min at room temperature. The sections were observed with a stereomicroscope (MZ16, Leica) and images were taken with the Leica Application Suite V3.5.

Table 3.6. Settings used for the Laser Ablation and Inductively Coupled Plasma Mass Spectrometry devices

LA System	**Teledyne Cetac LSX-213**	**ICP-MS**	**Thermo Element 2**
Laser energy	100% (~5.6 mJ)	RF Power	1330 W
Repetition rate	20 Hz	Cooling gas	15.5 L min^{-1}
Spot diameter	25 µm	Auxiliary gas	0.8 L min^{-1}
Scan speed	17 µm s^{-1}	Nebulizer gas (Ar)	0.8 L min^{-1}
Ablation mode	single line scan	Cones	Ni (skimmer and sampler)
Carrier gas (He)	1 L min^{-1}	Isotopes	^{13}C, ^{31}P, ^{32}S, ^{55}Mn, ^{56}Fe, ^{63}Cu, ^{64}Zn
Cryogenic cell T	-20° C	Sample time	5 ms
		Mass window	100%
		Samples per peak	10

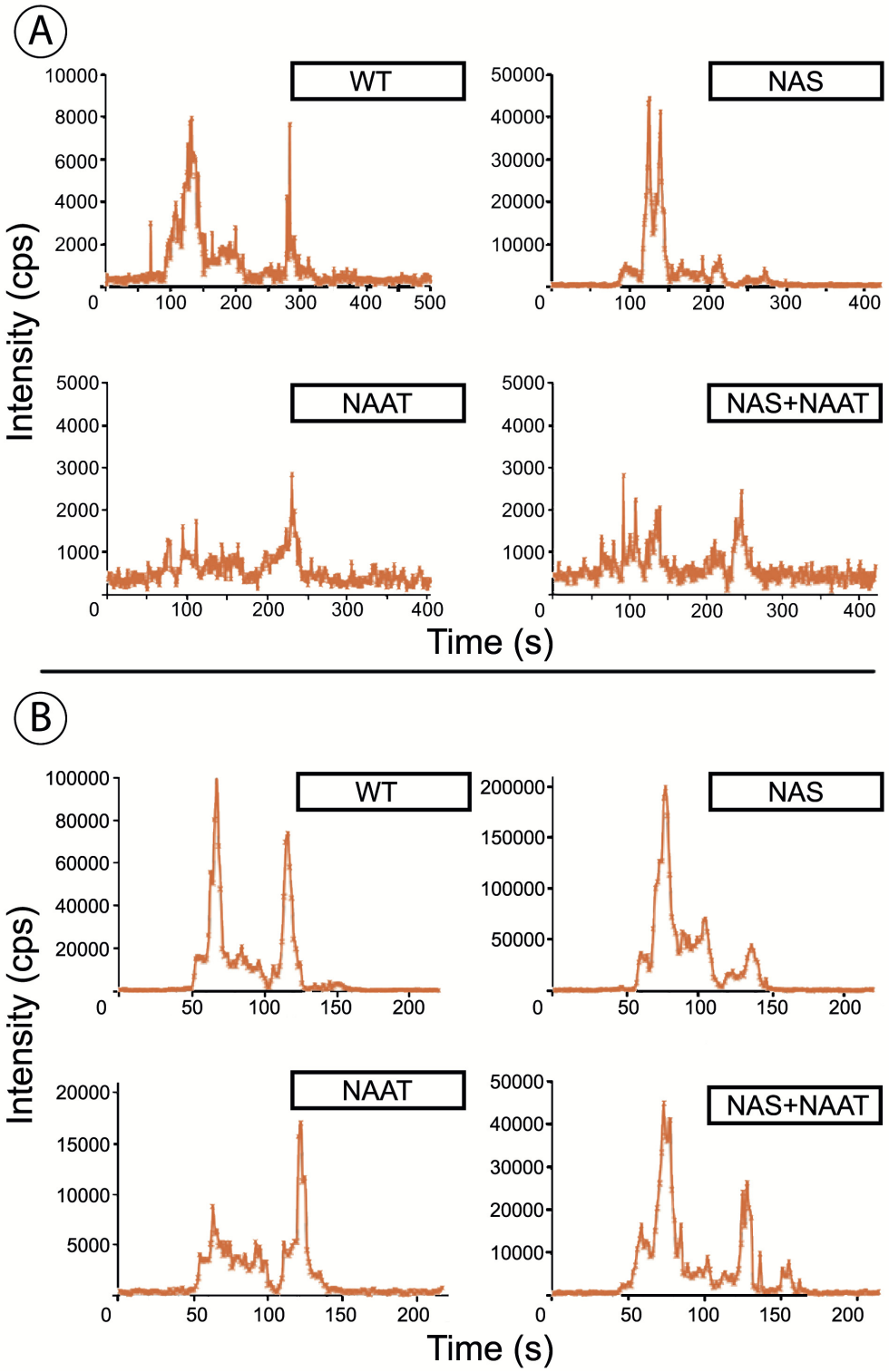

Fig. 3.12. ICP-MS signal intensity for ^{56}Fe (in counts per second, cps) in seeds of different rice genotypes obtained with laser spot diameters of 10 (A) and 25 µm (B). Parallel lines for each laser spot diameter were run adjacently in the same seed to minimize variability

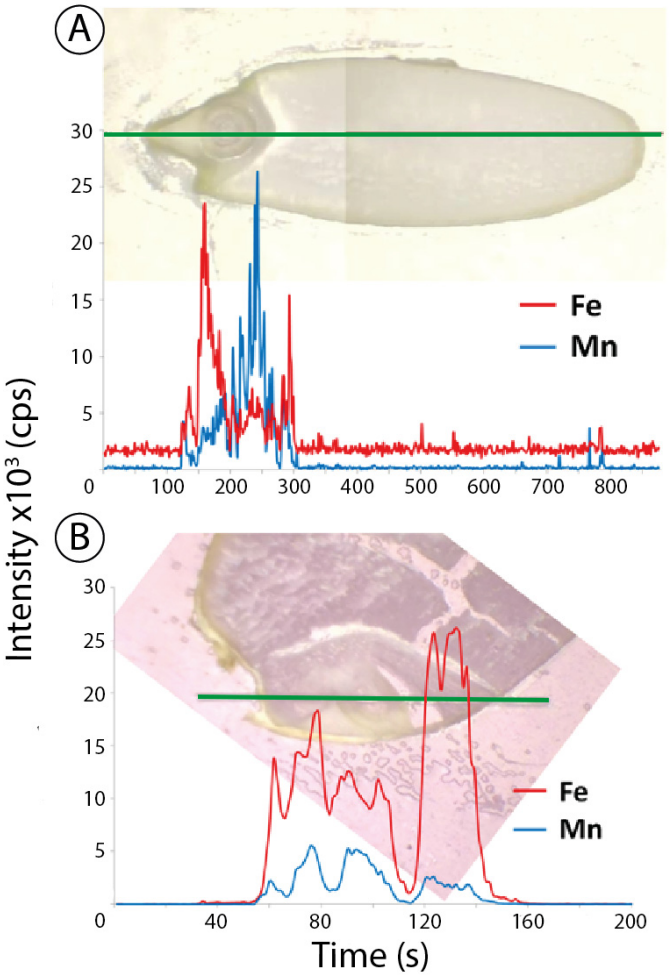

Fig. 3.13. ICP-MS ^{56}Fe and ^{55}Mn signal intensities (in *cps*) for scans across the longitudinal section of the seed (A) and along the embryo structures (B)

3.9. Statistical analysis

Statistical analysis was carried out using IBM SPSS Statistics v. 22 (New York, USA). Data for tomato were analyzed using an ANOVA test ($p < 0.05$) for the different treatments at a given time (*e.g.*, +Fe *vs.* -Fe *vs.* Fe resupply at 0 hours) and for a given treatment at different times. Then, a comparison of means was carried out using Tukey's or Games-Howell's tests, depending on Levene test for variance homogeneity ($p < 0.05$).

Rice data (NA, DMA and metal micronutrients) were analyzed using an ANOVA test ($p < 0.05$), comparing genotypes (*OsNAS1* and *HvNAATb* overexpressors) or treatments (in the case of the *Osfrdl1* rice experiments) with the WT in control conditions. Then, a comparison of means was carried out using Tukey's or Games-Howell's tests, depending on Levene test for variance homogeneity ($p < 0.05$).

Chapter 4

Results

Section 4.1

Objective 1 Results

Effects of iron status on the concentrations of metal micronutrients, nicotianamine and carboxylates in tomato plant fluids

In this chapter the concentrations of different organic compounds and metal micronutrients related to Fe transport are shown for different compartments (root and leaf apoplastic fluids and symplastic extracts, as well as and xylem sap) in a time-course experiment with tomato plants cv. FER with different Fe supply. These treatments included conditions of Fe-sufficiency (+Fe), Fe-deficiency (-Fe) and Fe resupply after a Fe-deficiency treatment (-Fe*). Before Fe resupply, root FCR was primed using low concentration Fe pulses to increase Fe acquisition rates of -Fe plants and to obtain fluids with a high Fe concentration (see Section 3.3).

4.1.1. Effects of iron deficiency on leaf Chl levels

A few days after imposing the Fe-deficiency treatment, tomato plants developed the first visible symptoms. The most visible indicator of deficiency, the *leaf iron chlorosis*, appeared 4 days after imposing Fe-deficiency, and was intense at day 11 (Fig. 4.1).

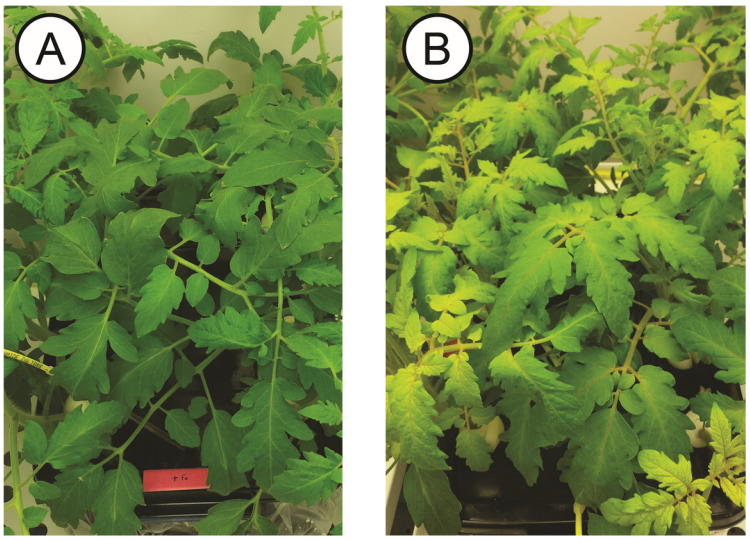

Fig. 4.1. Tomato plants after 11 days of growth. *A*, Fe-sufficient plants; *B*, Fe-deficient plants.

This was accompanied by decreases in leaf SPAD readings (which is a proxy for chlorophyll concentration) when compared to the values found in leaves of Fe-sufficient plants. The time-course evolution of the SPAD values with the different treatments is shown in Fig. 4.2. Iron sufficient leaves (young and developed) showed no changes during the treatment, with chlorophyll values being between 40 and 50 SPAD units (Fig. 4.2; values shown include those of young and developed leaves because there were no significant differences between them).

In the case of Fe-deficient leaves, the SPAD levels decreased progressively both in young and developed leaves, with the lowest values being found in the young ones. When the nutrient solution was supplemented with Fe pulses (of 0.5 µM Fe(III)-EDTA to boost Fe acquisition capacity (black arrows in Fig. 4.2; Zouari *et al*., 2001), no significant effects on the leaf SPAD values of the Fe-deficient plants were found (both in young and developed leaves; Fig. 4.2). Final SPAD values after 11 days in Fe-deficiency conditions were approximately 4-8 in the young leaves and 25-28 in the developed ones.

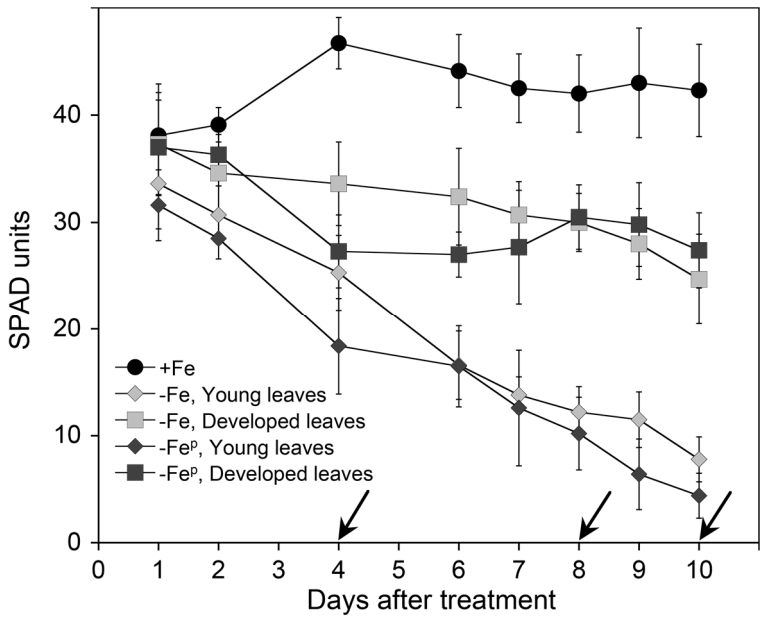

Fig. 4.2. Changes in leaf SPAD values induced by Fe deficiency in tomato FER plants. Plants were pre-grown for 14 d in nutrient solution with 45 µM Fe(III)-EDTA at pH 5.5, and then grown for 10 d with 45 µM Fe(III)-EDTA (+Fe), with 0 µM Fe (-Fe) or with 0 µM Fe but delivering 0.5 µM Fe(III)-EDTA pulses at days 4, 8 and 10 after imposing the Fe-deficiency treatment (-Fe^{p}) (Fe pulses are marked with arrows). Data are means ± SD, n = 8

4.1.2. Induction of root FCR activity with Fe pulses

The FCR activity measured at day 11 was 7.7 ± 0.8, 2.2 ± 0.1 and 55.8 ± 6.3 nmol Fe reduced g root FW^{-1} min^{-1} in Fe-sufficient, Fe-deficient and Fe-deficient plants treated with Fe pulses, respectively (Fig. 4.3). Therefore, the final reductase activities in Fe-deficient plants treated with Fe pulses was 8-fold higher than those in +Fe plants and 25-fold higher than those in -Fe plants. Values obtained were similar to those found in Zouari *et al*. (2001), where the highest FCR activity found was 50 nmol Fe reduced g root FW^{-1} min^{-1}, much higher than the maximum in the cv. "Tres Cantos" used in the preliminary experiments (7.8 nmol Fe reduced g root FW^{-1} min^{-1}, data not shown).

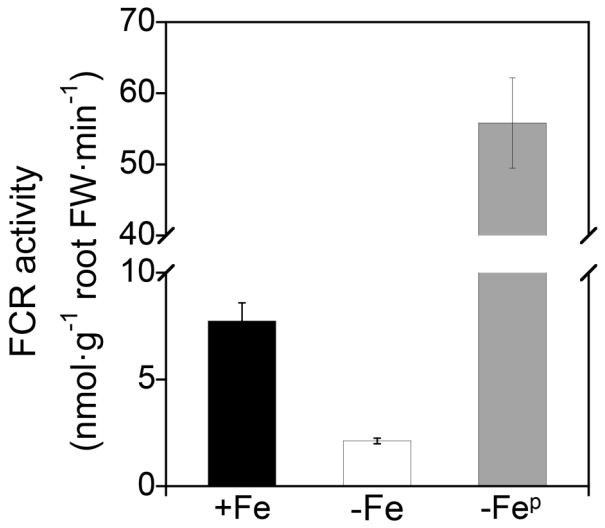

Fig. 4.3. Root FCR activity in intact FER tomato plants at day 11. Plants were grown with Fe (+Fe), without Fe (-Fe) and without Fe but treated with 0.5 µM Fe pulses to the nutrient solution (-Fe^p). Data are means ± SE, n = 4-8

4.1.3. Root and leaf fluid sampling yield

The mean volume obtained for the root apoplastic fluid was 106 ± 17 µL (mean ± SE; n = 20), whereas the root symplastic extract volume obtained was one order of magnitude larger, in the range from 2 to 4 mL (since the volume of symplastic extract obtained was quite large, only a volume range is given). Similarly, the apoplastic fluid volume recovered from leaves was 128 ± 55 µL (mean ± SE; n = 40) whereas the symplastic extract volume obtained was in the range of 0.5 to 2 mL.

The total tissue fresh weight (FW) loss is shown in Table 4.1. Therefore, the symplast extract volume accounts for a large part of the weight loss in the root and leaf tissues during extraction, whereas the apoplastic fluid accounts only for a low fraction of the total.

Table 4.1. Initial and final fresh weight (FW, in g) and weight loss (in %) in roots and leaves after the extraction of the apoplastic fluid and the symplastic soluble fraction. Data are means ± SE, n = 20 for roots and n = 30 for leaves

	Roots	**Leaves**
Initial FW (g)	8.85 ± 0.98	3.45 ± 1.01
Final FW (g)	4.21 ± 0.84	2.13 ± 0.78
Total FW loss (%)	57 ± 5	39 ± 8

4.1.4. Changes in metal micronutrient concentrations in plant fluids

Data on metal concentrations are shown below in Figures 4.4-4.7 and in Tables 4.2-4.5 (statistical significances at $p \leq 0.05$ are shown only in the Tables for easy reading of the Figures), and are described in the next subsections according to the plant tissues (roots, xylem sap and leaves). In all cases, data shown are for Fe-sufficient (+Fe), Fe-deficient (-Fe) and Fe-resupplied plants (thereafter called -Fe*). In the latter case, tomato plants having experienced the 0.5 μM Fe(III)-EDTA pulses described above were fully resupplied with Fe at day 11 *via* a complete replacement of the nutrient solution with 45 μM Fe(III)-EDTA. In the figures, the light and dark periods in the growth chamber are indicated in the X-axis.

All apoplastic fluid and xylem sap samples analyzed have little contamination by symplastic components as judged by the results of the *c-mdh* assay (values in the analyzed fluids were < 3% of the *c-mdh* activities present in the extracts of the same tissues and treatments).

4.1.4.1. Root apoplastic fluid and symplastic extract

The root, as the entrance point of micronutrients from the growth medium, is prone to undergo changes upon Fe resupply. The time course changes in the concentrations of Fe, Mn, Cu and Zn in the root apoplastic fluid and the symplast extract in the treatments studied are shown in Figure 4.4 and Table 4.2.

Root apoplastic fluid

Fe

The initial Fe concentration in the root apoplastic fluid of Fe-sufficient plants (+Fe) was 281 μM (this was 3 days after a full nutrient solution change). Then, the Fe concentration decreased significantly to 166 and 89 μM after 12 and 48 h, respectively. On the other hand, the Fe deficient plants (-Fe) always had very low Fe concentrations (≤ 35 μM), with no significant changes between sampling times. Iron resupply induced a large increase of Fe concentration in the root apoplastic fluid, rising 9- and 24-fold with respect to the initial value after 12 h and 24 h, respectively. This increase was transient, and after 48 h the Fe concentration in the Fe-resupply treatment went down by 72% (to *ca*. 111 μM), to values close to those found in the Fe-sufficient control values at this time sampling.

Regarding differences between treatments, the Fe concentration was significantly higher in the root apoplastic fluid of +Fe plants than that of -Fe plants with the exception of the 24 h samples. The Fe concentrations in the Fe-resupplied plants were similar to those of the +Fe plants at 12 and 48 h but much higher at 24 h.

Mn

The Mn concentration in root apoplastic fluid ranged from 47 to 220 µM in all treatments. Significant decreases in Mn concentration with time were found in +Fe plants (with a 34% decrease after 12 h), in -Fe plants (a 62% decrease from 12 to 24 h) and in Fe-resupplied plants (-Fe*) (a 72% decrease after 12 h). When comparing treatments, the -Fe plants showed the highest Mn concentrations at 12 h, whereas the lowest were in the Fe-resupplied plants at 12 and 48 h.

Cu

The Cu concentrations did not have major changes with treatments or time, and were in a range between 9 and 33 µM in the root apoplastic fluid. The only significant Cu concentration changes were found in the -Fe plants: they were lower at 48 h than at 12 and 24 h. No significant differences were found when comparing treatments at any sampling time in the apoplastic fluid of roots.

Zn

The root apoplastic fluid Zn concentration was between 28 and 75 µM in all treatments, with only minor changes with time. The only significant changes were for +Fe and Fe-resupplied plants (-Fe*), which showed a 2-fold increase from 0 to 48 h. When comparing treatments, the Zn concentration was similar in all sampling times with the exception of those in the Fe-resupplied plants (-Fe*), which were significantly higher than those in the +Fe and -Fe treatments at 24 and 48 h, respectively.

Root symplastic extract

Fe

In the root symplastic extract, the Fe concentration was generally lower than that in the apoplastic fluid, in the range of 135 µM at 0 h (3 days after a nutrient solution change) to 57 µM in +Fe plants at 48 h, and consistently below 24 µM in -Fe plants (Figure 4.4 and Table 4.2). In the Fe-resupplied plants (-Fe*), the Fe concentration in the symplastic extract increased significantly after 12 h (22-fold, up to 141 µM), and then decreased significantly

from 24 to 48 h by 40%, to reach final values of 74 µM, values similar to those found in +Fe plants at this sampling time.

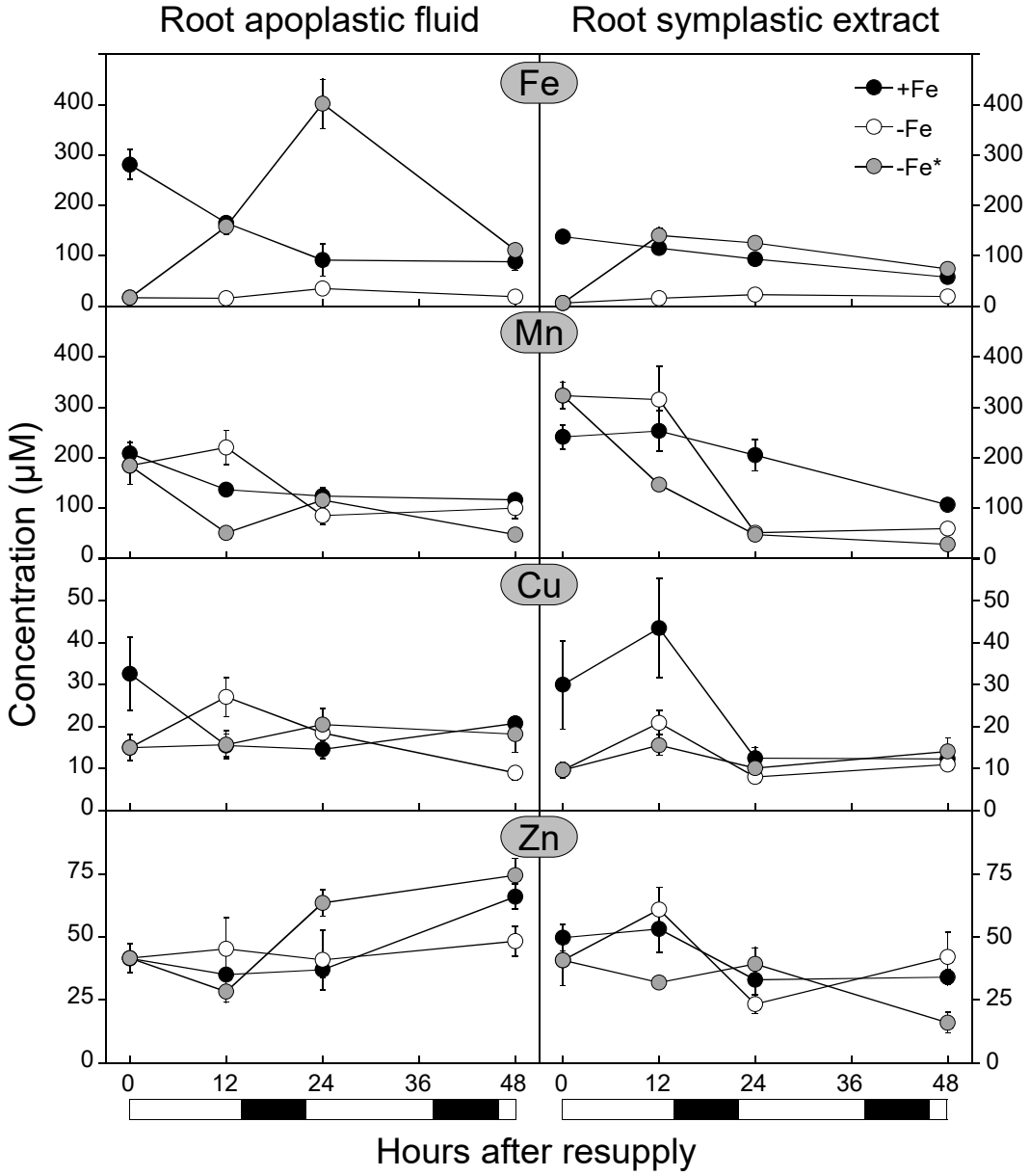

Fig. 4.4. Concentrations of Fe, Mn, Cu and Zn in the root apoplastic fluid and root symplastic extracts of tomato plants as affected by Fe deficiency and resupply. Plants were pre-grown for 14 d in nutrient solution with 45 µM Fe(III)-EDTA at pH 5.5, and then grown for 11 d with 45 µM Fe(III)-EDTA (+Fe), with 0 µM Fe (-Fe) or with 0 µM Fe but delivering 0.5 µM Fe(III)-EDTA pulses at days 4, 8 and 10 after imposing the Fe-deficiency treatment (-Fe*). Then, on day 11, a group of -Fe* plants were moved to nutrient solution containing 45 µM Fe(III)-EDTA (-Fe*, Fe resupply). Samples were taken at 0, 12, 24 and 48 h after the start of the Fe-resupply experiment. White and black boxes indicate light and dark periods, respectively. Data are means ± SE, n = 4-8

Table 4.2. Concentrations of Fe, Mn, Cu and Zn in root apoplastic fluid and symplastic extract in Fe-sufficient (+Fe), Fe-deficient (-Fe) and Fe-resupplied (-Fe*) plants at different sampling times (0, 12, 24 and 48 h). Groups were made based in Tukey or Games-Howell test (according to variance homogeneity test) with $p < 0.05$. Capital letters represent groups between different treatments at the same hour (rows) whereas lower case letters indicate groups of the same treatment at different hours (columns). Data are means SE, n = 4-8

	Root apoplastic fluid						Root symplastic extract					
Time (h)	**+Fe**		**-Fe**		**-Fe***		**+Fe**		**-Fe**		**-Fe***	
					Fe							
0	281.2 ± 30.0	B c	16.8 ± 3.2	A a	16.8 ± 3.2	A a	135.1 ± 11.8	B b	6.3 ± 1.4	A a	6.3 ± 1.4	A a
12	165.6 ± 3.8	B b	15.8 ± 4.2	A a	158.0 ± 14.7	B b	115.3 ± 6.9	B b	15.8 ± 3.4	A a	140.5 ± 15.4	B c
24	91.7 ± 31.6	A ab	35.0 ± 7.3	A a	402.2 ± 48.7	B c	93.6 ± 10.2	B ab	23.1 ± 2.6	A a	125.5 ± 8.8	C c
48	88.5 ± 17.6	B a	19.0 ± 3.2	A a	111.2 ± 11.6	B b	57.4 ± 5.1	B a	19.4 ± 5.9	A a	74.1 ± 10.6	B b
					Mn							
0	208.6 ± 22.7	A b	184.2 ± 37.0	A ab	184.2 ± 37.0	A b	241.3 ± 23.8	A b	323.4 ± 26.9	A b	323.4 ± 26.7	A c
12	136.8 ± 11.0	B a	220.3 ± 34.6	C b	50.7 ± 5.7	A a	253.3 ± 39.3	B b	315.4 ± 65.9	AB b	146.7 ± 11.2	A b
24	123.7 ± 17.2	A a	84.8 ± 17.7	A a	116.0 ± 21.6	A ab	205.3 ± 30.7	B b	51.1 ± 11.8	A a	47.5 ± 11.5	A a
48	116.4 ± 6.15	B a	99.7 ± 20.5	B a	47.4 ± 11.9	A a	106.5 ± 10.8	C a	59.1 ± 10.3	B a	27.9 ± 4.6	A a
					Cu							
0	32.6 ± 8.8	A a	15.0 ± 3.1	A ab	15.0 ± 3.1	A a	30.0 ± 10.5	A a	9.7 ± 1.8	A a	9.7 ± 1.8	A a
12	15.5 ± 2.7	A a	27.1 ± 4.7	A b	15.7 ± 3.3	A a	43.5 ± 11.8	A a	20.9 ± 2.9	A b	15.6 ± 2.5	A a
24	14.6 ± 2.1	A a	18.5 ± 1.7	A b	20.4 ± 3.8	A a	12.5 ± 2.6	A a	8.0 ± 0.4	A a	10.1 ± 2.6	A a
48	20.8 ± 1.4	A a	9.0 ± 1.6	A a	18.2 ± 4.2	A a	12.3 ± 0.9	A a	11.0 ± 1.1	A a	14.1 ± 3.2	A a
					Zn							
0	41.5 ± 2.5	A a	41.5 ± 5.8	A a	41.2 ± 5.8	A a	49.7 ± 5.4	A a	40.7 ± 10.1	A ab	40.7 ± 10.1	A b
12	35.0 ± 2.1	A a	45.3 ± 12.5	A a	28.3 ± 4.3	A a	53.2 ± 9.3	A a	60.9 ± 8.9	A b	31.8 ± 1.7	A b
24	37.0 ± 3.1	A a	40.9 ± 12.0	AB a	63.5 ± 5.3	B ab	33.0 ± 7.3	A a	23.3 ± 3.6	A a	39.3 ± 6.5	A b
48	66.0 ± 4.8	AB b	48.3 ± 5.9	A a	74.5 ± 6.8	B b	34.0 ± 3.1	B a	42.1 ± 10.0	AB ab	15.9 ± 4.1	A a

Regarding treatments, +Fe plants showed higher symplastic extract Fe concentration than -Fe plants at all sampling times, whereas the Fe-resupplied plants (-Fe*) showed the highest Fe concentration at 24 h.

Mn

The Mn concentration in the root symplastic extract decreased by 56% in +Fe plants in the final 48 h sampling, whereas in -Fe plants a decrease of 84% was found from 12 to 24 h. In the Fe-resupplied plants (-Fe*) significant decreases in root symplastic extract Mn concentration (by 55 and 85%) were found after 12 and 24 h, respectively, when compared with the initial concentration.

Regarding treatments, the highest Mn concentrations in root symplastic extract were found in the +Fe plants at 24 and 48 h, whereas the lowest was found in Fe-resupplied plants (-Fe*) at 48 h. The Mn concentration in -Fe plants at 48 h was lower than in +Fe plants.

Cu

The Cu concentrations in the root symplastic extract did not have major changes with treatments or time, and were in a range between 8 and 44 μM. The only significant change was found in the -Fe plants: they were larger at 12 h than at the other sampling times.

No significant differences were found when comparing treatments at any sampling time in the symplastic extract of roots.

Zn

In the root symplastic extract, the Zn concentration showed little changes with time or treatment, and were in the range from 16 to 61 μM in all treatments. The only significant Zn concentration changes were found in the -Fe plants, which was decreased by 61% from 12 to 24 h, and in the Fe-resupplied plants (-Fe*), which showed a 60% reduction from 24 to 48 h.

When comparing treatments, only the +Fe plants at 48 h showed a significantly higher Zn concentration than that in the Fe-resupplied plants (-Fe*).

4.1.4.2. Xylem sap

The metal micronutrients concentrations in the xylem sap of the different treatments and times are shown in Figure 4.5 and Table 4.3.

Fe

The Fe concentration was not significantly different in the +Fe plants and the -Fe ones (values in the ranges 17-32 and 9-15 µM, respectively). Iron resupply led to a large increase in xylem sap Fe concentration: values were 9- and 13-fold higher after 12 and 20 h, respectively, when compared to those at 0 h. After that, Fe concentrations were lower in samples taken in the light than in those taken in the dark: 60% decreases occurred between 20 and 24 h, and between 44 and 48 h. The final Fe concentration at 54 h was 53 µM. Regarding treatments, the -Fe* plants had the highest values at 12 and 24 h.

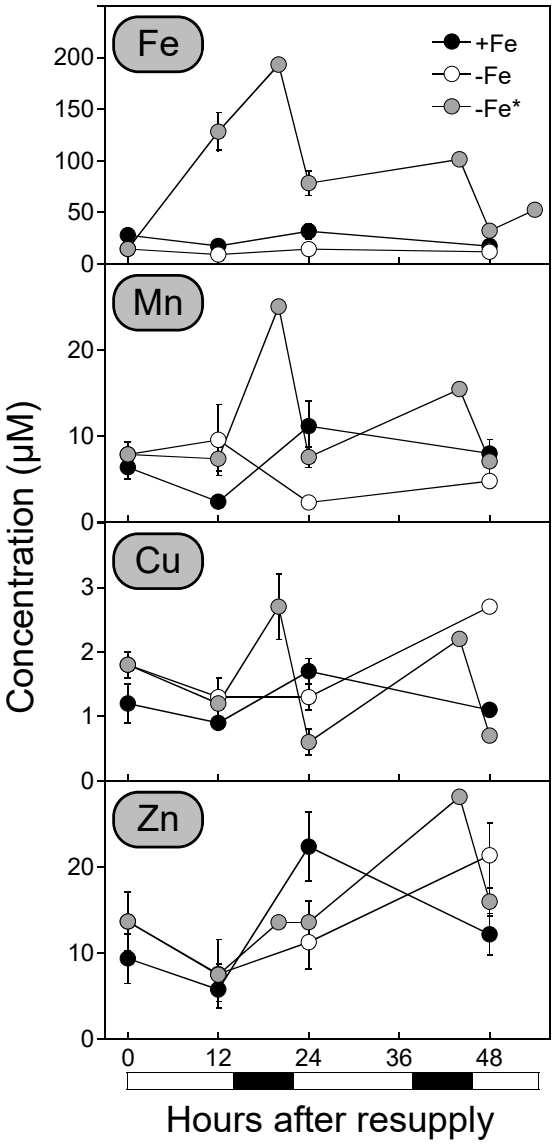

Fig. 4.5. Concentrations of Fe, Mn, Cu and Zn in the xylem sap of tomato plants as affected by Fe deficiency and resupply. Treatments were as described in Fig. 4.4. Data are means ± SE, n = 2-10

Mn

The xylem sap Mn concentrations in both the +Fe and -Fe plants were in the range from 2 to 11 µM. In the case of Fe-resupplied plants (-Fe*) they also had a similar Mn concentration, approximately 7-8 µM, at sampling times 0, 12, 24 and 48 h. However, higher Mn concentrations, 25 and 15 µM, were observed at times 20 and 44 h, respectively.

Cu

The Cu concentration in xylem sap was always below 3 µM, with +Fe and -Fe plants showing a quite stable concentration, lower than 2 µM, at all sampling times, with the only exception of the -Fe plants at 48 h, which reached 2.7 µM (a 2-fold increase in relation to -Fe plants at 12-24 h). Comparing treatments, the -Fe* plants had at 24 h lower values than those of the +Fe plants and at 48 h lower values than those of the -Fe plants.

Zn

The Zn concentration in xylem sap was in the range 5 to 22 µM in +Fe and -Fe plants. In the +Fe plants, a 4-fold increase in the Zn concentration was found from 12 to 24 h. No significant differences in Zn concentration were found between treatments at any of the sampling times studied.

Table 4.3. Concentrations of Fe, Mn, Cu and Zn in the xylem sap of Fe-sufficient (+Fe), Fe-deficient (-Fe) and Fe-resupplied (-Fe*) plants at different sampling times (0, 12, 24 and 48h in +Fe and -Fe plus 20 and 44 h in -Fe*). Groups were made based in Tukey or Games-Howell test (according to variance homogeneity test) with $p < 0.05$. Capital letters represent groups between different treatments at the same hour (rows) whereas lower case letters indicate groups of the same treatment at different hours (columns). Data are means ± SE, n = 2-10 with the exception of -Fe* 44 h, which was only 1. *n.d., not determined*

Time (h)	+Fe		-Fe		-Fe*	
			Fe			
0	27.9 ± 6.1	A a	14.5 ± 4.4	A a	14.5 ± 4.4	A a
12	17.4 ± 5.7	A a	9.2 ± 3.6	A a	128.3 ± 18.3	B c
20	n.d.		n.d.		193.2 ± 4.5	d
24	31.7 ± 7.4	A a	14.4 ± 3.1	A a	78.3 ± 12.0	B c
44	n.d.		n.d.		101.3	
48	17.3 ± 2.9	A a	11.8 ± 5.8	A a	32.2 ± 5.4	A a
54	n.d.		n.d.		52.5 ± 5.1	b
			Mn			
0	6.4 ± 1.4	A b	7.9 ± 1.4	A b	7.9 ± 1.4	A a
12	2.4 ± 0.3	A a	9.6 ± 4.1	AB ab	7.4 ± 1.4	B a
20	n.d.		n.d.		25.1 ± 0.7	b
24	11.2 ± 2.9	B b	2.3 ± 0.4	A a	7.6 ± 1.2	B a
44	n.d.		n.d.		15.5	
48	8.0 ± 1.6	A b	4.8 ± 0.8	A ab	7.1 ± 1.6	A a
			Cu			
0	1.2 ± 0.3	A a	1.8 ± 0.2	A ab	1.8 ± 0.2	A c
12	0.9 ± 0.1	A a	1.3 ± 0.3	A a	1.2 ± 0.2	A b
20	n.d.		n.d.		2.7 ± 0.5	c
24	1.7 ± 0.2	B a	1.2 ± 0.2	AB a	0.6 ± 0.2	A a
44	n.d.		n.d.		2.2	
48	1.1 ± 0.1	A a	2.7 ± 0.1	B b	0.7 ± 0.1	A a
			Zn			
0	9.4 ± 2.9	A a	13.7 ± 3.4	A a	13.7 ± 3.4	A ab
12	5.8 ± 1.4	A a	7.6 ± 4.0	A a	7.5 ± 1.3	A a
20	n.d.		n.d.		13.6 ± 0.2	b
24	22.4 ± 4.0	A b	11.3 ± 3.1	A a	13.6 ± 2.5	A ab
44	n.d.		n.d.		28.2	
48	12.2 ± 2.4	A ab	21.4 ± 3.8	A a	16.0 ± 1.7	A b

4.1.4.3. Leaf apoplastic fluid

The metal micronutrients concentrations in leaf apoplastic fluid of young and developed leaves of the different treatments and times are shown in Figure 4.6 and Table 4.4.

Fe

The leaf apoplastic fluid Fe concentration in +Fe plants was in the range 4-16 μM in young leaves, with the highest concentration found at 12 hours (16 μM, a 4-fold increase in relation to the 0 h Fe concentration), and in the range 17-20 μM in developed leaves (no significant changes were found in this case). In -Fe plants, the Fe concentration in young leaves was similar to those in the +Fe plants, 5-11 μM, whereas in the developed leaves the Fe concentration was generally lower than those in the +Fe plants (8-15 μM). The only significant difference with time in -Fe leaves was a decrease by 47% at 12 h in the developed leaves. Iron resupply (-Fe*) led to a 2-fold increase in leaf apoplastic fluid Fe concentration after 24 h in young leaves, whereas in developed leaves the increase was by 67% and was detected at 12 h. After this Fe concentration peak, the Fe concentration in Fe-resupplied plants decreased towards control levels in young leaves (*ca.* 11 μM) and to even lower concentrations than those in +Fe plants in developed leaves (*ca.* 9 μM).

Regarding treatments, significantly higher Fe concentrations were found in +Fe plants in young and developed leaves at 48 h and in developed leaves at 24 h when compared with those in the -Fe plants. Meanwhile, the Fe-resupplied plants showed the highest concentrations at 24 h in young leaves and at 12 h in developed leaves.

Mn

The Mn concentrations in the apoplastic fluid of +Fe plants were in the ranges 5-11 and 16-45 μM in young and developed leaves, respectively. In -Fe plants, the Mn concentrations were in the ranges 4-12 and 12-44 μM in young and developed leaves, respectively. The only significant changes found for these treatments was a 2-fold increase in Mn concentration in young +Fe leaves from 12 to 48 h, a 3-fold Mn concentration increase in developed leaves of +Fe plants from 0 to 12 h, and a 70% decrease in developed leaves of -Fe plants from 0 to 24 h. In the apoplastic fluid of Fe-resupplied plants (-Fe*) the Mn concentration in developed leaves showed a 2-fold increase at 12 h to decrease afterwards by 66%, whereas no significant effect in Mn concentrations were found in young leaves. Regarding treatments, at 0 h, the values in the developed leaves of the +Fe plants were significantly lower when compared with those of the -Fe and -Fe* treatments.

Cu

The Cu concentration was quite stable in all leaves and treatments, with most values between 1 and 5 μM. The only remarkable differences were found in developed leaves, with a 2-fold increase in Cu concentration in the +Fe plants from 0 to 24 h, a 47% decrease in the -Fe plants from 12 to 24 h, and a 40% decrease in the -Fe* plants from 0 to 12 h. Regarding treatments, the +Fe developed leaves showed higher Cu concentrations than the -Fe and -Fe* plants at 24 and 48 h.

Zn

The Zn concentration in apoplastic fluid was similar in all treatments at the start of the experiment for both leaf ages (7 and 12 μM for young leaves in the +Fe and -Fe plants, respectively; 13 and 23 μM for developed leaves in +Fe and -Fe treatments, respectively). The Zn concentration in apoplastic fluid of +Fe plants showed a 3-fold increase in both young and developed leaves after 24 h and 48 h, respectively, whereas in the -Fe plants it increased 2-fold in developed leaves from 12-24 to 48 h. In the -Fe* plants a 3-fold increase in young leaves from 12 to 24 h and a 57% decrease in developed leaves from 0 to 12 h were found. The only significant difference among treatments was found in -Fe developed leaves at 12 h, which showed a higher Zn concentration than the +Fe developed leaves.

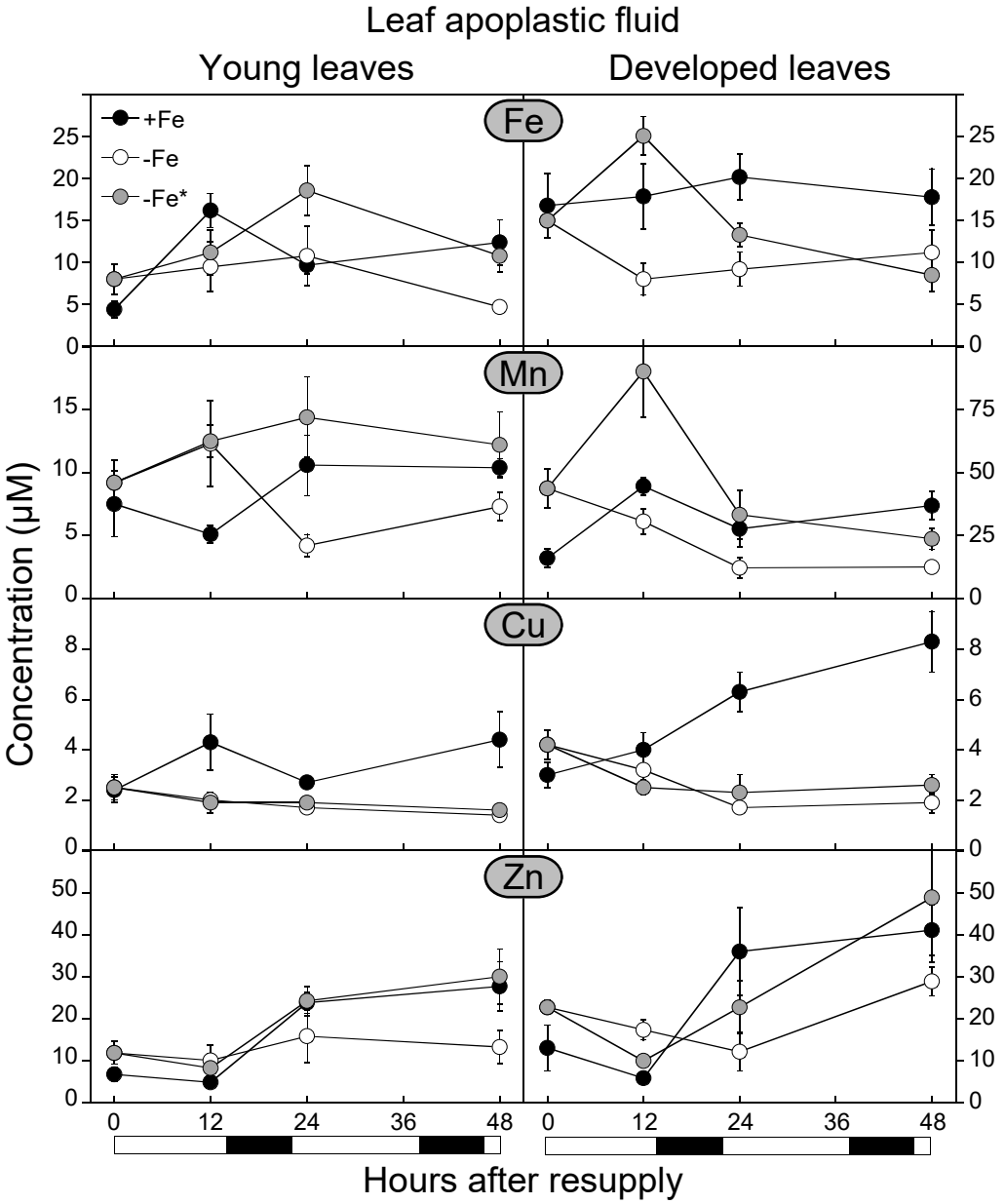

Fig. 4.6. Concentrations of Fe, Mn, Cu and Zn in the leaf apoplastic fluid of tomato plants as affected by Fe deficiency and resupply. Treatments were as described in Fig. 4.4. Leaves sampled were the 1st, 2nd and 3rd (developed leaves) and the 4th, 5th and 6th (young leaves) from the cotyledons. Data are means ± SE, n = 3-12

Table 4.4. Concentrations of Fe, Mn, Cu and Zn in leaf apoplastic fluid of young and developed leaves in Fe-sufficient (+Fe), Fe-deficient (-Fe) and Fe-resupplied (-Fe*) plants at different sampling times (0, 12, 24 and 48 h). Groups were made based in Tukey or Games-Howell test (according to variance homogeneity test) with $p < 0.05$. Capital letters represent groups between different treatments at the same hour (rows) whereas lower case letters indicate groups of the same treatment at different hours (columns). Data are means ± SE, n = 3-12

	Young leaves						Developed leaves					
Time (h)	**+Fe**		**-Fe**		**-Fe***		**+Fe**		**-Fe**		**-Fe***	
Fe												
0	4.4 ± 1.0	A a	8.0 ± 1.8	A a	8.0 ± 1.8	A a	16.8 ± 3.9	A a	15.0 ± 2.1	A b	15.0 ± 2.1	A a
12	16.2 ± 2.0	A b	9.5 ± 3.0	A a	11.2 ± 2.7	A ab	17.9 ± 3.9	AB a	8.0 ± 1.9	A a	25.0 ± 2.3	B b
24	9.7 ± 1.1	A ab	10.8 ± 3.5	AB a	18.6 ± 3.0	B b	20.2 ± 2.6	B a	9.2 ± 2.0	A a	13.3 ± 1.4	AB a
48	12.3 ± 2.7	B b	4.7 ± 0.5	A a	10.8 ± 1.9	B ab	17.8 ± 3.4	B a	11.2 ± 2.7	A ab	8.5 ± 2.0	A a
Mn												
0	7.5 ± 2.3	A ab	9.2 ± 1.8	A a	9.2 ± 1.8	A a	16.0 ± 3.8	A a	43.7 ± 7.7	B b	43.7 ± 7.7	B a
12	5.1 ± 0.7	A a	12.3 ± 3.4	A a	12.5 ± 1.3	A a	44.6 ± 3.5	A b	30.6 ± 5.0	A ab	90.2 ± 18.1	A b
24	10.6 ± 2.4	A ab	4.2 ± 0.9	A a	14.4 ± 3.2	A a	27.7 ± 7.3	A ab	12.1 ± 4.1	A a	33.3 ± 9.7	A a
48	10.4 ± 0.7	A b	7.3 ± 1.1	A a	12.2 ± 2.6	A a	36.9 ± 5.5	A b	21.2 ± 5.0	A a	23.7 ± 4.3	A a
Cu												
0	2.4 ± 0.5	A a	2.5 ± 0.5	A a	2.5 ± 0.5	A a	3.0 ± 0.5	A a	4.2 ± 0.6	A b	4.2 ± 0.6	A b
12	4.3 ± 1.1	A a	2.0 ± 0.3	A a	1.9 ± 0.3	A a	4.0 ± 0.7	A ab	3.2 ± 0.5	A b	2.5 ± 0.3	A a
24	2.7 ± 0.2	A a	1.6 ± 0.1	A a	1.9 ± 0.2	A a	6.2 ± 0.8	B b	1.7 ± 0.2	A a	2.3 ± 0.7	A a
48	4.4 ± 1.1	A a	1.4 ± 0.1	A a	1.6 ± 0.1	A a	8.3 ± 1.2	B b	1.9 ± 0.3	A a	2.6 ± 0.4	A a
Zn												
0	6.7 ± 1.7	A a	11.8 ± 2.7	A a	11.8 ± 2.7	A a	13.0 ± 5.4	A a	22.7 ± 1.7	A ab	22.7 ± 1.7	A b
12	4.8 ± 0.7	A a	10.0 ± 3.7	A a	8.2 ± 3.4	A a	5.8 ± 1.0	A a	17.3 ± 2.4	B a	9.9 ± 1.4	AB a
24	23.8 ± 2.5	A b	15.8 ± 6.3	A a	24.2 ± 3.5	A b	36.0 ± 10.4	A ab	12.1 ± 4.4	A a	22.7 ± 6.3	A ab
48	27.7 ± 5.8	A b	13.2 ± 4.0	A a	30.0 ± 6.6	A b	41.1 ± 5.9	A b	28.9 ± 3.5	A b	48.9 ± 15.5	A ab

4.1.4.4. Leaf symplastic extract

The changes in the metal micronutrient concentrations in leaf symplastic extract are shown in Fig. 4.7 and Table 4.5.

Fe

The Fe concentration in the symplast was similar in both young and developed leaves of Fe-sufficient plants (in the range 23-39 μM at all sampling times), whereas the Fe-deficient plants showed somewhat lower concentrations, between 10 and 30 μM. The Fe-resupply treatment increased the Fe concentration 3-fold over the initial values at 24 hours in young leaves. However, in the case of developed leaves the increase in Fe concentration (2-fold) was significant only at 48 h in the cases of the +Fe and -Fe* plants.

Regarding treatments, +Fe plants showed higher Fe concentrations than -Fe plants at 0 and 12 h in young leaves and at 12 and 48 h in developed leaves. The -Fe* plants had the highest values in young leaves at 24 and 48 h.

Mn

The Mn concentration in the symplastic extract was generally higher in the developed leaves than in the young ones. In the young leaves of +Fe plants Mn was in the range 31-50 μM range at all sampling times, without significant changes with time. In the developed leaves of +Fe plants, the concentration was in the 38-82 μM range, with a 2-fold increase at 24 h. In the young leaves of -Fe plants no significant changes in concentration were found (values in the range 29-41 μM), whereas in the developed leaves Mn concentrations increased significantly by 1.2-fold from 24 to 48 h. In the Fe resupplied plants (-Fe*) there was a 1.5-fold increase in Mn concentration in young leaves from 0 to 48 h, whereas in the developed leaves the Mn concentration did not change significantly in spite of the large concentration range (167-243 μM).

Regarding treatments, the Fe-resupplied plants showed the highest Mn concentration in young leaves at 48 h. In developed leaves the Mn concentration was higher in the -Fe plants than in +Fe plants in all sampling times excepting at 12 h, whereas the Fe-resupplied plants showed the highest Mn concentrations at 24 and 48 h.

Cu

The Cu concentration in the symplastic fluid of young leaves was similar in all treatments and sampling times, with levels between 15 and 36 μM. Some significant decreases in Cu concentrations were found: an increase in +Fe plants from 0 to 12 h (1.5-fold), and decreases in +Fe plants from 12 to 48 h (62%), in -Fe plants from 0 to 24 and from 24 to 48 h (by 17 and 24%, respectively), and in -Fe* plants from 0 to 24 h (by 30%). In developed leaves Cu concentrations were in the range 9-31 μM; significant changes were found in the +Fe plants, with a 1.4-fold increase at 12 h followed by a 56% decrease from 24 at 48 h, in -Fe plants, with a 52% decrease from 12 to 48 h, and in Fe-resupplied plants (-Fe*), with a 35% decrease in the 24 h value when compared to the 0 h one.

When comparing treatments, no significant differences were found in young leaves, whereas the +Fe developed leaves showed higher Cu concentration than the -Fe plants with the exception of the values at 0 h. Only at 48 h the Fe-resupplied plants (-Fe*) Cu concentration was higher than that in the -Fe plants.

Zn

The concentration of Zn was similar in the symplastic fluid in all treatments and leaf ages (22-74 μM), although some significant differences were found. In young leaves, a 2-fold increase was found from 12 to 24 h in +Fe plants and a transient decrease was found in -Fe plants from 12 to 24 h, whereas in the symplastic extract of +Fe developed leaves a 3-fold increase was found from 12 to 24 h.

Regarding treatments, in young leaves Zn concentration was the highest in +Fe plants and the lowest in -Fe plants at 24 h, whereas -Fe* plants had higher concentrations than +Fe and -Fe plants at 12 and 48 h, respectively. In developed leaves, when compared to the +Fe plants a higher Zn concentration was found in the -Fe and -Fe* plants at 0 and 12 h, whereas in the -Fe* plants at 48 h values were higher than those in the -Fe ones.

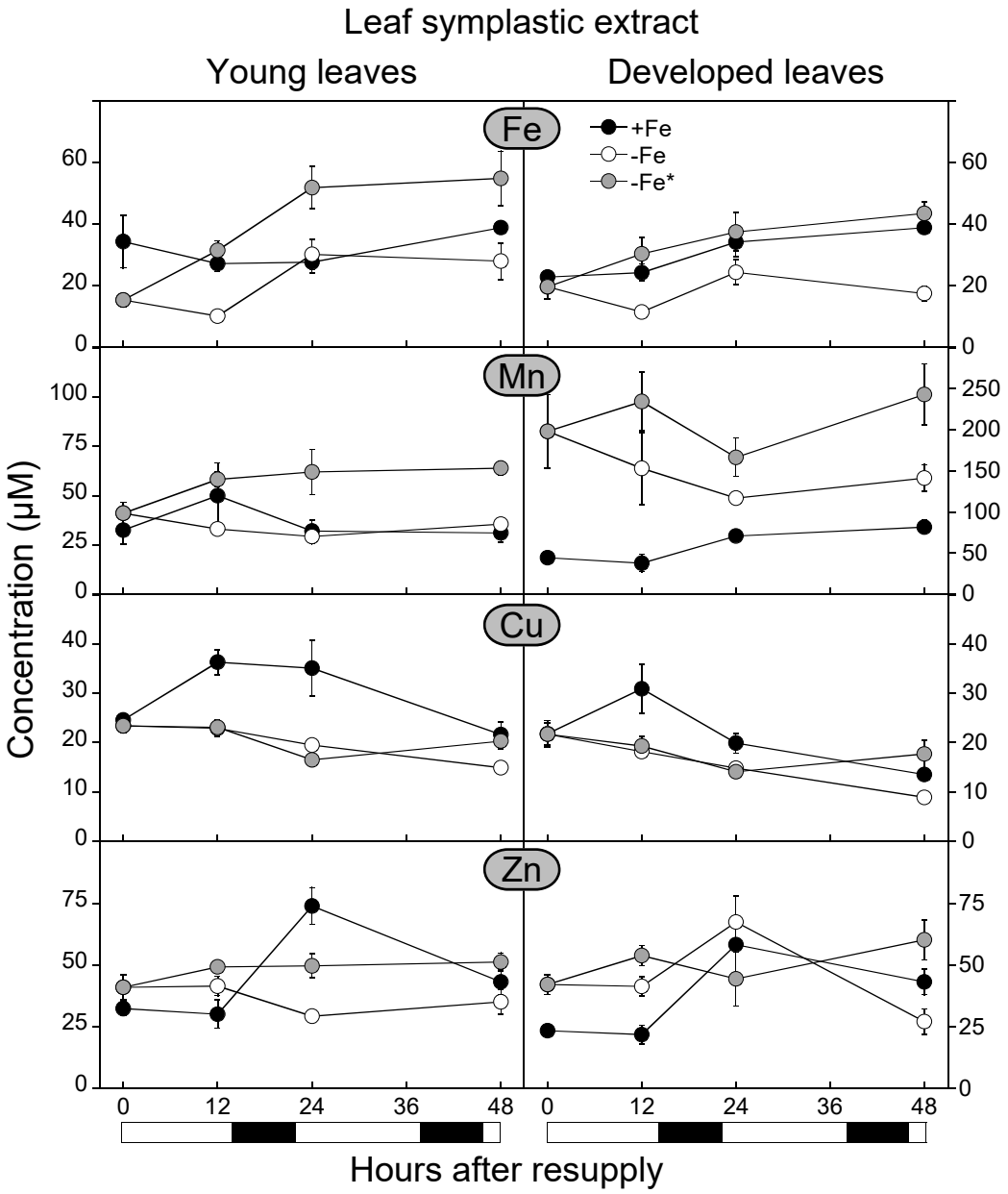

Fig. 4.7. Concentrations of Fe, Mn, Cu and Zn in the leaf symplastic extracts of tomato plants as affected by Fe deficiency and resupply. Treatments were as described in Fig. 4.4. Leaves sampled were the 1st, 2nd and 3rd (developed leaves) and the 4th, 5th and 6th (younger leaves) from the cotyledons. Data are means ± SE, n = 3-12

Table 4.5. Concentrations of Fe, Mn, Cu and Zn in the leaf symplastic extract of young and developed leaves in Fe-sufficient (+Fe), Fe-deficient (-Fe) and Fe-resupplied (-Fe*) plants at different sampling times (0, 12, 24 and 48 h). Groups were made based in Tukey or Games-Howell test (according to variance homogeneity test) with $p < 0.05$. Capital letters represent groups between different treatments at the same hour (rows) whereas lower case letters indicate groups of the same treatment at different hours (columns). Data are means ± SE, n = 3-12

Time (h)	Young leaves						Developed leaves					
	+Fe		-Fe		-Fe*		+Fe		-Fe		-Fe*	
Fe												
0	34.3 ± 8.6	B a	15.3 ± 2.1	A a	15.3 ± 2.1	A a	22.8 ± 1.0	A a	19.6 ± 3.8	A a	19.6 ± 3.8	A a
12	27.1 ± 3.5	B a	10.1 ± 0.4	A a	31.4 ± 3.1	B ab	24.2 ± 2.7	B a	11.4 ± 0.5	A a	30.3 ± 5.3	A ab
24	27.6 ± 3.5	A a	30.1 ± 4.9	AB b	51.8 ± 6.8	B b	34.1 ± 4.8	A ab	24.3 ± 4.0	A a	37.4 ± 6.2	A ab
48	38.8 ± 1.9	A a	27.8 ± 5.9	A ab	54.8 ± 8.8	B b	38.8 ± 2.0	B b	17.4 ± 2.4	A a	43.4 ± 3.6	B b
Mn												
0	32.5 ± 7.3	A a	41.1 ± 5.5	A a	41.1 ± 5.5	A a	44.5 ± 7.0	A a	198.1 ± 44.9	B ab	198.1 ± 44.9	B a
12	49.9 ± 16.5	A a	33.1 ± 0.9	A a	58.2 ± 3.8	A ab	37.7 ± 10.6	A a	153.3 ± 43.8	AB ab	234.4 ± 35.7	B a
24	32.0 ± 5.7	A a	29.2 ± 3.8	A a	62.0 ± 11.6	A ab	70.9 ± 2.9	A b	116.9 ± 4.8	B a	166.6 ± 23.7	C a
48	31.0 ± 4.4	A a	35.5 ± 3.3	A a	63.9 ± 3.5	B b	81.6 ± 8.1	A b	141.3 ± 16.3	B b	243.0 ± 37.6	C a
Cu												
0	24.6 ± 0.9	A a	23.4 ± 1.4	A c	23.4 ± 1.4	A b	21.8 ± 2.6	A b	21.7 ± 2.2	A b	21.7 ± 2.2	A b
12	36.3 ± 2.5	B b	22.9 ± 1.7	A bc	23.1 ± 1.6	A ab	30.9 ± 5.0	B c	18.2 ± 0.7	A b	19.3 ± 2.0	A ab
24	35.1 ± 5.6	B ab	19.5 ± 0.2	A b	16.5 ± 1.4	A a	19.9 ± 2.0	B ab	14.8 ± 1.1	A ab	14.1 ± 1.3	A a
48	21.6 ± 2.0	B a	14.9 ± 0.7	A a	20.3 ± 1.6	B ab	13.5 ± 0.6	B a	8.9 ± 0.3	A a	17.7 ± 2.7	B ab
Zn												
0	32.3 ± 2.6	A a	40.1 ± 5.0	A b	40.9 ± 5.0	A a	23.3 ± 1.1	A a	42.1 ± 3.9	B a	42.1 ± 3.9	B a
12	30.0 ± 5.7	A a	41.1 ± 3.7	AB b	49.2 ± 2.4	B a	21.7 ± 3.8	A a	41.3 ± 3.8	B a	53.8 ± 4.1	B a
24	73.9 ± 7.4	C b	29.2 ± 3.8	A a	49.6 ± 4.9	B a	58.2 ± 11.7	A b	67.4 ± 10.7	A a	44.3 ± 10.9	A a
48	43.1 ± 5.2	AB ab	35.0 ± 5.1	A ab	51.2 ± 3.7	B a	43.1 ± 5.2	AB b	27.0 ± 5.2	A a	60.2 ± 8.0	B a

4.1.5. Changes in nicotianamine concentrations in tomato plant fluids

4.1.5.1. Root apoplastic fluid and symplastic extract

The NA concentration in the root apoplastic fluid changed with the sampling time (Fig. 4.8 and Table 4.6). The initial concentration of NA in the +Fe and -Fe treatments was approximately 42-44 µM, and it decreased in +Fe plants to 15 µM (by 67%) at 24 h and in -Fe plants to 12 µM (by 72%) at 48 h. In the Fe resupplied plants (-Fe*) there was a large increase (2.5-fold) in NA concentration to 103 µM at 12 h, and then the NA values remained stable at 24 h and decreased to 45 µM (by 50%) from 24 to 48 h.

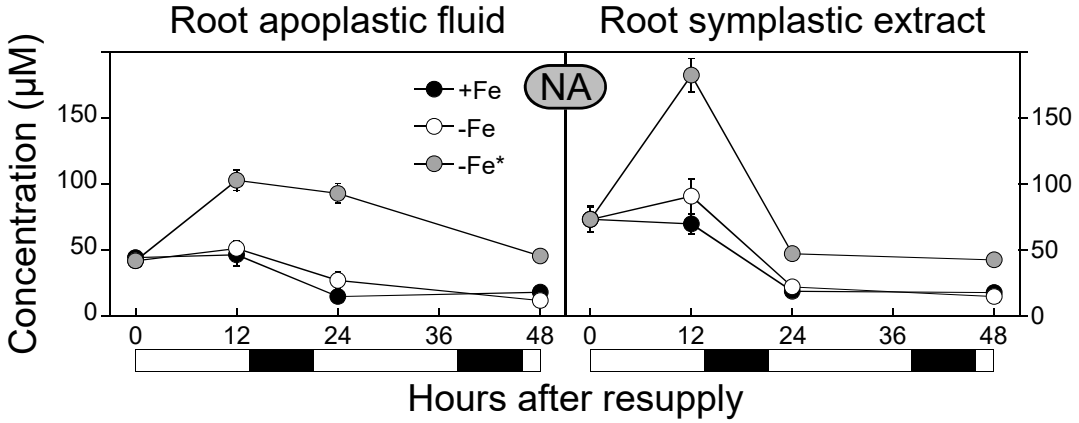

Fig. 4.8. Nicotianamine (NA) concentrations in root apoplastic fluid and root symplastic extracts of tomato plants as affected by Fe deficiency and resupply. Treatments were as described in Fig. 4.4. Samples were taken at 0, 12, 24 and 48 h after the start of the Fe-resupply experiment. Data are means ± SE, n = 4-9

Regarding treatments, NA concentrations in the root apoplastic fluid were not significantly different in the +Fe and -Fe treatments, whereas those in the -Fe* plants were significantly higher than those in the other treatments at 12, 24 and 48 h.

In the root symplastic extract, the initial NA concentration was 73 µM in the +Fe and -Fe treatments, and then decreased to 15-18 µM (by 70-75%) after 24-48 h. In the Fe resupplied plants (-Fe*) there was a large increase (2.5-fold) in NA concentration to 182 µM at 12 h, followed by a decrease to 47-42 µM (by 74-77%) at 24-48 h.

Regarding treatments, NA concentrations in the root symplastic extract were not significantly different in the +Fe and -Fe treatments, whereas those in the -Fe* plants were significantly higher at 12, 24 and 48 h.

Table 4.6. Concentrations of NA in tomato fluids from Fe-sufficient (+Fe), Fe-deficient (-Fe) and Fe-resupplied (-Fe*) plants at different sampling times (0, 12, 24 and 48 h, plus 20 and 44 h in xylem sap of -Fe*). Groups were made based in Tukey or Games-Howell test (according to variance homogeneity test) with $p < 0.05$. Capital letters represent groups between different treatments at the same hour (rows) whereas lower case letters indicate groups of the same treatment at different hours (columns). Data are means ± SE, n = 2-20. *n.d. not determined*

Time (h)	+Fe		-Fe		-Fe*		+Fe		-Fe		-Fe*	
	Root apoplastic fluid						**Root symplastic extract**					
0	44.0 ± 5.4	A b	41.6 ± 2.3	A b	41.6 ± 2.1	A a	73.1 ± 9.7	A b	73.0 ± 9.2	A b	73.0 ± 9.2	A a
12	46.3 ± 8.4	A b	51.0 ± 5.7	A b	102.6 ± 3.1	B b	69.6 ± 7.9	A b	90.6 ± 13.0	A b	182.1 ± 12.8	B b
24	14.6 ± 1.2	A a	26.9 ± 6.1	A ab	92.7 ± 6.8	B b	18.6 ± 1.0	A a	21.8 ± 1.7	A a	47.0 ± 3.9	B a
48	17.9 ± 1.9	A a	11.5 ± 0.8	A a	45.3 ± 8.8	B a	17.6 ± 1.0	A a	14.5 ± 0.3	A a	42.4 ± 2.8	B a
	Xylem sap											
0	12.4 ± 2.0	A b	8.9 ± 1.3	A a	8.9 ± 1.3	A a						
12	5.3 ± 1.5	A a	12.1 ± 1.5	B a	13.4 ± 1.6	B a						
20	n.d.		n.d.		11.9 ± 1.1	a						
24	14.3 ± 1.8	A b	10.6 ± 0.7	A a	12.3 ± 0.7	A a						
44	n.d.		n.d.		10.1 ± 0.9	a						
48	10.9 ± 0.6	A b	11.6 ± 0.3	A a	9.5 ± 0.9	A a						
	Young leaf apoplastic fluid						**Developed leaf apoplastic fluid**					
0	9.6 ± 0.7	A a	11.4 ± 1.0	A b	11.4 ± 1.0	A b	13.0 ± 1.8	B b	6.2 ± 0.3	A a	6.2 ± 0.3	A a
12	19.8 ± 3.8	B b	7.0 ± 0.8	A a	7.1 ± 0.9	A a	14.7 ± 1.7	B b	10.3 ± 0.3	A bc	7.1 ± 0.9	A ab
24	11.7 ± 1.5	A a	12.9 ± 2.0	A ab	9.7 ± 0.4	A ab	8.4 ± 0.6	A a	12.6 ± 0.8	B c	15.9 ± 2.6	B c
48	15.4 ± 2.7	B ab	9.5 ± 0.3	A ab	8.1 ± 0.2	A a	8.9 ± 0.8	A a	8.9 ± 0.4	A b	8.1 ± 0.2	A b
	Young leaf symplastic extract						**Developed leaf symplastic extract**					
0	67.2 ± 2.8	B a	50.3 ± 6.0	A a	50.3 ± 6.0	A a	33.0 ± 3.8	A b	42.4 ± 9.1	A a	42.4 ± 9.1	A a
12	72.9 ± 5.7	A a	56.0 ± 5.7	A a	55.2 ± 5.0	A a	21.0 ± 1.3	A a	38.6 ± 3.0	B a	35.0 ± 3.1	B a
24	71.8 ± 1.5	B a	62.3 ± 1.9	A a	75.3 ± 6.1	AB ab	21.6 ± 1.6	A a	57.9 ± 7.2	B a	51.5 ± 4.8	B ab
48	69.0 ± 7.6	A a	55.8 ± 2.8	A a	89.9 ± 2.9	B b	23.9 ± 2.8	A ab	42.2 ± 2.8	B a	70.2 ± 4.2	C b

4.1.5.2. Xylem sap

The NA concentration in the xylem sap was in the range 5-15 µM for all treatments and sampling times (Fig. 4.9 and Table 4.6). The only significant difference found was for the +Fe treatment at 12 hours, at which the NA concentration was 5 µM, 57% lower than the initial one (12 µM); consequently, the NA concentration at 12 h was lower (50%) in +Fe plants that in the -Fe and resupplied (-Fe*) ones. This minimum corresponds to the end of the light period, in a pattern similar to that found for the metal micronutrients (see section 4.4.2).

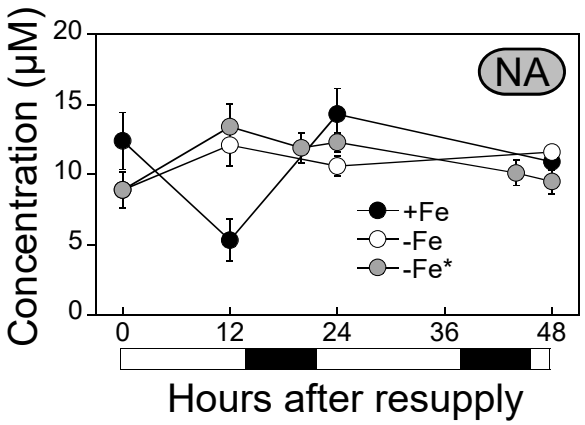

Fig. 4.9. Nicotianamine (NA) concentration in the xylem sap of tomato plants as affected by Fe deficiency and resupply. Treatments were as described in Fig. 4.4. Data are means ± SE, n = 2-6

4.1.5.3. Leaf apoplastic fluid

The NA concentration in the leaf apoplastic fluid was always in the range 6-20 µM, with only minor differences between treatments or leaf age (Fig. 4.10 and Table 4.6). In young leaves, NA concentrations in the leaf apoplastic fluid of +Fe plants showed an increase from 10 to 20 µM from 0 to 12 h, and then a decrease to 12 µM at 24 h. The NA concentrations in -Fe and Fe-resupplied (-Fe*) plants were always in the range 7-13 µM, with a 38% decrease in the NA concentration being found at 12 h when compared to those at 0 h in both treatments. In developed leaves, a decrease in NA concentration (43%) was found in the leaf apoplastic fluid of +Fe plants from 12 to 24 h, whereas significant 2- and 3-fold increases were found in the -Fe and -Fe* plants at 12 and 24 h, respectively, followed by decreases in both cases at 48 h.

Regarding treatments, the NA concentrations in young leaves were much lower in the -Fe and -Fe* plants than in the +Fe ones at 12 and 48 h. In developed leaves, the -Fe and -Fe* plants had less NA in the apoplastic fluid when compared to the +Fe plants at 0 and 12 h. However, at 24 h the opposite was true, with the -Fe and -Fe* plants having more NA than +Fe ones.

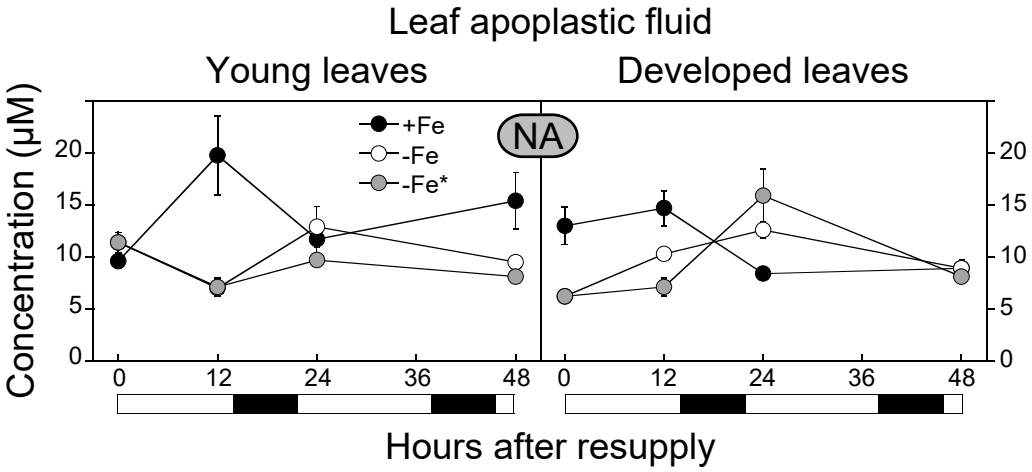

Fig. 4.10. Nicotianamine (NA) concentrations in the leaf apoplastic fluid of tomato plants as affected by Fe deficiency and resupply. Treatments were as described in Fig. 4.4. Leaves sampled were the 1st, 2nd and 3rd (developed leaves) and the 4th, 5th and 6th (younger leaves) from the cotyledons. Data are means ± SE, n = 4-20 with the exception of developed leaves -Fe 12h that were only 2

4.1.5.4. Leaf symplastic extract

In young leaves, the concentrations of NA in the leaf symplastic extract were in the range 50-90 µM (Fig. 4.11 and Table 4.6). In the +Fe and -Fe plants no changes were detected in the NA concentration with time. In the case of the Fe resupplied plants (-Fe*), the concentration of NA in the symplastic extract increased 2-fold from 0-12 to 48 h. In developed leaves, the concentrations of NA in the leaf symplastic extract were in the range 21-71 µM. A 36% reduction (from 33 to 21 µM) was observed in the +Fe plants from 0 to 12 h, and a 2-fold increase was observed in the -Fe* plants at 48 h when compared with the value at 0 h. No differences were found between the different sampling times in -Fe plants.

Regarding differences between treatments, the symplastic NA concentrations in young leaves of +Fe plants were somewhat higher than those in the -Fe ones at 0 and 24 h, and somewhat lower than those in the -Fe* plants at 48 h. In contrast, in developed leaves, a lower concentration (48% decrease) was observed in +Fe plants when compared to the -Fe and -Fe* ones at 12, 24 and 48 h. The highest NA concentration was found in-Fe* plants at 48 h.

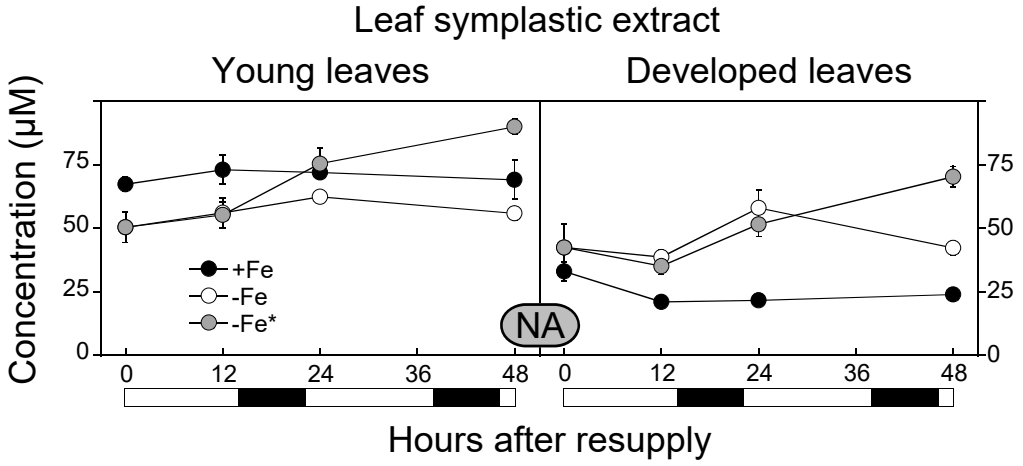

Fig. 4.11. Nicotianamine (NA) concentration in the leaf symplastic extract of tomato plants as affected by Fe deficiency and resupply. Treatments were as described in Fig. 4.4. Leaves sampled were the 1st, 2nd and 3rd (developed leaves) and the 4th, 5th and 6th (younger leaves) from the cotyledons. Data are means ± SE, n = 4-11

4.1.6. Changes in carboxylate concentrations

4.1.6.1. Root apoplastic fluid and symplastic extract

Root apoplastic fluid

In the root apoplastic fluid, the carboxylate concentrations were found in different concentration ranges: 2-oxoglutarate, *Cit* and *Mal* were in the mM range, whereas succinate and fumarate were in the µM one (Fig. 4.12 and Table 4.7).

2-oxoglutarate

The 2-oxoglutarate concentration in the root apoplastic fluid of +Fe and -Fe plants was in the range 1-7 mM. In the root apoplastic fluid of +Fe plants the initial concentration of 2-oxoglutarate was 5 mM and decreased to 1 mM at 48 h. In -Fe plants, the initial concentration was 7 mM, decreased to 2 mM at 12 h, and increased to 5 mM at 48 h. In the -Fe* plants, the initial concentration was 7 mM, it decreased to 2 mM after 12 h, and then increased to 6 mM at 24 h.

When comparing treatments, the concentration of 2-oxoglutarate was higher in +Fe plants than in the -Fe and -Fe* plants at 12 h, whereas the opposite occurred at 48 h. At this time, the -Fe plants had the highest 2-oxoglutarate concentration.

Citrate

The *Cit* concentration in the root apoplastic fluid of +Fe and -Fe plants was in the range 1-6 mM. The *Cit* concentration in root apoplastic fluid increased 2-fold at 48 h in +Fe and at 12 h in -Fe plants when compared to the initial values. On the other hand, in Fe-resupplied plants (-Fe*) the *Cit* concentration increased 4-fold at 24 h, followed by an 82% decrease at 48 h.

When comparing treatments, the concentration of *Cit* in the -Fe* plants was much higher than those in +Fe and -Fe plants at 24 h, and lower than those in the +Fe and -Fe plants at 48 h.

Malate

The *Mal* concentration in the root apoplastic fluid of +Fe and -Fe plants was in the range 1-4 mM. The *Mal* concentration in root apoplastic fluid of +Fe plants increased by 1.4-fold in the range 0-48 h, whereas in the -Fe plants it decreased by 45% at 12 h and increased to 1.7 mM at 48 h. In the -Fe* plants there was a 65% decrease in *Mal* at 12 h followed by a 4-fold increase at 24 h and another 66% decrease at 48 h.

When comparing treatments, the *Mal* concentration in root apoplastic fluid was higher in the +Fe plants than in the -Fe and -Fe* plants at 12 and 48 h, whereas at 24 h the -Fe* plants showed the highest *Mal* concentrations.

Succinate

The succinate concentration in root apoplastic fluid of +Fe and -Fe plants was 119-194 µM across all sampling times, with the only significant change being a 1.6-fold increase in the +Fe plants from 0 to 48 h. In the -Fe* plants the succinate concentration decreased from 119 µM at 0 h to values below LOQ at 12 hours, and then increased to 476 µM at 24 h (this concentration was 4-fold higher than at 0 h). Finally, the concentration decreased to 118 µM at 48 h.

When comparing treatments, the succinate concentration in -Fe* plants was lower than those in the +Fe and -Fe plants at 12 h, and the highest at 24 h. At 48 h, the succinate concentration in the +Fe plants was higher than those in the -Fe and -Fe* plants.

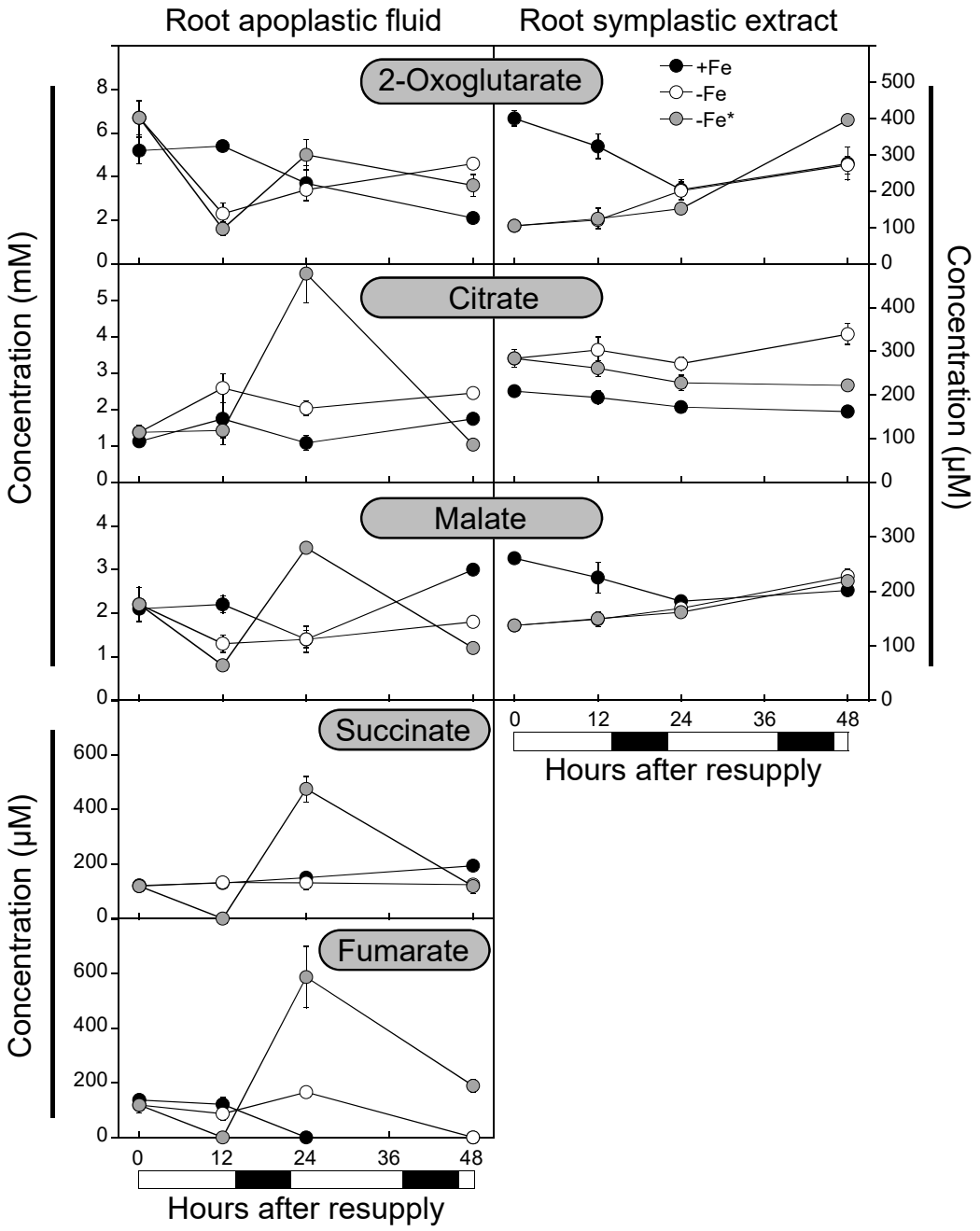

Fig. 4.12. Carboxylates concentrations in the root apoplastic fluid and root symplastic extract of tomato plants as affected by Fe deficiency and resupply.
Treatments were as described in Fig. 4.4. Data are means ± SE, n = 3-4

Table 4.7. Concentrations of carboxylates in root apoplastic fluid and symplastic extract in Fe-sufficient (+Fe), Fe-deficient (-Fe) and Fe-resupplied (-Fe*) plants at different sampling times (0, 12, 24 and 48 h). Groups were made based in Tukey or Games-Howell test (according to variance homogeneity test) with $p < 0.05$. Capital letters represent groups between different treatments at the same hour (rows), whereas lower case letters indicate groups of the same treatment at different hours (columns). < LOQ, below limit of quantification. 2-oxoglutarate, citrate and malate in root apoplastic fluid are expressed in mM, the others in µM. Data are means ± SE, n = 3-4

Time (h)	Root apoplastic fluid						Root symplastic extract					
	+Fe		-Fe		-Fe*		+Fe		-Fe		-Fe*	
2-oxoglutarate												
0	5.2 ± 0.6	A b	6.7 ± 0.8	A d	6.7 ± 0.8	A b	400 ± 21	B c	105 ± 3	A a	105 ± 3	A a
12	5.4 ± 0.7	B b	2.3 ± 0.2	A a	1.6 ± 0.3	A a	324 ± 34	B bc	121 ± 11	A a	124 ± 28	A a
24	3.7 ± 0.7	A b	3.4 ± 0.7	A b	5.7 ± 1.2	A b	204 ± 27	A a	201 ± 24	A b	152 ± 16	A a
48	1.1 ± 0.1	A a	4.6 ± 0.1	C c	3.6 ± 0.5	B b	276 ± 45	A ab	272 ± 25	A b	396 ± 14	B b
Citrate												
0	1.1 ± 0.0	A a	1.4 ± 0.0	A a	1.4 ± 0.2	A a	208 ± 8	A b	284 ± 19	B a	284 ± 19	B a
12	1.7 ± 0.6	A ab	2.6 ± 0.1	A b	1.4 ± 0.2	A a	194 ± 15	A ab	303 ± 29	B a	261 ± 18	AB a
24	1.1 ± 0.2	A ab	2.0 ± 0.1	A ab	5.7 ± 0.8	B b	172 ± 10	A ab	272 ± 16	C a	228 ± 18	B a
48	1.7 ± 0.0	B b	2.4 ± 0.0	C b	1.0 ± 0.1	A a	162 ± 5	A a	339 ± 24	C a	222 ± 9	B a
Malate												
0	2.1 ± 0.1	A a	2.2 ± 0.1	A c	2.2 ± 0.4	A b	261 ± 6	B b	137 ± 4	A a	137 ± 4	A a
12	2.2 ± 0.2	B a	1.2 ± 0.0	A a	0.8 ± 0.1	A a	225 ± 28	B ab	149 ± 13	A a	150 ± 7	A ab
24	1.4 ± 0.3	A a	1.4 ± 0.1	A ab	3.5 ± 0.1	B c	172 ± 10	A a	169 ± 7	A a	162 ± 8	A b
48	3.0 ± 0.1	C b	1.7 ± 0.1	B b	1.2 ± 0.1	A ab	202 ± 3	A a	228 ± 13	AB b	219 ± 2	B c
Succinate												
0	122.0 ± 19.1	A a	119.2 ± 5.8	A a	119.2 ± 18.7	A a						
12	130.4 ± 18.9	B a	132.5 ± 12.5	B a	< LOQ							
24	150.0 ± 15.0	A ab	131.2 ± 12	A a	475.7 ± 47.9	B b						
48	194.0 ± 14.7	B b	124.2 ± 5.9	A a	118.4 ± 26.2	A a						
Fumarate												
0	137.3 ± 4.7	A a	118.9 ± 5.8	A a	118.9 ± 27.9	A a						
12	121.2 ± 23.7	B a	86.9 ± 12.5	B a	< LOQ							
24	< LOQ		165.8 ± 12	A a	587.1 ± 112.7	B b						
48	< LOQ		< LOQ		189.1 ± 22.7	a						

Fumarate

The fumarate concentration in root apoplastic fluid of +Fe and -Fe plants was in the range from below the LOQ (the LOQ for fumarate in the root apoplastic fluid matrix was approximately 80 μM) to 166 μM. The concentration dropped below the LOQ in the +Fe plants at 24 and 48 h and in the -Fe ones at 48 h. In the -Fe* plants fumarate was below the LOQ at 12 h, whereas at 24 h the fumarate concentration increased 5-fold (when compared with 0 h) and then decreased by 68% at 48 h.

When comparing treatments, the fumarate concentration in -Fe* plants was the lowest at 12 h, whereas at 24 h the highest values were found in the -Fe* plants and the lowest in the +Fe plants. At 48 h the only values above the LOQ were for the -Fe* plants.

Root symplastic extract

In root symplastic extract the carboxylate concentration values were always lower than those in root apoplastic fluid (Fig. 4.12 and Table 4.7). 2-oxoglutarate, *Cit* and *Mal* were found in the μM range, whereas succinate and fumarate were below LOQ in all samples.

2-oxoglutarate

The 2-oxoglutarate concentration in the root symplastic extract was in the range 105-400 μM. In the +Fe plants, the lowest 2-oxoglutarate concentrations in the root symplastic extract were found at 24 h. In the -Fe and -Fe* plants, significantly higher concentrations (2- to 4-fold) were found at 24-48 and 48 h, respectively, than at the other sampling times.

When comparing the different treatments, the 2-oxoglutarate concentration in the root symplastic fraction was higher in the +Fe plants than in the -Fe and -Fe* plants at 0 and 12 h, and it was higher in the -Fe* plants than in the other two treatments at 48 h.

Citrate

The *Cit* concentration in root symplastic extract was in the range 161-340 μM. The only difference with time was found in the +Fe treatment, which showed a 23% decrease from 0 to 48 h.

Regarding differences between treatments, the *Cit* concentration in the root symplastic fraction was higher in -Fe than in +Fe plants at all sampling times (2-fold on average), whereas in the Fe-resupplied (-Fe*) plants the increases over the +Fe values were significantly different at 0, 24 and 48 h.

Malate

The *Mal* concentration in root symplastic extract was in the range 137-261 µM. A 30% decrease in *Mal* concentration in the root symplastic fraction of +Fe plants was found between 0 and 24 h, whereas in the -Fe increased 1.7-fold from 0-24 to 48 h. In the -Fe* plants a 1.2-fold increase occurred from 0 to 24 h and a further 1.4-fold one from 24 to 48 h.

When comparing the treatments, the *Mal* concentration in root symplastic extract of +Fe plants was higher than that in -Fe and -Fe* plants at 0 and 12 h. The *Mal* concentration in the -Fe* plants were higher than that in the +Fe ones at 48h.

Succinate and fumarate

The succinate and fumarate concentrations in root symplastic extract in all treatments and sampling times were below the LOQ, which were approximately 100 and 75 µM, respectively, in the original root symplastic extract matrix.

4.1.6.2. Xylem sap

The carboxylate concentrations in tomato xylem sap at different treatments and times are shown in Fig. 4.13 and Table 4.8. The most abundant carboxylate, in the mM range, was *Mal*, whereas 2-oxoglutarate, *Cit*, succinate and fumarate concentrations were found in the µM range.

2-oxoglutarate

The concentrations of 2-oxoglutarate in the xylem sap were in the range from below the LOQ to 139 µM. In the +Fe plants, there was a 2-fold increase from 12 to 24 h, whereas no changes with sampling time were found in the -Fe treatment. In the -Fe* plants there was a 70% decrease from 0 to 12 h, and by 48 h values were below the LOQ.

Regarding treatments, the concentrations found in the -Fe* plants were the lowest at 12, 24 and 48 h.

Citrate

The concentrations of *Cit* in the xylem sap were in the range from 147-449 µM. No changes in the xylem sap *Cit* concentration with time were found in the +Fe plants. In contrast, a significant decrease (28%) in the xylem sap *Cit* concentration was found in the -Fe plants from 12 to 24 h. As it occurs in the -Fe plants, the xylem sap *Cit* concentration of

the -Fe* plants decreased with time (46 and 26% decreases from 0 to 12 and from 24 to 48 h, respectively).

Regarding differences between treatments, the xylem sap *Cit* concentration was approximately 2-fold higher in -Fe than in +Fe plants at 0 and 12 h. In the case of the -Fe* plants, the xylem sap *Cit* concentration was higher (1.7-fold) than that found in the +Fe plants at 24 h.

Malate

The concentrations of *Mal* in the xylem sap were in the range from 0.6-3.6 mM. The *Mal* concentration was quite constant in the xylem sap of +Fe plants with time, whereas a significant decrease (61%) was found in the -Fe plants from 0 to 12 h, followed by a 3-fold increase at 24 h and a 35% decrease at 48 h. In the -Fe* plants, the xylem sap *Mal* concentration decreased by 82% at 12 h, followed by a 2-fold increase from 12-24 to 48 h.

Regarding differences between treatments, the xylem sap *Mal* concentrations at 0 h were lowest in the +Fe plants. At 12, 24 and 48 h the lowest values were found in the-Fe* plants. Values at 24 h were lower in the +Fe plants than in the -Fe ones.

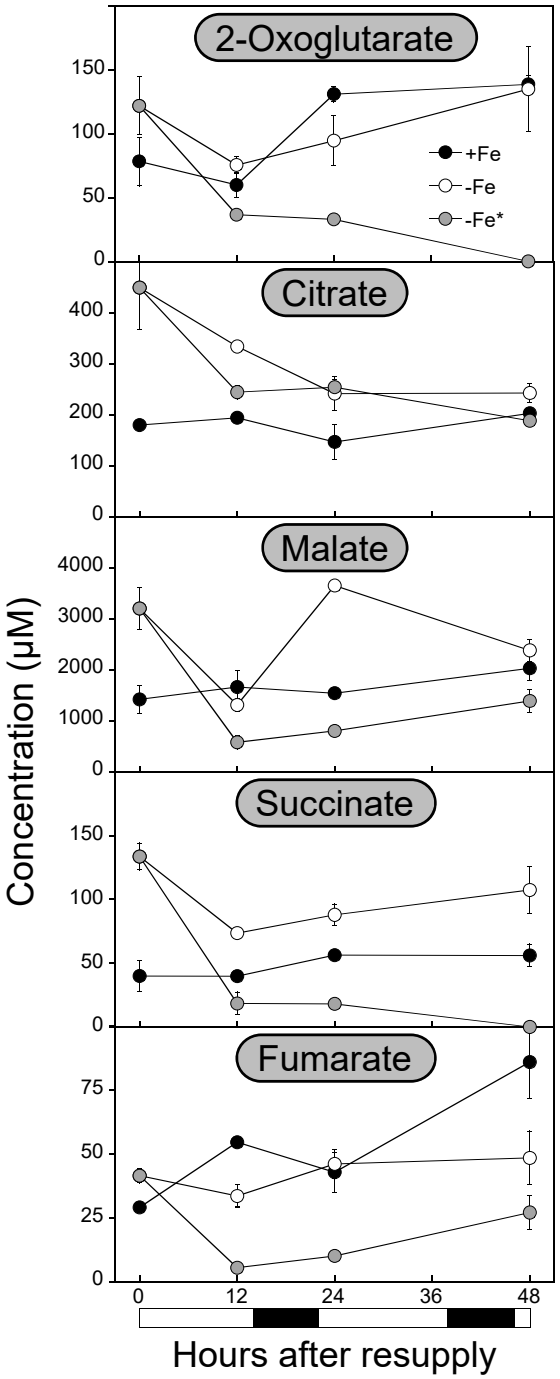

Fig. 4.13. Carboxylate concentrations in the xylem sap of tomato plants as affected by Fe deficiency and resupply. Treatments were as described in Fig. 4.4. Data are means ± SE, n = 3

Table 4.8. Concentrations of carboxylates in the xylem sap in Fe-sufficient (+Fe), Fe-deficient (-Fe) and Fe-resupplied (-Fe*) plants at different sampling times (0, 12, 24 and 48 h). Groups were made based in Tukey or Games-Howell test (according to variance homogeneity test) with $p < 0.05$. Capital letters represent groups between different treatments at the same hour (rows), whereas lower case letters indicate groups of the same treatment at different hours (columns). < LOQ, below limit of quantification. All data is expressed in µM with the exception of malate, which is in mM. Data are means ± SE, n = 3

Time (h)	+Fe		-Fe		-Fe*	
			2-oxoglutarate			
0	78.4 ± 18.9	A a	122.0 ± 22.7	A a	122.0 ± 22.7	A b
12	59.9 ± 9.6	B a	75.5 ± 6.9	B a	36.6 ± 3.3	A a
24	131.2 ± 6.1	B b	94.7 ± 19.6	B a	33.0 ± 1.8	A a
48	138.8 ± 6.6	A b	135.1 ± 33.2	A a	< LOQ	
			Citrate			
0	179.5 ± 5.2	A a	448.9 ± 81.8	B b	448.9 ± 81.8	B c
12	193.8 ± 9.6	A a	333.3 ± 7.4	C b	243.9 ± 13.0	B b
24	146.6 ± 34.2	A a	241.5 ± 33.3	AB a	253.6 ± 14.5	B b
48	202.3 ± 5.5	A a	242.3 ± 18.7	A a	188.1 ± 4.4	A a
			Malate			
0	1.4 ± 0.3	A a	3.2 ± 0.4	B bc	3.2 ± 0.4	B c
12	1.7 ± 0.3	B a	1.2 ± 0.1	B a	0.6 ± 0.1	A a
24	1.5 ± 0.1	B a	3.6 ± 0.0	C c	0.8 ± 0.0	A a
48	2.0 ± 0.2	B a	2.4 ± 0.2	B b	1.4 ± 0.2	A b
			Succinate			
0	39.9 ± 12.0	A a	133.7 ± 10.4	B c	133.7 ± 10.4	B b
12	39.8 ± 2.1	B a	73.6 ± 1.6	C a	18.4 ± 8.6	A a
24	56.3 ± 8.3	B a	87.9 ± 2.1	C b	18.1 ± 0.8	A a
48	56.1 ± 8.6	A a	107.4 ± 18.6	B bc	< LOQ	
			Fumarate			
0	29.1 ± 0.9	A a	41.5 ± 2.7	B a	41.5 ± 2.7	B c
12	54.6 ± 1.9	C b	33.6 ± 4.5	B a	5.5 ± 1.3	A a
24	42.9 ± 7.9	B ab	46.1 ± 2.9	B a	10.1 ± 2.1	A a
48	86.0 ± 14.1	B c	48.5 ± 10.5	AB a	27.1 ± 6.5	A b

Succinate

The concentrations of succinate in the xylem sap were in the range from below the LOQ (*ca.* 15 µM) to 134 µM. The concentration of succinate in the xylem sap of +Fe plants was quite stable at all sampling times (40-57 µM), whereas in -Fe plants succinate concentration was 134 µM at 0 h and decreased by 45% at 12 h, to increase by 1.5-fold from 12 to 48 h. Upon Fe resupply, the succinate concentration in xylem sap was reduced by 86% in the first 12 h and decreased below the LOQ from 24 to 48 h.

Regarding differences between treatments, the concentration of succinate was higher in -Fe than those in +Fe plants at all sampling times. In the case of the -Fe* plants, values were the lowest at 12, 24 and 48 h.

Fumarate

The concentrations of fumarate in the xylem sap were in the range from 6-86 μM. In the +Fe plants, the fumarate concentrations increased 2-fold from 0 to 12 and again from 24 to 48 h, whereas in the -Fe plants they showed no significant changes with time (34-49 μM). In the -Fe* plants, fumarate decreased 87% in the first 12 h, and then increased 5-fold from 12-24 to 48 h.

Regarding differences between treatments, the concentration of fumarate in the -Fe* treatment was the lowest at sampling times 12, 24 and 48 h. In the case of the 0 h sampling, the concentration of fumarate was higher in the -Fe plants than in the +Fe ones, whereas the opposite occurred at 12 h.

4.1.6.3. Leaf apoplastic fluid

The carboxylate concentrations in the leaf apoplastic fluid of young and developed leaves are shown in Fig. 4.14 and Table 4.9. The leaf apoplastic fluid was the only plant fluid where it was possible to quantify the carboxylate *cis*-aconitate. In the apoplastic fluid the *Cit* and *Mal* concentrations were found in the mM range in both young and developed leaves, whereas the *cis*-aconitate, 2-oxoglutarate, succinate and fumarate concentrations were in the μM range. The carboxylate concentrations in the apoplastic fluid of developed leaves were generally higher than those present in the apoplastic fluid of young leaves.

Citrate

The *Cit* concentrations in the apoplastic fluid for all treatments were 0.4-1.8 mM and 1.6-13.6 mM in young and developed leaves, respectively. In young leaves, the *Cit* concentrations in apoplastic fluid of +Fe plants were always in the range 0.4-0.6 mM, with no significant changes with time. In the -Fe plants, *Cit* concentrations were 1.8 mM at 0 h and decreased by 56% at 24 h. In the -Fe* plants, the *Cit* concentrations decreased by 50% at 12 h, increased 2-fold after 24 h and decreased again by 66% at 48 h. In the developed leaves, +Fe plants showed a quite constant *Cit* concentration (in the range 3.4-5.7 mM), whereas in -Fe plants the concentration was 5.1 mM at 0 h and decreased by 69% after 24 h. In the Fe-resupplied plants (-Fe*) the *Cit* concentration increased 2-fold from 0-12 to 24-48 h.

Regarding differences among treatments, in the apoplastic fluid of young leaves the *Cit* concentrations were the lowest in the +Fe plants at all sampling times, whereas the

highest *Cit* concentrations corresponded to the -Fe* plants at 24 h and the -Fe plants at 48 h. In developed leaves, the only differences among treatments were found at 24 and 48 h, with the highest *Cit* concentrations in the -Fe* plants and the lowest ones in the -Fe ones.

Malate

The *Mal* concentrations in the apoplastic fluid of young leaves were in the range 0.4-1.5 mM, whereas in developed ones they were in the range from 1.3 to 9.7 mM. In the young leaf apoplastic fluid of +Fe plants, the *Mal* concentration at 0-12 h was 0.4 mM, and then increased 2-fold at 24-48 h. In the -Fe and -Fe* plants, the initial *Mal* concentration was 1.4 mM and had decreased by 50% and 57% at 48 h, respectively. In developed leaf apoplastic fluid, +Fe plants showed a *Mal* concentration from 2.5 to 4.9 mM, with no significant changes with time. In the -Fe plants *Mal* concentration decreased from 2.0-2.9 mM at 0-12 h to 1.3 mM at 24-48 h (a 35-55% decrease), whereas in the -Fe* plants the *Mal* concentration increased 3- and 5-fold at 12-24 and 48 h, respectively, when compared to the value at 0 h.

Regarding treatments, the leaf apoplastic fluid of young leaves at 0 and 12 h in the -Fe and -Fe* plants showed higher *Mal* concentrations than those in the +Fe plants, whereas at 24 h and 48 h the -Fe* and +Fe plants showed the highest concentration, respectively. In developed leaves, the apoplastic fluid *Mal* concentrations were the lowest in the -Fe plants at all sampling times, whereas the -Fe* plants showed the highest concentrations at 24 and 48 h.

cis-aconitate

cis-aconitate was found in a concentration range from below the LOQ to 27 µM in young leaves and 18-192 µM in developed ones. *cis*-aconitate was hardly detected in the samples because of its low concentration and the high LOQ of the method (0.245 µM in the standard mixture; equivalent to 4.91 pmol injected, and approximately 15 µM in the original undiluted sample, taking into account the matrix effect).

In the apoplastic fluid of young leaves in the +Fe plants, *cis*-aconitate was found below the LOQ at 0 and 12 h, whereas at 24 and 48 h it was 18-19 µM. In the -Fe plants, the concentration was 15-21 µM at 0, 24 and 48 h, and below the LOQ at 12 h. In -Fe* plants, it decreased by 33% at 12 h and then increased 2-fold at 24 h. In developed leaves, *cis*-aconitate in the +Fe plants was 60 µM and decreased by 56% at 12 h, whereas in -Fe plants

it was 30-50 µM at 0-24 h, and decreased to 24 µM at 48 h. In the -Fe* plants the concentration increased 5-fold from 0-12 to 24-48 h.

Regarding treatments, in the leaf apoplastic fluid of young leaves the highest *cis*-aconitate concentration was found at 0 h in -Fe plants, at 12 and 24 h in the -Fe* plants and at 48 h in the +Fe plants. In developed leaves, the highest *cis*-aconitate concentrations was found at 0 h in the +Fe plants, at 12 h in -Fe plants, and at 24 and 48 h in the -Fe* plants.

2-oxoglutarate

The 2-oxoglutarate concentration was in the range 32-230 µM in young leaves and 141-1194 µM in developed ones. In the young leaf apoplastic fluid of +Fe plants the concentration was 32-36 µM at 0-12 h, increased 3-fold at 24 h and decreased by 40% at 48 h. In -Fe plants, the concentration was 190 µM at 0 h, it decreased by 51% at 12 h and then increased to 175-119 at 24-48 h. In -Fe* plants, a 60% decrease in 2-oxoglutarate was found from 0 to 12 h, followed by a 3-fold increase at 24 h and a 62% decrease at 48 h. In the apoplastic fluid of developed leaves, the 2-oxoglutarate concentration in +Fe plants was 216 µM, and had increased by 67% at 24 h. In the -Fe plants, the concentration did not change significantly with time. In the -Fe* plants, the 2-oxoglutarate concentration increased 3- and 6-fold at 12-24 and 48 h, respectively, when compared to the initial concentration.

Regarding treatments, the lowest concentrations of 2-oxoglutarate in young leaf apoplastic fluid were always found in +Fe plants. Values in the +Fe plants were significantly lower to those in the -Fe and -Fe* plants at 48 and 24 h, respectively. In developed leaves, the highest concentrations of 2-oxoglutarate were found in the -Fe* plants at 24 and 48 h. The -Fe plants showed a significantly lower concentration than that found in the +Fe plants at 48 h.

Succinate

The succinate concentration in the apoplastic fluid of young leaves was in the range 18-202 µM, whereas in the developed ones the concentration was from 49 to 230 µM. The succinate concentration in the young leaf apoplastic fluid of +Fe plants was 19 µM at 0-12 h and increased 2- to 4-fold at 24-48 h. In the -Fe plants the concentration was in the range 96-202 µM, with no significant changes with sampling time. In the -Fe* plants, succinate was 201 µM at 0 h and had decreased by 72% at 12 h, with no further significant changes at longer sampling times. In the apoplastic fluid of developed leaves, concentrations were in the range 49-71 µM and 83-100 µM for +Fe and -Fe plants, respectively, with no significant

changes in the treatments with time. In the -Fe* plants, a 2- to 3-fold increase in the succinate concentration was found from 0-24 to 48 h.

Regarding differences between treatments in the apoplastic fluid of young leaves, the -Fe plants showed the highest succinate concentrations at 0, 12 and 24 h, although there were no significant differences with the values found in the -Fe* plants at 12 h and 24 h, and with those in the +Fe plants at 48 h. At the 48 h sampling time, the concentration in the -Fe plants was significantly higher than that in the -Fe* ones. In the case of the developed leaves, the succinate concentration in the -Fe and -Fe* plants were generally higher than those in the +Fe plants, with the exception of -Fe plants at 12 and 48 h, where concentrations were not significantly different to those in the +Fe ones.

Fumarate

The fumarate concentration in apoplastic fluid was found from 3 to 34 µM in young leaves and from 4 to 99 in developed ones. In young leaves, the fumarate concentration was 3-7 µM and 13-33 in +Fe and -Fe plants, respectively, with no significant differences with time, whereas in the Fe-resupplied plants (-Fe*) the concentration decreased by 80% from 18-33 µM at 0-24 h to 6 µM at 48 h. In developed leaves, the fumarate concentration in the +Fe plants was 25 µM at 0 h, increased 2-fold at 12 h and then decreased by 63-61% at 24-48 h. In the -Fe plants, it increased 2-fold from 0 to 48 h. In the -Fe* plants, fumarate increased 3-fold from 0 to 12 h and then decreased by 85% at 24 h and a further 70% at 48 h.

Regarding treatments, the highest fumarate concentrations in young leaf apoplastic fluid were in the -Fe and -Fe* plants, and at 48 h the values was even higher in the -Fe plants than in the -Fe* ones. In the case of the developed leaves, fumarate concentration was similar in all treatments at 0 h but was the highest in the -Fe* plants at 12 h. At 24 and 48 h, the highest concentrations were found in the -Fe plants.

4.1.6.4. Leaf symplastic extract

It was not possible to quantify the carboxylate concentrations in the symplastic extracts of leaves because of problems in the chromatographic separation. In spite of the removal of proteins from the samples, the high matrix complexity of these plant fluids led to column saturation and overpressure, and these problems remained unsolved in most samples after in-depth column cleaning procedures. Furthermore, even in cases when a succesful separation was achieved, the high matrix complexity led to ionization suppression in the ESI source during the MS detection.

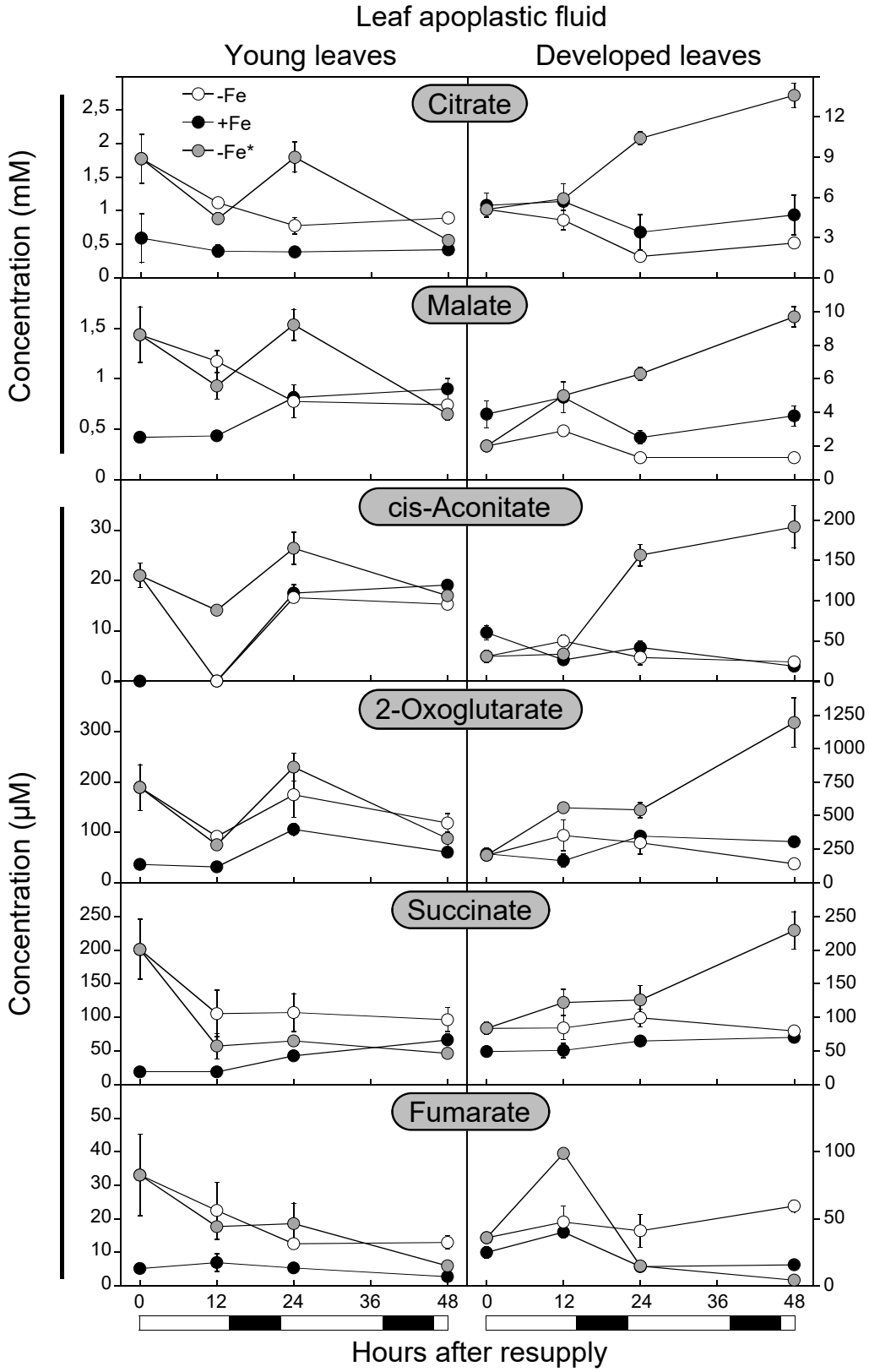

Fig. 4.14. Organic acid concentrations in the leaf apoplastic fluid of tomato plants as affected by Fe deficiency and resupply. Treatments were as described in Fig. 4.4. Leaves sampled were the 1st, 2nd and 3rd (developed leaves) and the 4th, 5th and 6th (younger leaves) from the cotyledons. Data are means ± SE, n = 3-4 with the exception of developed leaves -Fe 12 h that were only 2

Table 4.9. Concentrations of carboxylates in the leaf apoplastic fluid of young and developed leaves in Fe-sufficient (+Fe), Fe-deficient (-Fe) and Fe-resupplied (-Fe*) plants at different sampling times (0, 12, 24 and 48 h). Groups were made based in Tukey or Games-Howell test (according to variance homogeneity test) with $p < 0.05$. Capital letters represent groups between different treatments at the same hour (rows), whereas lower case letters indicate groups of the same treatment at different hours (columns). < LOQ, below limit of quantification. Citrate and malate are expressed in mM, whereas cis-aconitate, 2-oxoglutarate, succinate and fumarate are expressed in µM. Data are means ± SE, n = 3-4

Time (h)	Young leaves						Developed leaves					
	+Fe		-Fe		-Fe*		+Fe		-Fe		-Fe*	
Citrate												
0	0.6 ± 0.0	A a	1.8 ± 0.4	B b	1.8 ± 0.4	B c	5.4 ± 0.9	A a	5.1 ± 0.3	A b	5.1 ± 0.3	A a
12	0.4 ± 0.0	A a	1.1 ± 0.0	B ab	0.9 ± 0.1	B b	5.7 ± 1.3	A a	4.3 ± 0.7	A b	5.8 ± 0.2	A a
24	0.4 ± 0.0	A a	0.8 ± 0.1	B a	1.8 ± 0.2	C c	3.4 ± 0.5	B a	1.6 ± 0.2	A a	10.4 ± 1.3	C b
48	0.4 ± 0.0	A a	0.9 ± 0.0	C a	0.6 ± 0.0	B a	4.6 ± 0.9	B a	2.3 ± 0.2	A a	13.6 ± 1.5	C b
Malate												
0	0.4 ± 0.0	A a	1.4 ± 0.3	B b	1.4 ± 0.3	B b	3.9 ± 0.8	B a	2.0 ± 0.2	A b	2.0 ± 0.2	A a
12	0.4 ± 0.0	A a	1.2 ± 0.1	B b	0.9 ± 0.1	B ab	4.9 ± 0.9	B a	2.9 ± 0.3	A b	5.0 ± 0.2	B b
24	0.8 ± 0.0	A b	0.8 ± 0.2	A ab	1.5 ± 0.2	B b	2.5 ± 0.4	B a	1.3 ± 0.2	A a	6.3 ± 0.8	C b
48	0.9 ± 0.1	B b	0.7 ± 0.0	A a	0.6 ± 0.0	A a	3.8 ± 0.6	B a	1.3 ± 0.0	A a	9.7 ± 1.1	C c
***cis* -aconitate**												
0	< LOQ		21.0 ± 2.4	A a	21.0 ± 2.4	A b	60.3 ± 9.1	B b	30.7 ± 8.1	A ab	30.7 ± 8.1	A a
12	< LOQ		< LOQ		14.1 ± 1.2	A a	26.5 ± 2.9	A a	49.9 ± 6.5	B b	33.7 ± 1.9	A a
24	17.5 ± 1.7	A a	16.6 ± 0.7	A a	26.4 ± 3.2	B b	41.8 ± 7.8	A ab	29.5 ± 9.6	A ab	156.6 ± 13.2	B b
48	19.1 ± 0.6	B a	15.3 ± 0.2	A a	17.0 ± 0.5	AB ab	18.6 ± 1.3	A a	23.9 ± 3.2	A a	191.7 ± 26.4	B b
2-oxoglutarate												
0	36.4 ± 7.3	A a	189.5 ± 45.4	B b	189.5 ± 45.4	B b	215.7 ± 38.6	A a	205.1 ± 16.1	A a	205.1 ± 16.1	A a
12	31.6 ± 5.0	A a	92.1 ± 8.8	B a	75.4 ± 6.6	B a	164.2 ± 48.7	A a	352.1 ± 115.0	AB a	559.5 ± 12.6	B b
24	106.1 ± 12.1	A c	174.8 ± 44.3	AB b	229.8 ± 27.1	B b	347.6 ± 27.1	A b	297.6 ± 84.9	A a	542.5 ± 58.7	B b
48	60.7 ± 4.9	A b	118.8 ± 18.1	B b	87.9 ± 19.3	AB a	305.7 ± 39.5	B b	141.0 ± 13.4	A a	1194.0 ± 181.6	C c
Succinate												
0	18.5 ± 1.6	A a	201.1 ± 44.7	B a	201.1 ± 44.7	B b	49.0 ± 6.3	A a	83.6 ± 8.5	B a	93.6 ± 8.5	B a
12	18.5 ± 1.7	A a	105.4 ± 34.6	B a	57.2 ± 18.8	AB a	50.5 ± 10.4	A a	84.2 ± 17.7	AB a	122.0 ± 19.3	B a
24	42.6 ± 3.8	A b	107.1 ± 27.9	B a	64.8 ± 5.6	B a	64.7 ± 2.8	A a	99.3 ± 13.3	B a	125.9 ± 21.4	B a
48	66.2 ± 8.2	AB b	96.4 ± 18.0	B a	46.3 ± 6.9	A a	70.2 ± 8.1	A a	79.6 ± 5.5	A a	229.5 ± 27.8	B b
Fumarate												
0	5.2 ± 0.5	A a	33.1 ± 12.2	B a	33.1 ± 12.2	B b	25.0 ± 4.3	A a	36.0 ± 3.4	A a	36.0 ± 3.4	A c
12	7.0 ± 2.6	A a	22.5 ± 8.4	B a	17.7 ± 3.8	B b	40.1 ± 2.4	A b	47.7 ± 11.8	A ab	98.8 ± 3.5	B d
24	5.4 ± 1.3	A a	12.6 ± 0.4	B a	18.6 ± 6.4	B b	14.9 ± 1.8	A a	41.2 ± 12.3	B ab	14.5 ± 1.5	A b
48	2.8 ± 0.1	A a	13.0 ± 2.0	C a	6.0 ± 0.7	B a	15.8 ± 1.4	B a	59.6 ± 4.3	C b	4.3 ± 0.3	A a

4.1.7. Changes in ligand:metal ratios

The ratios NA:Fe, *Cit*:Fe and *Mal*:Fe in the different fluids studied were calculated from the raw data (using the concentrations found in each sample replicate), and are shown in Tables 4.10-4.13.

4.1.7.1. Root apoplastic fluid and symplastic extract

Root apoplastic fluid

NA:Fe

In the root apoplastic fluid, the NA:Fe ratios were in the range 0.1-3.6 (Table 4.10). In the +Fe plants the ratios were in the lower part of this range (0.1-0.3), and there were no changes with time. In the -Fe plants, the initial root apoplastic NA:Fe ratio at 0-12 h was 3.5-3.6, and decreased by 86% at 24-48 h. In the Fe-resupplied plants (-Fe*) a 84% decrease was also found between 0 and 12 h, to decrease further (by 66%) from 12 to 24 h and finally increase by 2.5-fold from 24 to 48 h.

Regarding treatments, the root apoplastic fluid in the +Fe plants had the lowest NA:Fe ratios at all sampling times, with the exception of the samples at 24 h, were the values in the +Fe and -Fe* plants were similar. The NA:Fe ratios in the root apoplastic fluid of the -Fe plants were the highest at 0 and 12 h.

Cit:Fe

In the root apoplastic fluid, the *Cit*:Fe ratios were in the range 5-204. In +Fe plants, this ratios were in the lower part of this range (5-36), and increased 3-fold from 0-12 to 24-48 h, whereas in the -Fe plants a 71% decrease was found from 0-12 to 24 h, followed by a 3-fold increase at 48 h. In the -Fe* plants, the root apoplastic *Cit*:Fe ratios decreased by 94% from 0 to 12 h, followed by a 1.5-fold increase from 12 to 48 h.

Regarding treatments, the apoplastic fluid of -Fe plants showed the highest *Cit*:Fe ratios, whereas the +Fe plants showed a higher ratio than the -Fe* plants at 24 h.

Mal:Fe

The *Mal*:Fe ratios in the root apoplastic fluid were in the range 6-117. In +Fe plants, this ratios were in the lower part of this range (10-37), with a 3-fold increase occurring from 0-12 to 24-48 h. In the -Fe plants a 55% decrease was found from 0-12 to 24 h, followed by

a 3-fold increase from 24 to 48 h. In the Fe-resupplied plants (-Fe*) the *Mal*:Fe ratios decreased by 93% from 0 to 12 h, and then increased 2-fold from 24 to 48 h.

Regarding treatments, the highest *Mal*:Fe ratios were found in the -Fe plants, whereas the lowest occurred in the -Fe* plants.

Root symplastic extract

NA:Fe

In the case of the root symplastic extract, the NA:Fe ratios were in the range 0.2-15.0 (Table 4.10). In +Fe plants, the ratios were in the lower part of this range (0.2-0.6), with a 50-66% decrease occurring from 0-12 to 24-48 h. In -Fe plants, a large decrease (94%) was found between 0-12 and 24-48 h. In the case of Fe-resupplied plants (-Fe*), a 88% decrease in the NA:Fe ratio was observed from 0 to 12 h, followed by a further 73% decrease from 12 to 24-48 h.

Regarding treatments, the root symplastic extract of the +Fe plants had the lowest NA:Fe ratios at all sampling times, with the exception of the samples at 24 h, were the values in the +Fe and -Fe* plants were similar. The NA:Fe ratios in the root symplastic extract of the -Fe plants were the highest at all sampling times.

Cit:Fe

In the root symplastic extract, the *Cit*:Fe ratio was in the range 1.6-82.2 (Table 4.10). The +Fe plants had *Cit*:Fe ratios in the lower part of this range (1.6-2.8), and showed a 2-fold increase from 0-12 to 24-48 h. In the -Fe plants, an 82% decrease was found from 0-12 to 24 h, followed by a 3-fold increase at 48 h. In the Fe-resupplied plants (-Fe*), a large decrease (97%) was found from 0 to 12 h, with no further changes in the next sampling times.

Regarding treatments, in the root symplastic extract the -Fe plants showed higher *Cit*:Fe ratios in all sampling times than those of the +Fe and -Fe* plants, which were not significantly different.

Mal:Fe

In the symplastic extract, the *Mal*:Fe ratios were in the range 1.4-34.7 (Table 4.10). The *Mal*:Fe ratios in the +Fe plants were in the lower part of this range (2.1-3.5), and a 2-fold increase was observed from 24 to 48 h. In the -Fe plants, a 72% decrease was observed from

0 to 12 h, followed by a 2-fold increase from 24 to 48 h. In the -Fe* plants, the *Mal*:Fe ratio showed a 96% decrease from 0 to 12-24 h and a 2-fold increase from 12-24 to 48 h.

Regarding treatments, in the root symplastic extract the *Mal*:Fe ratios were the highest in the -Fe plants, whereas those in the +Fe and -Fe* plants were similar at 12, 24 and 48 h.

Table 4.10. Ligand:Fe ratios in tomato root apoplastic fluid and symplastic extract in Fe-sufficient (+Fe), Fe-deficient (-Fe) and Fe-resupplied (-Fe*) plants at different sampling times (0, 12, 24 and 48 h). Groups were made based in Tukey or Games-Howell test (according to variance homogeneity test) with $p < 0.05$. Capital letters represent groups between different treatments at the same hour (rows) whereas lower case letters indicate groups of the same treatment at different hours (columns). Data are means ± SE, n = 3-4

Root apoplastic fluid

Time (h)	+Fe		-Fe		-Fe*	
			NA:Fe			
0	0.1 ± 0.1	A a	3.5 ± 0.9	B b	3.5 ± 0.9	B c
12	0.2 ± 0.1	A a	3.6 ± 1.0	C b	0.6 ± 0.0	B b
24	0.3 ± 0.1	A a	0.5 ± 0.3	A a	0.2 ± 0.0	A a
48	0.3 ± 0.0	A a	0.6 ± 0.1	B a	0.5 ± 0.0	B b
			***Cit*:Fe**			
0	5.6 ± 1.1	A a	195.2 ± 9.8	B b	195.2 ± 9.8	B c
12	13.6 ± 2.1	A a	203.3 ± 24.1	B b	11.5 ± 2.5	A a
24	35.7 ± 8.5	B b	59.3 ± 11.8	C a	13.8 ± 3.1	A ab
48	21.4 ± 2.6	A b	158.6 ± 31.9	B b	17.8 ± 1.0	A b
			***Mal*:Fe**			
0	10.1 ± 1.6	A a	90.6 ± 5.6	B b	90.6 ± 5.6	B c
12	13.3 ± 2.1	B a	93.0 ± 4.2	C b	6.7 ± 1.6	A a
24	46.8 ± 13.7	B b	42.0 ± 7.8	B a	10.9 ± 3.6	A a
48	36.8 ± 4.6	B b	116.8 ± 31.9	C b	20.6 ± 1.1	A b

Root symplastic extract

Time (h)	+Fe		-Fe		-Fe*	
			NA:Fe			
0	0.6 ± 0.1	A b	14.5 ± 3.6	B b	14.5 ± 3.6	B c
12	0.6 ± 0.1	A b	7.0 ± 1.8	C b	1.8 ± 0.3	B b
24	0.2 ± 0.0	A a	0.9 ± 0.2	B a	0.4 ± 0.0	A a
48	0.3 ± 0.0	A a	1.3 ± 0.2	C a	0.6 ± 0.1	B a
			***Cit*:Fe**			
0	1.6 ± 0.1	A a	82.2 ± 28.3	B b	82.2 ± 28.3	B b
12	1.7 ± 0.1	A a	23.3 ± 4.4	B b	2.4 ± 0.6	A a
24	2.2 ± 0.3	A b	12.0 ± 1.9	B a	2.0 ± 0.3	A a
48	2.8 ± 1.2	A b	30.4 ± 6.7	B b	3.6 ± 0.7	A a
			***Mal*:Fe**			
0	2.1 ± 0.1	A a	34.7 ± 10.5	B b	34.7 ± 10.5	B c
12	2.3 ± 0.1	A a	12.0 ± 2.5	B a	1.5 ± 0.5	A a
24	2.3 ± 0.3	A a	7.6 ± 1.5	B a	1.4 ± 0.2	A a
48	3.5 ± 0.4	A b	20.3 ± 4.0	B b	3.5 ± 0.5	A b

4.1.7.2. Xylem sap

NA:Fe

The NA:Fe ratios were in the range 0.1-1.6, and showed no significant differences with time in +Fe and -Fe xylem sap (Table 4.11). In the case of Fe-resupplied plants (-Fe*), the NA:Fe ratios decreased by 87% from 0 to 12 h, and then increased 4-fold from 24 to 48 h.

Regarding treatments, the -Fe plants showed the highest NA:Fe ratios at 12 and 48 h, whereas the lowest ratios were found in -Fe* plants.

Cit:Fe

The xylem sap *Cit*:Fe ratios were in the range 3-99 (Table 4.11). In the +Fe plants the ratios were in the lower part of this range (4-17) and showed no significant changes with time, whereas in the -Fe plants the range was 19-102 and a major decrease (81%) was found from 0 to 24 h. In the -Fe* plants, the *Cit*:Fe ratio decreased by 98% from 0 to 12 h, followed by a 2-fold increase from 12-24 to 48 h.

Regarding treatments, the -Fe plants showed higher *Cit*:Fe ratios than the +Fe plants at 0, 24 and 48 h, whereas the +Fe plants showed higher ratios than the -Fe* plants at 12 h.

Mal:Fe

The *Mal*:Fe ratios in xylem sap were found in the range 5-754 (Table 4.11). In +Fe plants, the ratios were in the lower part of this range (47-122), and a 2-fold increase was found from 0 to 12 h followed by a 57% decrease at 24 h. On the other hand, in the -Fe plants the range was 218-754 and no differences were found with time. In contrast, in the Fe-resupplied plants (-Fe*) there was a drastic decrease (by 99%) in the *Mal*:Fe ratios from 0 to 12 h, and a large increase from 12-24 to 48 h.

Regarding treatments, the *Mal*:Fe ratios were the highest in -Fe plants at 0, 24 and 48 h, whereas the +Fe plants showed higher ratios than the -Fe* ones at 12 and 24 h.

4.1.7.3. Leaf apoplastic fluid

NA:Fe

The NA:Fe ratios in the apoplastic fluid were found between 0.5-2.3 and 0.4-1.9 in young and developed leaves, respectively (Table 4.12). The only significant difference with time was found in the developed leaves of -Fe plants, which showed a 3-fold increase from 0-12 to 24-48 h.

Table 4.11. Ligand:Fe ratios in tomato xylem sap in Fe-sufficient (+Fe), Fe-deficient (-Fe) and Fe-resupplied (-Fe*) plants at different sampling times (0, 12, 24 and 48 h). Groups were made based in Tukey or Games-Howell test (according to variance homogeneity test) with $p < 0.05$. Capital letters represent groups between different treatments at the same hour (rows) whereas lower case letters indicate groups of the same treatment at different hours (columns). Data are means ± SE, n = 3-4

	Xylem Sap					
Time (h)	**+Fe**		**-Fe**		**-Fe***	
			NA:Fe			
0	0.4 ± 0.1	A a	1.5 ± 0.2	B a	1.5 ± 0.2	B c
12	0.4 ± 0.1	B a	1.6 ± 0.6	C a	0.2 ± 0.0	A a
24	0.4 ± 0.1	B a	0.8 ± 0.2	B a	0.1 ± 0.0	A a
48	0.7 ± 0.1	B a	1.5 ± 0.5	C a	0.4 ± 0.0	A b
			***Cit*:Fe**			
0	6.6 ± 1.8	A a	101.7 ± 39.7	B b	101.7 ± 39.7	B c
12	16.2 ± 8.0	B a	52.8 ± 27.4	B ab	2.3 ± 0.1	A a
24	4.2 ± 0.7	A a	19.3 ± 6.3	B a	3.1 ± 0.5	A a
48	12.0 ± 0.8	A a	31.1 ± 10.7	B ab	6.9 ± 0.7	A b
			***Mal*:Fe**			
0	48.9 ± 13.3	A a	753.7 ± 286.6	B a	753.7 ± 286.6	B c
12	110.8 ± 24.3	B b	218.7 ± 118.6	B a	5.3 ± 0.8	A a
24	47.4 ± 14.9	B a	276.7 ± 56.3	C a	9.7 ± 1.4	A a
48	122.4 ± 51.5	A ab	318.0 ± 118.6	B a	51.5 ± 10.1	A b

Regarding treatments, the only differences in young leaves were found at 0 h, when the -Fe plants had a higher NA:Fe ratio than that found in the +Fe plants, and at 24 h, when +Fe plants had higher NA:Fe ratios than those found in the -Fe* plants. In the developed leaves the -Fe plants showed the highest NA:Fe ratios at 12, 24 and 48 h, and in the -Fe* plants this ratio was higher than that found in +Fe plants at 24 h.

Cit:Fe

The *Cit*:Fe ratios were in the ranges 16-789 and 191-999 in young and developed leaves, respectively (Table 4.12). In young leaves, the *Cit*:Fe ratios in the +Fe plants were in the lower part of the range (16-81), and showed a 66% decrease from 0 to 12 h followed by a large increase at 24-48 h. In the -Fe plants the *Cit*:Fe ratio decreased by 78% in the first 12 h. The Fe-resupplied plants (-Fe*) showed a 79% decrease in the *Cit*:Fe ratios from 0 to 12 h and a further decrease (53%) from 12 to 24-48 h. In the developed leaves no significant changes were found with time.

Regarding treatments, in the young leaf apoplastic fluid the *Cit*:Fe ratios were higher in -Fe plants than the +Fe plants at 0 and 12 h. In developed leaves this ratio was higher in the +Fe than in the -Fe plants at 12 and 24 h. At 12 h, the *Cit*:Fe ratio of the -Fe* plants was also higher than that of the -Fe plants, whereas at 24 h the *Cit*:Fe ratio of the -Fe* plants was lower than that in the +Fe plants.

Table 4.12. Ligand:Fe ratios in tomato leaf apoplastic fluid in Fe-sufficient (+Fe), Fe-deficient (-Fe) and Fe-resupplied (-Fe*) plants at different sampling times (0, 12, 24 and 48 h). Groups were made based in Tukey or Games-Howell test (according to variance homogeneity test) with $p < 0.05$. Capital letters represent groups between different treatments at the same hour (rows) whereas lower case letters indicate groups of the same treatment at different hours (columns). Data are means ± SE, n = 3-4

	Young leaf						Developed leaf					
Time (h)	**+Fe**		**-Fe**		**-Fe***		**+Fe**		**-Fe**		**-Fe***	
	NA:Fe						**NA:Fe**					
0	0.9 ± 0.3	A a	2.3 ± 0.2	B a	2.3 ± 0.2	B a	0.7 ± 0.2	A a	0.5 ± 0.1	A a	0.5 ± 0.1	A a
12	0.8 ± 0.2	A a	1.2 ± 0.8	A a	0.9 ± 0.5	A a	1.7 ± 0.2	A a	0.4 ± 0.0	B a	0.5 ± 0.1	A a
24	1.2 ± 0.2	B a	1.9 ± 0.8	AB a	0.5 ± 0.1	A a	0.5 ± 0.1	A a	1.9 ± 0.3	C b	0.8 ± 0.1	B a
48	1.3 ± 0.3	A a	2.2 ± 0.6	A a	1.0 ± 0.1	A a	0.5 ± 0.1	A a	1.4 ± 0.3	B b	0.8 ± 0.3	AB a
	***Cit*:Fe**						***Cit*:Fe**					
0	47 ± 6	A b	789 ± 193	B b	789 ± 193	B c	460 ± 124	A a	360 ± 119	A a	360 ± 119	A a
12	16 ± 2	A a	175 ± 70	B a	165 ± 14	B b	448 ± 68	B a	191 ± 9	A a	375 ± 64	B a
24	78 ± 7	A c	58 ± 25	A a	87 ± 12	A a	641 ± 165	B a	235 ± 53	A a	245 ± 41	A a
48	81 ± 23	A bc	98 ± 29	A a	69 ± 4.3	A a	680 ± 88	AB a	403 ± 83	A a	999 ± 361	A a
	***Mal*:Fe**						***Mal*:Fe**					
0	35 ± 7	A b	952 ± 298	B b	952 ± 298	B b	307 ± 67	B a	142 ± 40	A a	142 ± 40	A a
12	19 ± 4	A a	203 ± 43	B ab	149 ± 93	B a	411 ± 66	B a	121 ± 30	A a	317 ± 54	B a
24	87 ± 18	A c	121 ± 59	A a	77 ± 12	A a	389 ± 99	B a	196 ± 68	AB a	182 ± 28	A a
48	81 ± 23	AB bc	165 ± 35	B a	79 ± 4	A a	485 ± 71	B a	202 ± 40	A a	816 ± 196	B b

Mal:Fe

The *Mal*:Fe ratios were in the ranges 19-952 and 121-816 in young and developed leaves, respectively (Table 4.12). In young leaves, the *Mal*:Fe ratios in the +Fe plants were in the lower part of the range (19-87), and showed a 46% decrease from 0 to 12 h followed by a 4-fold increase from 12 to 24-48 h, whereas the -Fe plants showed a 87% decrease from 0 to 24 h. In the Fe-resupplied plants (-Fe*) the *Mal*:Fe ratio decreased by 84% from 0 to 12 h. In developed leaves the only difference with time was found in Fe-resupplied plants (-Fe*), with a 4-fold increase from 24 to 48 h.

Regarding treatments, the -Fe young leaves had the highest *Mal*:Fe ratios at 0 h, whereas the lowest ones were found in +Fe plants at 0 and 12. In developed leaves, the highest *Mal*:Fe ratios were found in +Fe plants, although no significant differences were found with the values observed in the -Fe plants at 24 h and with those in the -Fe* plants at 12 and 48 h. The -Fe* *Mal*:Fe ratios were also higher than those in -Fe plants at 12 and 48 h.

4.1.7.4. Leaf symplastic extract

The NA:Fe ratios in the symplastic extract were in the ranges 1.5-5.4 and 0.6-3.4 in young and developed leaves, respectively (Table 4.13). In young leaves, the NA:Fe ratios in the +Fe plants were in the lowest part of the range (1.5-2.5), and showed a 40% decrease from 0 to 48 h. In the -Fe plants a 51% decrease was observed from 0-12 to 24-48 h, whereas in the -Fe* plants a 59% decrease was observed from 0 to 12 h. In developed leaves, the +Fe plants showed a 70% decrease from 0-12 to 24-48 h, whereas in the -Fe* plants a 50% decrease was found from 0 to 12 h.

Regarding treatments, the -Fe plants showed the highest NA:Fe ratios in young leaves at 0, 12 and 48 h and in developed leaves at 12, 24 and 48 h. The -Fe* plants had higher NA:Fe ratios than those found in the +Fe plants in developed leaves at 24 and 48 h.

Table 4.13. NA:Fe ratios in tomato leaf symplastic fluid in Fe-sufficient (+Fe), Fe-deficient (-Fe) and Fe-resupplied (-Fe*) plants at different sampling times (0, 12, 24 and 48 h). Groups were made based in Tukey or Games-Howell test (according to variance homogeneity test) with $p < 0.05$. Capital letters represent groups between different treatments at the same hour (rows) whereas lower case letters indicate groups of the same treatment at different hours (columns). Data are means ± SE, n = 3-4

Time (h)	+Fe	-Fe	-Fe*
	Young leaf		
0	2.5 ± 0.3 A b	4.4 ± 0.6 B b	4.4 ± 0.6 B b
12	2.1 ± 0.6 A ab	5.4 ± 0.5 B b	1.8 ± 0.3 A a
24	2.0 ± 0.3 A ab	2.3 ± 0.4 A a	1.5 ± 0.3 A a
48	1.5 ± 0.1 A a	2.5 ± 0.5 B a	1.4 ± 0.1 A a
	Developed leaf		
0	2.0 ± 0.4 A b	2.8 ± 0.4 A a	2.8 ± 0.4 A b
12	1.5 ± 0.4 A b	3.4 ± 0.4 B a	1.4 ± 0.1 A a
24	0.6 ± 0.1 A a	3.2 ± 0.5 C a	1.3 ± 0.2 B a
48	0.6 ± 0.1 A a	2.4 ± 0.2 C a	1.7 ± 0.2 B a

Section 4.2

Objective 2 Results

Contribution of Cit, NA and DMA to the long-distance Fe transport in rice plants

This Chapter describes the effects of the lack of the xylem *Cit* transporter FRDL1 on the root and leaf concentrations of Fe, NA and DMA in rice plants grown under Fe-sufficient and -deficient conditions in hydroponics. Also, the Chapter describes the effects of foliar applications of *Cit* to WT and mutant *Osfrdl1* plants on the levels of the Fe, NA and DMA.

4.2.1. Changes in chlorophyll concentration

The time-course of the leaf chlorophyll concentration (SPAD readings) in Fe-sufficient (+Fe) and Fe-deficient (-Fe) WT and *Osfrdl1* plants foliar-treated with *Cit* (+*Cit*) or untreated (-*Cit*) are shown in Fig. 4.15.

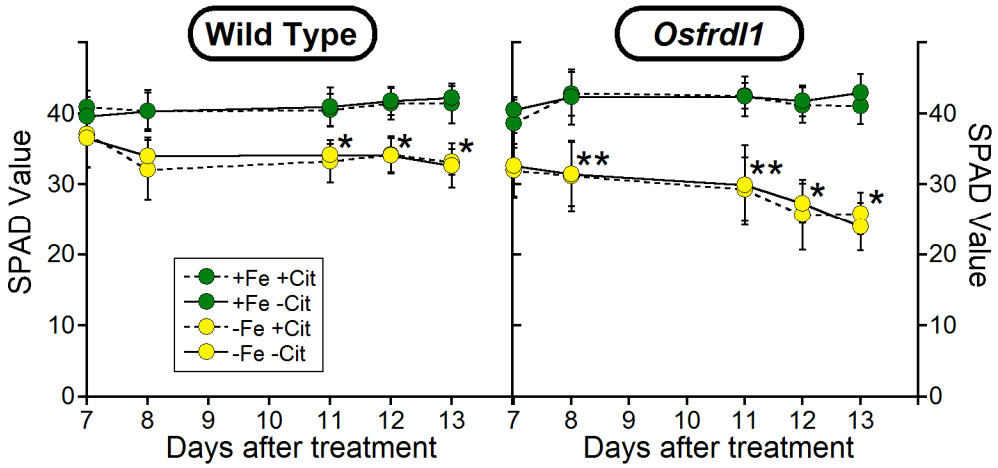

Fig. 4.15. Time-course of the SPAD levels in rice leaves of WT and *Osfrdl1* mutants grown with 0.2 µM Fe (-Fe) or 10 µM $FeSO_4$ (+Fe) and foliar-treated with (+Cit) or without (-Cit) 20 mM citrate. Values shown are means ± SD (n = 12), asterisks indicate significant differences among treatments at a given day (ANOVA test, * $p < 0.05$, ** $p < 0.10$)

The SPAD values were affected by the Fe supply and genotype but not by the exogenous *Cit* treatments. The +Fe plants of both genotypes (grown with 10 µM $FeSO_4$) did not develop chlorosis symptoms, with SPAD values in the range 35-45 regardless of the application of exogenous *Cit*. The -Fe treatment (0.2 µM $FeSO_4$) led to a decrease in SPAD values to 20-35 in both genotypes. The chlorosis developed sooner and more intensely in *Osfrdl1* than in the WT plants. On the other hand, the *Cit* application to -Fe plants did not affect SPAD levels regardless of the genotype.

4.2.2. Carboxylate concentrations in xylem sap

The xylem sap concentrations of *Cit* and *Mal* in +Fe and -Fe WT and *Osfrdl1* plants are shown in Fig. 4.16. In +Fe plants, the *Cit* and *Mal* concentrations were 197 and 242 µM in the WT and 53 and 218 µM in the *Osfrdl1* mutant, respectively. The low xylem sap *Cit* levels found in *Osfrdl1* plants confirmed the loss of function of the FRDL1 protein as reported Yokosho *et al.* (2009). In both genotypes, *Cit* concentrations were not affected significantly by Fe deficiency, whereas *Mal* concentrations increased 1.5- and 2-fold with Fe deficiency in the WT and *Osfrdl1* plants, respectively (in the latter case, the increase was significant only at $p < 0.10$). This increase in *Mal* is in line with the increases in xylem sap *Mal* found in barley, another *Poaceae* species (López-Millán *et al*., 2012).

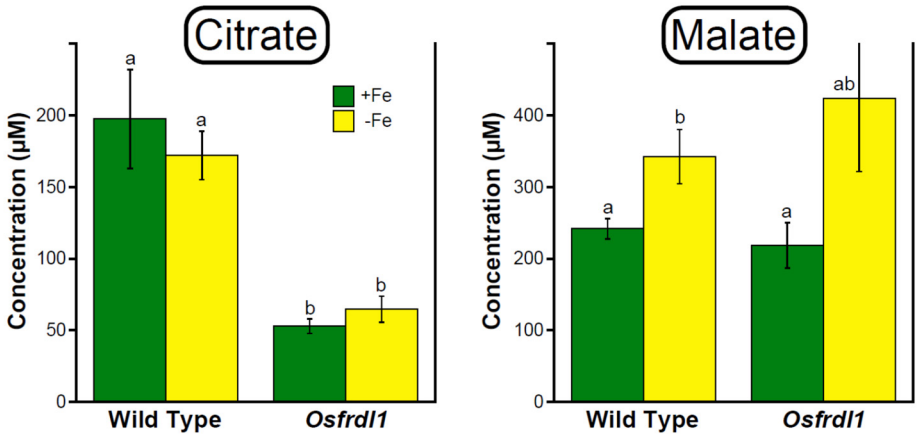

Fig. 4.16. Concentrations of *Cit* and *Mal* in the xylem sap of WT and *Osfrdl1* plants grown for 14 days with 10 µM (+Fe) or 0.2 µM (-Fe) $FeSO_4$. Values shown are means ± SD, n = 3. Different letters above the columns indicate significant differences among treatments and genotypes (Tukey's test, $p < 0.05$)

4.2.3. Iron concentration in leaf and root tissues

The leaf and root Fe concentrations of +Fe and -Fe WT and *Osfrdl1* plants treated with (+*Cit*) or without (-*Cit*) *Cit* are shown in Fig. 4.17. All +Fe plants showed high root Fe concentrations, with values between 2500 and 3700 µg g^{-1}, with no significant differences among genotypes or *Cit* treatments. In contrast, the root Fe concentration of -Fe plants was one order of magnitude lower, below 200 µg g^{-1}, regardless of the genotype and *Cit* treatment. The application of *Cit* did not lead to significant changes in root Fe concentrations.

In the case of leaves, the Fe concentrations were in the range 90-290 µg g^{-1}. The Fe concentrations of the +Fe WT plants not treated with *Cit* were 165 µg g^{-1}, much lower than those of the rest of the +Fe plants (240-290 µg g^{-1}). In the -Fe plants, leaf Fe concentrations were below 120 µg g^{-1}, and were significantly lower than those in the +Fe treatment in the cases of the +*Cit* WT and in both the +*Cit* and -*Cit Osfrdl1* plants.

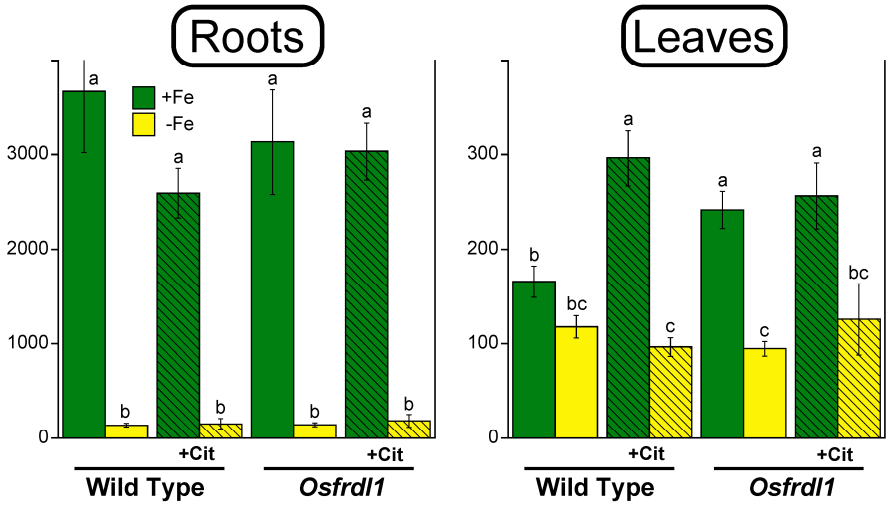

Fig. 4.17. Root and leaf Fe concentrations of WT and *Osfrdl1* plants grown for 14 days with 10 µM (+Fe) or 0.2 µM (-Fe) $FeSO_4$ and foliar-treated with (+Cit) or without 20 mM citrate. Data are means ± SD of 4 replicates. Different letters above the columns indicate significant differences among treatments and genotypes (Tukey's test, $p < 0.05$)

4.2.4 Nicotianamine and 2'-deoxymugineic acid concentrations in root and leaf tissues

4.2.4.1. Roots

In roots, DMA was more abundant that NA, with concentrations of 12-61 and 0.4-3.8 µg g^{-1}, respectively (Fig. 4.18).

The root NA concentrations of the +Fe plants not treated with *Cit* were 2.9 and 2.3 µg g^{-1} in WT and *Osfrdl1*, respectively, and *Cit* application did not cause significant changes. In the -Fe plants not treated with *Cit* the NA concentrations in WT and *Osfrdl1* were 3.1 and 0.4 µg g^{-1}, respectively, which indicates that Fe deficiency causes a strong decrease in the root NA concentration in the mutant.

When *Cit* was applied to the -Fe plants, the NA concentrations were 1.5 and 2.1 µg g^{-1} in WT and *Osfrdl1*, respectively. Therefore, *Cit* applications led to a marked decrease

(56%) in the NA root concentration in the -Fe WT and to a large increase (5-fold) in the NA root concentration in -Fe *Osfrdl1*.

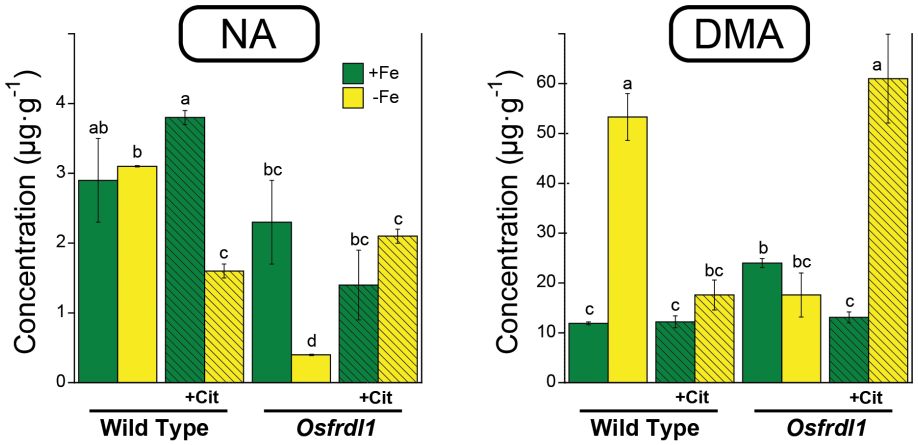

Fig. 4.18. Root NA and DMA concentrations of WT and *Osfrdl1* plants grown for 14 days with 10 µM (+Fe) or 0.2 µM (-Fe) $FeSO_4$ and foliar-treated with (+Cit) or without 20 mM citrate. Data are means ± SD of 4 replicates. Different letters above the columns indicate significant differences among treatments and genotypes (Tukey's test, $p < 0.05$)

Concerning the root DMA concentrations in the +Fe plants not treated with *Cit*, they were 12 and 24 µg g^{-1} in WT and *Osfrdl1*, respectively. When *Cit* was applied to these plants, no changes were found in the WT and a 55% decrease was found in *Osfrdl1*. In the -Fe plants not treated with *Cit*, the DMA concentrations were 53 and 18 µg g^{-1} in WT and *Osfrdl1*, respectively, which evidences an effect of Fe deficiency (a 4-fold increase) only in the WT plants. When *Cit* was applied to -Fe plants, the DMA concentrations increased 3-fold in the *Osfrdl1* plants, whereas a 67 % decrease occurred in the WT.

4.2.4.2 Leaves

In leaves DMA was also more abundant than NA, with concentrations in the ranges of 16-120 and 0.8-5.0 µg g^{-1} (Fig. 4.19), respectively. This indicates that leaves were generally richer in DMA than roots. The leaf NA concentrations of +Fe plants not treated with *Cit* were 5.0 and 3.9 µg g^{-1} in WT and *Osfrdl1*, respectively, and when *Cit* was applied to these plants no significant changes in the NA concentrations were found. The NA concentrations of -Fe plants not treated with *Cit* were in the range of 0.8-1.2 µg g^{-1} in both genotypes, which evidences that Fe deficiency caused major decreases in NA

concentrations (72-84%) regardless of the genotype. The application of *Cit* to -Fe plants did not affect leaf NA concentrations in both genotypes.

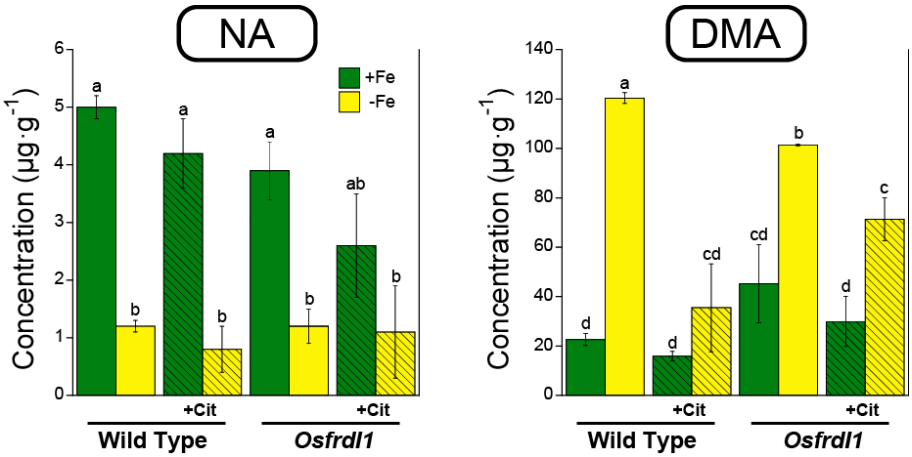

Fig. 4.19. Leaf NA and DMA concentrations of WT and *Osfrdl1* plants grown for 14 days with 10 µM (+Fe) or 0.2 µM (-Fe) $FeSO_4$ and foliar-treated with (+Cit) or without 20 mM citrate. Data are means ± SD of 4 replicates. Different letters above the columns indicate significant differences among treatments and genotypes (Tukey's test, $p < 0.05$)

The leaf DMA concentrations of +Fe plants not treated with *Cit* were 22.6 and 45.2 µg g^{-1} in WT and *Osfrdl1*, respectively. When *Cit* was applied to these plants no significant changes in DMA concentrations were found. The DMA concentrations of -Fe plants not treated with *Cit* were in the range of 101-120 µg g^{-1} in both genotypes, indicating that Fe deficiency leads to increases in DMA concentration (4.5- and 2.6-fold in WT and *Osfrdl1*, respectively). When *Cit* was applied to the -Fe plants, the DMA concentrations decreased markedly (71 and 30% decreases in WT and *Osfrdl1*, respectively).

Section 4.3

Objective 3 Results

Effects of the overexpression of NA and DMA synthesis genes on the localization of metal micronutrients and metal ligands in rice seed

In this Chapter, the changes in the concentrations of NA, DMA and metal micronutrients in the embryo and endosperm of rice seeds as affected by the overexpression of *nicotianamine synthase* (*OsNAS*) and/or the expression of barley *nicotianamine aminotransferase* (*HvNAAT*) are shown. Also, quantitative maps for the metal concentrations in rice seed sections, obtained by LA-ICP-MS, are used to depict the effects on element distribution in the different structures of the rice embryos in four genotypes (WT, *OsNAS*, *HvNAAT* and *OsNAS+HvNAAT*).

4.3.1. Characterization of rice transgenic lines

Rice transformation allowed the generation of transgenic lines with different degrees of *OsNAS1* and *HvNAATb* overexpression (alone or in combination), as shown in the RNA Northern blots of leaves for six selected lines (Fig. 4.20). Two different lines of each type were studied: lines 92 and 267 for *OsNAS1*, 7 and 67 for *HvNAATb* and 89 and 98 for *OsNAS1* + *HvNAATb*. The mRNA abundance for *OsNAS1* and *HvNAATb* was different in each line, even when lines overexpressed the same gene. The expression of *OsNAS1* was higher in line 92 than in line 267, the expression of *HvNAATb* was much higher in line 67 than in line 7, and the expression of both *OsNAS1* and *HvNAATb* were higher in line 98 than in line 89.

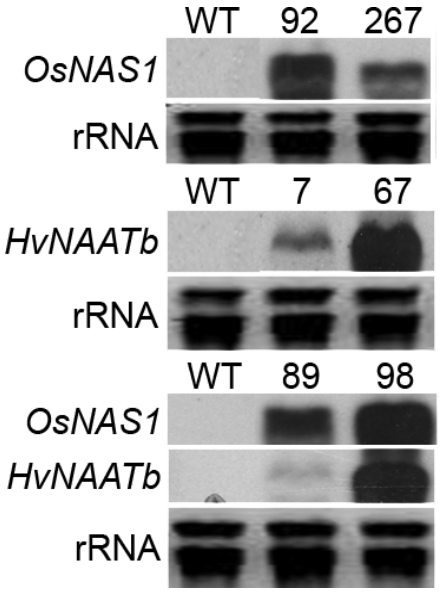

Fig. 4.20. RNA blot showing transgene expression in the leaf tissue of WT and trangenic lines overexpressing *OsNAS1* and/or expressing *HvNAATb*. rRNA: ribosomal RNA

4.3.2 Concentrations of nicotianamine and 2'deoxymugineic acid in the embryo and endosperm of rice seeds

As indicated in the Materials and Methods section, the embryo and endosperm part of the seeds were separated using a razor blade, and therefore both sample include parts of the aleurone layer.

The overexpression of *OsNAS1* and/or the expression of *HvNAAT* led to changes in the concentrations of NA and DMA in both the embryo and endosperm (Fig. 4.21). In WT rice, the NA concentration in the embryo was 6.0±1.5 μg g^{-1}, whereas in the endosperm the NA

concentration was below the limit of quantification (LOQ). In the WT seeds DMA was found at concentrations of 24.2±1.5 μg g^{-1} in the embryo and 13.5±1 μg g^{-1} in the endosperm. Therefore, the DMA/NA ratio in the embryo was approximately 4.

The overexpression of *OsNAS1* increased the NA concentrations in the embryo (15- and 2.5-fold in lines 92 and 267, respectively) and in the endosperm (reaching values well above the LOQ, 29.1±4.8 and 6.4±0.1 μg g^{-1} in lines 92 and 267, respectively). The concentrations of DMA also increased in the embryo in line 92 (3.5-fold) but did not change significantly in line 267, and increased in the endosperm (10.5- and 6.2-fold in lines 92 and 267, respectively). Therefore, the embryo DMA/NA ratios decreased with the overexpression of *OsNAS1*, from the control values of 4 down to approximately 1 and 3 for lines 92 and 267, respectively. On the other hand, the endosperm DMA/NA ratios were 5 and 13 for lines 92 and 267, respectively. It is remarkable that the overexpression of *OsNAS1* boosts the production not only of NA but also of DMA, probably because of the higher substrate availability for NAAT.

The expression of *HvNAATb* did not change significantly the NA concentrations in both the embryo and endosperm, whereas the effects on DMA differed between lines. In line 7, the DMA concentration in the embryo showed a large increase (4.2-fold) but in the endosperm it was decreased by 71%. In contrast, in line 67 the DMA concentration was unaffected in the embryo and increased 2-fold in the endosperm. The DMA/NA ratios in the embryo increased with the expression of *HvNAATb* from the control values of 4 up to 34 and 10 for lines 7 and 67, respectively.

In the two double transgenic lines (89 and 98), the effects of the overexpression *OsNAS1* and expression of *HvNAATb* on the NA and DMA concentrations were different. In line 89, the NA concentrations increased both in the embryo (a 3.0-fold increase) and the endosperm (to 16.8 μg NA g^{-1}), and the DMA concentrations also increased in both tissues (4.1- and 9.2-fold in the embryo and endosperm, respectively). However, in line 98 the NA concentrations decreased (although only significantly at $p < 0.10$) by 76% in the embryo and were below the LOQ in the endosperm, whereas the DMA concentration showed very large increases in both tissues (12- and 19-fold in the embryo and endosperm, respectively). Therefore, the embryo DMA/NA ratios increased in *OsNAS1+HvNAATb* seeds from the control values of 4 up to 7 and 185 for lines 89 and 98, respectively. The endosperm DMA/NA ratio for line 89 was 7. The concentrations of NA and DMA in seeds are in line with the abundance of *OsNAS1* and *HvNAATb* found in each line

(Fig. 5.1): in line 89 seeds were richer in both NA and DMA than the WT ones, whereas in line 98 seeds were poorer in NA and richer in DMA than the WT ones.

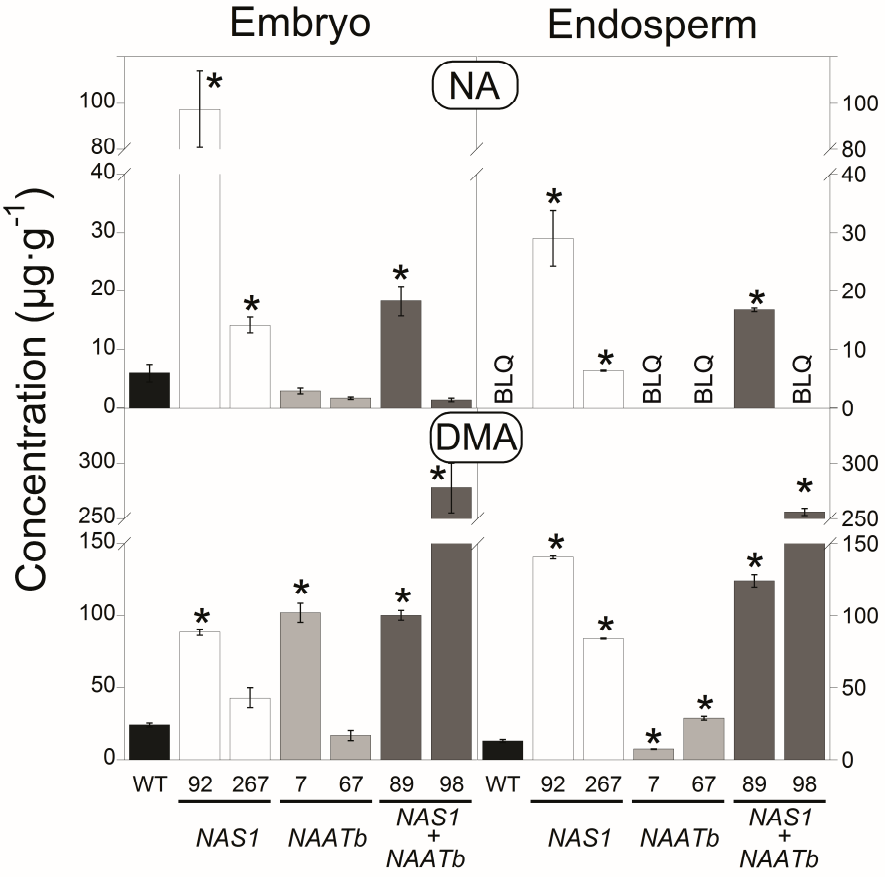

Fig. 4.21. NA and DMA concentrations in the embryo and endosperm of WT and transgenic rice seeds. Asterisks indicate significant differences (t-Student test, $p < 0.05$) when compared against the concentrations in the WT. Values shown are means ± SE, n = 3-4, *BLQ: below LOQ*

4.3.3. Metal concentrations in the embryo and endosperm of rice seeds

The concentrations of Fe, Mn, Cu and Zn in the embryo and endosperm are shown in Fig. 4.22. In the WT, the Fe concentration was 99 ± 6 µg g^{-1} in the embryo and 20 ± 1 µg g^{-1} in the endosperm. The Fe concentrations were higher in all four lines overexpressing *OsNAS1* (92, 267, 98 and 89), both in the embryo (1.3- to 2.1-fold higher) and the endosperm (1.7- to 2.9- fold). In contrast, the Fe concentration did not change much in lines expressing *HvNAATb*: the only significant change in the Fe concentration was found in the endosperm of line 7, which was reduced by 33% when compared with the concentration in the WT.

In the case of Zn, the concentrations in the WT were 102 ± 1 µg g^{-1} in the embryo and 21 ± 1 µg g^{-1} in the endosperm. In the case of the *OsNAS1* overexpressors, the Zn concentration

generally increased significantly in the embryo (1.3- and 1.2-fold in lines 92 and 267, respectively) and endosperm (2.5- and 1.3-fold in lines 92 and 267, respectively). The expression of *HvNAATb* did not lead to significant changes in Zn concentrations in the embryo and endosperm in relation to the WT. In the case of the *OsNAS1+HvNAATb* genotypes, in line 89 the Zn concentration did not change in the embryo and increased 2.5-fold in the endosperm, whereas in line 98 the Zn concentration was reduced by 40% in the embryo and was unaffected in the endosperm.

Regarding Mn, the concentrations in the WT were 76 ± 1 μg g^{-1} in the embryo and 16 ± 2 μg g^{-1} in the endosperm. In the embryo, the Mn concentration was reduced in the *OsNAS1* overexpressor line 267 and the *OsNAS1+HvNAATb* line 89 (in both cases by 18%) and increased by 25% in the *HvNAATb* overexpressor line 7. In the endosperm, the only significant change was found in the *OsNAS1* overexpressor line 92, which showed a 42% increase when compared to the WT value.

In the case of Cu, the WT concentrations were 10 ± 1 μg g^{-1} in the embryo and 7 ± 1 μg g^{-1} in the endosperm. In the embryo, the Cu concentrations increased in the *OsNAS1* overexpressor line 267 (1.3-fold) and the *OsNAS1+HvNAATb* lines 89 (2-fold) and 98 (2-fold), whereas no significant changes were found in the rest of lines studied. In the endosperm, the only changes found in Cu concentrations were a decrease in the *OsNAS1* overexpressor line 92 (27%) and increases of 1.2 and 1.4-fold in the *OsNAS1* overexpressor line 267 and the *OsNAS1+HvNAATb* line 89, respectively.

4.3.4. Correlations between metal ligand and metal concentrations in the embryo and endosperm

The correlations between the concentrations of metal ligands and metals and in the embryo and endosperm, using data obtained from all rice lines, are shown in Table 4.14. In the embryo, the DMA concentration was correlated significantly only with the concentration of Cu (r^2 of 0.736; $p < 0.01$), whereas the NA concentration was correlated significantly with those of Fe and Zn (r^2 of 0.599 and 0.561, respectively; $p < 0.05$). On the other hand, the concentration of Fe was correlated significantly with those of Mn (r^2 0.587; $p < 0.05$), Cu (r^2 0.579; $p < 0.05$) and specially Zn (r^2 0.787; $p < 0.01$), whereas the concentration of Mn was correlated significantly with that of Zn (r^2 0.854; $p < 0.01$). In the endosperm, the concentration of DMA was strongly correlated with that of Fe (r^2 0.951; $p < 0.01$), but no correlation was found with those of other metals. The concentration of NA was highly correlated with those of Mn and Zn (r^2 0.831 and 0.895,

respectively; $p < 0.01$), but not with that of Fe. The only relationship between metal micronutrients in this tissue was found between Zn and Mn (r^2 0.876; $p < 0.01$).

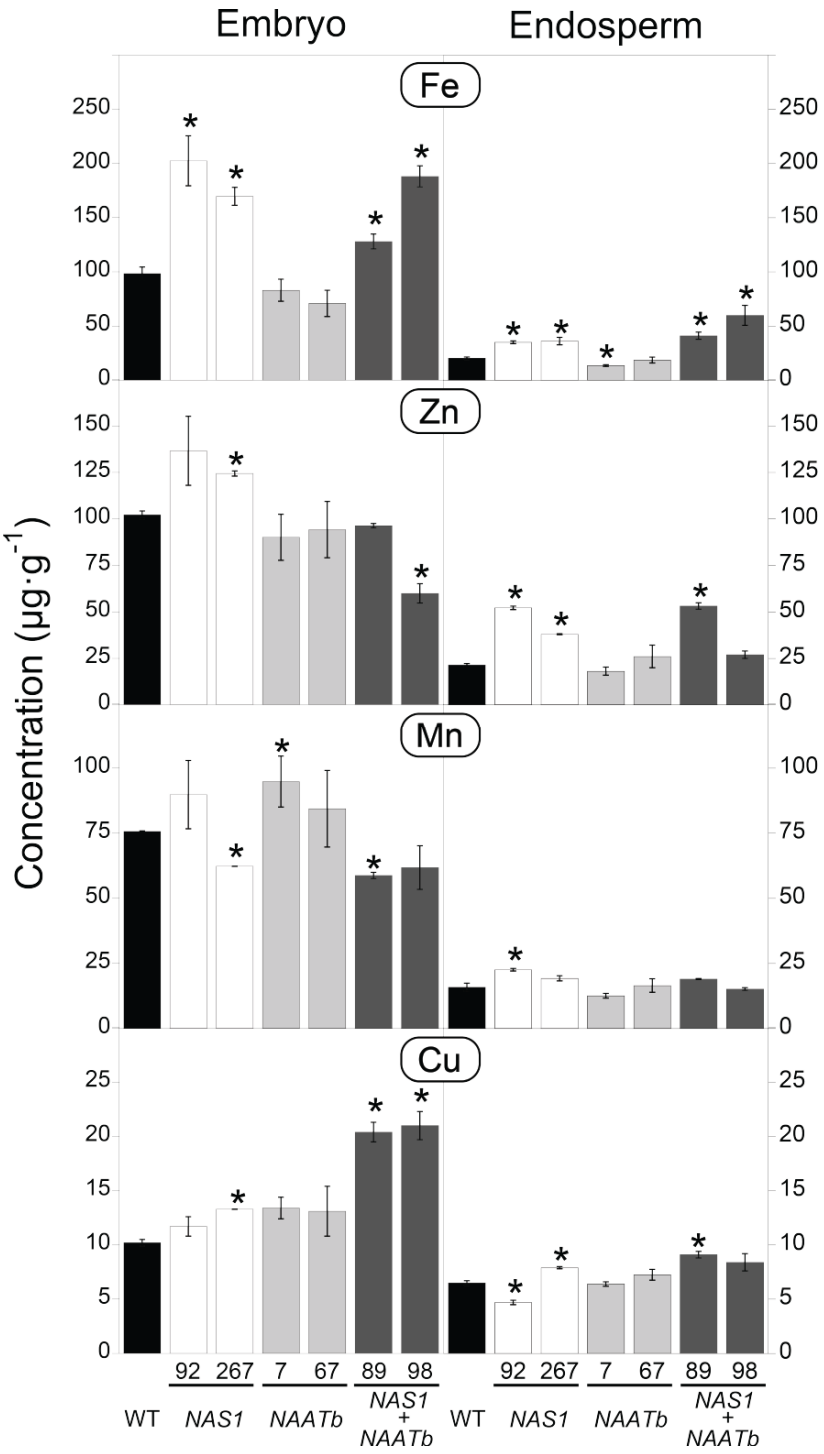

Fig. 4.22. Concentrations of Fe, Mn, Cu and Zn in the embryo and endosperm of WT and transgenic rice seeds. Asterisks indicate significant differences (t-Student test, $p < 0.05$) when compared against the concentrations in the WT. Values shown are means ± SE, n = 3-4, *BLQ: below LOQ*

Table 4.14. Pearson correlations between the concentrations of NA, DMA, Fe, Mn, Cu and Zn in embryo and endosperm of rice seeds

Embryo					
	DMA	**NA**	**Mn**	**Fe**	**Cu**
DMA	1				
NA	0.018	1			
Mn	0.069	0.427	1		
Fe	0.352	**0.599***	**0.587***	1	
Cu	**0.736****	-0.096	0.296	**0.579***	1
Zn	-0.103	**0.561***	**0.854****	**0.787****	0.188
Endosperm					
	DMA	**NA**	**Mn**	**Fe**	**Cu**
DMA	1				
NA	0.297	1			
Mn	0.276	**0.831****	1		
Fe	**0.951****	0.231	0.283	1	
Cu	0.324	-0.341	-0.176	0.458	1
Zn	0.409	**0.895****	**0.876****	0.424	0.07

**, significant differences at $p < 0.01$; *, significant differences at $p < 0.05$

Table 4.15. Pearson correlations between the sum of NA and DMA and the ratio NA/DMA with the concentrations of concentrations of NA, DMA, Fe, Mn, Cu and Zn in embryo and endosperm of rice seeds

Embryo		
	NA+DMA	**NA/DMA**
DMA	**0.939****	-0.223
NA	0.361	**0.930****
Mn	0.211	0.205
Fe	**0.535***	0.36
Cu	**0.653***	-0.407
Zn	0.097	0.401

Endosperm		
	NA+DMA	**NA/DMA**
DMA	**0.993****	0.274
NA	0.407	**0.950****
Mn	0.366	**0.891****
Fe	**0.938****	0.247
Cu	0.268	-0.325
Zn	0.502	**0.890****

**, significant differences at $p < 0.01$; *, significant differences at $p < 0.05$

The correlations between the sum of NA and DMA and the ratio NA/DMA with the concentrations of metal and metal ligands in the embryo and endosperm were calculated using the data from all lines (Table 4.15). In the embryo, the sum of the concentrations of NA and DMA was significantly correlated with the concentrations of Fe and Cu (r^2 0.535 and 0.653, respectively; $p < 0.05$), whereas the NA/DMA ratio was not correlated significantly with the concentrations of any metal micronutrient. In the endosperm, the sum of the NA and DMA concentrations was correlated significantly only with the concentration of Fe (r^2 0.938; $p < 0.01$), whereas the ratio NA/DMA was strongly correlated with the concentrations of Mn and Zn (r^2 0.891 and 0.890, respectively; $p < 0.01$).

4.3.5. Selection of the optimal rice seed section

Sections of rice seeds were taken using the protocol described by Johnson *et al.* (2011) with some modifications, and 60 µm-thick sections (*vs*. 70 µm in the original method) were obtained without causing a major disruption of the seed embryo structures. For the metal localization study three different cut types were considered: lateral-longitudinal (Fig. 4.23a), lateral (Fig. 4.23b) and longitudinal dorso-ventral (Fig. 4.23c). The longitudinal dorso-ventral cut (Fig. 4.23c) was selected as the optimal one, based on the number of tissues contained in the section and the significant variability in the metal concentration in any given tissue (see below). This cut (Fig. 4.24) allowed for the simultaneous visualization of the root (RP) and leaf primordia (LP), as well as other seed structures, including the scutellum (SC) -that surrounds the primordia-, the transfer cell layer (TC) between the embryo and the endosperm, and the aleurone layer (AL) that covers both the embryo and the starchy endosperm (SE). In contrast, the lateral and lateral-longitudinal sections (Fig. 4.23 *a* and *b*) were not used because i) both cuts only allow the visualization of either the leaf or root primordia tissues, ii) the coverage of the embryo area is always less comprehensive than that in the longitudinal dorso-ventral cut, and iii) the variability of the element concentrations within a given structure was quite large, as explained in detail below (Section 4.3.7). For example, the Fe mapping obtained using the longitudinal dorso-ventral allowed to find that the tip of the leaf primordia tissue had higher Fe concentrations than the basal zone, whereas neither the lateral nor the lateral-longitudinal cuts could detect this difference.

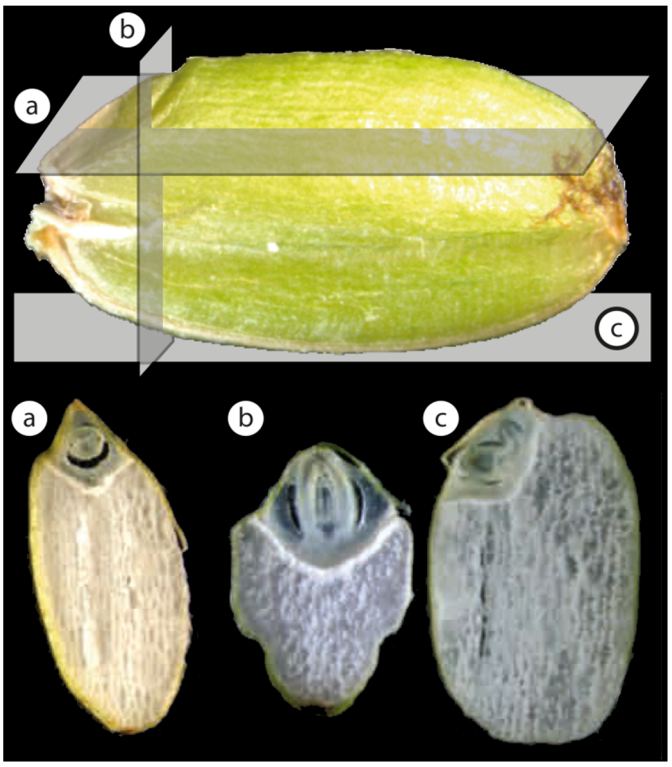

Fig. 4.23. Rice seed sections obtained with the vibrating microtome: lateral-longitudinal section (*a*), lateral section (*b*), and longitudinal dorso-ventral section (*c*)

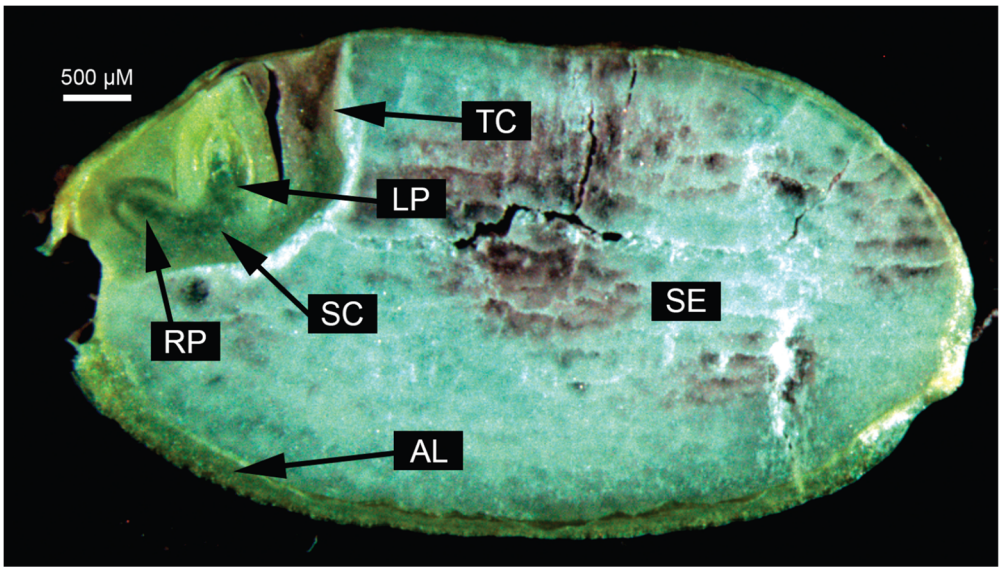

Fig. 4.24. Longitudinal dorso-ventral 60 µm-thick section of a rice seed.
S) scutellum, RP) root primordium, LP) leaf primordium, TC) transfer cells layer, AL) aleurone layer, SE) starchy endosperm

4.3.6. Perls staining of rice seed sections

Perls staining was used as a first approach to determine a qualitative distribution of Fe in rice seeds, since it is a fast and relatively easy technique to assess Fe accumulation in the tissues. It should be stated that this method only allows the detection of labile Fe (including Fe hydroxides, inorganic Fe and complexes with *Cit* and NA; Rios *et al.,* 2016; Fig. 4.25). Differences in Perls staining were found between the different rice genotypes studied (Fig. 4.26).

In the WT, seeds showed a light blue coloration in the scutellum and some parts of the aleurone layer and a more intense color in the transfer cell layer between the embryo and endosperm. In the *OsNAS1* overexpressor genotype (line 92) the whole embryo was intensely colored, with the blue color being especially intense in the root primordia and scutellum. The leaf primordium showed a light coloration, whereas the aleurone layer was more stained than in the WT. The transfer cell layer was also stained in this line. In the *HvNAATb* expressor genotype (line 67), the scutellum was less stained than in the *OsNAS* line, whereas the transfer cell layer and the root primordium were intensely colored. The aleurone layer showed only a light stain. The double transgenic line *OsNAS1+HvNAATb* (89) showed a pattern similar to that observed in the *HvNAATb* line, but the staining was much more intense. The Perls stain was very strong in the scutellum, root primordium, transfer cell layer and aleurone layer.

None of the lines showed a blue coloration in the endosperm. This is likely due to the chelation and/or integration of the existing Fe by/with molecules that would not permit the formation of the Perls stain (*e.g.*, phytate). Considering the typical Fe concentrations found in rice endosperm excluding the aleurone layer (4 µg g^{-1} DW) and assuming an endosperm water content of about 20%, one may expect average Fe concentrations of approximately 60 µM, which should be still detectable using Perls (Rios *et al*., 2016). The absence of significant Perls stain in the endosperm suggests that the presence of labile Fe forms is unlikely if they are homogeneously distributed in the endosperm.

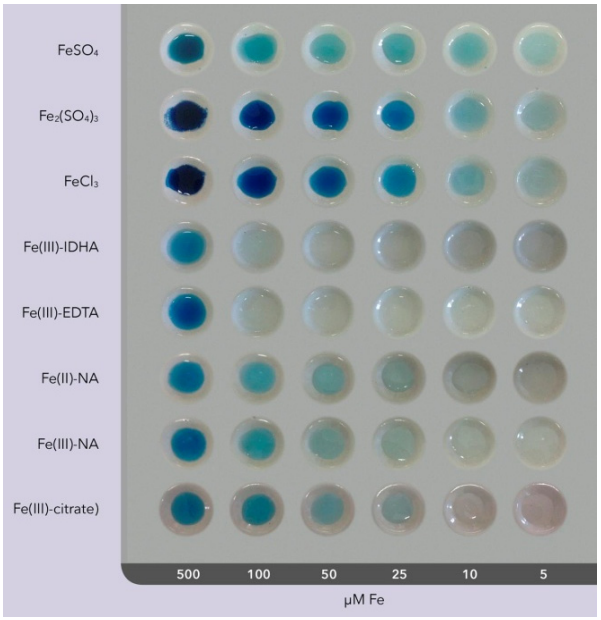

Fig. 4.25. Image of Perls blue stain with the different Fe compounds (from Rios *et al.,* 2016)

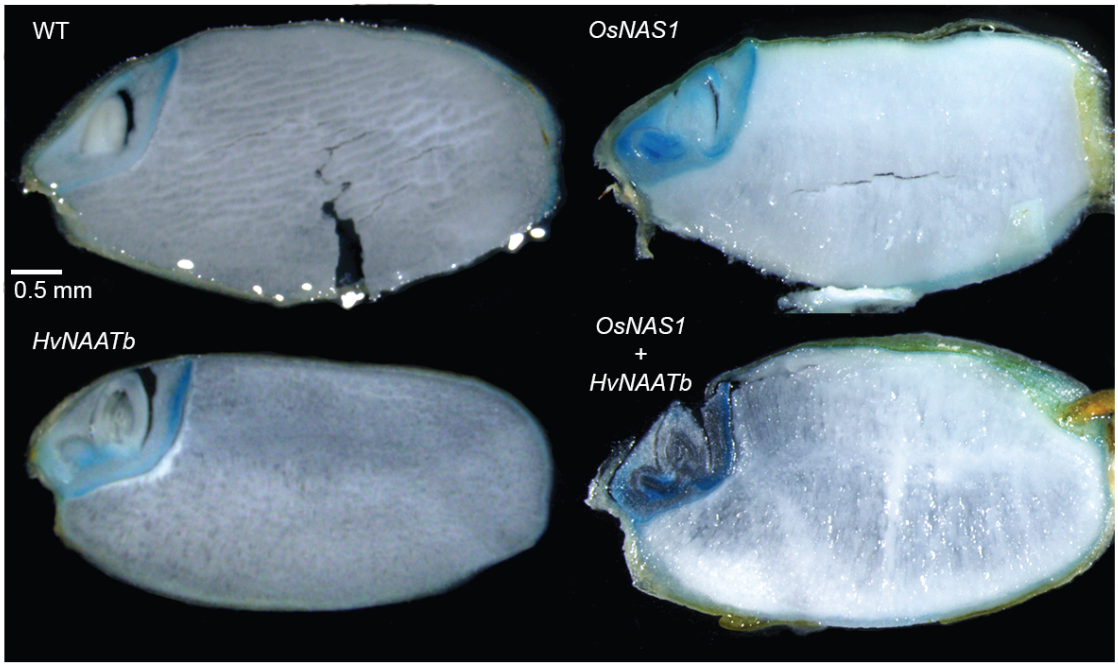

Fig. 4.26. Perls staining of longitudinal dorso-ventral sections of WT and transgenic rice seeds

4.3.7. Element localization in rice seeds with LA-ICP-MS

The elemental quantitative maps obtained with LA-ICP-MS from the WT and two lines each of the rice genotypes studied are shown in Fig. 4.27, along with the corresponding optical views of the sections analyzed. The color scales used in Fig. 4.27 represent the concentrations for each element, with the lowest ones in dark blue and the highest ones in red (for a given element, the same scale was used in all genotypes). ^{56}Fe, ^{64}Zn, ^{63}Cu and ^{55}Mn were expressed in µg element g^{-1} DW (parts per million; ppm) and ^{31}P and ^{32}S were expressed in % (w/w). The maps obtained had a good spatial resolution, allowing for the differentiation of elemental concentrations between embryo structures. It should be noted that for line 7, slight differences between the optical view and the maps ocurred because the seed section was broken during analysis, causing the shift of a piece of the lower part of the endosperm.

The first remarkable aspect is the preferential accumulation in the embryo, which had high concentrations of most elements, whereas in the endosperm the element concentrations were generally lower or below the LOQ, with the only exceptions of ^{32}S and ^{63}Cu. Large differences in element distribution and concentration were found among the different genotypes (Fig. 4.27).

In the special case of Fe, maps are also presented using different concentration scales for each sample in one line of each genotype (Figure 4.28) for a better understanding of the distribution in the different structures of the seed sections. In the WT seeds, Fe was found mainly in the transfer cell layer and root primordium (in a concentration range of 150-220 µg Fe g^{-1} DW), whereas much lower concentrations were found in the aleurone layer (25-40 µg Fe g^{-1} DW) and the endosperm (5-15 µg Fe g^{-1} DW) (Figs. 4.27 and 4.28). In the seeds of the *OsNAS1* overexpressor lines 92 and 267, Fe was increased in the root primordia as well as in the scutellum (Fig. 4.27), with concentrations from 250 to 575 µg Fe g^{-1} DW (line 267 in Fig. 4.28). The *HvNAATb* expressor lines 7 and 67 showed lower Fe concentrations in the embryo than those found in the WT (Fig. 4.27), and in line 67 this element was preferentially in the transfer cell (50-200 µg Fe g^{-1} DW) and aleurone layers (50-100 µg Fe g^{-1} DW; Fig. 4.28). In the double transgenic lines *OsNAS1+HvNAATb*, Fe concentrations were similar than those found in *OsNAS1* in the root primordia, higher (up to 800 µg Fe g^{-1} DW) than those found in both WT and *OsNAS1* in the transfer cell layer, and lower (from 250 to 300 µg Fe g^{-1} DW) than those found in the *OsNAS1* (but still higher that those in the WT) in the scutellum (Fig. 4.27 for both lines and in Fig. 4.28 for line 89). No changes in starchy endosperm Fe concentration were found among genotypes.

In the case of Zn, there were large differences in concentrations between the different seed parts, with the distribution being quite similar in all genotypes (Fig. 4.27). As in the case of Fe, Zn maps are also presented using different concentration scales in one line of each genotype to better appreciate differences among genotypes (Figure 4.28). The WT seed showed the highest Zn concentration in the leaf primordia, ranging from 500 to 1200 μg g^{-1} DW, with the concentration in the scutellum and transfer cells being *ca.* 300 μg Zn g^{-1} DW (Figs. 4.27 and 4.28). The *OsNAS1* overexpressor showed similar values in the leaf primordium than those found in the WT, whereas in the root primordium and scutellum the Zn concentration increased (1500 and 400-600 μg Zn g^{-1} DW, respectively) when compared with the WT. The *HvNAATb* lines showed the maximum Zn concentrations in the leaf primordium and the transfer cell layer, reaching values of *ca.* 500 and 200 μg Zn g^{-1} DW, respectively, which were lower than those in the WT. The double transgenic lines also showed increases in Zn concentrations when compared to the WT, although these (400-700 μg Zn g^{-1} DW in the leaf and root primordia and below 300 μg Zn g^{-1} DW in the scutellum) were lower than those found in *OsNAS1* overexpressors. The Zn concentration in endosperm was always between 10 and 30 μg Zn g^{-1} DW regardless of the genotype.

Manganese was localized in high concentrations (150 to 350 μg Mn g^{-1} DW) in the leaf and root primordia, with the Mn concentrations in the transfer cell and aleurone layers being similar in all genotypes with the exception of the double transgenic *OsNAS1+HvNAATb* line 89 (Fig. 4.27). In this line, the Mn concentration in the cited tissues were generally higher (200-400 μg Mn g^{-1} DW) than the other lines. In the endosperm, Mn was not detected for any genotype.

Copper was the less abundant micronutrient of those investigated, and differences in distribution between genotypes were less marked (Fig. 4.27). This element was found in the whole embryo and in the aleurone layer, with concentrations in the range of 8 to 20 μg Cu g^{-1} DW. In the embryo, the two double transgenic lines (89 and 98) had the highest concentrations of Cu, whereas the two *HvNAATb* lines (7 and 67) had the lowest ones.

Phosphorus was present with similar distribution and concentrations in all genotypes investigated (Fig. 4.27). This element was mainly located in the embryo and the aleurone layer (at concentrations between 1 and 2%) and was not detected in the endosperm.

Sulphur was present in the whole embryo and the endosperm, and it was mainly located in the leaf and root primordia and the aleurone layer, at concentrations of approximately 0.2%, without any consistent difference among genotypes (Fig. 4.27). It is also worth to remark the gradient of S concentrations, from high in the aleurone layer to low in the endosperm.

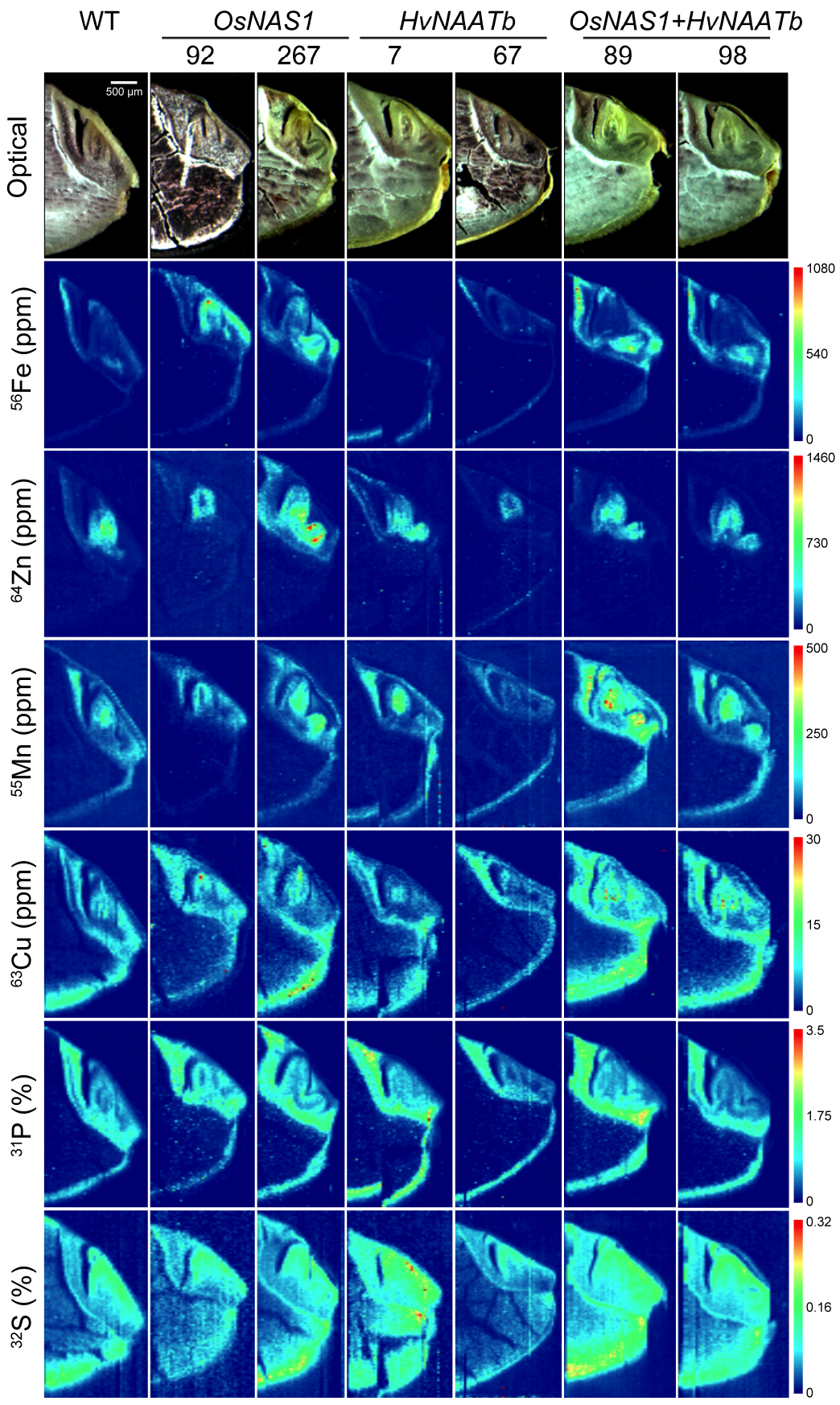

Fig. 4.27. Quantitative elemental maps of WT and transgenic rice seeds sections

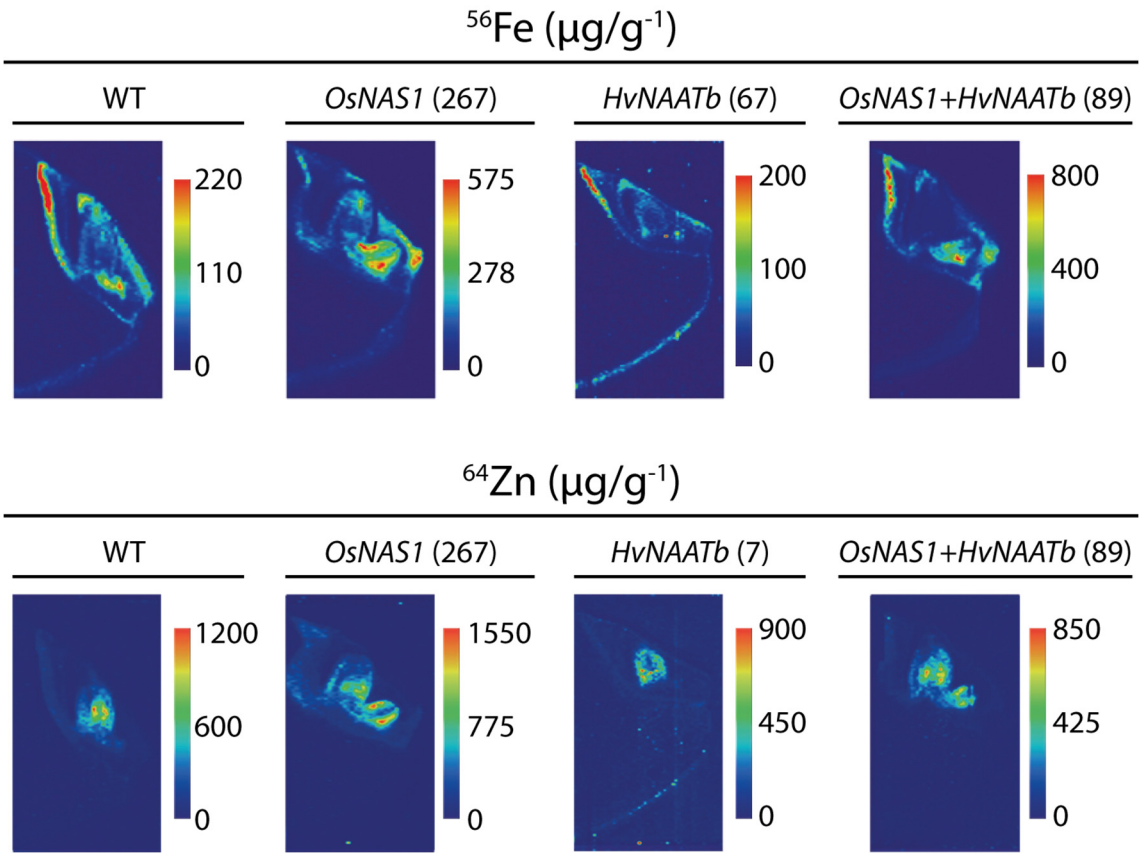

Fig. 4.28. Elemental maps of ^{56}Fe and ^{64}Zn in WT and transgenic rice seeds sections

Section 4.4

Phloem Sap Results

I. Phloem sap Fe and NA concentrations as affected by Fe deficiency in oilseed rape

II. Performance of phloem sap extraction in rice

This Chapter includes data on the purity and Fe and NA concentrations in the phloem sap sampled using bleeding from Fe-sufficient (+Fe) and Fe-deficient (-Fe) oilseed rape plants, as well as the phloem sap volumes obtained using aphids with the stylectomy protocol from WT and *OsNAS1* overexpressor rice plants.

4.4.1. Oilseed rape phloem sap

4.4.1.1 Sugar concentrations

The concentrations of glucose, fructose, and sucrose were measured to assess phloem sap purity (Table 4.16). The concentration of sucrose in the phloem sap was *ca*. 380 mM, whereas glucose and fructose concentrations were in the range from 1.5 to 6.1 mM. Iron deficiency did not affect the sucrose and glucose concentrations and decreased by 38% the fructose concentration. Therefore, reducing sugars accounted for 2.2 and 1.7% of the total sugars in +Fe and -Fe samples, respectively. These values are similar to those obtained in other phloem sap studies (Giavalisco *et al*., 2006; Mendoza-Cózatl *et al.*, 2008), and are indicative of highly pure phloem sap. These results also indicate that there are no major differences in phloem sap purity between treatments.

Table 4.16. Sucrose, glucose and fructose (in mM) concentrations in the phloem sap from Fe-sufficient (+Fe) and Fe-deficient (-Fe) *Brassica napus* plants. Values are means ± SD, n = 7. Different letters within a row indicate statistically significant differences (Student's t-test, $p < 0.05$)

	+Fe	-Fe
Sucrose (mM)	374 ± 39 a	384 ± 54 a
Glucose (mM)	6.1 ± 0.4 b	5.0 ± 0.6 b
Fructose (mM)	2.4 ± 0.5 b	1.5 ± 0.3 a
Reducing sugars/total sugars	2.2 ±3.3 b	1.7 ± 0.4 a

4.4.1.2 Iron and nicotianamine concentrations

Time-courses of the Fe and NA concentrations in oilseed rape phloem sap are shown in Figure 4.29. The Fe concentrations in the phloem sap of +Fe plants were higher than those in the -Fe plants (2- to 7-fold higher, on the average 4-fold) at all sampling times. The NA concentration in the phloem sap was also higher in the +Fe plants, although the difference was smaller than in the case of Fe (1.2- to 1.5-fold higher, an average of 1.4-fold) at all sampling times. The NA:Fe ratios in the Fe-sufficient plants were in the 0.4-0.8 range, whereas in Fe-deficient plants the ratios were in the 1.0-2.1 range.

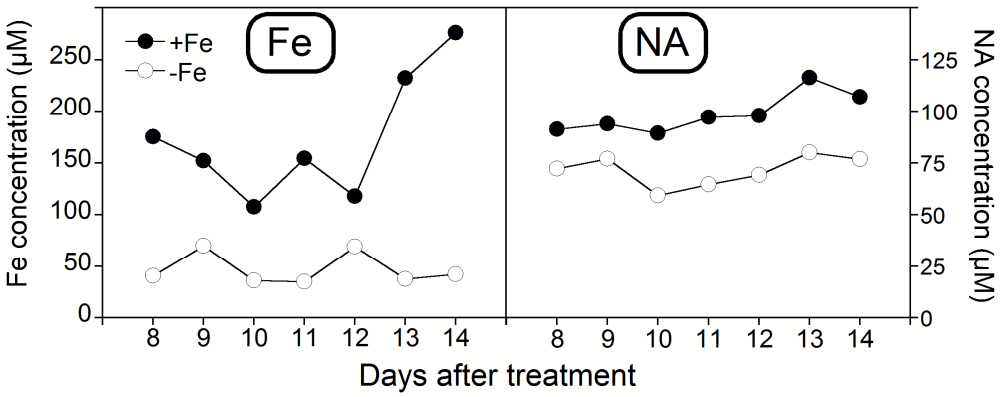

Fig. 4.29. Time-course of Fe and NA concentrations in phloem sap from Fe-sufficient (+Fe) and Fe-deficient (-Fe) oilseed rape plants. Plants were grown until flowering and then transferred to a 45 µM Fe(III)-EDTA (+Fe) or 0 µM Fe (-Fe) treatments

4.4.2. Rice phloem sap

The volumes of phloem sap obtained from WT and *OsNAS1* overexpressor rice plants with the stylectomy protocol are shown in Table 4.17.

The small volumes obtained from rice plants (1.6 µL and 2.7 µL in total) did not allow the quantification of metals nor NA in this fluid. Since the metal and NA quantification methods used requires at least 2000 and 60 µL of liquid for analysis, respectively, samples should be diluted 1:2000 and 1:60. Since the Fe and NA concentrations reported in rice phloem sap are in the ranges of 40-74 and 66-83 µM, respectively (Ando *et al*., 2012; Yoneyama *et al*., 2015), the 1:2000 and 1:60 dilutions of the samples would lead to Fe and NA concentrations of 0.02-0.04 and 1.1-1.4 µM. These concentrations are near or below the limit of quantification (LOQ) of the instruments used for the metal (ICP-MS, LOQ = 0.02 µM) and NA (HPLC-ESI-MS, LOQ = 5 µM in standards, without considering possible matrix effects) analyses.

In addition, to determine the purity of the samples more volume would be needed for the determination of sugars or, at least, measuring the pH.

Table 4.17. Volumes of phloem sap obtained with the stylectomy protocol. Several aphids were used for each plant, allowing obtaining different aliquots from the same plant

Wild type	
Plant	**Volume (nL)**
Plant 1	388
	299
	296
	500
Plant 2	0
Plant 3	0
Plant 4	0
Plant 5	163
Total	**1646**

OsNAS1	
Plant	**Volume (nL)**
Plant 1	0
Plant 2	0
Plant 3	476
	67
	436
	32
Plant 4	476
	480
	240
	460
	48
Total	**2715**

Because of all the stated above, the determination of metals and metal ligands in rice phloem sap could not be carried out, and further samplings would be required until enough volume could be obtained. This minimum volume required is considered to be at least 10 μL.

Chapter 5

Discussion

The next pages discuss Fe transport in relation to NA in the fluids of Strategy I plants affected by Fe-deficiency and Fe-resupply (Section 5.1), as well as in the tissues of a Strategy II plant affected either by the lack of a *Cit*-mediated long distance Fe transport (Section 5.2) or by the overexpression of NA and DMA synthesis (Section 5.3). The changes in Fe and NA and the relationships with other metals and metal-ligands are critically analyzed and causes and effects of these changes are proposed.

Section 5.1

Objective 1 Discussion

Effects of iron status on the concentrations of metal micronutrients, nicotianamine and carboxylates in tomato plant fluids

In this Thesis, the first comprehensive analysis of metal micronutrients and organic ligand concentrations in plant fluids with a high degree of purity has been carried out, using the Strategy I species tomato. The results obtained are discussed following the flow of Fe within the plant (Fig. 5.1) starting with short-distance transport in roots, continued with long-distance transport *via* xylem and finally with short-distance transport in young and developed leaves.

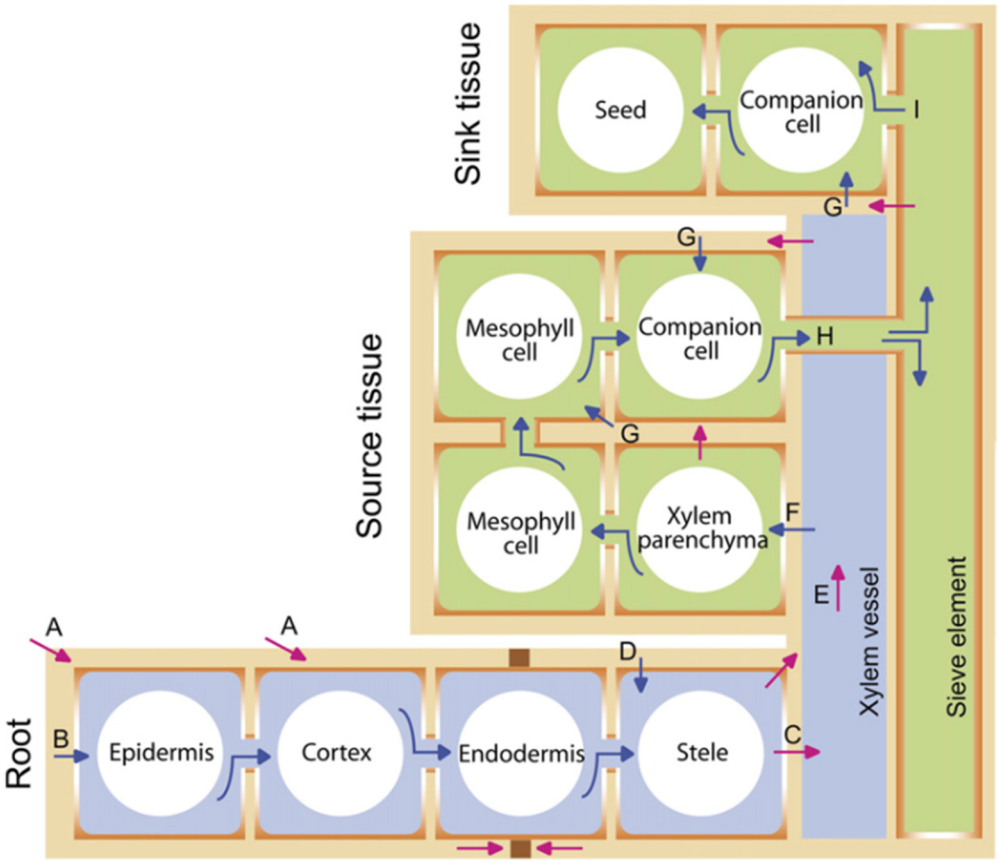

Fig. 5.1. Fe transport from the soil to the seed. Red arrows represent speculative flow of apoplastic Fe; blue arrows indicate Fe movement into symplastic space. After initial diffusion from the soil (A), Fe is imported into epidermal or cortex cells (B). Once in the cytoplasm, Fe moves through symplastic passages to the stele and then is exported into a xylem vessel (C). Apoplastic leakage is blocked by the Casparian strip (shown in brown boxes). Fe precipitates in root apoplast is re-absorbed under Fe-deficiency (D). Fe is transported to the shoot through the transpiration stream (E) and imported into the leaf cytoplasm (F). Fe precipitates in shoot apoplast are remobilized on demand of sink tissues (G). Fe moves through symplastic passages from a source tissue to a sink tissue *via* phloem loading (H) and unloading (I). From Kim and Guerinot (2007)

Data obtained allows for the assessment of the short- and long-distance transport of Fe in different compartments of the whole plant. The results obtained (Figs. 4.4-14 and Tables 4.2-9) are summarized in Figs. 5.2-5.3. In these Figures, Fe is shown as red dots and the major metal ligands NA and *Cit* are shown as blue squares and green triangles, respectively. The role of NA in Fe transport will be discussed in the next Sections in relation to carboxylates and other metals as affected by Fe deficiency and Fe resupply.

5.1.1. Effects of iron status on the concentrations of metal micronutrients and metal ligands in roots

Metal micronutrients in the root apoplastic fluid and symplastic extract

Roots of plants grown under Fe deficiency conditions generally have reduced Fe concentrations and increased concentrations of other metal micronutrients such as Mn, Cu and Zn. This has been previously reported in pea (Cohen *et al*., 1998), sugar beet (López-Millán *et al*., 2001a) and "Tres Cantos" tomato (Carrasco-Gil *et al*., 2016). Upon Fe resupply, root Fe concentrations have been shown to increase rapidly in tomato (Zamboni *et al*., 2016), as well as in other species such as sugar beet (López-Millán *et al*., 2001a) and maize (Thoiron *et al*., 1997). However, no direct analyses of metal concentrations in root fluids in conditions of Fe deficiency and resupply have been published so far. On the other hand, it has been reported that most of the root Fe is located in the apoplastic space in Fe-sufficient and Fe-deficient plants resupplied with Fe. This has been shown in different species, including tomato (Becker *et al*., 1992), wheat (Zhang *et al*., 1991) and red clover (Jin *et al*., 2007). This information was always obtained (indirectly) by determining the Fe concentrations before and after washing roots with a solution containing an Fe chelating agent (usually EDTA or bipyridyl) to remove metal apoplastic contents, a protocol that provides apoplastic and symplastic Fe contents expressed on a root mass basis. Therefore, this Thesis is the first study to measure metal concentrations directly in both root apoplastic and symplastic extracts.

The decreases found in root apoplastic and symplastic Fe concentrations in response to Fe deficiency are in line with previous studies with tomato whole root tissues (Carrasco-Gil *et al*., 2016; Zamboni *et al*., 2016) (Fig. 5.2; see also Fig. 4.4 and Table 4.2). Then, upon Fe-resupply to Fe-deficient tomato plants the root apoplastic fluid Fe concentration increased 9- and 24-fold after 12 and 24 hours, respectively (up to 400 μM;

Figs. 5.2-5.3; see also Fig. 4.4 and Table 4.2), and later on it decreased at 48 hours to values similar to those found in the Fe-sufficient controls (Figs. 5.2-5.3). In the root symplastic extract, the Fe concentration increased to a maximum at 12 hours, to reach values similar to those found in +Fe plants, and then decreased slowly with time (Figs. 5.2-5.3; see also Fig. 4.4 and Table 4.2). These results suggest that the Fe acquired by root epidermal cells reaches progressively the root apoplastic space, leading to further transport into the vascular tissues and also helping to avoid the toxicity that would appear if symplastic Fe concentrations are too high. A tight regulation of the symplastic extract Fe concentration is supported by the moderate concentrations found in the extracts of Fe-sufficient and Fe-resupplied plants, which were always lower than 150 μM. The high apoplastic fluid Fe concentrations at 24 h after resupply could be associated to the stop of the xylem sap flow during the dark period, since the xylem sap transpiration stream, providing continuous loading and transport of elements to the upper parts of the plant, is only active during the light period (from 0 h to 14 h after resupply). The occurrence of labile Fe pools in the root cell walls under these circumstances (which could be possibly remobilized at a later point) cannot be excluded without further experiments.

Root concentration increases have been reported for other metal micronutrients upon Fe deficiency, and attributed to the low specificity of the root IRT1 transporter, which is capable to transport not only Fe(II) but also other divalent metals such as Zn(II), Mn(II) and Cd(II) (Korshunova *et al*., 1999, Vert *et al*., 2002; Barberon *et al*., 2014). However, the lack of major changes in the concentration of these metals in tomato root fluids with Fe deficiency (see Fig. 4.4 and Table 4.2) suggests that they could have been immobilized in the root cell walls. Also, upon Fe-resupply the IRT1 transporter could be saturated with Fe(II), impairing to some extent the transport of divalent metals other than Fe (Korshunova *et al*., 1999). Indeed, after Fe-resupply the Mn concentrations decreased both in the apoplastic fluid and symplastic extracts. However, the effects of Fe-resupply on Zn were different, with concentrations increasing 2-fold at 24 h in the root apoplastic fluid and being unchanged in the root symplastic extracts. Therefore, the changes in root fluid metal concentrations cannot be explained only by the saturation of IRT with Fe.

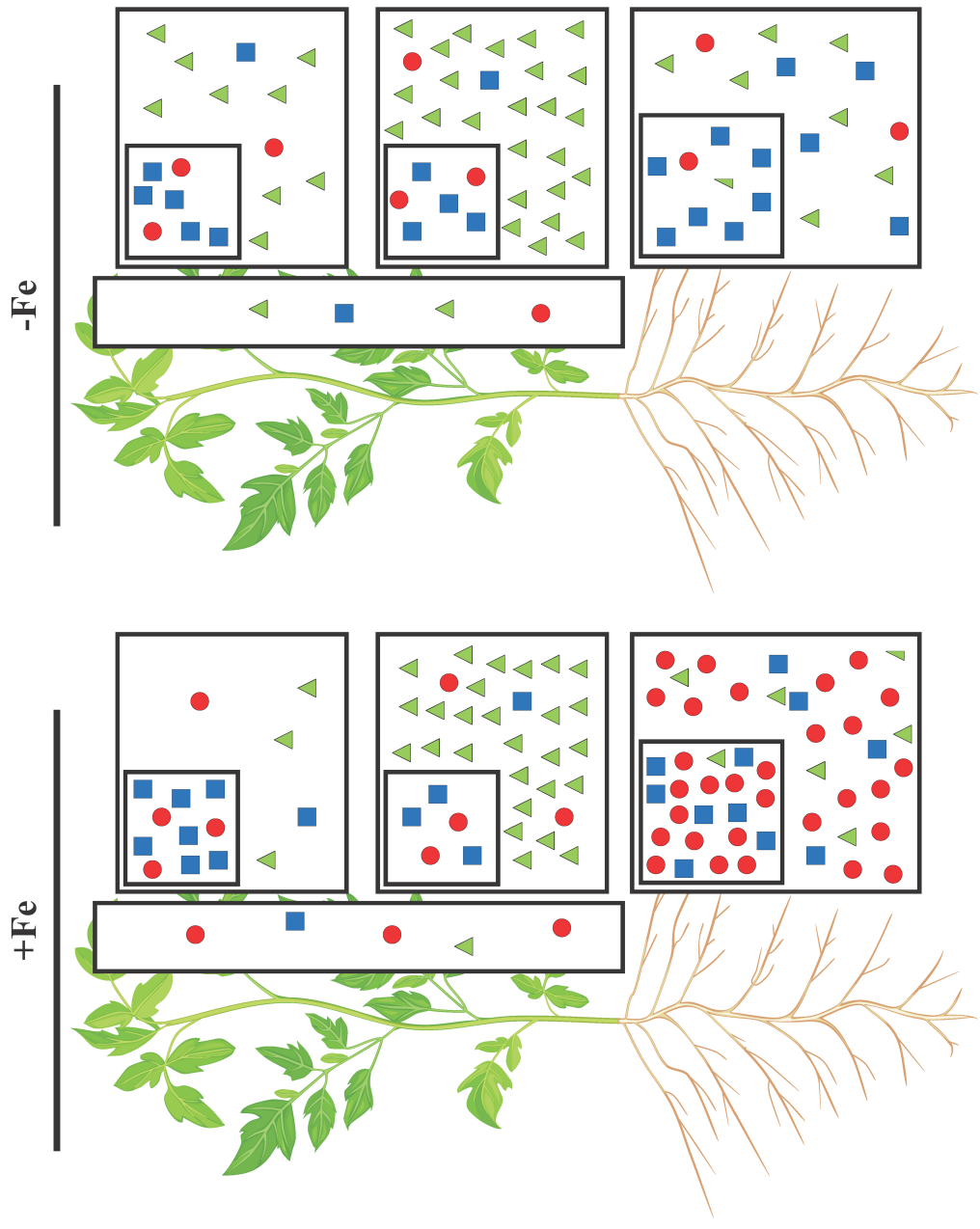

Fig. 5.2. Schematic representation of the effect of Fe deficiency on Fe, NA and *Cit* concentrations in xylem sap, apoplastic fluid and intracellular extracts of tomato plants. **Cit* concentrations in leaf symplastic extract are not depicted, no data are available due to matrix interferences. ● Fe (10 µM) ■ NA (10 µM) ▲ *Cit* (200 µM)

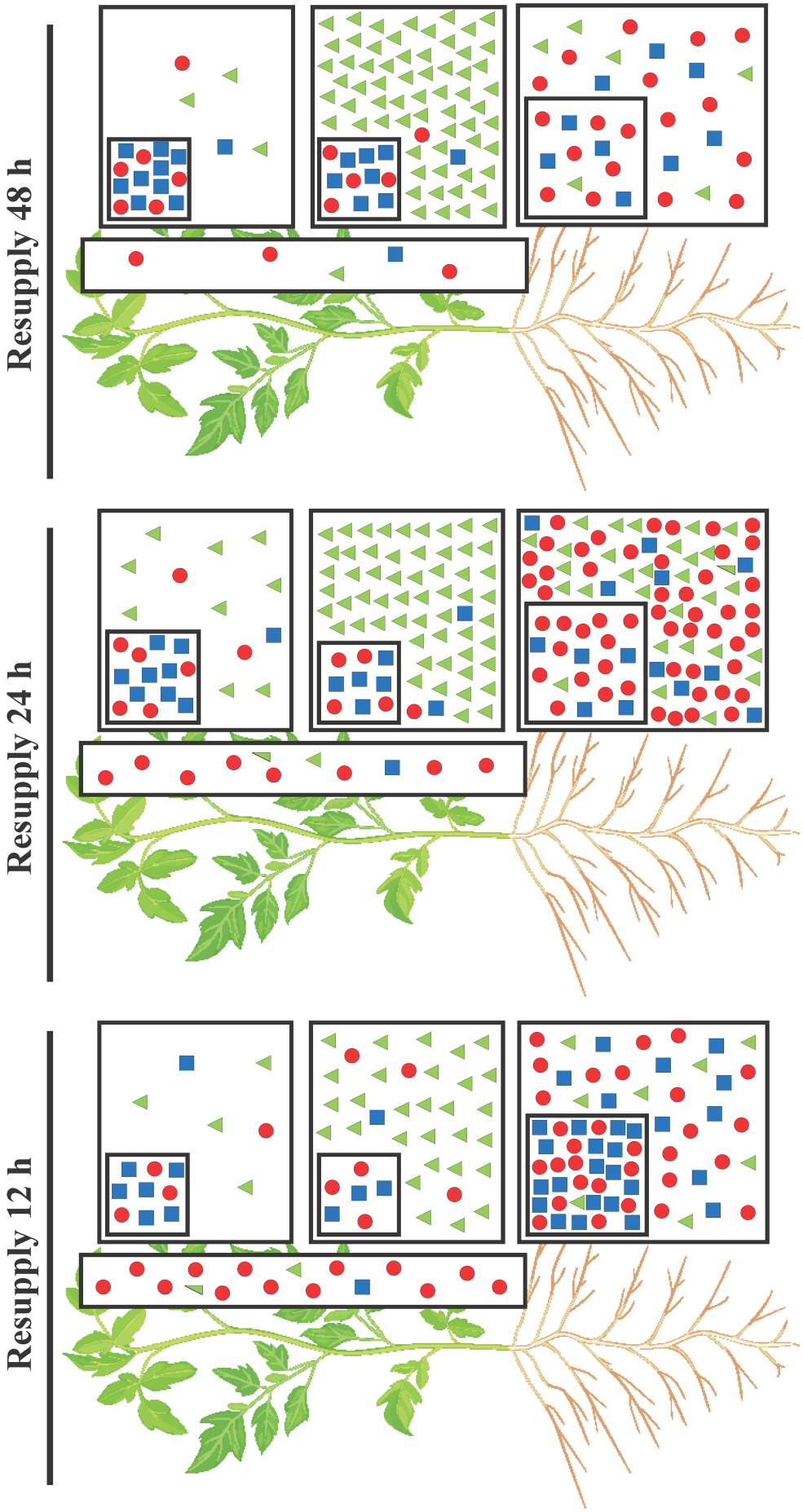

Figure 5.3. Schematic representation of the effect of Fe deficiency and Fe resupply on Fe, NA and *Cit* concentrations in xylem sap, apoplastic fluid and intracellular extracts of tomato plants. **Cit* concentrations in leaf symplastic extract are not depicted. No data are available due to matrix interferences.

Nicotianamine in the root apoplastic fluid and symplastic extract

Nicotianamine is synthesized by the enzyme NAS, which is localized in the cytoplasm associated to the plasma membranes (Higuchi *et al*., 1994, Yang *et al*., 2015 Nozoye *et al*., 2014a). This enzyme is known to be induced in response to Fe deficiency in *A. thaliana* and melon (Waters *et al*., 2014), but until now data on the NA concentrations in whole roots of Strategy I species are still scarce. Nicotianamine concentrations reported so far in roots of Fe-sufficient and Fe-deficient *A. thaliana* plants are in the ranges 20-30 and 40-60 μg g^{-1} FW, respectively (Deinlein *et al*., 2012; Haydon *et al*., 2012; Tsednee *et al*., 2014). In sugar beet roots, relative increases of 8-, 13- and 2.5-fold have been reported with Fe-deficiency and after 24 and 72 h Fe-resupply, respectively, using a metabolomics GC-MS approach (Rellán-Álvarez *et al*., 2010b).

The concentrations of NA reported here for tomato root apoplastic fluid and symplastic extract from tomato plants were in the ranges 11-103 μM and 14-183 μM, respectively, and were similar in the Fe-sufficient and Fe-deficient plants (Fig. 5.2; see also Fig. 4.8 and Table 4.6). The concentrations of NA were higher than those of Fe in the case of the -Fe plants. Upon Fe-resupply, the NA concentration increased rapidly both in the symplastic extract and apoplastic fluid, accompanying the increases in Fe concentrations in these fluids that occur in the first 12 h (Figs. 5.2-5.3), and then decreased in the following hours. This supports that i) Fe resupply elicits the synthesis of NA in the cytoplasm, and ii) there is an active efflux of NA to the apoplastic fluid. This efflux may occur *via* transport of NA or metal-NA complexes through YSL transporters (Curie *et al*., 2009) or other members of the OPT family (Vasconcelos *et al*., 2008).

Carboxylates in the root apoplastic fluid and symplastic extract

The increases in carboxylate concentrations with Fe deficiency in whole roots have been well documented in tomato (López-Millán *et al*., 2009) and other species (Rabotti *et al*., 1995; Alhendawi *et al*., 1997; López-Millán *et al*., 2000b, 2001a; see Abadía *et al*., 2002 for a review). However, the effects of Fe-resupply to Fe-deficient plants in root carboxylate concentrations are much less documented. In sugar beet roots, general decreases in carboxylate concentrations with Fe-resupply were reported in the long term (96 h after resupply) (López-Millán *et al*., 2001a; Rellán-Álvarez *et al*., 2010b).

In the present tomato study, *Cit* was the only carboxylate increasing its concentration with Fe deficiency in both root apoplastic fluid and symplastic extract

during the full time course experiment (Fig 5.2; see also Fig. 4.12 and Table 4.7). The concentrations of other carboxylates either did not change significantly or were lower with Fe deficiency (Fig. 4.12 and Table 4.7). Both the increases in *Cit* and the decreases in *Mal* and 2-oxoglutarate concentrations in root symplastic extract are in agreement with previous results with tomato root tip extracts (López-Millán *et al*., 2009).

Iron resupply led to a decrease in the concentration of most carboxylates in the root apoplastic fluid at 12 h, with the only exception of *Cit* (Figs. 5.2-5.3; see also Fig. 4.12 and Table 4.7). This is likely a consequence of a fast metabolic readjustment, as reported in sugar beet roots (López-Millán *et al*., 2001a; Rellán-Álvarez *et al*., 2010b). The secretion of organic acids to the rizosphere (Keuskamp *et al*., 2015) and/or the export to the vascular stream (see below) may also contribute to the decrease in carboxylate concentrations with Fe resupply. The relatively high concentrations of carboxylates in the root apoplastic fluid at 24 h after resupply, occurring concomitantly with the Fe concentration maximum, are possibly associated to the stopped xylem sap flow at night time.

Root apoplastic and symplastic transport of iron facilitated by organic ligands

Iron can be transported either symplastically or apoplastically through the root cortex until the endodermis and Casparian strip, where Fe must enter cells to be transported symplastically into the vascular system (Fig 5.4). Tomato, as a Strategy I species, reduces Fe^{3+} complexes in the soil solution to Fe^{2+}, which is then taken up by the divalent ion transporter IRT1. Once inside the cell, the neutral pH of the cytoplasm (approximately 7.0) would allow for the formation of the stable Fe(II)-NA complex even in the presence of other metal ligands such as *Cit* (Rellán-Álvarez *et al*., 2008). The Fe(II)-NA complex is the most likely vehicle for Fe transport in the symplast of the root cortex.

In Fe-deficient plants the levels of symplastic Fe decreased when compared to the controls, whereas the symplastic NA concentrations were unaffected. On the other hand, Fe resupply led to a large increase both in Fe and NA symplastic concentrations after 12 h. Therefore, the NA:Fe ratio was higher than 1 both in the Fe-deficient and in the 12 h Fe-resupplied plants. Later on, at 24 and 48 h of Fe resupply, the NA:Fe ratios became lower than 1, down to values similar to those in Fe-sufficient plants (Table 4.10). This suggests that NA could play a role in Fe transport during the massive Fe root uptake (at 12 h after Fe resupply), helping to deliver the metal to the different organelles

(mitochondria, vacuoles, etc) and to neighbouring cells. Then, other metal chelators such as the carboxylates *Cit* and/or *Mal* (and perhaps storage proteins such as ferritin) could be involved in Fe homeostasis at longer resupply times.

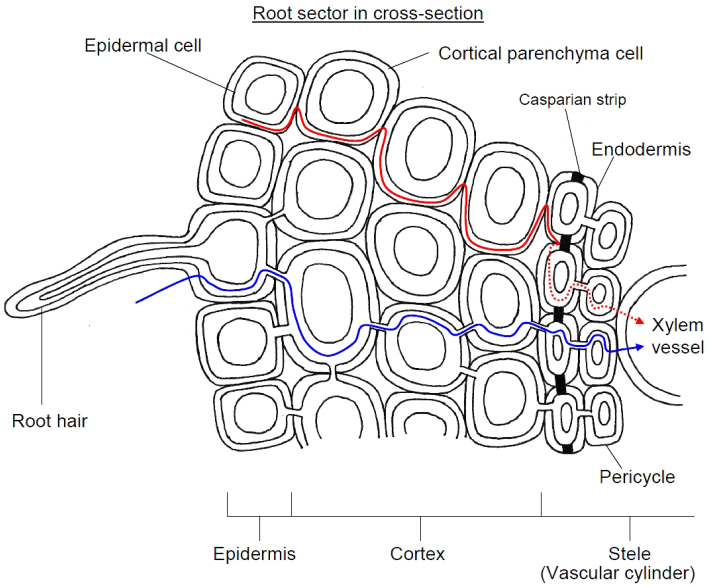

Fig. 5.4. Fe transport pathways in roots. In blue, the symplastic pathway through cells; in red, the apoplastic pathway up to the Casparian strip, where Fe is introduced in cells and continue through the symplastic way (red dotted line). Image from *www.cronodon.com*

In the case of the root apoplastic fluid, large increases in Fe, NA and carboxylate concentrations were found in response to Fe resupply. These values and the prevalent pH in this compartment (approximately 5.5) would support the formation of Fe complexes with both NA and carboxylates. Such complexes have been detected in other plant compartments with pH values close of 5.5 such as the tomato xylem sap ($Fe(III)_xCit_x$ x=2-3; Rellán-Álvarez *et al*., 2010a) and pea xylem sap and embryo sac liquid (Fe(II)-NA and $Fe(III)_3(Cit)_{(4-x)}(Mal)_x$ x=1-3; Flis *et al*., 2016). The occurrence of Fe(II)-NA complexes at pH 5.5 in presence of high concentrations of *Cit* was also demostrated in *in vitro* experiments using ESI-MS analyses (Rellán-Álvarez *et al*., 2008). However, data in this Thesis shows that the NA increase in the apoplastic fluid was never sufficient to reach the 1:1 NA:Fe ratio that would be expected if NA was the only player in Fe transport in roots (Figs. 8.2-8.3; Table 4.10). Therefore, the metal, NA and carboxylate concentrations, and the pH (and other factors) would determine the relative abundance of Fe-complexes with NA or carboxylates in the apoplastic fluid. Also, since Fe resupply led to an accumulation of Fe and NA in both the symplastic and apoplastic compartments,

an efflux of NA or metal-NA complexes from the symplast to the apoplast through YSL transporters seems likely. That NA facilitates transport of Fe at the root level has been evidenced previously by i) the accumulation of symplastic Fe in the roots in the NA-free tomato mutant *chloronerva*; ii) the decrease in root apoplastic Fe concentrations down to control values in the mutant *chloronerva* after the application of NA to the leaves (Becker *et al*., 1992), and iii) the alteration of subcellular and inter-organ partitioning of Fe, and in particular the decreased Fe concentrations in shoots, in plants overexpressing the ZINC-INDUCED FACILITATOR1 (ZIF1), which mediates NA vacuolar sequestration in roots (Haydon *et al*., 2012). Since the Casparian strip is a barrier for apoplastic Fe species, at that point Fe should enter the symplastic route, probably be chelated again by NA to reach the vascular parenchyma, and then possibly transferred to the xylem sap as (Fe(II) or Fe(III)) free ions by the IREG/FPN1 protein (Morrisey *et al*., 2009).

5.1.2. Effects of iron status on the concentrations of metal micronutrients and metal ligands in the xylem sap

Metal micronutrients in the xylem sap

The xylem sap has been, by far, the most studied fluid in tomato plants, due to the ease of sampling. The first study on this issue reported Fe concentrations of 28 μM in the xylem sap of Fe-sufficient tomato (Tiffin, 1966). Later on, studies in the 80's reported tomato xylem sap Fe concentrations in the range 2-9 μM (White *et al*., 1981a; Cataldo *et al*., 1988). Recent studies include values in the ranges 10-150 (Orera *et al*., 2010), 50-121 (Rellán-Álvarez *et al*., 2010a), 5-177 (Rellán-Álvarez *et al*., 2011a) and 4-6 μM (Terzano *et al*., 2013), with the highest xylem sap Fe concentrations being observed in Fe-deficient plants submitted to an Fe-resupply treatment.

The xylem sap Fe concentrations found in this work are in the range 9-194 μM, with Fe deficiency not causing any significant change in Fe concentrations (although values tended to be lower in Fe-deficient plants; this weak effect may be due to the particular genotype used in this Thesis). On the other hand, Fe resupply led to a xylem Fe concentration increase at 12 h, with a peak at 20 h (Figs. 4.5 and 5.3), in agreement with data in Rellán-Álvarez *et al*. (2010a and 2011a). The experimental approach used in this Thesis supports a relationship between the Fe concentrations in the roots and those in the xylem sap. During the first 24 h after Fe resupply, the root takes up Fe and transport to

the xylem occurs, likely through the (constitutively expressed) FPN1 transporter. The peaks in Fe concentrations in the xylem sap are likely to be enhanced during the dark period by the stop of the transpiration stream. Then, two days after Fe resupply the Fe concentration in the xylem sap decreased to values similar to those of the Fe-sufficient plants.

Regarding the concentrations of Mn, Cu and Zn in tomato xylem sap, concentrations of approximately 8, 5 and 6 μM, respectively, were reported for Fe-sufficient plants (White *et al*., 1981a), but as far as I know no information about changes with Fe-deficiency and Fe-resupply is available. This Thesis provides the first set of data regarding these micronutrients in conditions of Fe-deficiency and resupply. The concentrations of Mn in Fe-sufficient and Fe-deficient plants were similar to those found previously, whereas those of Cu and Zn were slightly lower and higher, respectively (White *et al*., 1981a). Iron resupply led to an increase in the concentration of these micronutrients only during the dark period (20 and 44 h), so that it can be also hypothesized that the changes are probably more related to the light/dark periods than to the plant Fe status. Since circadian rhythm effects have been found for Cu (Abdel-Ghany *et al*., 2009), it seems likely that the concentrations of other metal micronutrients may be also influenced by the light/dark cycles.

Nicotianamine in the xylem sap

Only two studies have described the NA concentrations in xylem sap of tomato plants, with the concentrations found being 15-20 and 10 μM (Pich and Scholz, 1996; Ariga *et al*., 2014). Much higher concentrations of NA (64 μM) were found in the xylem sap of *B. carinata*, with the concentrations being especially high in response to Ni stress (271 μM) (Irtelli *et al*., 2009). As far as I know no studies on the effects of Fe deficiency and resupply on the xylem sap NA concentrations have been carried out.

The values found in this Thesis for tomato were in the range 10-15 μM for all sampling times and treatments, in line with the values reported previously for this species (Pich and Scholz, 1996; Ariga *et al*., 2014). Results show that the xylem sap NA concentrations did not change with Fe deficiency and resupply (Figs. 4.9, 5.2-5.3). The lowest concentrations were found in Fe-sufficient plants at 12 h, and this may suggest a NA shortage at the end of the day.

Carboxylates in the xylem sap

Previous studies have shown that the xylem sap concentrations of *Cit* and *Mal* are increased by Fe deficiency in tomato (Brown and Tiffin, 1965; White *et al*., 1981a; López-Millán *et al*., 2009; Rellán-Álvarez *et al*., 2010a, 2011a) and other Strategy I species such as sugar beet (López-Millán *et al*., 2000a; Larbi *et al*., 2010) and others (see review Álvarez-Fernández *et al*., 2014). Increased carboxylate levels have been hypothesized to play roles in the transport of Fe and C *via* xylem to the shoot (López-Millán *et al*., 2000a). Iron resupply to "Tres Cantos" tomato plants led in the short-term to xylem sap concentration increases for different carboxylates such as *Cit*, 2-oxoglutarate and fumarate (Rellán-Álvarez *et al*., 2011a), whereas in the long-term Fe resupply to tomato and sugar beet plants decreased xylem sap carboxylate concentrations (López-Millán *et al*., 2000a; Larbi *et al*., 2010).

The results obtained in this Thesis for FER tomato xylem sap show that carboxylate concentrations increased with Fe-deficiency, in line with data in the previous studies cited above (Figs. 5.2-5.3; see also Fig. 4.13 and Table 4.8). However, in this tomato genotype carboxylate concentrations decreased upon Fe resupply in the short-term (at 12 h), in contrast with what was found in the genotype "Tres Cantos" (Rellán-Álvarez *et al*., 2011a). A possible explanation may be the existence of genotypic differences related to shoot Fe deficiency signaling. In the more efficient genotype FER, leaf mesophyll cells resupplied with Fe might respond in a more rapid way by increasing photosynthesis, thus requiring less C skeletons from the roots (for a review of Fe status signaling, see Gayomba *et al*., 2015).

Xylem sap transport of iron facilitated by organic ligands

Previously published evidence supports that NA is not essential for xylem Fe transport. The NA-deficient tomato mutant *chloronerva* accumulates Fe in developed leaves (Pich *et al*., 1994) and the *A. thaliana* NAS quadruple mutant (with very low levels of NA) also accumulates Fe in leaves (Klatte *et al*., 2009). Furthermore, no Fe-NA complex has been detected in xylem sap, with both *in silico* and *in vitro* speciation studies tending to exclude NA as a possible xylem Fe carrier at the slightly acidic pH values typical of xylem (von Wirén *et al*., 1999; Rellán-Álvarez *et al*., 2008). However, it has been recently suggested that NA may play a role in long distance transport of Fe when carboxylates are in short supply, a circumstance that occurs in the FRD mutants (Schuler *et al*., 2012), as well as

in plant species where the xylem sap is less acidic, such as field-grown *Prunus persica* trees (where the xylem sap pH is in the range from 6.5 to 7.5; Larbi *et al*., 2003; Rellán-Álvarez *et al*., 2011a). Since YSL proteins have been found in vasculature of Strategy I plants, it has been proposed that they are involved in metal-NA lateral transport between the xylem and phloem saps (Waters *et al*., 2007; Conte and Walker, 2011).

Results in this Thesis show that Fe deficiency did not affect consistently xylem sap Fe and NA concentrations, whereas Fe resupply to Fe-deficient plants led in the short term to large increases in xylem sap Fe concentrations, up to 193 μM, with this Fe increase not being accompanied by parallel changes in the xylem sap NA concentration (Figs. 5.2-5.3, see also Figs 4.4 and 4.9 and Tables 4.3 and 4.6). This supports again that NA is not likely to be involved directly in Fe long distance xylem sap transport. The NA concentrations observed suggest that NA could chelate instead Mn and/or Cu, since in most cases the concentrations of these metals were similar to those of NA. For instance, it is known that in the *chloronerva* mutant the long-distance transport of Cu is impaired, indicating the importance of NA in Cu trafficking (Pich and Scholz, 1996).

On the other hand, the xylem sap concentrations of carboxylates (mainly *Cit* and *Mal*) increased with Fe deficiency. The concentration ranges for Fe, *Cit* and *Mal* (32-193, 188-449 and 600-3200 μM, respectively) in Fe-resupplied plants would allow the formation of the Fe-carboxylate complexes not only with *Cit* as it was reported in xylem sap of tomato ($Fe(III)_3$-Cit_3; Rellán-Álvarez *et al*., 2010a) but also with *Mal* as in pea xylem sap and embryo sac liquid ($Fe(III)_3$-$(Cit)_{(4-x)}$-$(Mal)_x$; Flis *et al.*, 2016). The protein responsible for xylem sap *Cit* loading is FRD (Durrett *et al*., 2007; Yokosho *et al*., 2009), whereas no such transporter has been found for *Mal* so far. Oocytes expressing FRD3-GFP transport *Cit*, but not *Mal*, when used at comparable concentrations (30-50 mM) (Durrett *et al*., 2007). Carboxylates have been proposed to chelate other metals in this compartment, including Zn^{2+} (Monsant *et al*., 2011) and Mn^{2+} (Fernando *et al*., 2010). In summary, it seems that in the Strategy I plant tomato carboxylates could be important actors for Fe transport in the xylem sap.

5.1.3. Effects of iron status on the concentrations of metal micronutrients and metal ligands in leaf apoplastic fluid

Metal micronutrients in the leaf apoplastic fluid

Only a few studies have focused on the leaf apoplastic fluid Fe concentrations, with values reported being 2-4 μM in tomato (Barabasz *et al*., 2012), and 3-6 (López-Millán *et al*., 2000a) and 7-65 μM (Larbi *et al*., 2010) in sugar beet. Iron deficiency caused decreases in the leaf apoplastic fluid Fe concentration in sugar beet (López-Millán *et al*., 2000a; Larbi *et al*., 2010). The only study reporting leaf apoplastic Fe concentrations during a time-course Fe-resupply experiment with sugar beet showed a large increase in Fe concentration 24 h after Fe resupply and a rapid decrease towards control levels at 48 h (Larbi *et al*., 2010).

The Fe concentrations in the leaf apoplastic fluid found in this Thesis are somewhat higher than those reported earlier in the same species, between 4 and 25 μM (Fig. 5.2; see also Fig. 4.6 and Table 4.4), with somewhat higher concentrations in developed leaves (8-25 μM) than in young ones (4-19 μM). This may be due to the fact that developed leaves grew when the plants were still in pre-treatment nutrient solution, when there was still plenty of Fe for development. On the other hand, Fe deficiency did not affect significantly the Fe concentrations in the leaf apoplastic fluid (Fig. 5.2; see also Fig. 4.6 and Table 4.4). Upon Fe resupply, increases in Fe concentration were found in the leaf apoplastic fluid, with differences regarding leaf age: developed leaves were the first to receive a Fe flush, with an increase 12 h after resupply, whereas in young leaves the Fe concentration was not significantly increased until 24 h (Figs. 5.3; see also Fig. 4.6 and Table 4.4). This is possibly related to the transpiration rate (xylem sap import), which is much larger in the fully expanded leaves than in the developing ones. Young leaves are only partially fed by the xylem sap, with a considerable fraction of nutrients being imported through the phloem sap. Another interesting aspect is the decrease of Fe concentration in the apoplastic fluid of developed leaves from 12 h to 24 h after Fe-resupply, reaching concentrations similar to those in Fe-deficient plants (Figs. 5.2-5.3). This may be due to Fe acquisition by cells, export to the phloem sap or even the precipitation in cell walls.

Nicotianamine in the leaf apoplastic fluid

The NA concentration in whole *A. thaliana* leaves has been reported to be in the range 20-150 nmol g^{-1} FW (Haydon *et al*., 2012, Klatte *et al*., 2009; Mari *et al*., 2006). This Thesis is the first report for NA concentrations in leaf apoplastic fluid. Concentrations in the leaf apoplastic fluid were in the range from 6 to 20 µM NA, with Fe deficiency and resupply generally having no effect (Figs. 5.2-5.3; see also Fig 4.10 and Table 4.6). Those values are equivalent to < 1 nmol NA g^{-1} FW. This indicates that the NA levels in this compartment only account for a small fraction of the whole leaf NA.

Carboxylates in the leaf apoplastic fluid

The concentrations of carboxylates in the leaf apoplastic fluid have been studied only in a few papers until now. Citrate and *Mal* were found in the ranges 0.2-4 and 0.7-2 mM in sugar beet and 1.6-2 and 0.8-1.8 in pear tree, respectively, with Fe deficiency leading to increased carboxylate concentrations (López-Millán *et al*., 2000a, 2001b; Larbi *et al*., 2010). In both species, increases in leaf carboxylates were associated to decreases in chlorophyll (López-Millán *et al*., 2000a, 2001b). Also, Fe resupply to Fe-deficient sugar beet plants led to large decreases in leaf apoplastic fluid *Cit* concentrations after 24 h (Larbi *et al*., 2010).

In this Thesis, values found for *Cit* and *Mal* in leaf apoplastic fluid of tomato were in the ranges 0.4-14 and 0.4-10 mM, respectively (Fig 4.14 and Table 4.9), with concentrations being lower in young than in developed leaves. As mentioned before, developed leaves had higher leaf chlorophyll levels than the young ones, which were severely chlorotic. In tomato, changes in carboxylate concentrations were also related with leaf chlorosis as in the other species studied: young Fe-deficient leaves contained higher concentrations of carboxylates than their Fe-sufficient counterparts, whereas the developed leaves of both Fe-deficient and Fe-sufficient plants showed similar carboxylate concentrations.

Upon Fe resupply, carboxylate concentrations also showed different responses in developed and young leaves. In developed leaves, carboxylate concentrations increased upon Fe resupply, with *Cit* and *Mal* increasing 3- and 4-fold after two days, whereas in young leaves all carboxylate concentrations had a transient increase at 24 h but decreased to control levels after 48 h. These changes point out again to the main source of nutrients for each leaf: developed leaves have high transpiration rates and would receive higher

amounts of *Cit* and *Mal* from the xylem sap than young leaves, which are fed mainly by phloem. The drastic reduction of *Cit* and *Mal* from 24 to 48 h after Fe-resupply found in the apoplastic fluid of young leaves could be associated to the import of C skeletons by mesophyll cells to feed the energy metabolism (Krebs cycle). The reduction of apoplastic *Cit* levels along with a stable Fe supply would facilitate Fe acquisition by mesophyll cells, since previous studies reported a decrease of mesophyll cell FCR activity with high *Cit*:Fe ratios (González-Vallejo *et al*., 2000; Nikolic and Römheld, 1999).

Leaf apoplastic fluid transport of iron facilitated by organic ligands

The apoplastic fluid is a highly variable fluid, with many fluxes into and out of it in the form of liquids (xylem and phloem saps) and gases (O_2 and CO_2), which could affect metal and ligand concentrations. Thus, leaf apoplast data must be taken into consideration to study Fe transport, although the relevance of these data is always open to debate.

When comparing the Fe acquisition of leaf protoplasts from the NA-free tomato mutant *chloronerva* and its WT *Bonner Beste*, the plasma membrane FCR was found to be identical in both genotypes, whereas the uptake of Fe was higher in *chloronerva* protoplasts (Pich and Scholz, 1994). Also, the addition of NA to the protoplast uptake assay medium had no effect on the absorption of Fe, showing that NA is not essential for the transport of Fe at the plasma membrane level (Pich and Scholz, 1994). The difference in Fe content between protoplasts and whole leaves, which is a proxy for the apoplastic Fe concentration, showed that in *chloronerva* the lack of NA led to an accumulation of Fe in developed leaves both in the symplastic and apoplastic pools, being higher in the former (Pich and Scholz, 1994). Therefore, even if NA is not directly involved in Fe uptake at the cell level, it appears to be essential for the regulation of its distribution between the apoplastic and symplastic compartments (Curie *et al*., 2009; Schuler *et al.*, 2012).

The results in this Thesis show that the NA concentration in the apoplastic fluid of leaves did not change markedly with Fe deficiency or resupply (Figs. 5.2-5.3), and therefore support that NA is not involved directly in the transport of Fe from the xylem sap to the mesophyll cells. Also, the NA concentrations observed were never sufficient to chelate all the Fe present in the fluid, suggesting that, as in the case of the root apoplast, other metal ligands must be involved in transport of Fe at this stage. However, the fact that the pH of the leaf apoplastic fluid would allow the formation of the Fe-NA complex

may suggest that NA could still have a role in chelating a fraction of the total Fe present. On the other hand, the high concentration of carboxylates (mainly *Cit* and *Mal*) found in the apoplastic fluid and its slightly acidic pH (5.5 to 6.3) would favor the involvement of Fe-*Cit*-*Mal* complexes in the transport of Fe in this compartment. The decrease in the *Cit*:Fe ratios after Fe resupply would tend to favor the formation of the Fe_3Cit_3 complex, which could be an excellent substrate for the FCR as suggested by Rellán-Álvarez *et al*. (2010a). Unfortunately, since the LOD of the Fe-*Cit* species in the method developed by Rellán-Álvarez *et al*. (2010a) was 25-30 μM, and the Fe concentrations found in the apoplastic fluid in this Thesis was approximately 25 μM, it has not been possible to analyze Fe-*Cit* species so far. This underlines the difficulties of detecting the carboxylate-Fe complexes in apoplastic fluid.

5.1.4: Effects of iron status on the concentrations of metal micronutrients and metal ligands in leaf symplastic extracts

Micronutrients in leaf symplastic extracts

The concentrations of metal micronutrients in young and developed leaves of Fe-sufficient and Fe-deficient tomato plants have been reported in a recent study (Carrasco-Gil *et al*., 2016). The concentration ranges found were (in μg g^{-1} DW) 25-99, 40-300, 12-23 and 16-53 for Fe, Mn, Cu and Zn, respectively. Also, the same study showed that Fe deficiency led to decreases in the concentrations of Fe and increases in the concentrations of the other micronutrients.

In this Thesis, the metal micronutrient concentrations in the leaf symplastic extract of tomato plants (Figs. 5.2-5.3, see also Fig. 4.7 and Table 4.5) were comparable to those found in whole leaves by Carrasco-Gil *et al*. (2016). Iron deficiency caused a decrease in Fe concentrations in the symplastic extract of both young and developed leaves, although differences were significant only at some points of the time course.

Regarding the other micronutrients, significant increases only occurred for Mn and Zn in the symplastic extract of developed leaves and at some sampling times. Differences between the changes in whole leaves and leaf symplastic extracts could be attributable to metal allocation in solid phases not easily extractable by centrifugation, including cell membranes as well as structural elements such as cell walls and others (Terry and Abadía, 1986; Robson and Reuter, 1981; Broadley *et al*., 2009).

Upon Fe-resupply, the Fe concentrations in the symplastic extract of young leaves increased 2-fold in 12 h, matching with the increases in Fe concentration in root apoplastic fluid and symplastic extract and in xylem sap, whereas Fe concentrations in developed leaves did not change significantly at that time point (Figs. 5.2-5.3; see also Fig 4.7 and Table 4.5). Afterwards, the Fe concentration in the symplastic extract increased further, although at different paces in young (where a further increase was observed only at 24 h) and developed leaves (where it only increased from 24 h to 48 h). This could be explained again by the source of nutrients, mainly *via* xylem sap in developed leaves (minimal at night due to stomatal closure) and *via* phloem sap in young leaves. These data suggest the existence of an Fe concentration limit in leaf symplastic extracts (approximately 60 μM), as it also occurs in root symplastic extracts (approximately 150 μM).

An interesting change was found for Mn, since the Fe-resupplied plants showed higher concentrations of this micronutrient at 24 and 48 h after Fe resupply in both young and developed leaves. This increase could be due to the induction of Fe transporters of the ZIP or the NRAMP families, which transport metals into the cytosol and have a broad range of metal substrates (Socha and Guerinot, 2015). Once Fe-deficient cells start receiving Fe, the synthesis of the components of the photosynthetic chain is induced and Mn would be in high demand for the synthesis of PS II components such as the most well-known and best-documented example of a Mn-containing enzyme, the water-splitting system in PS II. In addition, Mn has a critical role in other metabolic processes, with up to 35 enzymes requiring Mn as a cofactor (Maschner, 1995), involving from the detoxification of ROS through MnSOD to decarboxylation and hydrolysis steps in the TCA cycle (*e.g.*, the enzyme *malate deshydrogenase*). Iron deficiency leads to the production of ROS as well as an increased respiration in all tissues (Zaharieva and Abadía, 2003; Zaharieva *et al*., 2004; Tewari *et al*., 2013). Also, a fast Fe flux in Fe-resupplied plants could produce transient Fe toxicity symptoms, which may lead to enhanced ROS production. Thus, Mn-, Cu- and Zn-containing SOD would be essential to limit or avoid oxidative damage.

Nicotianamine in leaf symplastic extracts

The NA concentrations in the leaf symplastic extract were affected by the leaf age and Fe status. The NA concentrations in leaf symplastic extract in the Fe-sufficient plants were 3-fold higher in young (67-73 μM) than in developed leaves (21-33 μM), whereas in the Fe-deficient plants NA concentrations were similar in leaves of both ages (*ca.* 40-50 μM)

(Fig. 5.2; see also Fig. 4.11 and Table 4.6). Therefore, Fe deficiency decreased NA levels in young leaves and increased them in developed ones. This again may be related to the source of nutrients for each leaf according to their age and Fe status, with young leaves being fed by the phloem sap, likely by metal-NA complexes. The different NA concentrations in Fe-sufficient plants suggest Fe phloem movement from the developed leaves to the young ones as it has been found in *H. vulgare* (Shi *et al*., 2012). In contrast, in Fe-deficient plants the low Fe levels available for trafficking could possibly explain the fact that NA levels in young and developed leaves were similar.

Upon Fe-resupply, the concentrations of NA in leaf symplastic extract were highest at 48 h in both young and developed leaves, and this occurred after the increase of Fe concentration in the same extract (Fig 5.3, see also Fig. 4.11 and Table 4.6). Thus, NA seems to be synthesized once Fe is delivered to cells, probably helping to chelate the micronutrient, avoiding toxicity and facilitating intracellular and intercellular transport. Also, in the developed leaves these Fe-NA complexes could be exported *via* phloem sap to the young leaves. The NA:Fe ratios in the leaf symplast tend to support the occurrence of Fe-NA complexes, specially in the case of the Fe-resupply (Table 4.13).

5.1.5. Concluding remarks on the effects of Fe status on the composition of tomato plant fluids

A general model for Fe transport in whole tomato plants is proposed in Fig. 5.5. Iron deficiency led to major decreases in Fe concentrations, especially in roots, and to general increases in the carboxylate concentrations. In contrast, the NA concentrations were not affected, suggesting that NA occurs in basal concentrations irrespective of the Fe levels.

Upon Fe resupply, a rapid and large increase in Fe concentration was found in the root apoplastic fluid and symplastic extract and the xylem sap, whereas in the leaves no changes in Fe concentrations were found in the apoplastic fluid and in the symplastic extract an increase was found only 24 hours after resupply. This points out to a strict regulation of Fe concentrations. The NA concentrations increased in the leaf and root symplastic extract in parallel to those of Fe, revealing a key role of NA in root Fe trafficking, and suggesting that NA synthesis is triggered upon Fe acquisition to buffer the metal ion and avoid oxidative damage as well as to facilitate Fe transport and delivery. Also, NA could contribute to Fe transport in roots *via* the symplastic and apoplastic pathways. The concentrations of major carboxylates (*Cit* and *Mal*) also increased upon

Fe resupply in the apoplastic fractions of leaves and roots, and these increases were found to be more intense after the Fe concentration peak in the apoplastic fluid in roots and developed leaves, whereas in the corresponding root symplastic extracts the increase in carboxylates was concomitant to the Fe peak. This supports a role for carboxylates in the root apoplastic fluid, and also points out the possible relevance of carboxylate compartmentalization in young leaves, which may affect Fe acquisition.

These data suggest that Fe is able to elicit NA synthesis in cells, where it is involved in intracellular chelation and metal transport, whereas in the apoplastic fluid carboxylates secreted by cells would be the main ligands involved in Fe transport. In the xylem sap, the relatively low NA concentrations found support that this ligand does not have a role in long distance transport, whereas it could be instead involved in the transport of other metal micronutrients such as Cu, Mn and Zn.

Since the lack of sampling protocols to obtain phloem sap from tomato plants have prevented filling the picture with phloem data from tomato, data from oilseed rape (another Strategy I plant species) have been also used. Data show that in the phloem sap of *B. napus* the concentrations of NA in Fe-sufficient plants are not high enough to chelate all the Fe present (Fig. 4.29), and therefore other ligands could be required for Fe translocation in this compartment.

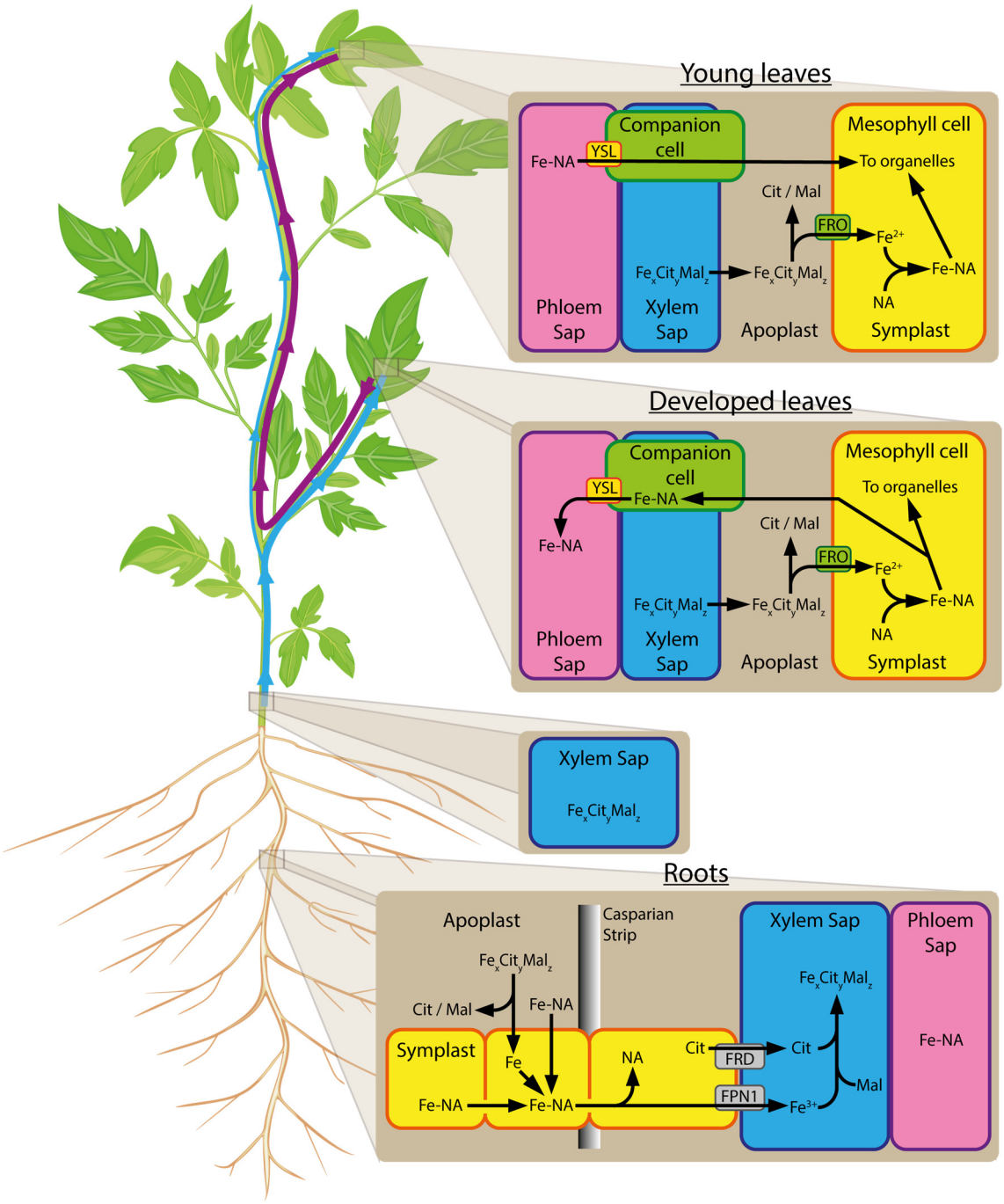

Fig. 5.5. Proposed model for iron transport assisted by ligands in tomato plants

Section 5.2

Objective 2 Discussion

Contribution of Cit, NA and DMA to the long-distance Fe transport in rice plants

OsFRDL1 was initially described as an homolog of AtFRD3 (Inoue *et al*., 2004) and its function in rice was characterized by Yokosho *et al*. (2009). The *Osfrdl1* mutant lacks the protein responsible for *Cit* (but not *Mal*) loading into the xylem sap, shows Fe precipitation in the vascular root tissues and develops Fe chlorosis in young leaves. Both root Fe precipitation and chlorosis were only observed when the external Fe supply was low, and it was suggested that other metallic cations would compete with Fe for the chelation by *Cit*, thus impeding Fe transport to the shoot (Yokosho *et al*., 2009). A new study has demonstrated that OsFRDL1 is also expressed in the upper nodes of rice at the reproductive stage, where it seems to be involved in the remobilization of apoplastic Fe in the shoot (Yokosho *et al*., 2016).

In this section I tested the hypothesis that in *Osfrdl1* plants grown with low Fe supply the ligands NA and/or DMA could play a role as an alternative Fe transport system, acting as a backup of the carboxylate-mediated transport system.

5.2.1. Iron and metal ligands in WT and *Osfrdl1*

Results in this Thesis confirm the loss of function of the OsFRDL1 protein in the *Osfrdl1* mutant plants. The mutant shows major decreases in the xylem sap *Cit* concentrations in both Fe treatments, and a consistent 2-fold increase in the xylem sap *Mal* concentration when grown under low Fe supply (see Section 4.2.2). These results are in line with those in the original paper of Yokosho *et al*. (2009), where upon Fe deficiency the xylem sap concentrations of both *Cit* and *Mal* increased in the WT whereas those of *Cit* decreased and *Mal* increased in *Osfrdl1*.

The Fe root and leaf concentrations found in this Thesis in *Osfrdl1* were not significantly different to those in the WT, regardless of Fe supply (see Section 4.2.3), suggesting the existence of an Fe transport system independent of *Cit*. This is in contrast with the results for *Osfrdl1* in Yokosho *et al*. (2009), which found even higher root Fe concentrations when plants were grown with a low Fe supply. This may be due to differences in the plant growth conditions.

In all tissues, genotypes, and Fe treatments DMA was more abundant than NA (see Section 4.2.4). Iron deficiency led to decreases in the NA concentrations in roots and leaves, with the only exception of WT roots. In contrast, Fe deficiency led to increases in DMA concentrations in roots and leaves, with the only exception of the *Osfrdl1* roots,

where concentrations of this ligand were unaffected. Therefore, the differences between DMA and NA concentrations were generally more marked in Fe-deficiency conditions. The fact that this trend was not observed in *Osfrdl1* roots may be due to the export of DMA from roots to the shoots and/or the nutrient solution.

5.2.2. Iron and metal ligands in WT and *Osfrdl1* upon *Cit* treatment

Assuming that carboxylates and the NA/DMA pair could play a complementary role in Fe transport within the plant, it was tested if foliar *Cit* application to Fe-deficient plants could revert the concentration of these ligands towards control values.

When plants were grown with an adequate Fe supply, foliar *Cit* application in the WT led to 2-fold increases in leaf Fe concentrations, without affecting NA and DMA concentrations in root and leaf tissues (Figs. 4.17, 4.18 and 4.19). In contrast, in *Osfrdl1* plants foliar treatment with *Cit* did not change Fe and NA concentrations whereas root DMA concentrations decreased to the WT levels. A possible explanation for these data is that *Cit* application leads to the remobilization of apoplastic Fe in Fe-sufficient WT plants, whereas in Fe-sufficient *Osfrdl1* plants it leads to an impairment of the DMA synthesis or to the export to the growth medium.

When plants were grown with a low Fe supply, foliar *Cit* application did not change the Fe concentrations in any genotype, whereas marked changes in NA and DMA concentrations were observed, being different in each genotype. In the WT plants, the root and leaf DMA concentrations decreased to values similar to those in the Fe-sufficient WT, whereas NA concentrations decreased only in the roots. In contrast, *Osfrdl1* plants treated with *Cit* showed large increases of NA and DMA in roots whereas leaf DMA was decreased and leaf NA did not change. A possible explanation for these data is that *Cit* application leads to a decreased synthesis of NA and DMA in Fe-deficient WT plants, whereas in Fe-deficient *Osfrdl1* plants it leads to an impairment of the DMA transport from roots to shoots.

5.2.3. Concluding remarks on long-distance Fe transport in rice

Osfrdl1 is able to mobilize as much Fe as the WT to the aerial organs even though the *Cit* transporter is no longer active. This may be related to the fact that the *Cit* concentration in the xylem sap of *Osfrdl1* is still maintained at approximately 50 μM. Another possible ligand contributing to Fe mobilization is *Mal*, that increased 2-fold by Fe deficiency (Fig

4.16). However, it is unlikely that *Mal* alone could be the alternative ligand to *Cit* in *Osfrdl1*, since the *Mal* concentrations in the xylem sap were similar in the WT and *Osfrdl1* grown with the same Fe supply. Also, Fe complexed only with *Mal* has not been detected in xylem sap of either Strategy I or II plants. However, a fraction of the Fe in the xylem sap could still be transported *via* mixed Fe-*Cit*-*Mal* complexes as it was recently found in pea, a Strategy I species (Flis *et al.*, 2016). Therefore, other Fe ligands can be involved in maintaining the Fe concentrations in aerial organs in the *Osfrdl1* mutant.

The changes in DMA and NA concentrations observed in WT and *Osfrdl1* with Fe deficiency and foliar *Cit* aplications suggest that these ligands are involved in Fe long-distance transport. Upon Fe deficiency, DMA may act in a separate Fe long-distance transport mechanism, complementing the Fe-carboxylate pathway in rice and perhaps other graminaceous plants, whereas it is unlikely that NA could participate in long distance Fe transport because the NA:Fe ratios found are extremely low (<0.1 in Fe-sufficient plants). The involvement of DMA in Fe long distance transport is also supported by other findings, since: i) DMA (synthesized from NA) is present in larger concentrations than NA in both roots and shoots, and differences are larger in Fe deficiency conditions (Bashir *et al*., 2006; this study); ii) NAAT, acting in the first step of the conversion of NA into DMA, and TOM1, the transporter involved in DMA secretion to the rizhosphere and xylem sap loading, are expressed in the vascular tissue of roots and shoots (Inoue *et al*., 2008; Nozoye *et al*., 2011); iii) the YSL15 transporter, known to transport Fe(III)-DMA, is also present in the vasculature (Inoue *et al*., 2009); iv) co-elution of DMA and Fe has been observed in rice xylem sap, supporting the occurrence of a Fe-DMA complex in this fluid (Ariga *et al*., 2014), and v) the Fe(III)-DMA complex has been identified in rice phloem sap (Ando *et al*., 2012). To determine whether *Cit* and DMA have complementary roles in the transport of Fe from roots to shoots *via* xylem, it would be necessary to analyze the xylem sap Fe(III)-DMA concentrations in WT and *Osfrdl1* plants grown under different Fe status.

A model for Fe trafficking in WT and *Osfrdl1* plants is proposed in Fig 5.6. The Fe acquisition mechanism from the soil would be common for both rice genotypes. The protein TOM1 secretes DMA to the rhizosphere, which then chelates Fe(III), and the Fe(III)-DMA complex is subsequently taken up by the plasma membrane protein YSL15 and then transported to the stele (Inoue *et al*., 2009; Lee *et al*., 2009a). At this point, the WT would be able to export free Fe, *Cit* and DMA to the xylem sap through FPN1

(Morrisey *et al*., 2009), FRDL1 (Yokosho *et al*., 2009) and TOM1 (Nozoye *et al*., 2011), respectively, whereas the *Osfrdl1* mutant would have reduced *Cit* loading because of the lack of the transporter. Both WT and *Osfrdl1* plants could also be able to load Fe(III)-DMA into the xylem sap *via* YSL15 (Inoue *et al*., 2009; Lee *et al*., 2009a). In this compartment Fe-*Cit*-*Mal* and/or Fe-DMA complexes would form, with Fe-DMA complexes being favored in *Osfrdl1* due to the lower *Cit* concentration, and transported to the shoots (this aspect is pointed out in Figure 5.6 by the size of each complex in the xylem sap panel). In the phloem sap, both Fe-NA and Fe-DMA complexes would be involved in Fe transport, with possible lateral Fe-DMA transport between xylem and phloem sap, specially at the nodes (Aoyama *et al*., 2009). On the other hand, the exogenous *Cit* application to the leaves would remobilize precipitated Fe pools that, upon reaching the cells, could lead to down-regulation of Fe deficiency responses, such as NA and DMA synthesis in roots and DMA translocation from roots to shoots.

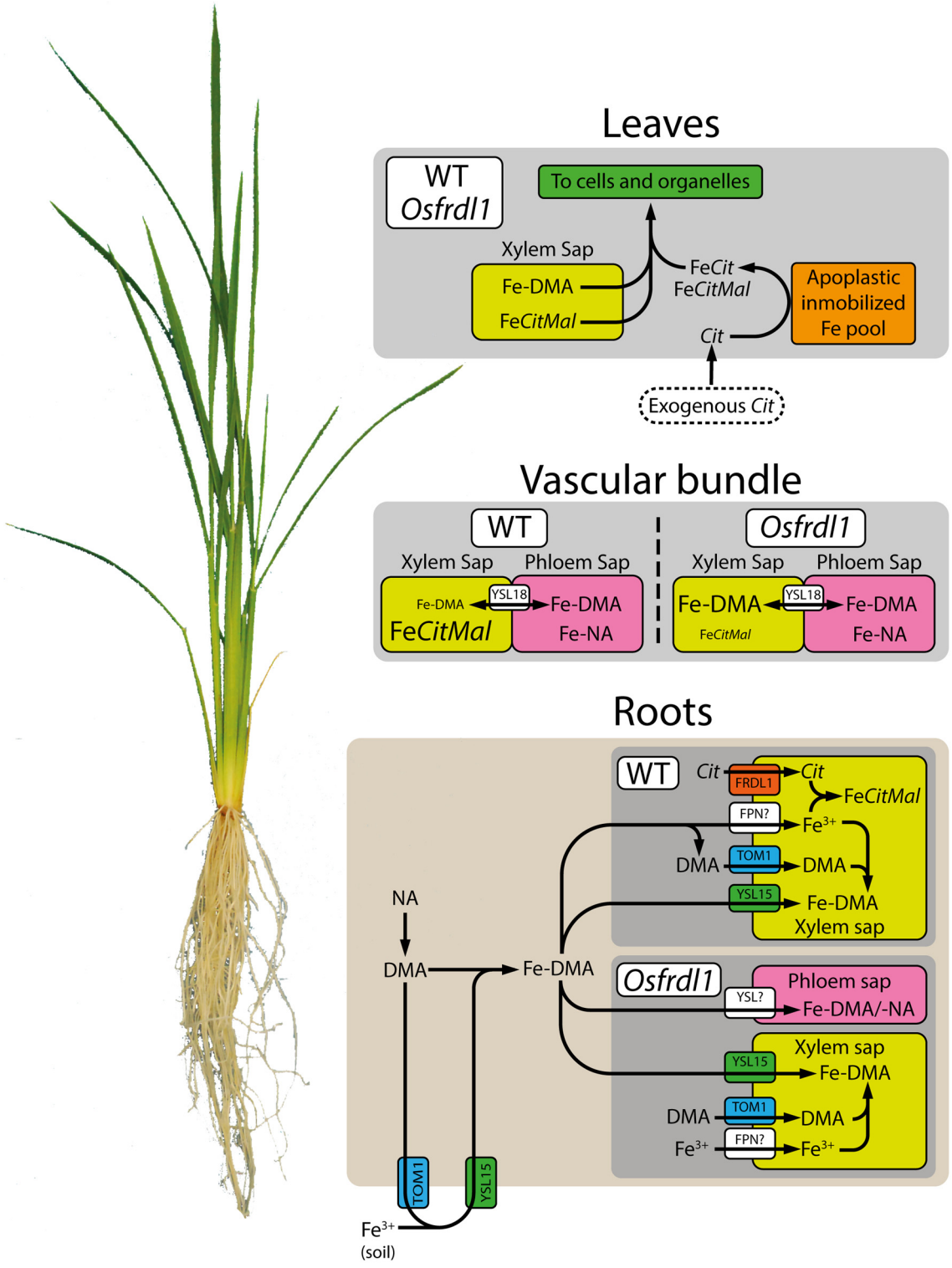

Fig. 5.6. Possible Fe long distance transport mechanisms in WT and *Osfrdl1* rice plants. Relative contribution of Fe-*Cit* and Fe-DMA in the xylem sap is reflected by the letter size of each complex.

Section 5.3

Objective 3 Discussion

Effects of the overexpression of NA and DMA synthesis genes on the localization of metal micronutrients and metal ligands in rice seed

The next pages discuss Fe transport in relation to NA and its derivative DMA within the seed of a particularly relevant Strategy II crop species, rice. This Thesis includes the first in-depth study of the possible role of DMA in the allocation of metal micronutrients in the embryo and endosperm.

5.3.1. Concentrations of metals and metal ligands in rice seeds

Unpolished rice seeds usually have approximately 4 μg Fe g^{-1} DW (Zheng *et al*., 2010; Johnson *et al*., 2011; Trijatmiko *et al*., 2016). However, the typical concentrations in polished rice seeds are generally below 4 μg Fe g^{-1} DW (Pfeiffer and McClafferty, 2008), because of the preferential Fe localization in the embryo, aleurone and sub-aleurone layers, which are removed in the polishing process (Lombi *et al.,* 2011; Lu *et al*., 2013).

Iron biofortification has been successfully achieved in rice seeds by increasing NA synthesis, either alone or in combination with increases in the expression of ferritin and/or YSL2. Increases achieved so far in polished grains were from 1-4 μg Fe g^{-1} DW in the different WT cultivars up to 14-19 μg Fe g^{-1} DW in the grains of the transgenic plants (Zheng *et al*., 2010; Johnson *et al*., 2011; Trijatmiko *et al*., 2016). Some of these studies also reported Fe concentrations in unpolished rice seeds, which include tissues with high Fe concentrations such as the aleurone layer and the embryo, and they were in the range from 20 to 64 μg Fe g^{-1} DW (Johnson *et al*., 2011; Lee *et al*., 2009b; Zheng *et al*., 2010). In all studies, transgenic rice lines with increased NA levels led to increased Fe and Zn concentrations both in the embryo and endosperm (Lee *et al*., 2009b; Masuda *et al*., 2013; Trijatmiko *et al*., 2016).

In this Thesis, the overexpression of *OsNAS1* in combination with the expression of *HvNAATb* also led to increases in the Fe concentrations in unpolished rice seed endosperm, up to 60 μg Fe g^{-1} DW (Fig. 4.22). The contribution of the aleurone layer to the total Fe concentration should be very low in the embryo and endosperm fractions used, since it accounts for a very small percentage (<1%) of the total seed weight. The WT and transgenic lines used led to different results (Figs. 4.21 and 4.22), which are discussed in the next paragraphs according to the overexpressed genes.

In the WT the concentrations of DMA were always higher than those of NA. The NA and DMA concentrations in the embryo were 6 and 24 μg g^{-1} DW, respectively, whereas in the endosperm the concentrations of NA and DMA were lower, below the

LOQ and 13 μg g^{-1} DW, respectively. The metal (Fe/Zn) concentrations were 99/102 and 20/21 μg g^{-1} DW in the embryo and endosperm, respectively. Therefore, the embryo was richer in ligands and metal micronutrients than the endosperm. Whereas no data have been reported before for NA and DMA in the embryo, the endosperm values obtained here are in line with those reported previously (*ca*. 4 and 15 μg NA and DMA g^{-1} DW, respectively, in polished rice; Masuda *et al*., 2013; Trijatmiko *et al*., 2016).

The overexpression of *OsNAS1* led to results as good as those of previous studies with transgenic rice regarding the concentrations of NA, DMA and metals (Lee *et al*., 2009b; Zheng *et al*., 2010; Johnson *et al*., 2011; Trijatmiko *et al*., 2016). There were large increases both for NA (97 and 29 μg g^{-1} DW in the embryo and endosperm) and DMA concentrations (88 and 140 μg g^{-1} DW in the embryo and endosperm), and these increases were accompanied by increases in Fe (to 202 and 36 μg g^{-1} DW in the embryo and endosperm) and Zn concentrations (to 136 and 52 μg g^{-1} DW in the embryo and endosperm). These results are in line with previous studies reporting that the overexpression of *NAS* genes lead to increases in the rice seed concentrations of NA, Fe, Zn (Zheng *et al*., 2010; Johnson *et al*., 2011; Masuda *et al*., 2013; Trijatmiko *et al*., 2016), and DMA (Masuda *et al*., 2013; Trijatmiko *et al*., 2016).

The overexpression of *OsNAS1+HvNAATb* led to similar or even better results when compared with those obtained with with *OsNAS1* overexpression alone. The two transgenic lines *OsNAS1+HvNAATb* were different: one of them (line 89) had increases in NA and DMA in the embryo and endosperm (the NA/DMA concentrations were 18/100 μg^{-1} DW in the embryo and 16/124 μg g^{-1} DW in the endosperm), whereas the second one (line 98) had NA concentrations similar to the WT while DMA concentrations were very high (278 and 256 μg g^{-1} DW in the embryo and endosperm, respectively). The Fe concentrations in these two lines were increased, when compared with the WT, both in the embryo (188 and 128 μg g^{-1} DW) and the endosperm (41 and 60 μg g^{-1} DW). In contrast, when compared with the WT, the Zn concentration only increased in the endosperm of the line with high NA and DMA (to 53 μg g^{-1} DW), whereas it decreased in the embryo of the line with high DMA only (to 60 μg g^{-1} DW). This indicates that the ratio NA/DMA strongly influences Zn allocation in seeds.

Finally, the expression of *HvNAATb* alone led to poor results when compared to those overexpressing *OsNAS1* alone or *OsNAS1+HvNAATb*. The two lines expressing *HvNAATb* showed low NA concentrations in the embryo (3 and 2 μg g^{-1} DW) and no

changes in the NA concentrations in the endosperm, whereas the concentration of DMA increased in the embryo in only one of the lines (line 7; to 102 μg g^{-1} DW) and in the endosperm of the other (line 67; to 29 μg g^{-1} DW). In contrast, in line 7 a decrease in DMA was found in the endosperm (7 μg g^{-1} DW). The Fe and Zn concentrations in embryo and endosperm of these transgenic lines were quite similar to those in the WT, although in line 7, with lower endosperm DMA concentrations, a decrease in endosperm Fe concentration (14 μg g^{-1} DW) was found.

These results allow for hypothesizing relationships between ligands and metal micronutrient concentrations, which are also supported by the corresponding Pearson correlation coefficients (Table 4.14). In the endosperm, Fe was highly correlated with DMA but not with NA, whereas NA was highly correlated with Zn. In contrast, in the embryo both Fe and Zn concentrations were correlated with NA but not with DMA, and DMA was correlated with Cu. All these data support that DMA can play a relevant role in endosperm Fe loading and/or storage, and also that Fe and Zn can compete for NA during seed loading. Based on these results, we hypothesize the existence of Fe-NA, Zn-NA and Cu-DMA complexes in the embryo and Fe-DMA and Zn-NA complexes in the endosperm. All these complexes can play different roles in seed metal loading and storage.

5.3.2. Localization of elements in rice seeds

Several authors have studied the distribution of micronutrients in WT and/or transgenic seeds using Synchrotron-based μ-XRF or LA-ICP-MS imaging techniques (Takahashi *et al*., 2009; Johnson *et al*., 2011; Lombi *et al*., 2011; Kyriacou *et al*., 2014; Basnet *et al*., 2014; Trijatmiko *et al*., 2016). In most studies μ-XRF techniques have been used, which provide high resolution but only relative metal levels based on X-ray fluorescence intensity data. Only one study has used LA-ICP-MS, reporting quantitative concentration images of Zn and other toxic metals (As, Pb, Cd, etc.) in seeds of rice plants grown in contaminated soils (Basnet *et al*., 2014). In all these imaging studies, the embryo and aleurone layer showed high concentrations of micronutrients, with the endosperm showing lower, homogeneous micronutrient concentrations. In the case of NAS overexpressors (alone or in combination with other genes) a further accumulation of Fe and Zn in the embryo and aleurone layer has been found (Johnson *et al*., 2011; Trijatmiko *et al*., 2016).

This Thesis shows for the first time quantitative concentration images of several elements (Fe, Mn, Cu, Zn, P and S) in WT and transgenic rice seeds overexpressing *OsNAS1* and/or expressing *HvNAATb* (Figs. 4.27 and 4.28). In the WT, micronutrients (Fe, Mn, Cu and Zn) were mainly localized in the embryo and aleurone layer, in agreement with previous studies. These micronutrients are localized mainly in the leaf (180-200 and 800-1000 μg g^{-1} DW for Fe and Zn, respectively) and root primordia (180-200 and 200-300 μg g^{-1} DW for Fe and Zn, respectively). Iron was also found at high concentrations in the transfer cell layer (*ca*. 250 μg Fe g^{-1} DW), whereas Mn and Cu were mainly in the scutellum (50-100 and 5-10 μg g^{-1} DW for Mn and Cu, respectively). The only metal detected in the external area of the endosperm was Cu, in contrast with previous studies that were able to detect also a homogenous distribution for Zn in the endosperm. This may be due to technical reasons, since we used LA-ICP-MS instead of μ-XRF, and thinner sections than those used in the other studies. In the case of P, this element was mainly in the embryo and the aleurone layer, in the later case probably in the form of the P-rich molecule phytate that can chelate divalent cations (Persson *et al.,* 2009). Sulphur, usually found in proteins as a component of methionine and cysteine, was mainly in the embryo, the aleurone layer and the outer part of endosperm, in the latter case probably in the form of storage proteins such as gluteins and prolamins (Kim *et al*., 2013; Lee *et al*., 2015).

The overexpression of *OsNAS1* and/or the expression of *HvNAATb* led to changes in metal localization within the seed. There were large Fe concentration increases both in the root primordia (to 400-800 μg g^{-1} DW) and scutellum (from the WT values of 100-150 ppm to 400-600 μg g^{-1} DW), whereas in the transfer cell layer the Fe concentration increased only in the case of the *OsNAS1+HvNAATb* lines (to 800 μg g^{-1} DW). These results are in agreement with previous studies with *NAS* overexpressors, which found an increase of Fe concentration in the embryo, aleurone and subaleurone layers (Johnson *et al*., 2011; Kyriacou *et al*., 2014; Trijatmiko *et al*., 2016). Regarding Zn, the overexpression of *OsNAS1* led to a large increase in the Zn concentration only in the root primordia (to 1000-1500 μg g^{-1} DW), whereas the *OsNAS1+HvNAATb* lines showed no major changes in Zn concentration images. A similar result was reported with NAS overexpressors by Johnson *et al*. (2011). Zinc is known to accumulate in root tips during rice seed germination (Takahashi *et al*., 2009) and this Zn increase in meristematic tissues has been explained by its function in protein synthesis and structural components

(Cakmak, 2000). No changes in metal allocation were observed for Mn and Cu, although the concentrations were 2-fold higher in the *OsNAS1+HvNAATb* lines, suggesting that NA and/or DMA have an effect on seed Mn/Cu loading but not in their distribution. Increases of these metals without changes in allocation were also found in NAS overexpressors by Johnson *et al*. (2011). The concentrations and allocation of P and S were unchanged in the overexpressor lines in comparison to the WT.

5.3.3. Concluding remarks on the nicotianamine- and 2'-deoxymugineic acid-facilitated transport of metal micronutrients within the rice seed

Results in this Thesis confirm that NA is critical in seed Fe and Zn loading and distribution and also reveal that DMA plays a significant role in these processes.

The overexpression of *OsNAS1* (alone or in combination with the expression of *HvNAATb*) led to increases in NA (in 3 out of the 4 lines studied) and DMA and Fe concentrations (in all lines), with the highest Fe concentration occurring in the *OsNAS1+HvNAATb* line that had the highest concentration of DMA but no increases in NA. In the case of Zn, concentrations increased in 3 out of 4 lines, and the line where Zn did not change was that with the highest Fe concentration. In previous studies, it has been proposed that DMA is also involved in the long-distance transport of Fe and Zn (Nishiyama *et al*., 2012, Clemens *et al*., 2013).

It is likely that the speciation of Fe and Zn (complexed with NA or DMA) may affect the distribution in developing seeds due to the specificity of the different YSL family transporters, which also vary in tissue localization and abundance. In rice, 18 proteins of this family have been found (Koike *et al*., 2004), and 4 of them (OsYLS2, OsYLS15, OsYLS16 and OsYLS18) have been found to be expressed in the rice seed (Table 5.1). These OsYSL proteins have been reported to transport different metal complexes: Fe(II)-NA and Mn(II)-NA in the case of YLS2 (Koike *et al*., 2004), Fe(II)-NA (Inoue *et al*., 2009) and Fe(III)-DMA (Lee *et al*., 2009a, Inoue *et al*., 2009) in the case of YSL15, Cu(II)-NA (Zheng *et al*., 2012) and Fe(III)-DMA (Kakei *et al*., 2012) in the case of YSL16, and Fe(III)-DMA in the case of YSL18 (Aoyama *et al*., 2009) (Table 5.1). Another transporter not present in seeds, YSL6, has been reported to transport Mn(II)-NA (but not Mn(II)-DMA) for Mn detoxification (Sasaki *et al*., 2011).

Table 5.1. Substrates transported by YSL proteins present in rice seeds.

	NA	DMA	Fe(II)-NA	Fe(III)-NA	Fe(II)-DMA	Fe(III)-DMA	Mn(II)-NA	Mn(II)-DMA	Cu(II)-NA	Cu(II)-DMA	Zn(II)-NA	Zn(II)-DMA
YSL2[1]	X	X	√	X	*nt*	X	√	X	X	*nt*	X	*nt*
YSL15[2]	*nt*	*nt*	X	X	X	√	X	*nt*	*nt*	*nt*	*nt*	*nt*
YSL15[3]	*nt*	*nt*	√	X	X	√	X	*nt*	*nt*	*nt*	*nt*	*nt*
YSL16[4]	*nt*	*nt*	X	*nt*	*nt*	*nt*	*nt*	*nt*	√	*nt*	X	*nt*
YSL16[5]	*nt*	*nt*	X	*nt*	*nt*	√	*nt*	*nt*	*nt*	*nt*	*nt*	*nt*
YSL16[6]	*nt*	*nt*	*nt*	*nt*	*nt*	*nt*	*nt*	*nt*	*nt*	*nt*	*nt*	*nt*
YSL18[7]	*nt*	*nt*	X	*nt*	*nt*	√	*nt*	*nt*	nt	nt	X	X

nt, not tested

[1] Koike *et al*. (2004); [2] Lee *et al*. (2009); [3] Inoue *et al*. (2009); [4] Zheng *et al*. (2012); [5] Kakei *et al*. (2012); [6] Lee *et al*. (2012); [7] Aoyama *et al*. (2009)

Although no direct evidence for a Zn(II)-NA or Zn(II)-DMA transporter protein has been found so far in rice, the existence of such transporters is supported by the identification in this plant species of Zn(II)-NA in the xylem sap (Nishiyama *et al*., 2012) and Zn(II)-DMA in the phloem sap (Suzuki *et al*., 2008), as well as by the fact that the maize root YS1 protein is capable of transporting Zn(II)-DMA (Schaaf *et al*., 2004). The existence of Zn transporters is also supported by the concomitant increase in the expression of 8 out of 18 OPT transporters (not pertaining to the YSL clade) and the Zn translocation from the endosperm to the embryo that occurs during rice germination (Takahashi *et al*., 2009). Due to the high number of YSL and other OPT proteins potentially involved in translocation of the metal-NA and/or -DMA complexes in developing rice seeds, it is likely that one of this proteins could be able to specifically transport Zn(II)-NA or Zn(II)-DMA. To give insight into this issue, a detailed characterization of the localization and the substrate(s) transported by each of the YSL and other OPT proteins would be required.

A tentative model for metal loading, distribution and storage in rice seeds is proposed in Fig 5.7. The Fe-NA and Fe-DMA complexes would be transported *via* xylem and/or phloem saps and then distributed *via* two different pathways, one through the embryo (Fig 5.7, panel 1) and a second one through the aleurone layer (Fig 5.7, panel 2). The Fe(III)-DMA complex has been already found in the phloem sap (Ando *et al*., 2012), and there are some non-conclusive indications that the same metal species may occur in the xylem sap (Ariga *et al*., 2014).

The embryo pathway is described in Fig 5.7, panel 1. This pathway would be preferentially fed *via* phloem sap, with Fe being imported as Fe(III)-DMA through YSL15 (YSL16/18 proteins may also be involved) and perhaps Fe(II)-NA through YSL2 and YSL15. Some Fe(III)-DMA influx from the xylem sap may occur at this stage, also through YSL15. Once in the embryo tissues, Fe(II)-NA would be a relevant species that could function as intra- and inter-cellular distributor of Fe, with the complexes Zn(II)-NA and Cu(II)-DMA being also likely present. Then, it can be hypothesized that Fe(II)-NA would be exported to the transfer cell layer *via* YSL2, a ligand exchange with DMA would occur, and Fe(III)-DMA would be exported to the endosperm *via* YSL15/16/18.

The aleurone layer pathway is described in Fig 5.7, panel 2. In this case, the input *via* xylem sap would be enhanced by the transpiration of the lemma and the palea, the small leaves that cover the seeds and form the husk after seed development is completed (Hoshikawa, 1989), although a contribution from the phloem is also possible. Therefore, Fe(III)-DMA coming *via* the xylem and/or phloem would enter the aleurone layer via YSL15, although it is also possible that a fraction of Fe(II)-NA may enter the aleurone layer from the phloem sap through YSL2. Then, Fe transport from the aleurone layer to the endosperm may occur as Fe(III)-DMA through YSL15/16/18 proteins, being also possible a transport of Fe(II)-NA through YSL2.

Once in the endosperm, the Fe(III)-DMA complex could be a relevant Fe storage compound that would be readily available once seed starts the germination process (and likely bioavailable for human and livestock feed). The expression of different OPT family proteins (Takahashi *et al*., 2009) as well as NAS, NAAT and DMAS proteins support the role of NA and DMA in metal mobilization during germination (Nozoye *et al*., 2007).

The transport of other micronutrients is expected to follow similar routes, although little information is available regarding the specific metal species and proteins involved. The YSL6 transporter was found to be important in Mn detoxification in vegetative tissues, but this protein was not found in reproductive tissues (Sasaki *et al*., 2011), whereas the YSL2 protein might be involved in the transport of Mn-NA from the embryo and aleurone layer to the endosperm (Koike *et al*., 2004). Regarding Cu, the YSL16 protein is expressed in embryo and aleurone layer and is able to transport Cu(II)-DMA complexes (Zheng *et al*., 2012), although there is still controversy regarding the function of this protein, since other authors found YSL16 capable to transport Fe(III)-DMA (Kakei *et al*., 2012; Lee *et al*., 2012).

In summary, it seems that metal upload into rice seeds may not be mediated exclusively by NA, and biofortification approaches should also look at DMA as a relevant metal ligand, since the concentrations of DMA are higher than those of NA both in the embryo and in the endosperm. Due to the high correlation between DMA and Fe in the endosperm, DMA could also be involved in the selective chelation and storage of a significant fraction of Fe in this tissue.

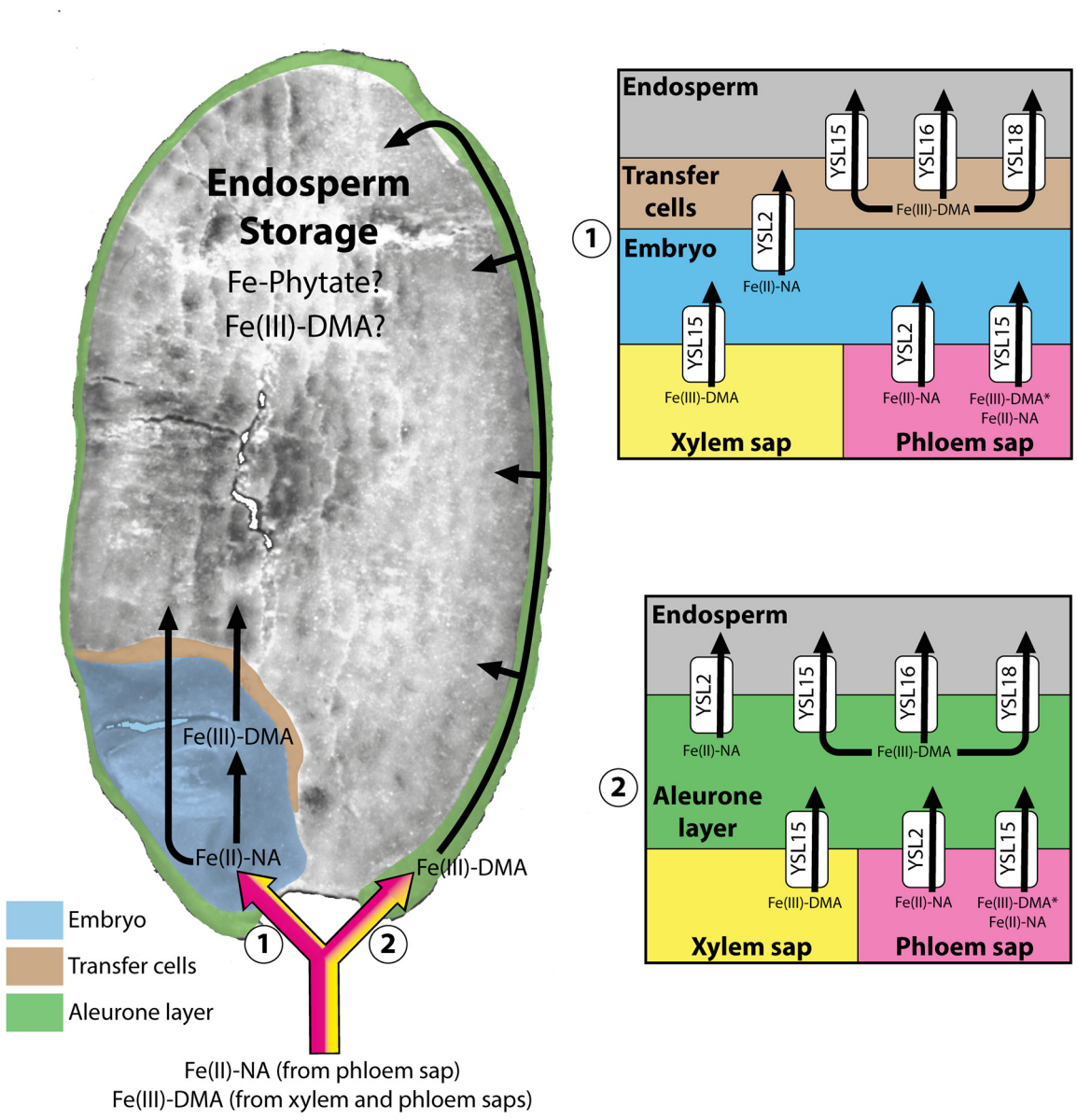

Fig. 5.7. A tentative model for Fe transport mechanisms within the rice seed.
1) embryo pathway, 2) aleurone layer pathway. The only Fe complex found so far in plants (Fe(III)-DMA in the phloem sap) is marked with an asterisk

Chapter 6

Concluding remarks and future prospects

Throughout the previous Chapters it is explained that Fe homeostasis in plants is regulated by different proteins, ligands and pathways that operate either simultaneously or separately, and that the plant Fe status affects this regulation. Novel and relevant roles for the metal ligands NA and its derivative DMA in plant Fe homeostasis are proposed in this Thesis. These include an involvement of these ligands in Fe buffering and distribution between compartments in roots and leaves of the Strategy I plant species tomato (Chapter 5, Section 1), the existence of a DMA-mediated Fe xylem transport pathway, complementing that mediated by carboxylates, in the Strategy II species rice (Chapter 5, Section 2), and an involvement of NA and DMA in the loading and distribution of Fe and Zn in rice seeds (Chapter 5, Section 3).

This Thesis presents the first comprehensive analysis of the concentrations of metal micronutrients, metal ligands and Kreb's cycle metabolites in the xylem sap, apoplastic fluids and symplastic extracts of tomato plants. The comparison of the concentrations of metals and ligands in Fe-sufficient, Fe-deficient, and Fe-deficient plants resupplied with Fe allows for a better understanding of the Fe traffic within the plant. In Fe-deficient tomato plants resupplied with Fe the synthesis of NA is elicited, likely leading to the chelation of Fe and its distribution *via* the root symplastic and apoplastic pathways. The Kreb's cycle, the core of the energetic metabolism in aerobic cells, is also boosted upon Fe ressuply, contributing to fuel the reducing power demand and providing carboxylates (mainly *Cit* and *Mal*) for short-distance root apoplastic Fe transport. The Fe transport to aerial organs is limited during the dark period by the cessation of the transpiration stream, causing a time lag between root Fe acquisition and leaf uptake. Nicotianamine does not seem to participate in xylem Fe transport, with *Cit* and *Mal* being instead the major Fe ligands, whereas NA seems to be a major Fe ligand in the phloem pathway. The relevance of NA and carboxylates in leaf Fe loading is markedly affected by leaf age, since the xylem and phloem sap are the major contributors for Fe transport in developed and young leaves, respectively. On the other hand, NA does not seem to be a player in short-distance Fe trafficking in the leaf apoplastic fluid, with *Cit* and *Mal* being involved at this stage. The low concentrations of metals and ligands reported in this study underline the need for improving current analytical methodologies to identify and quantify Fe-ligand complexes in plant fluids.

This Thesis also unveils novel functions for the NA derivative DMA in Fe transport in rice, a Strategy II plant species. The long-distance Fe transport facilitated by organic

ligands has been studied using foliar *Cit* applications to complement the *Osfrdl1* mutant, which is impaired in the *Cit* xylem loading. The results obtained strongly support that at least two root to shoot Fe transport systems exist in rice, one mediated by carboxylates and another by DMA, with NA not being involved. Thus, when carboxylates are less abundant in the xylem sap (as it occurs in the *Osfrdl1* mutant) DMA appears to be capable to mobilize some Fe from the roots to fulfill the demand of the shoot. The identification of the Fe-DMA complex in the xylem sap of *Osfrdl1* plants would be necessary to finally confirm this hypothesis.

The involvement of NA and its derivative DMA in metal micronutrient loading has been assessed in rice seeds by studying the localization (using MS technologies) of metals and ligands in plants overexpressing *OsNAS1* alone or in combination with the expression of *HvNAATb*. High levels of DMA appear to be crucial for increasing Fe loading in the seed, with final Fe concentrations reaching levels similar or even higher than those obtained with other biofortification approaches (overexpressing *NAS* genes alone or in combination with those of transport -*e.g.* YSL- or storage proteins -*e.g.* ferritin-). This supports that DMA could be a major direct player in Fe seed endosperm loading. The Fe concentration increases found in rice seeds in previous NAS overexpressor studies could be the consequence of increased DMA concentrations due to an enhanced NA synthesis. The relevance of DMA for Fe biofortification in rice is further supported by the high correlation between DMA and Fe concentrations in the endosperm. In contrast, NA concentrations correlated positively with Fe and Zn concentrations in the embryo and with Zn concentrations in the endosperm, supporting that NA is also a key ligand for biofortification of Strategy II crops. Research in the coming years should be directed towards the direct determination of metal complexes in plant fluids using LC-MS-based approaches and the localization of metal ligand complexes in the seeds by means of MALDI-MS imaging techniques.

Conclusions/Conclusiones

1) In Fe-deficient tomato (*Solanum lycopersicum*) plants resupplied with Fe, nicotianamine, citrate and malate are involved in Fe transport in the root apoplast.
2) In Fe-deficient tomato plants resupplied with Fe, nicotianamine is involved in Fe transport in the root symplast.
3) In Fe-deficient tomato plants resupplied with Fe, nicotianamine participates in the long-distance transport of Fe from the developed to young leaves *via* phloem sap but not *via* xylem sap.
4) In Fe-deficient tomato plants resupplied with Fe, the carboxylates citrate and malate are major actors in leaf apoplastic Fe trafficking, whereas nicotianamine does not play a major role at this stage.
5) In rice (*Oryza sativa*) plants, 2'-deoxymugineic acid has an complementary effect to that of citrate in Fe transport from root to shoots, whereas nicotianamine does not play a major role at this stage.
6) In rice seeds nicotianamine participates in Fe loading into the embryo, whereas 2'-deoxymugineic acid is the main ligand involved in Fe loading into the endosperm.
7) In rice seeds nicotianamine participates in Zn loading into the embryo and endosperm, whereas 2'-deoxymugineic acid is not involved in these processes.

1) En plantas de tomate (*Solanum lycopersicum*) deficientes en Fe y reabastecidas con dicho nutriente, los ligandos orgánicos nicotianamina, citrato y malato están involucrados en el transporte de Fe en el fluido apoplástico de raíz.

2) En plantas de tomate deficientes en Fe y reabastecidas con dicho nutriente, la nicotianamina está involucrada en el transporte de Fe en el simplasto de raíz.

3) En plantas de tomate deficientes en Fe y reabastecidas con dicho nutriente, la nicotianamina participa en el transporte a larga distancia de Fe desde las hojas desarrolladas a las hojas jóvenes *via* floema, pero no *via* xilema.

4) En plantas de tomate deficientes en Fe y reabastecidas con dicho nutriente, los carboxilatos citrato y malato son los ligandos principales en el tráfico de Fe en el fluido apoplástico de hoja, mientras que la nicotianamina no tiene un papel destacado en esta etapa.

5) En plantas de arroz (*Oryza sativa*), el ligando orgánico ácido 2'-deoximugineico tiene un papel complementario al del citrato en el transporte de Fe desde la raíz hasta las hojas, mientras que la nicotianamina no tiene un papel destacado en esta etapa.

6) En las semillas de arroz la nicotianamina participa en la carga de Fe en el embrión, mientras que el ácido 2'-deoximugineico es el principal ligando involucrado en la carga de Fe en el endospermo.

7) En las semillas de arroz la nicotianamina participa en la carga de Zn tanto en el embrión como en el endospermo, mientras que el ácido 2'-deoximugineico no está involucrado en estos procesos.

References

Abadía J, López-Millán AF, Rombolà A, Abadía A (2002) Organic acids and Fe deficiency: a review. *Plant Soil* 241: 75-86

Abadía J, Vázquez S, Rellán-Álvarez R, El-Jendoubi H, Abadía A, Álvarez-Fernández A, López-Millán AF (2011) Towards a knowledge-based correction of iron chlorosis. *Plant Physiol Biochem* 49: 471-482

Abdel-Ghany SE (2009) Contribution of plastocyanin isoforms to photosynthesis and copper homeostasis in *Arabidopsis thaliana* grown at different copper regimes. *Planta* 229: 767-779

Alam S, Kamei S, Kawai S (2001) Effect of iron deficiency on the chemical composition of the xylem sap of barley. *Soil Sci Plant Nutr* 47: 643-649

Alexou M, Peuke AD (2013) Methods for xylem sap collection. *Methods Mol Biol* 953: 195-207

Alhendawi RA, Römheld V, Kirkby EA, Marschner H (1997) Influence of increasing bicarbonate concentrations on plant growth, organic acid accumulation in roots and iron uptake by barley, sorghum and maize. *J Plant Nutr* 20: 1731-1753

Álvarez-Fernández A, Paniagua P, Abadía J, Abadía A (2003) Effects of Fe deficiency chlorosis on yield and fruit quality in peach (*Prunus persica* L Batsch). *J Agric Food Chem* 51: 5738-5744

Álvarez-Fernández A, Melgar JC, Abadía J, Abadía A (2011) Effects of moderate and severe iron deficiency chlorosis on fruit yield, appearance and composition in pear (*Pyrus communis* L.) and peach (*Prunus persica* L. Batsch). *Environ Exp Bot* 71: 280-286

Álvarez-Fernández A, Díaz-Benito P, Abadía A, López-Millán AF, Abadía J (2014) Metal species involved in long distance metal transport in plants. *Front Plant Sci* 5: 105

Alves S, Navais C, Simões Gonçalves ML, Correia dos Santos MM (2011) Nickel speciation in the xylem sap of the hiperaccumulator *Alyssum serpyllifolium* ssp Lusitanicum growing on serpentine soils of northeast Portugal. *J Plant Physiol* 168: 1715-1722

Anderegg G, Ripperger H (1989) Correlation between metal complex formation and biological activity of nicotianamine analogues. *J Chem Soc Chem Comm* 1989: 647-650

Ando Y, Nagata S, Yanagisawa S, Yoneyama T (2012) Copper in xylem and phloem saps from rice (*Oryza sativa*): the effect of moderate copper concentrations in the growth medium on the accumulation of five essential metals and a speciation analysis of copper-containing compounds. *Func Plant Biol* 40: 89-100

Anuradha K, Agarwal S, Batchu AK, Babu AP, Mallikarjuna Swamy BP, Longvah T, Sarla N (2012) Evaluating rice germplasm for iron and zinc concentration in brown rice and seed dimensions. *J Phytol* 4: 19-25

Aoyama T, Kobayashi T, Takahashi M, Nagasaka S, Usuda K, Kakei Y, Ishimaru Y, Nakanishi H, Mori S, Nishizawa NK (2009) OsYSL18 is a rice iron(III)-deoxymugineic acid transporter specifically expressed in reproductive organs and phloem of lamina joints. *Plant Mol Biol* 70: 681-692

Ariga T, Hazama K, Yanagisawa S, Yoneyama T (2014) Chemical forms of iron in xylem sap from graminaceous and non-graminaceous plants. *Soil Sci Plant Nutr* 60: 1-10

Armbruster DA, Pry T (2008) Limit of blank, limit of detection and limit of quantitation. *Clin Biochem Rev* 29: 49-52

Atkins CA, Smith PMC and Rodríguez-Medina C (2011) Macro-molecules in phloem exudates - a review. *Protoplasma* 248: 165-172

Banakar R, Álvarez-Fernández A, Abadía J, Capell T, Christou P (2016) A heterologous Fe (III) phytosiderophore transporter expressed in rice increases Fe uptake, translocation and seed loading but excludes heavy metals by selective Fe transport. *Plant Biotechnol J* 15: 423-432

Barabasz A, Wilkowska A, Ruszczyñsk A, Bulska E, Hanikenne M, Czarny M, Kraemer U, Antosiewicz DM (2012) Metal response of transgenic tomato plants expressing P1B-ATPase. *Physiol Plantarum* 145: 315-331

Barberon M, Dubeaux G, Kolb C, Isonoc E, Zelazny E, Vert G (2014) Polarization of IRON-REGULATED TRANSPORTER 1 (IRT1) to the plant-soil interface plays crucial role in metal homeostasis. *Proc Natl Acad Sci USA* 111: 8293-8298

Bashir K, Inoue H, Nagasaka S (2006) Cloning and characterization of deoxymugineic acid synthase genes from graminaceous plants. *J Biol Chem* 281: 32395-32402

Bashir K, Nishizawa NK (2006) Deoxymugineic acid synthase: a gene important for Fe-acquisition and homeostasis. *Plant Signal Behav* 1: 292

Basnet P, Amarasiriwardena D, Wub F, Fub Z, Zhang T (2014) Elemental bioimaging of tissue level trace metal distributions in rice seeds (*Oryza sativa* L) from a mining area in China. *Environ Pol* 195: 148-156

Becker JS, Dietrich RC, Matusch A, Pozebon D, Dressler VL (2008) Quantitative images of metals in plant tissues measured by laser ablation inductively coupled plasma mass spectrometry. *Spectrochim Acta B* 63: 1248-1252

Becker R, Grün M, Scholz G (1992) Nicotianamine and the distribution of iron into the apoplasm and symplasm of tomato (*Lycopersicon esculentum* Mill). *Planta* 187: 48-52

Benes I, Schreiber K, Ripperger H, Kircheiss A (1983) Metal complex formation by nicotianamine, a possible phytosiderophore. *Experientia* 39: 261-262

Bennett JH, Lee EH, Krizek DT, Olsen RA, Brown JC (1982) Photochemical reduction of iron II: plant related factors. *J Plant Nutr* 5: 335-344

Briat JF, Curie C, Gaymard F (2007) Iron utilization and metabolism in plants. *Curr Opin Plant Biol* 10: 276-282

Briat JF, Duc C, Ravet K, Gaymard F (2010) Ferritins and iron storage in plants. *Biochim Biophys Acta* 1800: 806-814

Briat JF, Dubos C, Gaymard F (2015) Iron nutrition, biomass production, and plant product quality. *Trends Plant Sci* 20: 33-40

Broadley MR, White PJ, Hammond JP, Zelko I, Lux A (2009) Zinc in plants. *New Phytol* 173: 677-702

Brown JC, Tiffin LO (1965) Iron stress as related to the iron and citrate occurring in stem exudates. *Plant Physiol* 40: 395-400

Brown JC, Chaney RL, Ambler JE (1971) A new tomato mutant inefficient in the transport of iron. *Physiol Plant* 25: 48-53

Cakmak I (2000) Possible roles of zinc in protecting plant cells from damage by reactive oxygen species. *New Phytol* 146: 185-205

Callahan DL, Baker AJM, Kolev SD, Wedd AG (2006) Metal ion ligands in hyperaccumulating plants. *J Biol Inorg Chem* (2006) 11: 2-12

Callahan DL, Roessner U, Dumontet V, Perrier N, Wedd AG, O'Hair RA (2008) LC-MS and GC-MS metabolite profiling of nickel(II) complexes in the latex of the nickel-hyperaccumulating tree *Sebertia acuminata* and identification of methylated aldaric acid as new nickel(II) ligand. *Phytochemistry* 69: 240-251

Carrasco-Gil S, Álvarez-Fernández A, Sobrino-Plata J, Millán R, Carpena-Ruiz RO, Leduc DL, Andrews JC, Abadía J, Hernández LE (2011) Complexation of Hg with phytochelatins is important for plant Hg tolerance. *Plant Cell Environ* 34: 778-791

Carrasco-Gil S, Siebner H, LeDuc DL, Webb SM, Millán R, Andrews JC, Hernández LE (2013) Mercury localization and speciation in plants grown hydroponically or in a natural environment. *Environ Sci Technol* 47: 3082-3090

Carrasco-Gil S, Rios JJ, Álvarez-Fernández A, Abadía A, García-Mina JM, Abadía J (2016) Effects of individual and combined metal foliar fertilization on iron- and manganese-deficient *Solanum lycopersicum* plants. *Plant Soil* 402: 27-45

Cataldo DA, McFadden KM, Garland TR, Wildung RE (1988) Organic constituents and complexation of Nickel(II), Iron(III), Cadmium(II), and Plutonium(IV) in soybean xylem exudates. *Plant Physiol* 86: 734-739

Cellier MFM (2012) Nramp: from sequence to structure and mechanism of divalent metal import. *Curr Top Membr* 69: 249-293

Cesco S, Neumann G, Tomasi N, Pinton R, Weisskopf L (2010) Release of plant-borne flavonoids into the rhizosphere and their role in plant nutrition. *Plant Soil* 329: 1-25

Christensen AH, Quail PH (1996) Ubiquitin promoter-based vectors for high-level expression of selectable and/or screenable marker genes in monocotyledonous plants. *Transgenic Res* 5: 213-218

Chu BB, Luo LQ, Xu T, Yuan J, Sun JL, Zeng Y, Ma YH, Yi S (2012) XANES study of lead speciation in duckweed. *Spectrosc Spect Anal* 32: 1975-1978

Chu HH, Chiecko J, Punshon T, Lanzirotti A, Lahner B, Salt DE, Walker EL (2010) Successful reproduction requires the function of Arabidopsis Yellow Stripe-Like 1 and Yellow Stripe-Like 3 metal-nicotianamine transporters in both vegetative and reproductive structures. *Plant Physiol* 154: 197-210

CIAAW (2016) Commission on Isotopic Abundances and Atomic Weights, International Union of Pure and Analytical Chemistry

Clemens S, Palmgren MG, Krämer U (2002) A long way ahead: understanding and engineering plant metal accumulation. *Trends Plant Sci* 7: 309-315

Clemens S, Deinlein U, Ahmadi H, Höreth S, Uraguchi S (2013) Nicotianamine is a major player in plant Zn homeostasis. *Biometals* 26: 623-632

Clemens S (2014) Zn and Fe biofortification: The right chemical environment for human bioavailability. *Plant Sci* 225: 52-57

Clemens S, Ma JF (2016) Toxic heavy metal and metalloid accumulation in crop plants and foods. *Annu Rev Plant Biol* 67: 489-512

Clinical and Laboratory Standards Institute (2015) EP17-A2: Evaluation of detection capability for clinical laboratory measurement procedures; approved guideline - 2nd edition 32: 8

Cohen CK, Fox TC, Garvin DF, Kochian LV (1998) The role of iron-deficiency stress responses in stimulating heavy-metal transport in plants. *Plant Physiol* 116: 1063-1072

Colangelo EP, Guerinot ML (2006) Put the metal to the petal: metal uptake and transport throughout plants. *Curr Opin Plant Biol* 9: 322-330

Conte SS, Walker EL (2011) Transporters contributing to iron trafficking in plants. *Mol Plant* 4: 464-476

Cornu J, Deinlein U, Höreth S, Braun M, Schmidt H, Weber M, Persson DP, Husted S, Schjoerring JK, Clemens S (2015) Contrasting effects of nicotianamine synthase knockdown on zinc and nickel tolerance and accumulation in the zinc/cadmium hyperaccumulator *Arabidopsis halleri*. *New Phytol* 206: 738-750

Culotta V, Scott RA (2013) Metals in Cells. John Wiley and Sons, New York, USA

Curie C, Briat JF (2003) Iron transport and signaling in plants. *Annu Rev Plant Biol* 54: 183-206

Curie C, Cassin G, Couch D, Divol F, Higuchi K, LeJean (2009) Metal movement within the plant: contribution of nicotianamine and yellow stripe 1-like transporters. *Ann Bot* 103: 1-11

Dannel F, Pfeffer H, Marschner H (1995) Isolation of apoplasmic fluid from sunflower leaves and its use for studies on influence of nitrogen supply on apoplasmic pH. *J Plant Physiol* 146: 273-278

De Benoist B, Egli I, Cogswell M (2008) Worldwide prevalence of anaemia 1993-2005. Geneva: World Health Organization

Deinlein U, Weber M, Schmidt H, Rensch S, Trampczynska A, Hansen TH, Husted S, Schjoerring JK, Talke IN, Krämer U, Clemens S (2012) Elevated nicotianamine levels in *Arabidopsis halleri* roots play a key role in zinc hyperaccumulation. *Plant Cell* 24: 708-723

Dinant S, Kehr J (2013) Sampling and analysis of phloem sap. *Methods Mol Biol* 953: 185-194

Donner E, Punshon T, Guerinot ML, Lombi E (2012) Functional characterization of metal(loid) processes in planta through the integration of synchrotron techniques and plant molecular biology. *Anal Bioanal Chem* 402: 3287-3298

Donnini S, Castagna A, Guidi L, Zocchi G, Ranieri A (2003) Leaf responses to reduced iron availability in two tomato genotypes: T3238FER (iron efficient) and T3238fer (iron inefficient). *J Plant Nut* 26: 2137-2148

Douchkov D, Gryczka C, Stephan UW, Hell R, Bäumlein H (2005) Ectopic expression of nicotianamine synthase genes results in improved iron accumulation and increased nickel tolerance in transgenic tobacco. *Plant Cell Environ* 28: 365-374

Durrett TP, Gassmann W, Rogers EE (2007) The FRD3-mediated efflux of citrate into the root vasculature is necessary for efficient iron translocation. *Plant Physiol* 144: 197-205

Duy D, Wanner G, Meda AR, von Wirén N, Soll J, Philippar K (2007) PIC1, an ancient permease in *Arabidopsis* chloroplasts, mediates iron transport. *Plant Cell* 19: 986-1006

Eide D, Broderius M, Fett J, Guerinot ML (1996) A novel iron-regulated metal transporter from plants identified by functional expression in yeast. *Proc Natl Acad Sci USA* 93: 5624-5628

European Food Safety Authority (2014) Scientific opinion on dietary reference values for zinc. *EFSA Journal* 12: 3844

European Food Safety Authority (2015) Scientific opinion on dietary reference values for iron. *EFSA Journal* 13: 4254

Fernando DR, Mizuno T, Woodrow IE, Baker AJM, Collins RN (2010) Characterization of foliar manganese (Mn) in Mn (hyper)accumulators using X-ray absorption spectroscopy. *New Phytol* 188: 1014-1027

Fiehn O (2003) Metabolic networks of *Cucurbita maxima* phloem. *Phytochemistry* 62: 875-886

Flis P, Ouerdane L, Grillet L, Curie C, Mari S, Lobinski, R (2016) Inventory of metal complexes circulating in plant fluids: a reliable method based on HPLC coupled with dual elemental and high-resolution molecular mass spectrometric detection. *New Phytol* 211: 1129-1141

Fourcroy P, Sisó-Terraza P, Sudre D, Savirón M, Reyt G, Gaymard F, Anunciacion Abadía A, Abadía J, Álvarez-Fernández A, Briat JF (2014) Involvement of the ABCG37 transporter in secretion of scopoletin and derivatives by *Arabidopsis* roots in response to iron deficiency. *New Phytol* 201: 155-167

Gayomba SR, Zhiyang Zhai Z, Jung H, Vatamaniuk OK (2015) Local and systemic signaling of iron status and its interactions with homeostasis of other essential elements. *Front Plant Sci* 6: 716

Giavalisco P, Kapitza K, Kolasa A, Buhtz A, Kehr J (2006) Towards the proteome of *Brassica napus* phloem sap. *Proteomics* 6: 896-909

Gogorcena Y, Larbi A, Andaluz S, Carpena RO, Abadía A, Abadía J (2011) Effects of cadmium on cork oak (*Quercus suber* L) plants grown in hydroponics. *Tree Physiol* 31: 1401-1412

González-Vallejo EB, Morales F, Cistué L, Abadía A, Abadía J (2000) Iron deficiency decreases the Fe(III)-chelate reducing activity of leaf protoplasts. *Plant Physiol* 122: 337-344

Grillet L, Ouerdane L, Flis P, Hoang MTT, Isaure MP, Lobinski R (2014) Ascorbate efflux as a new strategy for iron reduction and transport in plants. *J Biol Chem* 289: 2515-2525

Gupta RJ, Gangoliya SS, Singh NK (2015) Reduction of phytic acid and enhancement of bioavailable micronutrients in food grains. *J Food Sci Technol* 52: 676-684

Gutierrez-Carbonell E, Lattanzio G, Albacete A, Rios JJ, Kehr J, Abadía A, Grusak MA, Abadía J, López-Millán AF (2015) Effects of Fe deficiency on the protein profile of *Brassica napus* phloem sap. *Proteomics* 15: 3835-3853

Guttieri MJ, Bowen D, Dorsch JA, Raboy V, Souza E (2004) Identification and characterization of low phytic acid wheat. *Crop Sci* 44: 418-424

Harada E, Sugase K, Namba K, Iwashita T, Murata Y (2007) Structural element responsible for the Fe(III)-phytosiderophore specific transport by HvYS1 transporter in barley. *FEBS Letters* 581: 4298-4302

Harris WR, Sammons RD, Grabiak RC (2012) A speciation model of essential trace metal ions in phloem. *J Inorg Biochem* 116: 140-150

Haydon MJ, Cobbett CS (2007) Transporters of ligands for essential metal ions in plants. *New Phytol* 174: 499-506

Haydon MJ, Miki Kawachi M, Wirtz M, Hillmer S, Hell R, Krämer U (2012) Vacuolar nicotianamine has critical and distinct roles under iron deficiency and for zinc sequestration in *Arabidopsis*. *Plant Cell* 24: 724-737

Higuchi K, Kanazawa K, Nishizawa N-K, Chino M, Mori S (1994) Purification and characterization of nicotianamine synthase from Fe-deficient barley root. *Plant Soil* 165: 173-179

Hoshikawa K (1989) The growing rice plant: an anatomical monograph. Tokyo: Nobunkyo xvi

Huguet S, Bert V, Laboudigue A, Barthes V, Isaure MP, Llorens I, Schat H, Sarret G (2012) Cd speciation and localization in the hyperaccumulator *Arabidopsis halleri*. *Environ Exp Bot* 82: 54-65

Husted S, Persson DP, Laursen KH, Hansen TH, Pedas P, Schiller M, Hegelund JN, Schjoerring JK (2011) Review: The role of atomic spectrometry in plant science. *J Anal At Spectrom* 26: 52-79

Inoue H, Mizuno D, Takahashi M, Nakanishi H, Mori S, Nishizawa NK (2004) A rice FRD3-like (*OsFRDL1*) gene is expressed in the cells involved in long-distance transport. *Soil Sci Plant Nut* 50: 1133-1140

Inoue H, Takahashi M, Kobayashi T, Suzuki M, Nakanishi H, Mori S, Nishizawa NK (2008) Identification and localisation of the rice nicotianamine aminotransferase gene *OsNAAT1* expression suggests the site of phytosiderophore synthesis in rice. *Plant Mol Biol* 66: 193-203

Inoue H, Kobayashi T, Nozoye T, Takahashi M, Kakei Y, Suzuki K, Nakazono M, Nakanishi H, Mori S, Nishizawa NK (2009) Rice OsYSL15 is an iron-regulated iron(III)-deoxymugineic acid transporter expressed in the roots and is essential for iron uptake in early growth of the seedlings. *J Biol Chem* 284: 3470-3479

Irtelli B, Petrucci WA, Navari-Izzo F (2009) Nicotianamine and histidine/proline are, respectively, the most important copper chelators in xylem sap of *Brassica carinata* under conditions of copper deficiency and excess. *J Exp Bot* 60: 269-277

Ishimaru Y, Suzuki M, Tsukamoto T, Suzuki K, Nakazono M, Kobayashi T, Wada Y, Watanabe S, Matsuhashi S, Takahashi M, Nakanishi H, Mori S, Nishizawa NK (2006) Rice plants take up iron as an Fe^{3+}-phytosiderophore and as Fe^{2+}. *Plant J* 45: 335-346

Jeong J, Connolly EL (2009) Iron uptake mechanisms in plants: Functions of the FRO family of ferric reductases. *Plant Sci* 176: 709-714

Jin CW, You GY, He YF, Tang C, Wu P, Zheng SJ (2007) Iron deficiency-induced secretion of phenolics facilitates the reutilization of root apoplastic iron in red clover. *Plant Physiol* 144: 278-285

Johnson AAT, Kyriacou B, Callahan DL, Carruthers L, Stangoulis J, Lombi E, Tester M (2011) Constitutive overexpression of the *OsNAS* gene family reveals single-gene strategies for effective iron- and zinc-biofortification of rice endosperm. *PLoS ONE* 6(9): e24476

Kakei Y, Yamaguchi I, Kobayashi T, Takahashi M, Nakanishi H, Yamakawa T, Nishizawa NK (2009) A highly sensitive, quick and simple quantification method for nicotianamine and 2'-deoxymugineic acid from minimum samples using LC/ESI-TOF-MS achieves functional analysis of these components in plants. *Plant Cell Physiol* 50: 1988-1993

Kakei Y, Yasuhiro Ishimaru Y, Kobayashi T, Yamakawa T, Nakanishi H, Nishizawa MK (2012) OsYSL16 plays a role in the allocation of iron. *Plant Mol Biol* 79: 583-594

Kambe K, Tsuji T, Hashimoto A, Itsumura N (2015) The physiological, biochemical and molecular roles of zinc transporters in zinc homeostasis and metabolism. *Physiol Rev* 95: 749-784

Kato M, Ishikawa S, Inagaki K, Chiba K, Hayashi H, Yanagisa S, Yoneyama T (2010) Possible chemical forms of cadmium and varietal differences in cadmium concentrations in the phloem sap of rice plants (*Oryza sativa* L). *Soil Sci Plant Nutr* 56: 839-847

Kawai S, Takagi S, Sato Y (1988) Mugineic acid-family phytosiderophores in root-secretions of barley, corn and sorghum varieties. *J Plant Nutr* 11: 633-642

Kawai S, Kamei S, Matsuda Y, Ando R, Kondo S, Ishizawa A, Alam S (2001) Concentrations of iron and phytosiderophores in xylem sap of iron-deficient barley plants. *Soil Sci Plant Nutr* 47: 265-272

Keuskamp DH, Kimber R, Bindraban P, Dimkpa C, Schenkeveld WDC (2015) Plant exudates for nutrient uptake. *VFRC Report 2015/4*

Khouzam RB, Szpunar J, Holeman M, Lobinski R (2012) Trace element speciation in food: State of the art of analytical techniques and methods. *Pure Appl Chem* 84: 169-179

Kim S, Takahashi M, Higuchi K, Tsunoda K, Nakanishi H, Yoshimura E, Mori S, Nishizawa NK (2005) Increased nicotianamine biosynthesis confers enhanced tolerance of high levels of metals, in particular nickel, to plants. *Plant Cell Physiol* 46: 1809-1818

Kim SA, Punshon T, Lanzirotti A, Li L, Alonso JM, Ecker JR, Kaplan J, Guerinot ML (2006) Localization of iron in *Arabidopsis* seed requires the vacuolar membrane transporter VIT1. *Science* 214: 1295-1298

Kim SA, Guerinot ML (2007) Mining iron: Iron uptake and transport in plants. *FEBS Letters* 581: 2273-2280

Kim HJ, Lee JY, Yoon UH, Lim SH, Kim YM (2013) Effects of reduced prolamin on seed storage protein composition and the nutritional quality of rice. *Int J Mol Sci* 14: 17073-17084

Klatte M, Schuler M, Wirtz M, Fink-Straube C, Hell R, Bauer P (2009) The analysis of *Arabidopsis* nicotianamine synthase mutants reveals functions for nicotianamine in seed iron loading and iron deficiency responses. *Plant Physiol* 150: 251-271

Kobayashi T, Itai RN, Nishizawa NK (2014) Iron deficiency responses in rice roots. *Rice* 7: 17

Koike S, Inoue H, Mizuno D, Takahashi M, Nakanishi H, Mori S (2004) OsYSL2 is a rice metal-nicotianamine transporter that is regulated by iron and expressed in the phloem. *Plant J* 39: 415-424

Kolaj-Robin O, Russell D, Hayes KA, Pembroke JT, Soulimane T (2015) Cation diffusion facilitator family: structure and function. *FEBS Letters* 589: 1283-1295

Komal T, Mustafa M, Ali Z, Kazi AG (2015) Heavy metal contamination of soils: heavy metal uptake and transport in plants. *Soil Biology* 44: 181-194

Konz I, Fernández B, Fernández ML, Pereiro R, Sanz-Medel A (2012) Laser ablation ICP-MS for quantitative biomedical applications. *Anal Bioanal Chem* 403: 2113-2125

Konz I, Fernández B, Fernández ML, Pereiro R, Gonzalez-Iglesias H, Coca-Prados M, Sanz-Medel A (2014) Quantitative bioimaging of trace elements in the human lens by LA-ICP-MS. *Anal Bioanal Chem* 406: 2343-2348

Korshunova YO, Eide D, Clark WG, Guerinot ML, Pakrasi HB (1999) The IRT1 protein from *Arabidopsis thaliana* is a metal transporter with a broad substrate range. *Plant Mol Biol* 1999 40: 37-44

Köster J, Shi R, von Wirén N, Weber G (2011) Evaluation of different column types for the hydrophilic interaction chromatographic separation of iron-citrate and copper-histidine species from plants. *J Chromatogr A* 1218: 4934-4943

Krämer U, Talke IN, Hanikenne M (2007) Transition metal transport. *FEBS Letters* 581: 2263-2272

Krämer U (2010) Metal hyperaccumulation in plants. *Annu Rev Plant Biol* 61: 517-534

Krüger C, Berkowitz O, Stephan U, Hell R (2002) A metal-binding member of the late embryogenesis abundant protein family transports iron in the phloem of *Ricinus communis* L. *J Biol Chem* 277: 25062-25069

Küpper H, Mijovilovich A, Meyer-Klaucke W, Kroneck PM (2004) Tissue- and age-dependent differences in the complexation of cadmium and zinc in the cadmium/zinc hyperaccumulator *Thlaspi caerulescens* (Ganges ecotype) revealed by X-ray absorption spectroscopy. *Plant Physiol* 134: 748-757

Küpper H, Goetz B, Mijovilovich A, Kupper FC, Meyer-Klaucke W (2009) Complexation and toxicity of copper in higher plants I: characterization of copper accumulation, speciation, and toxicity in *Crassula helmsii* as a new copper accumulator. *Plant Physiol* 151: 702-714

Kyriacou B, Moore KL, Paterson D, de Jonge MD, Howard DL, Stangoulis J, Tester M, Lombi E, Johnson AAT (2014) Localization of iron in rice grain using synchrotron X-ray fluorescence microscopy and high resolution secondary ion mass spectrometry. *J Cereal Sci* 59: 173-180

Larbi A, Morales F, Abadía J, Abadía A (2003) Effects of branch solid Fe sulphate implants on xylem sap composition in field-grown peach and pear: changes in Fe, organic anions and pH. *J Plant Physiol* 160: 1473-1481

Larbi A, Morales F, Abadía A, Abadía J (2010) Changes in iron and organic acid concentrations in xylem sap and apoplastic fluid of iron-deficient *Beta vulgaris* plants in response to iron resupply. *J Plant Physiol* 167: 255-260

Lasat MM, Baker ALJM, Kochian LV (1998) Altered Zn compartmentation in the root symplasm and stimulated Zn absorption into the leaf as mechanisms involved in Zn hyperaccumulation in *Thlaspi caerulescens*. *Plant Physiol* 118: 875-883

Lattanzio G, Andaluz S, Matros A, Calvete JJ, Kehr J, Abadía A, Abadía J, López-Millán A-F (2013) Protein profile of *Lupinus texensis* phloem sap exudates: searching for Fe- and Zn-containing proteins. *Proteomics* 13: 2283-2296

Lee S, Chiecko JC, Kim SA, Walker EL, Lee Y, Guerinot ML, An G (2009a) Disruption of *OsYSL15* leads to iron inefficiency in rice plants. *Plant Physiol* 150: 786-800

Lee S, Jeon US, Lee SJ, Kima YK, Persson DP, Husted S, Schjørring JK, Kakei Y, Masuda H, Nishizawa NK, An G (2009b) Iron fortification of rice seeds through activation of the nicotianamine synthase gene. *Proc Natl Acad Sci USA* 106: 22014-22019

Lee S, Ryoo N, Jeon JS, Guerinot ML, An G (2012) Activation of rice Yellow Stripe1-Like 16 (OsYSL16) enhances iron efficiency. *Mol Cells* 33: 117-126

Lee HJ, Jo YM, Lee JY, Lim SH, Kim YM (2015) Lack of globulin synthesis during seed development alters accumulation of seed storage proteins in rice. *Int J Mol Sci* 16: 14717-14736

Leitenmaier B, Küpper H (2013) Compartmentation and complexation of metals in hyperaccumulator plants. *Front Plant Sci* 4: 374

Li L, Cheng X, Ling H (2004) Isolation and characterization of Fe(III)-chelate reductase gene LeFRO1 in tomato. *Plant Mol Biol Report* 54: 125-136

Liao MT, Hedley MJ, Woolley DJ, Brooks RR, Nichols MA (2000) Copper uptake and translocation in chicory (*Cichorium intybus* L cv Grasslands Puna) and tomato (*Lycopersicon esculentum* Mill cv Rondy) plants grown in NFT system I: Copper uptake and distribution in plants. *Plant Soil* 221: 135-142

Lindsay WL, Schwab AP (1982) The chemistry of iron in soils and its availability to plants. *J Plant Nut* 5: 821-840

Lindsay WL (1995) Chemical reactions in soils that affect iron availability to plants A quantative approach. In: *Iron Nutrition in Soils and Plants*. Abadía J (ed). Kluwer Academic Publishers, Dordrecht, The Netherlands

Lingle JC, Tiffin LO, Brown JC (1963) Iron uptake-transport of soybeans as influenced by other cations. *Plant Physiol* 38: 71-76

Lohaus G, Pennewis K, Sattelmacher B, Hussman M, Muehling KH (2001) Is the infiltration-centrifugation technique appropriate for the isolation of apoplastic fluid? A critical evaluation with different plant species. *Physiol Plant* 111: 457-465

Lombi E, Smith E, Hansen TH, Paterson D, de Jonge MD, Howard DL, Persson DP, Husted S, Ryan C, Schjoerring JK (2011) Megapixel imaging of (micro)nutrients in mature barley grains. *J Exp Bot* 62: 273-282

López-Millán AF, Morales F, Abadía A, Abadía J (2000a) Effects of iron deficiency on the composition of the leaf apoplastic fluid and xylem sap in sugar beet: implications for iron and carbon transport. *Plant Physiol* 124: 873-884

López-Millán AF, Morales F, Andaluz S, Gogorcena Y, Abadía A, de las Rivas J, Abadía J (2000b) Responses of sugar beet roots to iron deficiency. Changes in carbon assimilation and oxygen use. *Plant Physiol* 124: 885-897

López-Millán AF, Morales F, Gogorcena Y, Abadía A, Abadía J (2001a) Iron resupply-mediated deactivation of Fe-deficiency stress responses in roots of sugar beet. *Aust J Plant Physiol* 28: 171-180

López-Millán AF, Morales F, Abadía A, Abadía J (2001b) Iron deficiency-associated changes in the composition of the leaf apoplast fluid from field-grown pear (*Pyrus communis* L) trees. *J Exp Bot* 52: 1489-1498

López-Millán AF, Morales F, Gogorcena Y, Abadía A, Abadía J (2009) Metabolic responses in iron deficient tomato plants. *J Plant Physiol* 166: 375-384

López-Millán AF, Grusak MA, Abadía J (2012) Carboxylate metabolism changes induced by Fe deficiency in barley, a Strategy II plant species. *J Plant Physiol* 169: 1121-1124

Lu L, Tian S, Liao H, Zhang J, Yang X, John M Labavitch JM, Chen W (2013) Analysis of metal element distributions in rice (*Oryza sativa* L) seeds and relocation during germination based on X-ray fluorescence imaging of Zn, Fe, K, Ca, and Mn. *PLoS ONE* 8(2): e57360

Marentes E, Grusak MA (1998) Iron transport and storage within the seed coat of developing embryos of pea (*Pisum sativum* L). *Seed Sci Res* 8: 367-375

Mari S, Gendre D, Pianelli K, Ouerdane L, Lobinski R, Briat JF, Lebrun M, Czernic P (2006) Root-to-shoot long-distance circulation of nicotianamine and nicotianamine-nickel chelates in the metal hyperaccumulator *Thlaspi caerulescens*. *J Exp Bot* 57: 4111-4122

Marschner H, Römheld V, Kissel M (1986) Different strategies in higher plants in mobilization and uptake of iron. *J Plant Nutr* 9: 695-713

Marschner H (1995) Mineral Nutrition of Higher Plants. 2nd edition. Academic Press, London, U.K.

Masuda H, Usuda K, Kobayashi T, Ishimaru Y, Kakei Y, Takahashi M, Higuchi K, Nakanishi H, Mori S, Nishizawa NK (2009) Overexpression of the barley Nicotianamine Synthase gene *HvNAS1* increases iron and zinc concentrations in rice grains. *Rice* 2: 155-166

Masuda H, Kobayashi T, Ishimaru Y, Takahashi M, Aung MS, Nakanishi H, Mori S, Nishizawa NK (2013) Iron-biofortification in rice by the introduction of three barley genes participated in mugineic acid biosynthesis with soy bean ferritin gene. *Front Plant Sci* 4: 132

McNear DH, Chaney RL, Sparks DL (2010) The metal hyperaccumulator *Alyssum murale* uses nitrogen and oxygen donor ligands for Ni transport and storage. *Phytochemistry* 71: 188-200

McNear DH, Afton SE, Caruso JA (2012) Exploring the structural basis for selenium/mercury antagonism in *Allium fistulosum*. *Metallomics* 4: 267-276

Meija J, Montes-Bayón M, Caruso JA, Sanz-Medel A (2006) Integrated mass spectrometry in (semi)metal speciation and its potential in phytochemistry. *Trends Anal Chem* 25: 44-51

Mendoza-Cózatl DG, Emerald Butko E, Franziska Springer F, Justin W. Torpey JW, Elizabeth A. Komives EA, Julia Kehr J, Schroeder JI (2008) Identification of high levels of phytochelatins, glutathione and cadmium in the phloem sap of *Brassica napus*. A role for thiol-peptides in the long-distance transport of cadmium and the effect of cadmium on iron translocation. *Plant J* 54: 249-259

Mendoza-Cózatl DG, Jobe TO, Hauser F, Schroeder JI (2011) Long-distance transport, vacuolar sequestration, tolerance, and transcriptional responses induced by cadmium and arsenic. *Curr Opin Plant Biol* 14: 554-562

Mesko MF, Hartwig CA, Bizzi CA, Pereira JSF, Mello PA, Flores EMM (2011) Sample preparation strategies for bioinorganic analysis by inductively coupled plasma mass spectrometry. *Int J Mass Spectrom* 307: 123-136

Meyer S, Angeli AD, Fernie AR, Martinoia E (2010) Intra-and extra-cellular excretion of carboxylates. *Trends Plant Sci* 15: 40-47

Milner MJ, Kochian LV (2008) Investigating heavy-metal hyperaccumulation using *Thlaspi caerulescens* as a model system. *Ann Bot* 102: 3-13

Mimmo T, Del Buono D, Terzano R, Tomasi N, Vigani G, Crecchio C (2014) Rhizospheric organic compounds in the soil-microorganism plant system: their role in iron availability. *Eur J Soil Sci* 65: 629-642

Monicou S, Szpunar J, Lobinski R (2009) Metallomics: the concept and methodology. *Chem Soc Rev* 38: 1119-1138

Monsant AC, Kappen P, Wang Y, Pigram PJ, Baker AJM, Tang C (2011) *In vivo* speciation of zinc in *Noccaea caerulescens* in response to nitrogen form and zinc exposure. *Plant Soil* 348: 167-183

Morgan B, Lahav O (2007) The effect of pH on the kinetics of spontaneous Fe(II) oxidation by O_2 in aqueous solution - basic principles and a simple heuristic description. *Chemosphere* 68: 2080-2084

Morrissey J, Guerinot ML (2009) Iron uptake and transport in plants: the good, the bad and the ionome. *Chem Rev* 109: 4553-4567

Morrissey J, Baxter IR, Lee J, Li L, Lahner B, Grotz N, Jerry Kaplan J, Salt DE, Guerinot ML (2009) The Ferroportin metal efflux proteins function in iron and cobalt homeostasis in *Arabidopsis*. *Plant Cell* 21: 3326-3338

Murakami T, Ise K, Hayakawa M, Kamei S, Takagi S (1989) Stabilities of metal complexes of mugineic acid and their specific affinities for iron(III). *Chem Lett* 18: 2137-2140

Murashige T, Skoog F (1962) A revised medium for rapid growth and bio assays with tobacco tissue cultures. *Physiol Plantarum* 15: 473-497

Nakamura S, Akiyama C, Sasaki T, Hattori H, Chino M (2008) Effect of cadmium on the chemical composition of xylem exudates from oilseed rape plants (*Brassica napus* L). *Soil Sci Plant Nutr* 54: 118-127

Nikolic M, Römheld V (1999) Mechanism of Fe uptake by the leaf symplast: Is Fe inactivation in leaf a cause of Fe deficiency chlorosis? *Plant Soil* 215: 229-237

Nishiyama R, Kato M, Nagata S, Yanagisawa S, Yoneyama T (2012) Identification of Zn-nicotianamine and Fe-2-deoxymugineic acid in the phloem sap from rice plants (*Oryza sativa* L). *Plant Cell Physiol* 53: 381-390

Noma M, Noguchi M, Tamaki E (1971) A new amino acid, nicotianamine, from tobacco leaves. *Tetrahedron Lett* 12: 2017-2020

Nozoye T, Inoue H, Takahashi M, Ishimaru Y, Nakanishi H, Mori S, Nishizawa NK (2007) The expression of iron homeostasis-related genes during rice germination. *Plant Mol Biol* 64: 35-47

Nozoye T, Nagasaka S, Kobayashi T (2011) Phytosiderophore efflux transporters are crucial for iron acquisition in graminaceous plants. *J Biol Chem* 286: 5446-5454

Nozoye T, Tsunoda K, Nagasaka S, Bashir K, Takahashi M, Kobayashi T, Nakanishi H, Nishizawa NK (2014a) Rice nicotianamine synthase localizes to particular vesicles for proper function. *Plant Signal Behav* 9: e28660

Nozoye T, Kim S, Kakei Y, Takahashi M, Nakanishi H, Nishizawa NK (2014b) Enhanced levels of nicotianamine promote iron accumulation and tolerance to calcareous soil in soybean. *Biosci Biotechnol Biochem* 78: 1677-1684

Oliveira SR, Arruda M (2015) Application of laser ablation (imaging) inductively coupled plasma mass spectrometry for mapping and quantifying Fe in transgenic and non-transgenic soybean leaves. *J Anal At Spectrom* 30: 389-395

Orera I, Rodríguez-Castrillón JA, Moldovan M, García-Alonso JI, Abadía A, Abadía J, Álvarez-Fernández A (2010) Using a dual-stable isotope tracer method to study the uptake, xylem transport and distribution of Fe and its chelating agent from stereoisomers of an Fe(III)-chelate used as fertilizer in Fe-deficient Strategy I plants. *Metallomics* 2: 646-657

Ouerdane L, Mari S, Czernic P, Lebrun M, Lobinski R (2006) Speciation of non-covalent nickel species in plant tissue extracts by electrospray Q-TOFMS/MS after their isolation by 2D size exclusion hydrophilic interaction LC (SEC-HILIC) monitored by ICP-MS. *J Anal At Spectrom* 21: 676-683

Paesano R, Natalizi T, Berlutti F, Valenti P (2012) Body iron delocalization: the serious drawback in iron disorders in both developing and developed countries. *Pathog Glob Health* 106: 200-216

Pal R, Rai JPN (2010) Phytochelatins: peptides involved in heavy metal detoxification. *Appl Biochem Biotechnol* 160: 945-963

Palmer CM, Guerinot ML (2009) Facing the challenges of Cu, Fe and Zn homeostasis in plants. *Nat Chem Biol* 5: 333-340

Palmer LJ, Palmer LT, Pritchard J, Graham RD, Stangoulis JCR (2013) Improved techniques for measurement of nanolitre volumes of phloem exudate from aphid stylectomy. *Plant Methods* 9: 18

Parkhurst DF (1982) Stereological methods for measuring internal leaf structural variables. *Am J Bot* 69: 31-39

Patrick JW, Offler CE (2001) Compartmentation of transport and transfer events in developing seeds. *J Exp Bot* 52: 551-564

Persson DP, Hansen TH, Laursen KH, Schjoerring JK, Husted S (2009) Simultaneous iron, zinc, sulfur and phosphorus speciation analysis of barley grain tissues using SEC-ICP-MS and IP-ICP-MS. *Metallomics* 1: 418-426

Pfeiffer WH, McClafferty B (2008) Biofortification: breeding micronutrient dense crops *In:* Breeding major food staples. Kang MS, Priyadarshanpp PM (eds) pp: 61-91 Blackwell Publishing Ltd, Oxford, UK

Pianelli K, Mari S, Marquès L, Lebrun M, Czernic P (2005) Nicotianamine over-accumulation confers resistance to nickel in *Arabidopsis thaliana*. *Transgenic Res* 14: 739-748

Pich A, Scholz G, Stephan U (1994) Iron-dependent changes of heavy-metals, nicotianamine, and citrate in different plant organs and in the xylem exudate of two tomato genotypes - nicotianamine as a possible copper translocator. *Plant Soil* 165: 189-196

Pich A, Scholz G (1996) Translocation of copper and other micronutrients in tomato plants (*Lycopersicon esculentum* Mill): nicotianamine-stimulated copper transport in the xylem. *J Exp Bot* 47: 41-47

Pilon M, Tapken W (2016) Regulation of copper homeostasis in plants. *In:* Metals in cells. Culotta V, Scott RA (eds) pp: 289-300. John Wiley and Sons, New York, USA

Pittman JK (2005) Managing the manganese: molecular mechanisms of manganese transport and homeostasis. *New Phytol* 167: 733-742

Pottier M, Masclaux-Daubresse C, Yoshimoto K, Thomine S (2014) Autophagy as a possible mechanism for micronutrient remobilization from leaves to seeds. *Front Plant Sci* 5: 11

Puig S, Peñarrubia L (2009) Placing metal micronutrients in context: transport and distribution in plants. *Curr Opin Plant Biol* 12: 299-306

Rabotti C, De Nisi P, Zocchi C (1995) Metabolic implications in the biochemical responses to iron deficiency in cucumber (*Cucumis sativus* L.) roots. *Plant Physiol* 107: 1195-1199

Rellán-Álvarez R, Abadía J, Álvarez-Fernández A (2008) Formation of metal-nicotianamine complexes as affected by pH, ligand exchange with citrate and metal exchange: a study by electrospray ionization time-of-flight mass spectrometry. *Rapid Commun Mass Sp* 22: 1553-1562

Rellán-Álvarez R, Giner-Martínez-Sierra J, Orduna J, Orera I, Rodríguez-Castrillón JA, García-Alonso JI (2010a) Identification of a tri-iron(III), tri-citrate complex in the xylem sap of iron-deficient tomato resupplied with iron: new insights into plant iron long-distance transport. *Plant Cell Physiol* 51: 91-102

Rellán-Álvarez R, Andaluz S, Rodríguez-Celma J, Wohlgemuth G, Zocchi G, Álvarez-Fernández A, Fiehn O, López-Millán AF, Abadía J (2010b) Changes in the proteomic and metabolic profiles of *Beta vulgaris* root tips in response to iron deficiency and resupply. *BMC Plant Biol* 10: 120

Rellán-Álvarez R, El-Jendoubi H, Wohlgemuth G, Abadía A, Fiehn O, Abadía J (2011a) Metabolite profile changes in xylem sap and leaf extracts of strategy I plants in response to iron deficiency and resupply. *Front Plant Sci* 2: 66

Rellán-Álvarez R, López-Gomollón S, Abadía J, Álvarez-Fernández A (2011b) Development of a new High-Performance Liquid Chromatography-Electrospray Ionization Time-of-Flight Mass Spectrometry method for the determination of low molecular mass organic acids in plant tissue extracts. *J Agric Food Chem* 59: 6864-6870

Rios JJ, Carrasco-Gil S, Abadía A, Abadía J (2016) Using Perls staining to trace the iron uptake pathway in leaves of a *Prunus* rootstock treated with iron foliar fertilizers. *Front Plant Sci* 7: 893

Robinson NJ, Procter CM, Connolly EL, Guerinot ML (1999) A ferric-chelate reductase for iron uptake from soils. *Nature* 397: 694-697

Robson AD, Reuter DJ (1981) Diagnosis of copper deficiency and toxicity. In: Copper in soils and plants, eds. Academic Press, Sydney London New York

Rodríguez-Celma J, Lin WD, Guin-Mau F, Abadía J, López-Millán AF, Schimdt W (2013) Mutually exclusive alterations in secondary metabolism are critical for the uptake of insoluble iron compounds by *Arabidopsis* and *Medicago truncatula*. *Plant Physiol* 162: 1473-1485

Rodríguez-Celma J, Ceballos-Laita L, Michael A. Grusak MA, Javier Abadía J, López-Millán AF (2016) Plant fluid proteomics: Delving into the xylem sap, phloem sap and apoplastic fluid proteomes. *Biochim Biophys Acta* 1864: 991-1002

Rodríguez-Medina C, Atkins CA, Mann AJ, Jordan ME, Smith PMC (2011) Macromolecular composition of phloem exudate from white lupin (*Lupinus albus* L). *BMC Plant Biol* 11: 36

Rombolà AD, Brüggemann W, López-Millán AF, Tagliavini M, Abadía J, Marangoni B, Moog PR (2002) Biochemical responses to iron deficiency in kiwifruit (*Actinidia deliciosa*). *Tree Physiol* 22: 869-875

Roschzttardtz H, Conéjéro G, Curie C, Mari S (2009) Identification of the endodermal vacuole as the iron storage compartment in the *Arabidopsis* embryo. *Plant Physiol* 151: 1329-1338

Roschzttardtz H, Séguéla-Arnaud M, Briat JF, Vert G, Curie C (2011) The FRD3 citrate effluxer promotes iron nutrition between symplastically disconnected tissues throughout *Arabidopsis* development. *Plant Cell* 23: 2725-2737

Roschzttardtz H, Conéjéro G, Divol F, Alcon C, Verdeil JL, Curie C, Mari S (2013) New insights into Fe localization in plant tissues. *Front Plant Sci* 4: 350

Sagardoy R (2011) Effects of Zn and Cd toxicity on metal concentrations in the xylem sap of *B. vulgaris* and *S. esculentum*, in: Study of Zn and Cd homeostasis in higher plants. PhD Thesis, University of Zaragoza, Spain

Sagardoy R, Morales F, Rellán-Álvarez R, Abadía J, Abadía A, López-Millán AF (2011) Carboxylate metabolism in sugar beet plants grown with excess Zn. *J Plant Physiol* 168: 730-733

Salt DE, Prince RC, Pickering IJ, Raskin I (1995) Mechanisms of cadmium mobility and accumulation in indian mustard. *Plant Physiol* 109: 1427-1433

Salt DE, Prince RC, Baker AJM, Raskin I, Pickering IJ (1999) Zinc ligands in the metal hyperaccumulator *Thlaspi caerulescens* as determined using X-ray absorption spectroscopy. *Environ Sci Technol* 33: 713-717

Santi S, Schmidt W (2009) Dissecting iron deficiency-induced proton extrusion in *Arabidopsis* roots. *New Phytol* 183: 1072-1084

Sarret G, Pilon Smits EAH, Castillo Michel H, Isaure MP, Zhao FJ, Tappero R (2013) Use of synchrotron-based techniques to elucidate metal uptake and metabolism in plants. *Adv Agron* 119: 1-82

Sasaki A, Yamaji N, Xia J, Ma JF (2011) OsYSL6 is involved in the detoxification of excess manganese in rice. *Plant Physiol* 157: 1832-1840

Sattelmacher B (2001) The apoplast and its significance for plant mineral nutrition. *New Phytol* 149: 167-192

Schaaf G, Ludewig U, Erenoglu BE, Mori S, Kitahara T, von Wirén N (2004) ZmYS1 functions as a proton-coupled symporter for phytosiderophore- and nicotianamine-chelated metals. *J Biol Chem* 279: 9091-9096

Schander H (1939) The dependence upon external factors of chlorosis of *Lupinus luteus* seedlings in sand cultures. *Z Bodenk Pflanzenernähr* 12: 71-84

Schuler M, Rellán-Álvarez R, Fink-Straube C, Abadía J and Bauer P (2012) Nicotianamine functions in the phloem-based transport of iron to sink organs, in pollen development and pollen tube growth in *Arabidopsis*. *Plant Cell* 24: 2380-2400

Shi R, Weber G, Köster J, Reza-Hajirezaei M, Zou C, Zhang F, von Wirén N (2012) Senescence-induced iron mobilization in source leaves of barley (*Hordeum vulgare*) plants. *New Phytol* 195: 372-383

Silva AMN, Kong X, Parkin MC, Cammack R, Hider RC (2009) Iron(III) citrate speciation in aqueous solution. *Dalton Trans* 8616-8625

Sinclair SA, Krämer U (2012) The zinc homeostasis network of land plants. *Biochim Biophys Acta* 1823: 1553-1567

Sisó-Terraza P, Luis-Villarroya A, Fourcroy P, Briat JF, Abadía A, Gaymard F, Abadía J, Álvarez-Fernández A (2016a) Accumulation and secretion of coumarinolignans and other coumarins in *Arabidopsis thaliana* roots in response to iron deficiency at high pH. *Front Plant Sci* 7: 1711

Sisó-Terraza P, Rios JJ, Abadía J, Abadía A, Álvarez-Fernández A (2016b) Flavins secreted by roots of iron-deficient *Beta vulgaris* enable mining of ferric oxide via reductive mechanisms. *New Phytol* 209: 733-745

Smith RM, Martell AE (1989) Critical Stability Constants Vols 1-6, Plenum Press, New York

Socha AL, Guerinot ML (2015) Mn-euvering manganese: the role of transporter gene family members in manganese uptake and mobilization in plants. *Front Plant Sci* 5: 106

Song J, Yang YQ, Zhu SH, Chen GC, Yuan XF, Liu TT, Yu XH, Shi JY (2013) Spatial distribution and speciation of copper in root tips of cucumber revealed by μ-XRF and μ-XANES. *Biol Plantarum* 57: 581-586

Sperotto RA, Ricachenevsky FK, Waldow VA, Fett JP (2012) Iron biofortification in rice: it's a long way to the top. *Plant Sci* 190: 24-39

Steudle E, Smith JAC, Lüttge U (1980) Water-relation parameters of individual mesophyll cells of *Kalanchöe daigremontiana*. *J Plant Physiol* 66: 1155-1163

Stomph JT, Jiang W, Struik PC (2009) Zinc biofortification of cereals: rice differs from wheat and barley. *Trends Plant Sci* 14: 123-124

Stumm W, Morgan JJ (1996) Aquatic chemistry, chemical equilibria and rates in natural waters. John Wiley and Sons, New York

Sudhakar D, Duc LT, Bong B, Tinjuangjun P, Maqbool SB, Valdez M, Jefferson R, Christou P (1998) An efficient rice transformation system utilizing mature seed-derived explants and a portable, inexpensive particle bombardment device. *Transgenic Res* 7: 289-294

Suzuki M, Tsukamoto T, Inoue H, Watanabe S, Matsuhashi S, Takahashi M, Nakanishi H, Mori S, Nishizawa NK (2008) Deoxymugineic acid increases Zn translocation in Zn-deficient rice plants. *Plant Mol Biol* 66: 609-617

Takahashi M, Terada Y, Nakai I, Nakanishi H, Yoshimura E, Mori S, Nishizawa NK (2003) Role of nicotianamine in the intracellular delivery of metals and plant reproductive development. *Plant Cell* 15: 1263-1280

Takahashi M, Nozoye T, Kitajima N, Fukuda N, Hokura A, Terada Y, Nakai I, Ishimaru Y, Kobayashi T, Nakanishi H, Nishizawa NK (2009) *In vivo* analysis of metal distribution and expression of metal transporters in rice seed during germination process by microarray and X-ray fluorescence imaging of Fe, Zn, Mn, and Cu. *Plant Soil* 325: 39-51

Tehseen M, Cairns N, Sherson S, Cobbett CS (2010) Metallochaperone-like genes in *Arabidopsis thaliana*. *Metallomics* 2: 556-564

Terry N, Abadía J (1986) Function of iron in chloroplasts. *J Plant Nutr* 9: 609-646

Terzano R, Mimmo T, Vekemans B, Vincze L, Falkenberg G, Tomasi N (2013) Iron (Fe) speciation in xylem sap by XANES at a high brilliant synchrotron X-ray source: opportunities and limitations. *Anal Bioanal Chem* 405: 5411-5419

Tewari RK, Hadacek F, Sassmann S, Lang I (2013) Iron deprivation-induced reactive oxygen species generation leads to non-autolytic PCD in *Brassica napus* leaves. *Environ Exp Bot* 91: 74-83

Thoiron S, Pascal N, Briat JF (1997) Impact of iron deficiency and iron resupply during the early stages of vegetative development in maize (*Zea mays* L.). *Plant Cell Environ* 20: 1051-1060

Thomine S, Vert G (2013) Iron transport in plants: better be safe than sorry. *Curr Opin Plant Biol* 16: 322-327

Tian S, Lu L, Yang X, Webb SM, Du Y, Brown PA (2010) Spatial imaging and speciation of lead in the accumulator plant *Sedum alfredii* by microscopically focused synchrotron X-ray investigation. *Environ Sci Technol* 44: 5920-5926

Tiffin LO, Brown JC (1961) Iron chelates in soybean exudates. *Science* 135: 311-313

Tiffin LO (1966) Iron translocation I: plant culture exudate sampling iron-citrate analysis. *Plant Physiol* 41: 510-514

Trampczynska A, Küpper H, Meyer-Klaucke W, Schmidt H, Clemens S (2010) Nicotianamine forms complexes with Zn(II) *in vivo*. *Metallomics* 2: 57-66

Trijatmiko KR, Dueñas C, Tsakirpaloglou N, Torrizo L, Arines FM, Adeva C, Balindong J, Oliva N, Sapasap MV, Borrero J, Rey J, Francisco P, Nelson A, Nakanishi H, Lombi E, Tako E, Glahn RP, Stangoulis J, Chadha-Mohanty P, Johnson AT, Tohme J, Barry G, Slamet-Loedin IH (2016) Biofortified indica rice attains iron and zinc nutrition dietary targets in the field. *Sci Rep* 6: 19792

Tsednee M, Mak YW, Chen YR, Yeh KC (2012) Sensitive LC-ESI-Q-TOF-MS method reveals novel phytosiderophores and phytosiderophore-iron complexes in barley. *New Phytol* 195: 951-961

Tsednee M, Yang S, Lee D, Yeh K (2014) Root-secreted nicotianamine from *Arabidopsis halleri* facilitates zinc hypertolerance by regulating zinc bioavailability. *Plant Physiol* 166: 839-852

Turgeon R (2010) The puzzle of phloem pressure. *Plant Physiol* 154: 578-581

Ueno D, Iwashita T, Zhao FJ, Ma JF (2008) Characterization of Cd translocation and identification of the Cd form in xylem sap of the Cd-hyperaccumulator *Arabidopsis halleri*. *Plant Cell Physiol* 49: 540-548

Vasconcelos MW, Datta K, Oliva N, Khalekuzzaman M, Torrizo L, Krishnan S, Oliveira M, Goto F, Datta SK (2003) Enhanced iron and zinc accumulation in transgenic rice with the ferritin gene *Plant Sci* 164: 371-378

Vasconcelos MW, Li GW, Lubkowitz MA, Grusak MA (2008) Characterization of the PT clade of oligopeptide transporters in rice. *Plant Genome* 1: 77-88

Vasconcelos MW, Gruissem W, Bhullar NK (2017) Iron biofortification in the 21st century: setting realistic targets, overcoming obstacles, and new strategies for healthy nutrition. *Curr Opin Plant Biotech* 44: 8-15

Vert G, Grotz N, Dédaldéchamp F, Gaymard F, Guerinot ML, Briat JF, Curie C (2002) IRT1, an *Arabidopsis* transporter essential for iron uptake from the soil and for plant growth. *Plant Cell* 14: 1223-1233

Vogel-Mikuš K, Arcon I, Kodre A (2010) Complexation of cadmium in seeds and vegetative tissues of the cadmium hyperaccumulator *Thlaspi praecox* as studied by X-ray absorption spectroscopy. *Plant Soil* 331: 439-451

von Wirén N, Klair S, Bansal S, Briat JF, Khodr H, Shioiri T, Leigh RA and Hider RC (1999) Nicotianamine chelates both Fe(III) and Fe(II) implications for metal transport in plants. *Plant Physiol* 119: 1107-1114

Wada Y, Yamaguchi I, Takahashi M, Nakanishi H, Mori S, Nishizawa NK (2007) Highly sensitive quantitative analysis of nicotianamine using LC/ESI-TOF-MS with an internal standard. *Biosci Biotechnol Biochem* 71: 435-441

Wang M, Gruissem W, Bhullar NK (2013) Nicotianamine synthase overexpression positively modulates iron homeostasis-related genes in high iron rice. *Front Plant Sci* 4: 156

Waters BM, Blevins DG, Eide DJ (2002) Characterization of FRO1, a pea Ferric-Chelate Reductase involved in root iron acquisition. *Plant Physiol* 129: 85-94

Waters BM, Grusak MA (2007) Whole-plant mineral partitioning throughout the life cycle in *Arabidopsis thaliana* ecotypes Columbia, Landsberg erecta, Cape Verde Islands, and the mutant line *ysl1ysl3*. *New Phytol* 177: 389-405

Waters BM, Sankaran RP (2011) Moving micronutrients from the soil to the seeds: genes and physiological processes from a biofortification perspective. *Plant Sci* 180: 562-574

Waters BM, McInturf SA, Amundsen K (2014) Transcriptomic and physiological characterization of the *fefe* mutant of melon (*Cucumis melo*) reveals new aspects of iron-copper crosstalk. *New Phytol* 203: 1128-1145

Weber G, von Wirén N, Hayen H (2006) Analysis of iron(II)/iron(III) phytosiderophore complexes by nano-electrospray ionization Fourier transform ion cyclotron resonance mass spectrometry. *Rapid Commun Mass Spectrom* 20: 973-980

Wei ZG, Wong JW, Hong F, Zhao HY, Li HX, Hu F (2007) Determination of inorganic and organic anions in xylem saps of two contrasting oilseed rape (*Brassica juncea* L) varieties: Roles of anions in long-distance transport of cadmium. *Microchemical J* 86: 53-59

White MC, Decker AM, Chaney RL (1981a) Metal complexation in xylem fluid I: chemical composition of tomato and soybean stem exudates. *Plant Physiol* 67: 292-300

White MC, Decker AM, Chaney RL (1981b) Metal complexation in xylem fluid II: theoretical equilibrium model and computational computer program. *Plant Physiol* 67: 301-310

Wirth J, Poletti S, Aeschlimann B, Yakandawala N, Drosse B, Sonia Osorio, Tohge T, Fernie R, Günther D, Gruissem W, Sautter C (2009) Rice endosperm iron biofortification by targeted and synergistic action of nicotianamine synthase and ferritin. *Plant Biotechnol J* 7: 631-644

Wu B, Becker JS (2012) Imaging techniques for elements and element species in plant science. *Metallomics* 4: 403-416

Xiong H, Kakei Y, Kobayashi T, Guo X, Nakazono M, Takahashi H, Nakanishi H, Shen H, Zhang F, Nishizawa K, Zuo Y (2013) Molecular evidence for phytosiderophore-induced improvement of iron nutrition of peanut intercropped with maize in calcareous soil. *Plant Cell Environ* 36: 1888-1902

Xuan Y, Scheuermann EB, Meda AR, Hayen H, von Wirén N, Weber G (2006) Separation and identification of phytosiderophores and their metal complexes in plants by zwitterionic hydrophilic interaction liquid chromatography coupled to electrospray ionization mass spectrometry. *J Chromatogr A* 1136: 73-81

Xuan Y, Scheuermann EB, Meda AR, Jacob P, von Wirén N, Weber G (2007) CE of phytosiderophores and related metal species in plants. *Electrophoresis* 28: 3507-3519

Yamaguchi N, Ishikawa S, Abe T, Baba K, Arao T, Terada Y (2012) Role of the node in controlling traffic of cadmium, zinc, and manganese in rice. *J Exp Bot* 63: 2729-2737

Yang G, Lib J, Liu W, Yu Z, Shi Y, Lv B, Wang B, Han D (2015) Molecular cloning and characterization of MxNAS2, a gene encoding nicotianamine synthase in *Malus xiaojinensis*, with functions intolerance to iron stress and misshapen flower in transgenic tobacco. *Sci Hort* 183: 77-86

Yokosho K, Yamaji N, Ueno D, Mitani N, Ma JF (2009) OsFRDL1 is a citrate transporter required for efficient translocation of iron in rice. *Plant Physiol* 149: 297-305

Yokosho K, Yamaji M, Ma JF (2016) OsFRDL1 expressed in nodes is required for distribution of iron to grains in rice. *J Exp Bot* 67: 5485-5494

Yoneyama Y, Ishikawa S, Fujimaki S (2015) Route and regulation of zinc, cadmium, and iron transport in rice plants (*Oryza sativa* L) during vegetative growth and grain filling: metal transporters, metal speciation, grain Cd reduction and Zn and Fe biofortification. *Int J Mol Sci* 16: 19111-19129

Yoshimura E, Sakaguchi T, Nakanishi H, Nishizawa NK, Nakai I, Mori S (2000) Characterization of the chemical state of iron in the leaves of wild-type tomato and of a nicotianamine-free mutant chloronerva by X-ray Absorption Near-Edge Structure (XANES). *Phytochem Anal* 11: 160-162

Yruela I (2009) Copper in plants: acquisition, transport and interactions. *Funct Plant Biol* 36: 409-430

Yun W, Pratt ST, Miller RM, Cai Z, Hunter DB, Jarstfer AG, Kemner KM, Lai B, Lee HR, Legnini DG, Rodrigues W, Smith CI (1998) X-ray imaging and microspectroscopy of plants and fungi. *J Synchrotron Rad* 5: 1390-1395

Zaharieva TB, Abadía J (2003) Iron deficiency enhances the levels of ascorbate, glutathione, and related enzymes in sugar beet roots. *Protoplasma* 221: 269-275

Zaharieva TB, Gogorcena Y, Abadía J (2004) Dynamics of metabolic responses to iron deficiency in sugar beet roots. *Plant Sci* 166: 1045-1050

Zamboni A, Zanin L, Tomasi N, Pezzott M, Pinton R, Varanini Z, Cesco S (2012) Genome-wide microarray analysis of tomato roots showed defined responses to iron deficiency. *BMC Genomics* 13: 101

Zamboni A, Zanin L, Tomasi N, Avesani L, Pinton R, Varanini Z, Cesco S (2016) Early transcriptomic response to Fe supply in Fe-deficient tomato plants is strongly influenced by the nature of the chelating agent. *BMC Genomics* 17: 35

Zhang FS, Römheld V, Marschner H (1991) Role of the root apoplasm for iron acquisition by wheat plants. *Plant Physiol* 97: 1302-1305

Zhang C, Yu X, Ayre BG, Turgeon R (2012) The origin and composition of cucurbit "phloem" exudates. *Plant Physiol* 158: 1873-1882

Zheng L, Cheng Z, Ai C, Jiang X, Bei X, Zheng Y, Glahn RP, Welch RM, Miller DD, Lei XG, Shou H (2010) Nicotianamine, a novel enhancer of rice iron bioavailability to humans. *PLoS ONE* 5: e10190

Zheng L, Yamaji N, Yokosho K, Ma JF (2012) YSL16 is a phloem-localized transporter of the copper-nicotianamine complex that is responsible for copper distribution in rice. *Plant Cell* 24: 3767-3782

Zouari M, Abadía A, Abadía J (2001) Iron is required for the induction of root ferric quelate reductase activity in iron-deficient tomato. *J Plant Nutr* 24: 383-396

Publication

frontiers in
PLANT SCIENCE

REVIEW ARTICLE
published: 25 March 2014
doi: 10.3389/fpls.2014.00105

Metal species involved in long distance metal transport in plants

Ana Álvarez-Fernández, Pablo Díaz-Benito, Anunciación Abadía, Ana-Flor López-Millán and Javier Abadía*

Plant Nutrition Department, Aula Dei Experimental Station (CSIC), Zaragoza, Spain

Edited by:
Marta Wilton Vasconcelos, Universidade Católica Portuguesa, Portugal

Reviewed by:
John M. Ward, University of Minnesota, USA
Tadakatsu Yoneyama, The University of Tokyo, Japan

***Correspondence:**
Javier Abadía, Plant Nutrition Department, Aula Dei Experimental Station (CSIC), PO Box 13034, E-50080, Zaragoza, Spain
e-mail: jabadia@eead.csic.es

The mechanisms plants use to transport metals from roots to shoots are not completely understood. It has long been proposed that organic molecules participate in metal translocation within the plant. However, until recently the identity of the complexes involved in the long-distance transport of metals could only be inferred by using indirect methods, such as analyzing separately the concentrations of metals and putative ligands and then using *in silico* chemical speciation software to predict metal species. Molecular biology approaches also have provided a breadth of information about putative metal ligands and metal complexes occurring in plant fluids. The new advances in analytical techniques based on mass spectrometry and the increased use of synchrotron X-ray spectroscopy have allowed for the identification of some metal-ligand species in plant fluids such as the xylem and phloem saps. Also, some proteins present in plant fluids can bind metals and a few studies have explored this possibility. This study reviews the analytical challenges researchers have to face to understand long-distance metal transport in plants as well as the recent advances in the identification of the ligand and metal-ligand complexes in plant fluids.

Keywords: metals, metal complexes, phloem, transport, xylem

INTRODUCTION

To reach their final destination within the plant (e.g., organelles such as chloroplast or mitochondria) micronutrients taken up from the growth medium, including metals such as Fe, Mn, Zn, and Cu, must follow a complex path through a number of different plant compartments and membrane systems (Clemens et al., 2002; Colangelo and Guerinot, 2006; Briat et al., 2007; Haydon and Cobbett, 2007; Curie et al., 2009; Puig and Peñarrubia, 2009; Conte and Walker, 2011; Sinclair and Krämer, 2012). The vascular system, including the xylem and phloem conduits, is an essential segment for long distance translocation of micronutrients within this path. It has long been proposed that a significant fraction of metals would be present in plant fluids not as free ions but in less reactive chemical forms, e.g., non-covalently bound to organic compounds, to prevent uncontrolled binding and also because free metals often exert some degree of toxicity. The formation of metal complexes provides both solubility and shielding during long-distance transport, since the metallic atom is enveloped by an array of bound molecules or anions (the so-called ligands; in this review only ligands consisting in organic molecules are considered), which donate one or more electron pairs to the metal to form the complexes.

Indirect evidence for long distance, organic ligand-assisted transport of metals has been extensively reported. Possible ligand candidates are a range of small molecules, including organic acids -carboxylates- such as citrate (Cit) and malate (Mal), amino acids [including nicotianamine (NA), histidine (His), cysteine (Cys) and high-affinity Fe(III) chelating compounds derived from NA called phytosiderophores (PSs), such as mugineic (MA) and 2′-deoxymugineic (DMA) acids], as well as peptides and proteins (e.g., metallothioneins). In the case of toxic metals such as Cd, Hg, and others, plants also respond by synthesizing compounds such as the poly-glutathione peptides phytochelatins (PCs) that decrease the amount of free metal ions in plant fluids. Recent papers have reviewed the roles of NA (Curie et al., 2009; Clemens et al., 2013) and PCs (Pal and Rai, 2010) in plant metal homeostasis, the intra- and extracellular excretion of carboxylates (Meyer et al., 2010) and the plant metallo-chaperones (Tehseen et al., 2010). During the last decade, the identification of many genes involved in plant long-distance metal transport has also been achieved, and many reviews have covered this issue in relation to either several metals (Colangelo and Guerinot, 2006; Haydon and Cobbett, 2007; Krämer et al., 2007; Curie et al., 2009; Palmer and Guerinot, 2009; Puig and Peñarrubia, 2009; Krämer, 2010; Waters and Sankaran, 2011) or to specific ones such as Fe (Briat et al., 2007; Kim and Guerinot, 2007; Morrissey and Guerinot, 2009; Conte and Walker, 2011; Sperotto et al., 2012; Thomine and Vert, 2013), Zn (Sinclair and Krämer, 2012), Cu (Yruela, 2009), Mn (Pittman, 2005), and Cd (Mendoza-Cózatl et al., 2011).

To date, analytical data on the actual metal complexes existing in plant fluids are still scarce. This is relevant, because the chemical forms in which a metal occurs in solution (metal speciation) affect solubility, precipitation, acid/base equilibria, electron-transfer reactions, diffusivity, ability to undergo photolysis and others. The metal species existing in any given compartment determine biological activity, including the capability to be a substrate for membrane transport proteins involved in loading and unloading to xylem and phloem, as well as the possibility

that metal toxicity can occur. This review summarizes the current knowledge on metal species occurring in plant fluids [xylem sap, phloem sap and other fluids such as apoplastic fluid and embryo sac liquid (ESL)], and discusses general problems relevant to these studies as well as the methodological approaches currently used.

METHODS FOR PLANT FLUID SAMPLING AND INHERENT PROBLEMS

Metal translocation within plants is dynamic, with the composition of plant fluids often changing with time. This mandates to establish an adequate standard sampling protocol, including sampling time and others, which must be applied to all samples so that results are fully comparable. A major limitation in the analysis of plant fluids is the need for samples of adequate purity and in sufficient volume to carry out measurements. The purity of the fluid samples must always be assessed by measuring cytosolic and/or vacuolar components associated to cell rupture. The activities of cytosolic marker enzymes, such as Mal dehydrogenase (*mdh*) or others (López-Millán et al., 2000), or the concentrations of K as a vacuolar marker (Lohaus et al., 2001; Barabasz et al., 2012) are generally used with that purpose.

Xylem sap, the fluid contained in xylem vessels -composed of tracheary elements separated by rather large perforation plates-, is relatively easy to sample (reviewed by Alexou and Peuke, 2013). The most frequently used technique is de-topping plants and letting xylem to bleed after discarding the first drops (López-Millán et al., 2012). Other techniques involve centrifugation of excised stems (López-Millán et al., 2000) or the use of a Schölander pressure chamber (Larbi et al., 2003). With any of these extraction techniques the xylem sap volume sampled could reach several hundreds of μL.

The phloem sap, the fluid contained in sieve cells—separated by sieve plates—, is a special case, because there is still controversy about changes in composition induced by wounding (Atkins et al., 2011) and the presence of different types of phloem saps (Zhang et al., 2012). The purity of the phloem sap is usually assessed by measuring sugar concentrations and/or evaluating the presence of Rubisco proteins or transcripts (Giavalisco et al., 2006; Rodríguez-Medina et al., 2011; Lattanzio et al., 2013). Other authors consider pH values around 8.0 indicative of phloem purity (Ando et al., 2013). Some methods in use for phloem sap sampling (reviewed by Dinant and Kehr, 2013) are those involving an incision near the inflorescence (in *Cucurbitaceae*, *Brassicaceae* and some *Lupinus* species; Lattanzio et al., 2013), those using aphid or leaf-hopper stylectomy (with the disadvantage of resulting in minute phloem sap volumes, $\leq$1 μL per cut stylet; Ando et al., 2013), or by exudation of excised shoots maintained at >80% relative humidity in a closed chamber (the latter being only a qualitative approach; Marentes and Grusak, 1998). When using insect stylectomy, evaporation during sampling is a relevant issue; accurate determination of the phloem volume has been recently achieved by measuring the droplet diameter as it forms on the tip of the severed aphid stylet (Palmer et al., 2013).

The fluid in the apoplastic space in the leaf (free space outside the plasma membrane) is an interface between the xylem and the symplast. Some methods for leaf apoplastic fluid sampling involve direct centrifugation of leaves without petiole (previously centrifuged at low speed to remove xylem sap from the mid vein; López-Millán et al., 2000) or by using a Schölander pressure chamber (Larbi et al., 2003). Other authors infiltrate the leaves with a solution under vacuum and then obtain by centrifugation a leaf apoplastic wash fluid (Lohaus et al., 2001). Since the latter procedure leads to a dilution of the apoplastic fluid, concentrations should be corrected considering estimations of apoplastic volumes occupied by water and air, using vacuum infiltration with a ^{14}C-sorbitol labeled solution and silicone oil, respectively (Lohaus et al., 2001).

Recently, the ESL has been successfully used to study the processes of metal transport in pea seeds (Grillet et al., 2014). This liquid is enriched by the bulk flow of nutrients delivered by the seed coat and feeds the embryo.

METHODOLOGICAL APPROACHES TO UNRAVEL METAL SPECIES OCCURRING IN PLANT FLUIDS

Until recently, researchers had to rely on indirect methods to putatively identify the chemical forms of metals occurring in plant fluids. These methods were based on separate measurements of the concentrations of metals and possible ligands and the prediction of the existent chemical species by means of titration in "artificial" saps (Liao et al., 2000; Irtelli et al., 2009; Alves et al., 2011) or *in silico* by using a set of known, experimentally determined stability constants of metal-containing complexes and chemical speciation software; this was always done assuming that chemical equilibrium was achieved (White et al., 1981; López-Millán et al., 2000; Callahan et al., 2006; Harris et al., 2012). However, chemical equilibrium is unexpected in plant fluids, since continuous changes in composition usually occur in these dynamic plant compartments.

Molecular biology approaches have provided key information on putative metal ligands and metal complexes that could play a crucial role in inter- and intra-organ metal transport (see reviews by Briat et al., 2007; Haydon and Cobbett, 2007; Kim and Guerinot, 2007; Milner and Kochian, 2008; Palmer and Guerinot, 2009; Pal and Rai, 2010; Waters and Sankaran, 2011; Leitenmaier and Küpper, 2013; Thomine and Vert, 2013). Genotypes with loss-of-function of genes involved in the trafficking of metals, ligands and/or their metal complexes, as well as metal hyperaccumulator (e.g., *T. caerulescens*) plant species have been studied. Other approaches include mutant and transgenic lines with impaired or enhanced metal ligand synthesis; a classical example of impaired synthesis is the tomato mutant "*chloronerva*," which lacks NA (Pich and Scholz, 1996). Transgenic genotypes have also been constructed where the synthesis of ligands such as PCs is restricted to a specific tissue (Gong et al., 2003).

Another approach is searching for molecules with affinity for metals in plant fluids, using their immobilization by metal affinity chromatography (IMAC) followed by identification of the isolated molecules using some of the mass spectrometry (MS) techniques described below (Lattanzio et al., 2013). In this approach, the occurrence of the corresponding metal-ligand complex in plant fluids is only inferred from the presence of suitable ligands.

A further approach to identify metal complexes in plant tissues -including fluids- relies on the identification of the chemical

environment surrounding the metal by means of synchrotron X-ray absorption spectroscopy (XAS) techniques such as X-ray absorption near edge spectroscopy (XANES) and extended X-ray absorption fine structure spectroscopy (EXAFS) (Lombi et al., 2011; Donner et al., 2012). This has been used for different metals such as Fe (Yoshimura et al., 2000; Terzano et al., 2013), Mn (Yun et al., 1998), Cu (Küpper et al., 2009; Song et al., 2013), Zn (Salt et al., 1999; Küpper et al., 2004; Trampczynska et al., 2010; Lu et al., 2013), Ni (McNear et al., 2010), Cd (Salt et al., 1995; Vogel-Mikus et al., 2010; Huguet et al., 2012; Yamaguchi et al., 2012), Hg (Carrasco-Gil et al., 2011, 2013; McNear et al., 2012), and Pb (Tian et al., 2010; Chu et al., 2012). This technique allows direct *in situ* metal speciation in plants, without any preliminary extraction or preparation (see reviews by Lombi et al., 2011; Donner et al., 2012; Sarret et al., 2013). However, spectra are difficult to interpret when more than two or three species are dominant, and these techniques are generally used to confirm the presence of known species rather than to find new ones (Monicou et al., 2009). Furthermore, the applications of these techniques have been usually restricted to tissues from metal hyper-accumulators, due to the relatively low sensitivity (metal concentration should be higher than 10 $\mu g\ g^{-1}$ dry weight). In spite of that, some data on metal speciation have been reported for sap and vasculature tissues, although mainly in metal hyper-accumulator species. This has been done for Zn in *T. caerulescens* (Salt et al., 1999; Küpper et al., 2004; Trampczynska et al., 2010) and *Sedum alfredii* (Lu et al., 2013), for Cd in *Brassica juncea* (Salt et al., 1995) and *Arabidopsis halleri* (Huguet et al., 2012), and for Ni in *Alyssum murale* (McNear et al., 2010). Recently, the use of highly brilliant synchrotrons as X-ray sources has increased one order of magnitude the sensitivity of EXAFS for trace elements (e.g., below 1 $\mu g\ g^{-1}$ dry weight for Fe), thus allowing speciation of Fe in tomato xylem sap (Terzano et al., 2013) and Cd around the vascular bundles in node I -the one beneath the panicle- in *Oryza sativa* (Yamaguchi et al., 2012). Unfortunately, artifacts can arise from high intensity radiation damage to the sample (i.e., degradation of Fe(III) complexes with carboxylates and NA, as reported in Terzano et al., 2013).

Recent advances in analytical techniques, and specifically in MS, have enabled a new insight on metal speciation. The use of highly selective and sensitive molecular and metal-specific MS techniques has allowed the identification and quantification of individual, well-defined metal species in plant tissues (including metabolites and proteins), even at sub-nM levels (Meija et al., 2006; Monicou et al., 2009). These approaches generally use hyphenated techniques based on the separation of compounds by high-resolution techniques [e.g., liquid chromatography (HPLC) and capillary electrophoresis (CE)] and the determination of the metals and/or metal complexes by MS techniques [including inductively coupled plasma MS (ICP-MS), electrospray MS (ESI-MS), and others]. These new methodologies (reviewed by Monicou et al., 2009; Khouzam et al., 2012) offer unique advantages for the *de novo* identification of metallo-metabolites occurring at low concentrations, in particular in plant materials such as plant fluids that do not require multi-step extraction from the plant tissues. Metabolite structures can be elucidated using the empirical formulas of the parent compound and fragment ions (data provided by high-resolution and high-accuracy MS) and the lineage of fragment ions observed in tandem MS or multistage MS (MSn). Furthermore, complexes with metals having more than one stable isotope, such as Fe, Zn, Cu, Cd, and Hg, provide metal-specific isotopic signatures that allow for identification of MS signals corresponding to metal containing molecules (see an example for metal-NA complexes in Rellán-Álvarez et al., 2008). In the five past years, methods based on these analytical techniques have achieved the direct identification of several metal complexes with possible relevance in long distance transport, including carboxylate complexes with Fe(III) and Ni(II), NA and PS complexes with Fe(III), Fe(II), Ni(II), Co(II), Mn(II), Cu(II) and Zn(II), and His complexes with Cu(II) (Weber et al., 2006; Xuan et al., 2006, 2007; Rellán-Álvarez et al., 2008, 2010; Dell'mour et al., 2010; Köster et al., 2011a,b; Tsednee et al., 2012). However, until now only a few of these metal-ligand complexes have been really found in plant fluids (see below).

Another MS technique, high-precision multi-collection-ICP-MS (developed 20 years ago), which yields high-precision measurements of stable isotopes of transition elements (e.g., Fe, Cu, and Zn), has allowed the study of their fractionation during plant uptake and translocation (reviewed by von Blanckenburg et al., 2009). This technique provides information on the mechanisms involved in metal partitioning within the plant, but not on metal speciation or specific binding environments. Recent studies on fractionation of Fe and Cu stable isotopes, using plants relying on Strategy I or II for Fe uptake, have revealed that both metals undergo redox cycling during root-to-shoot translocation in Fe-deficient Strategy I plant species, but not in Strategy II ones (Guelke-Stelling and von Blanckenburg, 2007, 2012; Kiczka et al., 2010; Ryan et al., 2013). A recent *in silico* study predicted that redox Fe changes affect Fe isotopic fractionation, with Δ^{56}Fe (^{56}Fe/^{54}Fe) being 3‰ heavier in Fe(III)-PS than in Fe(II)-NA (Moynier et al., 2013). Even in the absence of redox Fe changes, changes in speciation alone would create up to 1.5‰ differences in Δ^{56}Fe: Fe(III)-PS is up to 1.5‰ heavier than Fe(III)-Cit and Fe(II)-NA is up to 1‰ heavier than Fe(II)-Cit (Moynier et al., 2013). These estimations are in agreement with the fact that roots of Strategy-II plants, which rely on Fe(III)-PS uptake, are isotopically heavier (by about 1‰) than the shoots, where Fe had presumably been transported as Fe(III)-Cit in the xylem or Fe(II)-NA in the phloem. Isotopic variations observed between younger and older leaves could also be explained by the occurrence of Fe acquisition *via* xylem and phloem (Moynier et al., 2013). Zinc sequestration in roots is mediated by a number of mass dependent processes that favor the heavier isotopes, including binding to cell walls, precipitation in intercellular spaces, binding to high affinity ligands in the root cell and sequestration in the vacuole (Aucour et al., 2011; Caldelas et al., 2011). Translocation processes of Zn within the plant also lead to significant fractionation of Zn stable isotopes, since shoots of several plant species were enriched in light isotopes, with the tallest species showing the largest fractionation in the youngest leaves (Moynier et al., 2009). This effect can be modified by the Zn status in those Zn hyper-accumulators that accumulate Zn mainly in the roots (e.g., *A. halleri*), due to the large fractionation that occurs before shoot Zn's re-translocation.

METALS IN PLANT FLUIDS

The study of long distance metal transport has traditionally used differences in metal accumulation ratios (root to shoot metal content ratios) within the plant, considering different scenarios (i.e., growth conditions, genotypes, etc.). Only recently, high-throughput elemental analysis technologies have allowed the characterization of the full ionome in a large number of lines of several plant species (www.ionomicshub.org) (Baxter et al., 2008; Singh et al., 2013). This information, in combination with bioinformatics and genetic tools, has yielded candidate genes coding for transporters as well as gene networks involved in long distance metal transport.

Direct analyses of metals in plant fluids have been carried out in a number of studies, and their concentrations are generally in the μM range (**Table 1**). Therefore, the use of sensitive analytical techniques such as graphite furnace atomic absorption spectroscopy (GAAS) or inductively coupled plasma-mass spectrometry (ICP-MS) is mandatory for their determination. Prior to the analyses and immediately after the sampling of plant fluids, metals are usually stabilized in the solution by acidifying it. To avoid metal cross-contamination, high purity acids (ultra trace analysis quality grade) should be used for sample acidification, and also for sample digestion and cleaning of all materials (Husted et al., 2011; Ando et al., 2013). Concentrations found in the xylem sap, phloem sap and leaf apoplastic fluid of different plant species are in the ranges 4–168 μM for Fe, 0.5–245 μM for Zn, 0.3–30 μM for Cu, 4–400 μM for Mn and nd–0.1 μM for Cd and Ni (**Table 1**). These concentrations usually increase when either the metals are in excess in the plant growth medium or when plants (specially those genotypes known as metal stress tolerant) are treated with control metal concentrations after a period of metal deficiency. In these cases concentrations may reach 120–177 μM Fe in tomato xylem sap (Orera et al., 2010; Rellán-Álvarez et al., 2010, 2011a), 148 μM Zn in sugar beet xylem sap (Sagardoy, 2012), 43 μM Cu in *O. sativa* phloem sap (Ando et al., 2013), 2300 μM Mn in *O. sativa* leaf apoplastic fluid (Führs et al., 2010) and 1–100 μM Cd in *O. sativa*, *B. vulgaris*, and *S. lycopersicum* (Mori et al., 2009; Kato et al., 2010; Sagardoy, 2012). Higher concentrations of metals in plant fluids are also found in hyper-accumulator species: up to 450 μM Ni (Mari et al., 2006) and 524 μM Zn (Lasat et al., 1998) in *T. caerulense*, up to 1750 μM Ni in *Alyssum lesbiacum* (Kerkeb and Krämer, 2003) and up to 100 μM Cd and 486 μM Zn in *A. halleri* (Ueno et al., 2008) (**Table 1**). Altered levels of metals in plant fluids are also found in mutant genotypes as well as in transgenic plants overexpressing or losing the function of either one or several gene components of the uptake, sequestration or transport mechanisms (Nakamura et al., 2008; Ishimaru et al., 2011; Sasaki et al., 2011). The addition of protein synthesis inhibitors or ligands to the growth media has also a large effect on the metal concentrations in plant fluids. For instance, the addition of cycloheximide to the hyper-accumulator *A. lesbiacum* led to a 70% reduction of the xylem sap Ni concentration, whereas the addition of His to the non-accumulator *B. juncea* increased Ni in xylem sap (Kerkeb and Krämer, 2003).

Transport metal studies have also been approached using radioactive or stable isotopes. Radioactive metal isotopes supplied to plants can be detected by autoradiography, both at the whole plant and/or organ level (Cakmak et al., 2000a,b; Erenoglu et al., 2002). The application of ^{59}Fe-citrate to source tissues of pea plants showed that Fe is complexed prior to phloem loading (Grusak, 1994). The high remobilization of ^{109}Cd from the leaves and stem to the maturing grain was associated with high accumulation of Cd in durum wheat grain (Harris and Taylor, 2001). A more recent example is the use of ^{109}Cd autoradiography in *A. halleri* (a Zn and Cd hyper-accumulator species) showing that after 3 weeks an enrichment of the leaf petiole, central vein and trichomes occurs, whereas after 9 weeks leaf edges were the most Cd-enriched tissues and Cd concentrations were lower in regions along leaf vascular bundles (Huguet et al., 2012). A visualization of metals at the microscopic level can be obtained using thin sections. For instance, ^{109}Cd radioisotope imaging using 30-μm thickness sections has demonstrated Cd xylem-phloem transfer immediately after root uptake in *O. sativa* (Kobayashi et al., 2013).

The use of stable metal isotopes and highly selective and sensitive ICP-MS detection has also allowed tracing long-distance transport of metals within plants. Metal sources labeled with stable isotopes and applied to the roots or to leaves were used to evaluate the translocation within the plant of ^{67}Zn (Watmough et al., 1999; Benedicto et al., 2011), ^{57}Fe (Rodríguez-Castrillón et al., 2008; Rojas et al., 2008; Orera et al., 2010), ^{54}Fe (Orera et al., 2010), and ^{207}Pb (Watmough et al., 1999). Recently, the application of stable isotopes combined with laser ablation ICP-MS has allowed to localize and quantify the metal tracer together with other metals in plant tissue thin sections. This has been applied for the quantitative imaging of Cu and other essential elements (such as K, Mg, Mn, P, S, and B) in the leaves of the Cu-tolerant plant *Elsholtzia splendens* treated with ^{65}Cu (Wu et al., 2009). Whereas these are useful approaches for analyzing the spatial distribution or temporal changes of metals within the plant, only a snapshot of the distribution of metal at a given moment can be obtained. In contrast, the Positron-Emitting Tracer Imaging System technique, PETIS, allows for real-time, image quantification studies of the movement of elements in intact plants. The uptake and translocation of metals has been investigated in several graminaceous species using PET tracers ^{52}Fe, ^{52}Mn, ^{62}Zn, and ^{107}Cd (Tsukamoto et al., 2006, 2009; Suzuki et al., 2008; Fujimaki et al., 2010; Ishikawa et al., 2011). For instance, this tool demonstrated the direct translocation of Fe from roots to young leaves *via* phloem in *H. vulgare* (Tsukamoto et al., 2009).

LIGANDS IN PLANT FLUIDS

Organic ligands involved in xylem and phloem metal translocation have been revealed mainly by physiological, genetic, and molecular studies, with the exception of some recent studies performing metabolite profiling using a combination of powerful analytical techniques (e.g., the LC-MS, GC-MS, and NMR analyses of latex of the Ni hyper-accumulator tree *Sebertia acuminata* by Callahan et al., 2008). Metal transport is associated with the occurrence in plant fluids of different classes of metal ligands, including: (i) compounds with just only O atoms as electron donors, such as different carboxylates (mainly Cit and Mal but also some less known ones such as methylated aldaric acid Callahan et al., 2008) and some *ortho*-dihydroxy phenolic compounds (e.g., protocatechuic acid; Ishimaru et al.,

Table 1 | Metal concentrations (in μM) in xylem sap, leaf apoplastic fluid and phloem sap in different plant species.

Species	Stress	Fe	Mn	Cu	Zn	Ni	Cd	References
XYLEM SAP								
A. lesbiacum^{H}	Ni					nd–1750^{S}		Kerkeb and Krämer, 2003
A. serpyllifolium^{H}	Ni					1000^{S}		Alves et al., 2011
A. halleri^{H}	Cd				486^{S}		nd–100^{S}	Ueno et al., 2008
A. thaliana		5^{G}–10						Durrett et al., 2007
B. vulgaris	Fe	2^{S}–6						López-Millán et al., 2000
	Fe	2^{S}–4–11^{SA}						Larbi et al., 2010
	Fe	4^{S}–15–30^{SA}						Orera et al., 2010
	Zn	5–9^{S}			20–148^{S}			Sagardoy, 2012
	Cd	5–11^{S}			20–26^{S}		<0.1–10^{S}	Sagardoy, 2012
B. carinata	Cu			0.3–1^{S}				Irtelli et al., 2009
B. juncea^{H}	Ni					175^{S}–500^{SA}		Kerkeb and Krämer, 2003
	Cd						nd–50^{S}	Salt et al., 1995
	Cd						nd–61^{S}	Wei et al., 2007a
B. napus	Cd	10–15^{S}	23–26^{S}	0.6–4^{S}	0.5–0.6^{S}		nd–12^{S}	Nakamura et al., 2008
	Cd	0.7^{S}–7					nd–11^{S}	Mendoza-Cózatl et al., 2008
B. oleracea			11–80		9–70			Shelp, 1987
H. vulgare	Fe	2^{S}–30	8–58^{S}	2–5^{S}	5–20^{S}			Alam et al., 2001
	Fe	nd–100^{SA}						Kawai et al., 2001
G. leucopteris		20	4	0.6	14			Hocking, 1983
G. max	Zn	1^{S}–6	7^{S}–10	1^{S}–6^{S}	3–28^{S}			White et al., 1981
N. glauca		11	4	2	22			Hocking, 1980
O. sativa		8^{G}–14						Yokosho et al., 2009
	Fe	4^{G,S}–6^{S}						Yokosho et al., 2009
	Fe	2^{S}–11						Kakei et al., 2009
	Cu	36^{S}–40	107^{S}–134–175^{S}	5–9^{S}	8–16^{S}			Ando et al., 2013
	Cu			0.2^{G}–1^{G}–5				Deng et al., 2013
		30^{G}–100	8–9^{G}				nd	Ishimaru et al., 2011
	Cd	15^{GS}–50^{S}	8^{GS}–8^{S}				5^{GS}–8^{S}	Ishimaru et al., 2011
	Cd	40^{S}–122^{S}			12^{S}–32^{S}		0.1^{S}–0.6^{S}	Yoneyama et al., 2010
	Cd						3^{S}–12^{S}	Kato et al., 2010
	Cd						<0.1–2^{S}	Uraguchi et al., 2009
P. communis	Fe	0.5^{S}–4						Larbi et al., 2003
P. persica	Fe	1^{S}–6						Larbi et al., 2003
S. lycopersicum	Fe	10^{S}–150^{SA}						Orera et al., 2010
	Fe	5^{S}–20–121^{SA}						Rellán-Álvarez et al., 2010
	Fe	5^{S}–15–177^{SA}						Rellán-Álvarez et al., 2011a
	Fe	4^{S}–6^{S}						Terzano et al., 2013
	Cu	13^{GSA}–43	15–56^{GS}	1^{G}–6	2^{GSA}–4^{G}			Pich and Scholz, 1996
	Zn	3^{S}–9	5^{S}–7	1^{S}–7	2–84^{S}			White et al., 1981
	Zn	32–89^{GS}			12–214^{GS}			Barabasz et al., 2012
	Cd	2^{S}–10			3–12^{S}		nd–95^{S}	Sagardoy, 2012
T. arvense	Zn				15–100^{S}			Lasat et al., 1998
T. caerulense^{H}	Zn				54–524^{S}			Lasat et al., 1998
	Ni					nd–450^{S}		Mari et al., 2006
LEAF APOPLASTIC FLUID								
B. vulgaris	Fe	3^{S}–6						López-Millán et al., 2000
	Fe	7^{S}–19–65^{SA}						Larbi et al., 2010
H. vulgare	Mn		11–22^{S}					Führs et al., 2010
O. sativa	Mn		400–2300^{S}					Führs et al., 2010
	Mn		150^{S}–600^{GS}					Sasaki et al., 2011

(Continued)

Table 1 | Continued

Species	Stress	Fe	Mn	Cu	Zn	Ni	Cd	References
P. communis	Fe	2^{S}–5						López-Millán et al., 2001
S. lycopersicum	Zn	2^{S}–4^{GS}			1^{S}–8^{GS}			Barabasz et al., 2012
PHLOEM SAP								
B. oleracea			4–76		78–245			Shelp, 1987
G. leucopteris		83	24	8	66			Hocking, 1983
N. glauca		168	16	19	243			Hocking, 1980
O. sativa	Cu	54^{S}–67–74^{S}	7^{S}–10	20^{S}–30–43^{S}	14^{S}–22–24^{S}			Ando et al., 2013
	Cd						nd–18^{S}	Tanaka et al., 2007
	Cd	50^{S}–63^{S}			34^{S}–115^{S}		0.1^{S}–0.5^{S}	Yoneyama et al., 2010
	Cd						1^{S}–3^{S}	Kato et al., 2010
R. communis		40–64	8–12	16–28	40–74			Schmidke and Stephan, 1995
		37						Schmidke et al., 1999

Specific cases are marked as follows: [S] High or low metal supply; [A] High or low metal supply in combination with a chemical (e.g., histidine, ABA, metal resupply); [G] Mutant or transgenic genotypes; and [H] Hyper-accumulator plant species. nd: not detected.

2011); (ii) compounds with O and N atoms as electron donors, such as amino acids (proteinogenic ones such as His and non-proteinogenic ones such as NA) and PSs (e.g., MA and DMA); and (iii) compounds with S atoms in which at least one of them acts as an electron donor, such as Cys, S-containing peptides (e.g., glutathione and their derivatives, PCs) and Cys-containing proteins (e.g., metallothioneins).

Carboxylates are usually found in the μM-mM range in plant fluids, whereas NA, DMA, His, PCs and others are generally in the μM range (examples are given in **Table 2**). Difficulties in determining ligands in plant fluids are inherent to their ability to form metal complexes. The total concentration of ligand (often very low) is distributed in different chemical forms: uncomplexed, complexed to different metals and even complexed to specific metals in different stoichiometries. Therefore, to prevent errors in ligand quantification, the conditions used during sample extraction, treatment and analytical determination seek either the complete dissociation of the existing metal-complexes (while preventing the formation of new ones) or the quantitative formation of the metal complexes [e.g., Fe(III)-PSs]. Also, derivatization of the ligands may be used. An example of the latter is the use of compounds such as fluorenylmethyloxycarbonyl to protect the amino groups of NA by blocking ligand atoms involved in metal complexation (these compounds also tag the ligand with a moiety that favors its detection) (Wada et al., 2007).

Classical analytical methodologies for organic ligands were based on direct HPLC-UV/VIS analyses for carboxylates (López-Millán et al., 2000), NA (Pich et al., 1994), PSs (Alam et al., 2001) and also for PCs (in the latter case, HPLC-UV/VIS is used in combination with pre- or post-column derivatization with UV/VIS-active tags, such as Ellman's reagent). New methodologies, based generally on HPLC-ESI-MS, have been developed using high resolution MS such as time-of-flight (TOF) MS for carboxylates (Rellán-Álvarez et al., 2011b and references therein) and NA and PSs (Wada et al., 2007; Kakei et al., 2009; Schmidt et al., 2011), Fourier transform ion cyclotron resonance-MS for NA and PSs (Weber et al., 2006), and quadrupole-TOF MS for NA and PSs (Tsednee et al., 2012). Other techniques have also been used, including CE coupled to UV/VIS (Xuan et al., 2007) or MS detection (Dell'mour et al., 2010), and GC-MS (for NA and/or PSs; Wirth et al., 2009; Rellán-Álvarez et al., 2011a). Nicotianamine and PSs have been analyzed, either using previous derivatization (Wada et al., 2007; Kakei et al., 2009; Schmidt et al., 2011) or by direct analysis (Xuan et al., 2007; Tsednee et al., 2012). In the case of PCs, analytical methods are also based on HPLC-MS techniques using either molecular detection (HPLC-ESI-MS and HPLC-ESI-MS/MS) or elemental detection (ICP-MS), and are often combined with derivatization (reviewed by Wood and Feldmann, 2012). For instance, N-(2-ferrocene-ethyl)maleimide is an electroactive pre-column tag that yields thiol-PCs conjugates, which can be separated and quantified by ESI-MS or ICP-MS detection, with detection limits for S at the nM level.

Quantification of ligands in plant fluids has been always done using external calibration with or without internal standardization. The latter is required when using HPLC-ESI-MS-based technologies, because the degree of ionization of a given analyte in different matrices can vary significantly and signal suppression (or enhancement) commonly occurs. Ideally, an isotope-labeled compound should be used as internal standard (IS) per each analyte to achieve accurate quantification; however, since isotope labeled compounds have a limited commercial offer and are quite expensive, either one or two isotope-labeled compounds or structural analogues are generally used. For instance, ^{13}C-labelled Mal and succinate have been used for quantification of carboxylates (Rellán-Álvarez et al., 2011b). For quantification of NA and PSs, different ISs, including structural NA analogs such as nicotyl-lysine (Wada et al., 2007) and nicotine (Tsednee et al., 2012), or ^{15}N-labelled NA produced using a recombinant *Schizosaccharomyces pombe* strain expressing NAS (Schmidt et al., 2011) have been used.

Since many carboxylates have more than one carboxylate group and some also have a α-hydroxycarboxylate binding center (i.e.,

Table 2 | Metal ligand concentrations (malate and citrate in mM and the rest in μM) in xylem sap, leaf apoplastic fluid and phloem sap.

Species	Stress	Malate	Citrate	NA	DMA	His	PCs	References
XYLEM SAP								
A. lesbiacum[H]	Ni					40–500[S]		Kerkeb and Krämer, 2003
A. serpyllifolium[H]	Ni	2[S]	0.5[S]			nd		Alves et al., 2011
A. deliciosa	Fe	0.2–0.4[S]						Rombolà et al., 2002
A. halleri[H]	Cd	0.02[S]	0.3[S]			12[S]		Ueno et al., 2008
A. thaliana			0.06[G]–0.09					Durrett et al., 2007
			0.2–0.9[G]					Schuler et al., 2012
B. vulgaris	Fe	2–30[S]	0.2–5[S]			nd–4[S]		López-Millán et al., 2000
	Fe	2–14[S]	1–3[S]					Larbi et al., 2010
	Zn	0.5[C]–2[S]	0.06–0.3[S]					Sagardoy et al., 2011
B. carinata	Cu			64–271[S]		17–140[S]		Irtelli et al., 2009
B. juncea[H]	Ni					40[S]–50		Kerkeb and Krämer, 2003
	Cd	0.02–0.23[S]	0.01[S]–0.7					Wei et al., 2007a
B. napus	Cd	0.7–0.9[S]	0.5–0.6[S]			66[S]–76		Nakamura et al., 2008
H. vulgare	Fe	0.01–0.03[S]	<0.01–0.02[S]		30–450[S]			Alam et al., 2001
	Fe				90[S]			Kawai et al., 2001
	Fe	0.8–5[S]	0.3–1.3[S]					López-Millán et al., 2012
G. max	Zn	0.04[S]–0.9	0.08[S]–1.5[S]			26[S]–62[S]		White et al., 1981
N. glauca						10		Hocking, 1980
O. sativa		0.15–0.18[G]	0.05[G]–0.1					Yokosho et al., 2009
	Fe	0.3[S]–0.4[GS]	0.1[GS]–0.2[S]					Yokosho et al., 2009
	Fe			10–18[S]	10–48[S]			Kakei et al., 2009
	Cu		0.08	28	34			Ando et al., 2013
P. communis	Fe	0.1–3	0.03–0.5[S]					Larbi et al., 2003
P. persica	Fe	0.7–2[S]	0.05–0.8[S]					Larbi et al., 2003
Q. suber	Cd	1–2[S]	0.5–1.2[S]					Gogorcena et al., 2011
S. lycopersicum	Fe	0.6–4[S]	0.04–0.6[S]					López-Millán et al., 2009
	Fe		0.01–0.17[S]					Rellán-Álvarez et al., 2010
	Cu			nd[GS]–20[S]				Pich and Scholz, 1996
	Zn	0.06[S]–0.8[S]	<0.04[S]–0.3[S]			6[S]–18		White et al., 1981
	Cd	0.1–0.3[S]	0.01[S]–0.03–0.06[S]					Sagardoy, 2012
T. arvense	Zn	0.1–0.3[S]	nd			110–140[S]		Lasat et al., 1998
	Ni					nd[S]–57		Persans et al., 1999
T. caerulense[H]	Zn	0.1–0.2[S]	nd		nd			Lasat et al., 1998
T. goesingense[H]	Ni					8–18[S]		Persans et al., 1999
LEAF APOPLASTIC FLUID								
B. vulgaris	Fe	0.7–2[S]	0.7–4[S]			<1–4[S]		López-Millán et al., 2000
	Fe		0.2–4[S]					Larbi et al., 2010
P. communis	Fe	1.6[S]–2	0.8–1.8[S]					López-Millán et al., 2001
PHLOEM SAP								
C. maxima		1.6	2.1					Fiehn, 2003
L. texensis		5.5	1.1					Lattanzio et al., 2013
N. glauca						370		Hocking, 1980
O. sativa	Cu		>0.08	66	152			Ando et al., 2013
	Cd		>0.001–>0.002[S]	66–83[S]	152–176[S]		nd–63[S]	Kato et al., 2010

[S] High or low metal supply; [G] Mutant or transgenic genotypes; and [H] Hyper-accumulator plant species. Nd, not detected; NA, nicotianamine; DMA, 2′-deoxymugineic acid; His, histidine; PCs, phytochelatins.

α-hydroxy acids such as Cit and Mal), they can act as mono- or poly-dentate (bidentate and so on) ligands, and form complexes with several metals (e.g., Fe, Mn, Cu, Ni, Zn, Pb, etc.). Carboxylates with shorter chains or closely packed carboxyl groups with adjacent alcohol groups (α-hydroxy acids) form stronger complexes. These characteristics, as well as the increases in carboxylate levels found in some metal-stressed plants (**Table 2**), have supported that carboxylates could be associated to long-distance metal transport. For instance, Fe-deficiency causes a well-known increase in carboxylate concentrations (mainly Cit) in xylem sap (Abadía

et al., 2002; Rellán-Álvarez et al., 2010) and leaf apoplastic fluid (López-Millán et al., 2000, 2001; Larbi et al., 2010). This occurs not only in several Strategy I plant species (**Table 2**; Abadía et al., 2002 and references therein; Rellán-Álvarez et al., 2010 and references therein) but also in Strategy II plant species (Alam et al., 2001; Yokosho et al., 2009; López-Millán et al., 2012), likely as a result of an increased anaplerotic C fixation mediated by the root phospoenolpyruvate carboxylase (López-Millán et al., 2000; Andaluz et al., 2002; López-Millán et al., 2012). This increased carboxylate flux in xylem sap would supply C to the Fe-deficient foliage that is deprived of C skeletons (López-Millán et al., 2000, 2012) and could also increase Fe supply via formation of Cit complexes with extracellular Fe pools (see below). This is in line with the use of citric acid in industry for cleaning and prevention of the clogging of pipes with colloidal and particulate Fe. An increased activity of citrate synthase (CS) and/or an overexpression of CS genes has been reported in plants grown with low Fe supply (e.g., *Beta vulgaris* López-Millán et al., 2000, *Pyrus communis* López-Millán et al., 2001, *A. thaliana* Thimm et al., 2001, *Actinidia deliciosa* Rombolà et al., 2002, *S. lycopersicum* López-Millán et al., 2009, *Pisum sativum* Jelali et al., 2010, *Malus xiaojinensis* Han et al., 2012 and citrus Martínez-Cuenca et al., 2013) and more recently in *M. xiaojinensis* plants grown with excessive Fe supply (Han et al., 2012). In fact, overexpression of an apple CS gene increased tolerance to Fe stress (low and excessive Fe supply) in transgenic *A. thaliana* and *Nicotiana tabacum* plants (Han et al., 2012, 2013). Increases in xylem carboxylate concentrations have also been described with other metal stresses, including excess of metals in crop (e.g., Zn in sugar beet Sagardoy et al., 2011 and Cd in tomato Sagardoy, 2012), and forest species (Cd in *Quercus suber* Gogorcena et al., 2011), as well as in metal hyper-accumulators (e.g., the Zn hyper-accumulator *T. caerulescens* Lasat et al., 1998, the Cd hyper-accumulator genotype of *B. juncea* L. Wei et al., 2007a and the Ni hyper-accumulator tree *S. acuminata* Callahan et al., 2008). It has been hypothesized that the increases in xylem carboxylates may constitute a general mechanism to cope with situations causing reduced photosynthetic activity (Sagardoy et al., 2011).

Catechols such as caffeic and protocatechuic acids are phenolic compounds with two adjacent hydroxyl groups in the aromatic ring, which have very high affinity for Fe(III). These compounds are involved in long-distance transport of Fe in *O. sativa*, since the mutant *phenolics efflux transporter* (*pez1*) had reduced concentrations of Fe, protocatechuic and caffeic acids in the xylem, along with increased root apoplasmic Fe (Ishimaru et al., 2011).

Histidine (His) is one of the strongest metal-coordinating ligands among the proteinogenic amino acids, and has three metal binding sites: carboxylate, α-amino and imidazole groups. The coordination to metals through the latter group forms rigid bonds and strong complexes, especially with Ni and Cu. However, evidence for a role of His in long-distance metal transport in plants is mostly related to Ni in the xylem of hyper-accumulators of the genus *Allysum*. Histidine (in the μM-mM range) and Ni xylem sap concentrations are significantly and linearly correlated in several *Alyssum* Ni hyper-accumulators (such as *A. lesbiacum*) in response to increased metal concentrations in the growth media (Krämer et al., 1996). This increased xylem loading of Ni is associated with constitutively higher root concentrations of His. Moreover, exogenous applications of His to either the roots or shoots of the non-accumulator plant species *Alyssum montanum* and *Brassica juncea* greatly increases the root-to-shoot mobility of Ni (Kerkeb and Krämer, 2003). In *A. lesbiacum* shoot His concentrations only increased when plants were exposed to Ni, and the levels of transcripts of the enzymes of the His biosynthesis pathway were constitutively higher in *A. lesbiacum* than in the non-accumulator *A. montanum*, especially for the first enzyme in the biosynthetic pathway, ATP-phosphoribosyltransferase (ATP-PRT) (Ingle et al., 2005). Moreover, the overexpression of an ATP–PRT cDNA in *A. thaliana* resulted in increases in shoot His and Ni tolerance (Wycisk et al., 2004). However, it has been recently reported that His does not play a role in Ni translocation in the xylem sap of *Alyssum* ssp. under field conditions (Alves et al., 2011; Centofanti et al., 2013). The Ni-His complex could occur in xylem sap under N-sufficient conditions, whereas under N-limited conditions, such as those usually found in the field, Ni translocation would occur as a free ion or complexed with carboxylates (Alves et al., 2011).

Nicotianamine (NA) and related molecules such as PSs are multi-dentate aminoacid chelators having more than one α-aminocarboxylate binding centers, which confer high affinity not only for Fe but also for other metals such as Zn, Cu, Mn, Ni, and Cd. Nicotianamine has affinity for Fe(III) and Fe(II), whereas PSs have an α-hydroxycarboxylate binding center that confers selectivity for Fe(III). Nicotianamine is ubiquitous in higher plants and present in all tissues, and is involved in plant metal trafficking (Curie et al., 2009; Clemens et al., 2013). In the NA-free tomato mutant *chloronerva*, which displays a strong interveinal chlorosis in young leaves, the long-distance transport of Cu but not that of Fe is impaired, indicating the importance of NA in Cu trafficking (Pich and Scholz, 1996). Unlike NA, PSs are restricted to grasses and secreted to the rhizosphere, and they are responsible for Fe and Zn acquisition (Suzuki et al., 2006). Both NA and PSs form metal stable complexes at the pH values occurring in plant fluids (von Wirén et al., 1999, 2000; Rellán-Álvarez et al., 2008). Furthermore, hydroxylated PSs such as MA and epi-MA have a higher affinity for Fe(III) than the non-hydroxylated DMA at the pH values from 5 to 7 typical of xylem sap, and this represents a competitive advantage when moving through slightly acid environments (von Wirén et al., 2000).

In xylem sap of *O. sativa*, NA and DMA concentrations are in the ranges 10–20 μM and 10–50 μM, respectively (Kakei et al., 2009), whereas in phloem sap higher concentrations were found, in the range of 66–83 for NA and 152–176 μM for DMA (Kato et al., 2010). Metal stresses caused increases in xylem sap NA or PSs concentrations in several species, including MA and DMA in Fe-deficient *H. vulgare* (Alam et al., 2001; Kawai et al., 2001), DMA in Fe-deficient *O. sativa* (Kakei et al., 2009), and NA in Cu-deficient Brassica (Irtelli et al., 2009) and Fe-deficient *Prunus persica* (Rellán-Álvarez et al., 2011a). Nickel-induced NA root-accumulation occurred in *T. caerulescens*, a Cd/Zn/Ni hyper-accumulator, but not in *T. arvense*, and this suggests that NA could be involved in Ni translocation *via* xylem in *T. caerulescens*, resulting in a higher capacity to transport Ni to shoots (Mari et al., 2006).

Phytochelatins are oligomers of the tri-peptide glutathione (-GluCysGly) and act as metal (Cd, Hg, Zn, and others) chelators through the thiol (-SH) group of Cys. Phytochelatins form a family of structures with increasing repetitions of the -Glu-Cys dipeptide units, followed by a terminal Gly, (-Glu-Cys)n-Gly or (-EC)n-Gly, where *n* generally ranges from 2 to 5 but can be as high as 11. A number of structural variants have been identified in a wide variety of plant species, and different metals, including Cd, Pb, Zn, and Hg, have been found to induce PCs production (reviewed by Pal and Rai, 2010). The occurrence of long-distance transport (either from shoot-to-root or from root-to-shoot) of PCs and some intermediates of their biosynthesis (e.g., **γ**-glutamylcysteine) during heavy-metal detoxification was first shown with transgenic and grafted Arabidopsis plants where PCs synthesis was restricted to specific tissues (Gong et al., 2003; Chen et al., 2006; Li et al., 2006). However, the direct determination of PCs in plant fluids has only been achieved more recently: glutathione and PCs were found in the phloem of Cd-treated *B. napus* (by HPLC coupled to both fluorescence and ESI-MS; Mendoza-Cózatl et al., 2008) and *O. sativa* (by CE-MS; Kato et al., 2010), and As-treated *R. communis* (by HPLC-ESI-MS; Ye et al., 2010). Lower concentrations of PCs (or trace levels) were found in the xylem of *B. napus* (Mendoza-Cózatl et al., 2008) and *R. communis* (Ye et al., 2010), suggesting that phloem is the major vascular system for PC-facilitated long-distance metal transport.

Proteins can also be involved in metal transport in fluids. A significant fraction of metals has been associated with the high molecular weight fraction in the phloem sap of *R. communis* (Fe Krüger et al., 2002) and *O. sativa* (Cu Ando et al., 2013 and Cd Kato et al., 2010). Among metal-binding proteins, metallothioneins (MTs) are low molecular weight (5–10 kDa), Cys-rich proteins, which are able to bind a variety of metals by the formation of mercaptide bonds with the numerous Cys residues present in the proteins (see review by Freisinger, 2011). Metallothioneins are implicated in several processes related to metal homeostasis, detoxification, distribution, and redox regulation, in particular under normal (non-stressed) physiological conditions. Evidence supports its role as metal carriers, mainly in the phloem sap. An up-regulation of MTs in *H. vulgare* was found during senescence (when metal remobilization occurs from senescing leaves), heavy metal treatments and Cu deficiency (Heise et al., 2007). Metallothioneins have been reported to occur in the phloem of *Apium graveolens* (Vilaine et al., 2003), *R. communis* (Barnes et al., 2004), *O. sativa* (Aki et al., 2008) and *L. texensis* (Lattanzio et al., 2013), when grown under non-stressed conditions. The induction of MTs (MT1) expression in leaf veins (and to a lesser extent in mesophyll cells) in response to Cu stress in *A. thaliana* suggest that this MT could be important for scavenging Cu in leaf veins (García-Hernández et al., 1998). Also, in hyper-accumulator plants, MTs could help detoxify the excess Cu accumulated by the high expression of the Cd/Zn ATPase HMA4 (Leitenmaier and Küpper, 2011, 2013).

CHALLENGES ANALYZING METAL COMPLEXES IN PLANT FLUIDS

Several challenges are faced when studying metal speciation in plant fluids, because of the changes in metal speciation that may occur at sampling and/or during storage, and especially during sample preparation, separation and determination (Husted et al., 2011). Challenges when attempting the analysis of the metal chemical form(s) existing in a plant fluid occur because: (i) dynamic metal–ligand systems such as those in plant fluids inevitably include labile or transient metal species; (ii) biochemical processes such as enzymatic activities may cause degradation of metal complexes, (iii) metal species occur in plant fluids at very low concentrations (in the μM range; see below; **Table 1**), (iv) the metal complex distribution strongly depends not only on pH, but also on the metal-to-ligand ratios (Weber et al., 2006; Xuan et al., 2006, 2007; Rellán-Álvarez et al., 2008). The latter is specially important in plant fluids, since unlike stable metal chelates with the hexadentate ligands NA and PSs, which always occur with 1:1 stoichiometry, many of the known metal ligands existing in xylem and phloem saps (e.g., amino acids and carboxylates) may act as bi- and tri-dentate ligands, resulting in numerous metal-ligand species with different stoichiometries and charge states (see examples for Fe-Cit complexes in Silva et al., 2009; Rellán-Álvarez et al., 2010). For instance, in a solution with a 1:2 Fe:Cit ratio and pH 4, up to thirteen different Fe-Cit species were detected in aqueous solution by ESI-MS, whereas only two species occurred in a solution prepared at 1:100 Fe:Cit ratio at the same pH (Silva et al., 2009). Also, even for stable metal species, ligand exchange reactions may occur (altering the actual composition of the sample) at any step previous to detection, due to the presence of competing ligands and/or redox mediators. Ligand exchanges have already been reported in the cases of Fe(III)-NA (with Cit; Rellán-Álvarez et al., 2008) and Fe(III)-DMA (with NA; Weber et al., 2006). Some of these challenges are especially critical in separation-based methods (e.g., HPLC, CE), because the separation of the free ligand does change the metal-to-ligand ratio, and also because the pH may change considerably when organic solvent modifiers are used (Rellán-Álvarez et al., 2008, 2010; Köster et al., 2011a).

Sampling and storage procedures (temperature, light, etc.), can be considered as key aspects to preserve the metal species occurring in samples during the whole analytical process (reviewed by Mesko et al., 2011). Temperature needs to be as low as possible to reduce metal species transformation. For this purpose, lyophilization and shock-freezing in liquid N are the most common procedures used to preserve metal species in fluids. The latter is considered the safest technique to prevent metal species changes because it can be performed immediately at the sampling site and also because sample is stored in an inert gas atmosphere. Light can cause changes in metal speciation because it can induce electron transfer reactions affecting the stability of the metal complexes and also the structural integrity of the ligands. For instance, photochemical reduction of Fe(III) complexes with ligands such as di- and tri-carboxylic acids is well known (Bennett et al., 1982), and are accompanied by oxidative decarboxylation of the ligand. This issue could limit the use of irradiation with high intensity synchrotron X-rays for metal speciation (Terzano et al., 2013).

Finally, accurate quantification of metal species, generally performed either on-line or off-line after separation, is currently carried out using metal (ICP-MS) or molecular (ESI-MS) detection, in combination with isotope dilution analysis (IDA) that requires the use of an isotopolog of the analyte. When ICP-MS

is used, a stable isotope of the metal is added after the separation of the metal complexes. For instance, Rellán-Álvarez et al. (2010) used ^{57}Fe post-column addition to quantify Fe-Cit species in tomato xylem sap. When molecular detection such as ESI-MS is used, the isotopolog should be either a metal complex with a stable isotope-labeled ligand, or alternatively a structural analogue of the ligand. As mentioned above, the limited supply of stable isotope labeled ligands is an additional constraint for metal speciation.

METAL SPECIES IN XYLEM SAP

Most of the studies exploring the chemical forms of metal complexes in plant fluids have been conducted using xylem sap. Metals occurring in the xylem sap may be preferentially complexed by the more acidic carboxylic acids (existing at concentrations from 2 to 9 mM in the xylem) rather than the much more basic amino acids (existing at concentrations from 1 to 3 mM in the xylem) due to the relatively acidic pH of this fluid, which is generally in the pH range from 5 to 6.5 (Harris et al., 2012).

A Fe(III)-Cit complex [tri-Fe(III), tri-Cit complex (Fe_3Cit_3)] was found for the first time in the xylem sap of tomato, using an integrated HPLC-MS approach, consisting in hydrophilic interaction liquid chromatography (HILIC) coupled to both ICP-MS and ESI-MS(TOF), combined with the use of stable isotope (^{54}Fe) labeling; the identification was based on exact molecular mass, isotopic signature, Fe determination and retention time (Rellán-Álvarez et al., 2010). Citrate had been considered for many years a likely candidate for Fe xylem transport, but the possible Fe-Cit species in the xylem sap were only predicted from the co-migration of Fe and Cit during paper electrophoresis of xylem sap (Tiffin, 1966) or from *in silico* calculations (von Wirén et al., 1999; López-Millán et al., 2000, 2001; Rellán-Álvarez et al., 2008). The Fe_3Cit_3complex was only found in xylem samples with Fe concentrations above 20 μM (the limit of detection for the complex), such as those in Fe-deficient plants after Fe-resupply. The complex could not be detected in Fe-deficient and control plants, which have lower xylem sap Fe concentrations. The existence of other Fe-Cit complexes is likely, and the complex Fe_2Cit_2 was also detected in Fe-Cit standards along with Fe_3Cit_3, with the allocation of Fe between the two complexes depending on the Fe:Cit ratio. Since in plant xylem sap a wide range of Fe to citrate ratios could exist, it is likely that both Fe(III)-Cit species could occur in different conditions (Rellán-Álvarez et al., 2010). Later, other Fe-Cit species were found along with Fe_3Cit_3 in *H. vulgare* leaf extracts using HILIC coupled to high-resolution Fourier transform ion cyclotron resonance (FT-ICR) MS (Köster et al., 2011a). More recently, the Fe speciation in tomato xylem sap was assessed for the first time using XANES on a highly brilliant synchrotron (PETRA III, beamline P06; Terzano et al., 2013). Although this study confirmed the occurrence of Fe(III)-Cit and also found Fe(III)-acetate complexes in xylem sap, the authors indicated that complexes found could be artifacts as a result of the high intensity radiation used. Studies with *FRD* mutants (i.e., *Atfrd3* and *Osfrdl1*), which lack a protein responsible for efflux of Cit in cells of the xylem vasculature, also support the role of Cit as a major ligand responsible for Fe complexation (Durrett et al., 2007; Yokosho et al., 2009). These mutants showed leaf chlorosis and low levels of Fe in xylem and leaves, as well as decreased Cit levels of in the xylem sap. Taken together, all these studies support that Fe-Cit is responsible for the translocation of an important fraction of Fe to the shoot, and that FRD mediated-Cit efflux is required to sustain normal rates of root–shoot Fe delivery. More recently, it was shown that FRD mediated-Cit efflux is also a major player in mobility of Fe in inter-cellular spaces lacking symplastic connections (Roschzttardtz et al., 2011).

The possible role of NA in long-distance Fe transport in the xylem is still being explored (Curie et al., 2009). However, strong evidence supports that this amino acid is not essential for xylem Fe transport: the NA-deficient tomato mutant *chloronerva* does accumulate Fe in old leaves (Pich et al., 1994) and the *A. thaliana* NA synthase (NAS) quadruple mutant (with low levels of NA) also accumulates Fe in leaves (Klatte et al., 2009). Until now, Fe-NA chelates have not been detected in xylem sap (Rellán-Álvarez et al., 2010), and *in silico* and/or *in vitro* speciation studies tend to exclude NA as a possible xylem Fe carrier at the slightly acidic pH values typical of xylem (von Wirén et al., 1999; Rellán-Álvarez et al., 2008). However, it has been recently suggested that NA may play a role in long distance transport of Fe when carboxylates are in short supply, as it occurs in *FRD* mutants (Schuler et al., 2012) or in plant species with less acidic xylem such in field-grown *Prunus persica* trees (where the xylem sap pH is in the range from 6.5 to 7.5 Larbi et al., 2003; Rellán-Álvarez et al., 2011a). The most accepted role of NA is in intra-organ Fe distribution, where this ligand could be crucial for xylem Fe unloading. Iron distribution within leaves is impeded in the tomato mutant *chloronerva* (Pich et al., 1994) that also showed a lower presence of Fe(II) ions in the veins when leaves were analyzed by XANES (Yoshimura et al., 2000). This suggests that the occurrence of Fe as Fe(II)-NA complex in leaf veins is crucial for the intra-organ Fe allocation (Yoshimura et al., 2000). No transporter responsible for moving Fe-complexes into the xylem sap has been conclusively identified so far, but it has been suggested that Fe-NA could be effluxed into the xylem by a yellow-stripe-like (YSL) transporter (Colangelo and Guerinot, 2006). Regarding PSs, only a minor peak assigned to Fe(III)-DMA was found in press sap from the roots of Fe-deficient wheat plants by HILIC-ESI-MS (Xuan et al., 2006).

The Zn species present in the xylem are still an open question (Clemens et al., 2013). Three studies tackling Zn speciation in xylem sap were carried out using EXAFS or XANES with the hyper-accumulators *T. caerulescens* (Salt et al., 1999; Monsant et al., 2011) and *S. alfredii* (Lu et al., 2013). In all cases, although the major fraction of Zn consisted in free hydrated Zn^{2+} ions, the remaining fraction was coordinated with carboxylates such as Cit and Mal. The occurrence of Zn-Cit in xylem sap was also predicted by *in silico* studies in non hyper-accumulator species (White et al., 1981; Mullins et al., 1986). However, other EXAFS study indicated that most of the Zn in petioles and stems of *T. caerulescens* is present as Zn-His (Küpper et al., 2004) and a recent study (including the re-evaluation of previous EXAFS spectra from this species) proposes His as a Zn ligand within cells and NA as Zn chelator involved in long distance transport (Trampczynska et al., 2010). In a recent room temperature XANES study with *T. caerulescens* intact plants, Zn-His and

Zn-phytate complexes were found in roots, whereas Zn(II)-Mal and Zn(II)-Cit were the major species in shoots (Monsant et al., 2011). *In vitro* metal exchange experiments also support the existence of the complex Zn(II)-NA in the xylem sap (Rellán-Álvarez et al., 2008). It has also been speculated that Zn would be associated with S ligands in Cys, GSH or PCs in hyper-accumulators (Milner and Kochian, 2008). In the Zn hyper-accumulator *A. halleri*, suppression of NA synthase (NAS2) resulted in strongly reduced NA root accumulation, and a concomitant decrease in root-to-shoot translocation of Zn (Deinlein et al., 2012). This study found NA and thiols as the dominant Zn ligands in the low molecular weight fraction of root extracts by using size-exclusion chromatography (SEC)-ICP-MS combined with off-line ESI-MS ligand detection in the Zn-containing LC fractions. The overexpression of *A. thaliana* ZINC-INDUCED-FACILITATOR1 (ZIF1) altered the subcellular partitioning of NA, which was accumulated in roots, and led to a Zn accumulation in roots at the expense of shoots (Haydon et al., 2012). This indicates that the formation of Zn(II)-NA could be responsible for Zn hyper-accumulation. However, the complex Zn(II)-NA has never been found in the xylem sap yet. In grasses, a Zn(II)-DMA complex was detected in press sap from roots of Fe-deficient wheat plants using HILIC-ESI-MS (Xuan et al., 2006).

The Cu(II)-DMA complex has been recently been found in xylem sap of *O. sativa* (Ando et al., 2013). The Cu(II)-DMA complex was identified by SEC combined with both off-line Cu determination (using GFAAS) and off-line molecular detection of the complex by ESI-MS, based on exact molecular mass and isotopic signature. In this study, the Cu, NA, and DMA xylem sap concentrations were 5, 28, and 34 μM, respectively (the molar ratio DMA:Cu was *ca.* 7). The same complex was already found in press sap from roots of Fe-deficient wheat plants, both using HPLC-MS (Xuan et al., 2006) and CE and UV-VIS detection (Xuan et al., 2007). The presence of Cu(II)-DMA is not unexpected, since it has a quite high stability constant (18.7; Murakami et al., 1989). Nicotianamine and DMA are present in comparable concentrations in the xylem, but Cu(II)-NA has not been found in xylem sap so far, in spite of having a similar stability constant to that of Cu(II)-DMA (18.6; Callahan et al., 2006). A preferential Cu complexation by DMA vs. NA was already predicted by *in silico* speciation (von Wirén et al., 1999). In plant species other than grasses, the low leaf Cu concentration found in the NA-free tomato mutant *chloronerva* is in strong support that Cu(II)-NA is involved in xylem Cu transport (Pich and Scholz, 1996). The EXAFS spectra of *T. caerulescens* shoots also suggested the presence of Cu(II)-NA (Mijovilovich et al., 2009). Further support for the role of NA in xylem Cu transport was obtained when the NA aminotransferase gene from *H. vulgare* was introduced into the non-graminaceous plant *N. tabacum*. When compared to wild type, these transgenic plants showed decreased Cu concentration in young leaves and flowers (Takahashi et al., 2003), attributable to the depletion of endogenous NA. The occurrence of a Cu-His complex has been reported in the xylem sap from the Ni hyper-accumulator *A. lesbiacum* by EXAFS (Krämer et al., 1996) and in *H. vulgare* leaf aqueous extracts by HILIC-FT-ICR/MS (Köster et al., 2011a).

Long-distance Ni transport has been demonstrated in hyper-accumulators (*Allysum* and *Thlaspi* species) coordinated with several ligands, including different carboxylates (e.g., Cit, Mal, etc.) and amino acids (e.g., NA and His). An in depth study of Ni ligands using a combination of advanced MS and NMR techniques in the latex of the Ni hyper-accumulator tree *S. acuminata* revealed the presence of Ni in complexes with methylated aldaric acid and Cit (Callahan et al., 2008). In this latex, containing 26% dry matter of Ni, Ni(II) was forming complexes of 1:2 stoichiometry [Ni(II):carboxylate] with these two carboxylates as well as with Mal, aconitate, erythronate, galacturonate, tartarate, aconitate, and saccharate. A $Ni(II)Cit_2$ complex (accounting for 99.4% of the Ni) was previously identified in an aqueous extract of *S. acuminata* using SEC monitorized on-line with ICP-MS, followed by off-line ESI-MS/MS analyses of the Ni-containing SEC-fractions (Schaumlöffel et al., 2003). In leaf extracts of several New Caledonia Ni hyper-accumulator plant species, Ni-Cit complexes were also found as the most prominent Ni containing ions detected by SEC-ESI-MS/MS (Callahan et al., 2012). In another Ni hyper-accumulator, *A. murale*, EXFAS studies indicated that Ni was found coordinated with Mal, His and other low molecular weight compounds in the plant sap and vasculature (McNear et al., 2010), and an *in silico* speciation study of the xylem sap of the hyper-accumulator *A. serpyllifolium* predicted approximately 18% of Ni bound to organic acids (Alves et al., 2011). However, a detailed study of the metal and ligand concentration in the xylem sap of Alyssum species treated with Ni for long periods indicated that most of the Ni in xylem sap of this species is present as the hydrated cation, and that the increases in His and other chelators may constitute only a short term response (Centofanti et al., 2013). The Ni(II)-NA complex is quite stable ($\log K = 16.1$) and accordingly Ni has also been found complexed by NA in hyper-accumulators as well as model plant species. Nickel(II)-NA was found in the xylem sap (Mari et al., 2006) and plant extracts (Vacchina et al., 2003; Ouerdane et al., 2006) of *T. caerulescens*, in a water extract of the latex in *S. acuminata* (Schaumlöffel et al., 2003), and in leaf extracts of New Caledonia Ni hyper-accumulator plant species (Callahan et al., 2012), using SEC-ESI-MS/MS or SEC in combination with ICP-MS detection and off-line ESI-MS/MS. In Arabidopsis xylem sap, the Ni(II)-NA complex was also detected using both HPLC-MS (Xuan et al., 2006) and CE coupled to UV-VIS (Xuan et al., 2007). On the other hand, studies on natural variation among *Arabidopsis* accessions indicated that a Ni(II)-Mal complex may also be involved in translocation of Ni from roots to shoots (Agraval et al., 2013).

In the case of toxic metals such as Cd, complexation with organic ligands in xylem vessels may not be necessary, because toxicity exerted in this apoplastic, extracellular system is low and may not require a metal detoxification strategy. In fact, using ^{113}Cd NMR analysis combined with a stable isotope (^{113}Cd) labeling technique, Cd was found as an ionic form in *A. halleri* xylem sap (Ueno et al., 2008). However, several EXAFS spectroscopy studies indicate that Cd is coordinated with O or N ligands in *B. juncea* xylem sap (Salt et al., 1995) and with O in aerial parts of *T. caerulescens* (Küpper et al., 2004), *A. halleri*

(Huguet et al., 2012) and *T. praecox* (Vogel-Mikus et al., 2010). In roots of *B. juncea*, a possible coordination of Cd with S ligands was also reported (Salt et al., 1995), with the bond length being similar to that of a purified Cd(II)-PC complex, supporting the occurrence of Cd(II)-PC complexes in plants (Salt et al., 1995). The occurrence of Cd association with PCs in the xylem sap of *B. juncea* has been proposed using SEC and off-line metal GFAAS, and using the retention times of several Cu-complexes with low molecular weight ligands (including PCs, GSH, Cys, organic acids, and inorganic anions) as a mean for identification (Wei et al., 2007b).

The chemical form of Al in xylem sap has been identified as the Al-Cit complex using ^{27}Al-NMR analysis in several Al hyper-accumulators, including *Fagopyrum esculentum* (Ma and Hiradate, 2000), *Melastoma malabathricum* (Watanabe and Osaki, 2001) and *Camellia sinensis* (Morita et al., 2004). Since Al in roots was as an Al-oxalate (1:3) complex, ligand exchange from oxalate to Cit should occur in these plant species (Ma and Hiradate, 2000; Watanabe and Osaki, 2001).

METAL SPECIES IN PHLOEM SAP

The distribution of micronutrients to developing organs of plants depends to a great extent on phloem transport. Unlike xylem, phloem consists of columns of living cells. Metals are sparingly soluble at the alkaline pH values typical of the phloem sap (pH range from 7 to 8), and they are also highly reactive species, with some of them such as Fe undergoing easily changes of valence that favor the production of highly reactive oxygen species *via* Fenton reactions. Therefore, metal complexation with appropriate ligands can provide solubility and shielding during phloem transport of metals to the nutrient sinks.

In the phloem sap of *O. sativa*, Fe has been found predominantly (77%) associated with high molecular weight molecules (using a 3 kDa membrane filter; Nishiyama et al., 2012). In this study, Fe-containing compounds or complexes of 10–30 kDa and the Fe(III)-DMA complex were detected in the phloem sap using anion exchange HPLC separation followed by an identification based on Fe determination and the comparison of the retention time with those of standards, in combination with exact molecular mass and Fe isotopic signature obtained using ESI-MS(TOF). A protein capable to bind Fe was described in the phloem sap of *R. communis* (ITP; Iron Transport Protein; Krüger et al., 2002) using two-dimensional gel electrophoresis protein separation (2-DE SDS-PAGE) followed by electro-blotting to PVDF membranes and staining of Fe-containing proteins with Ferene. Recently, two more low molecular weight Fe-binding proteins were also identified in *L. texensis* phloem sap using a similar approach combined with Fe affinity chromatography, although none of them are considered candidates for Fe transport (Lattanzio et al., 2013). The Fe(II)-NA complex has not been found so far in the phloem sap, although *in silico* and/or *in vitro* studies support that the Fe-NA complex is likely to occur at the neutral to basic pH values of the phloem sap (von Wirén et al., 1999; Rellán-Álvarez et al., 2008), and YSL transporters able to transport Fe-NA complexes have been described in *Arabidopsis* and *O. sativa* phloem vascular tissues (Curie et al., 2009). Perhaps NA is only important in Fe phloem loading (Schuler et al., 2012), and once in that compartment Fe may be transported in another form such as bound to proteins.

Almost all Zn in the *O. sativa* phloem sap was found associated with low molecular weight molecules when a 3 kDa membrane filter was used as a cut-off (Nishiyama et al., 2012). In this study, Zn was identified as the Zn(II)-NA complex, using SEC and off-line Zn determination and off-line ESI-MS, based on exact molecular mass, isotopic signature, and retention time. In *L. texensis* phloem sap, four low molecular weight Zn-binding proteins were identified using 2-DE SDS-PAGE, nanoLC-MS/MS and Zn affinity chromatography, one of them being a metallothionein-like protein type 2B, but they were not considered as good candidates for Zn transport (Lattanzio et al., 2013).

Regarding Cu, the phloem sap of *O. sativa* has been shown to contain the complexes Cu(II)-NA, Cu(II)-His and high-molecular-weight compounds >3 kDa (the latter being at least 30% of the total Cu) (Ando et al., 2013). Copper(II)-NA and Cu(II)-His were identified using SEC combined with both off-line Cu determination by GFAAS and molecular detection of the complex in the major Cu-containing fractions. Copper-containing proteins detected in phloem sap so far include Cu/Zn-superoxide dismutase, a Cu-chaperone (CCH homolog) and several MTs in *O. sativa* (Aki et al., 2008) and *L. texensis* (Lattanzio et al., 2013).

A Cd-containing complex has not been directly identified in the phloem sap so far. However, 90% of the Cd in the phloem sap from Cd-treated *O. sativa* plants was found in a complexed form using SEC-ICP-MS (Kato et al., 2010). Based on the elution times of *in vitro* prepared Cd-complexes with glutathione and several PCs and on the changes caused on Cd elution by sap digestion with proteinase K, it was proposed that Cd was found associated with a 13 kDa protein and SH-containing compounds. Cadmium has also been associated with S in the phloem and companion cells of *A. thaliana* using energy-dispersive X-ray microanalysis (van Belleghem et al., 2007). This, along with the occurrence of PCs in phloem of Cd-treated plants (see above) suggest the occurrence of Cd-PC complexes in the phloem sap.

Much less information is available on the chemical forms of other metals in the phloem sap. In *R. communis*, Mn was detected in association with low molecular peptides (van Goor and Wiersma, 1976), while Ni was shown to be complexed with negatively charged organic compounds with a molecular weight in the range of 1000–5000 Da (Wiersma and van Goor, 1979).

METAL SPECIES IN OTHER FLUIDS

The ESL is a fluid that facilitates metal transport from the seed coat to the embryo. Iron speciation in isolated *P. sativum* ESL was achieved using an integrated analytical approach, combining XANES, HILIC-ICP-MS, and HILIC-ESI-MS (Grillet et al., 2014). The application of the XANES technique indicated that most of the Fe was present as Fe(III), probably associated to carboxylates—although the XANES spectra of Fe-Cit and Fe-Mal could not be distinguished—with only a minor amount of Fe(II) species being present. Most (88%) of the Fe occurring in the ESL was found as the species $Fe(III)_3Cit_2Mal_2$, $Fe(III)_3Cit_3Mal$ (both are mixed ligand species) and $Fe(III)Cit_2$; only a minor amount of Fe(II)-NA was found using HILIC separation coupled to the two cited MS detectors. Metal species were identified

based on elution time, Fe determination, exact mass determination, isotopic signature, and MS^2 fragmentation pattern of the Fe species as identification tools. Pea embryos are capable of reducing Fe(III) in these complexes by effluxing to the ESL high amounts of ascorbate that chemically reduce Fe(III) from the Fe-Cit and Fe-Mal complexes. Ascorbate efflux also occurs in *A. thaliana* embryos and is significantly decreased, along with Fe concentrations, in ascorbate deficient mutants (Grillet et al., 2014). These data provide support for a new local Fe transport system that may play a major role to control Fe loading in seeds in dicotyledonous plants.

Apoplastic fluid composition is determined by the balance of import via xylem, absorption by cells, and export by phloem, and plays important roles in the transport and storage of mineral nutrients (Sattelmacher, 2001). However, as far as we know, there are no reports tackling direct metal speciation on apoplastic fluids. *In silico* calculations have been carried out to speciate Fe in leaf apoplastic fluid of *B. vulgaris* (López-Millán et al., 2000; Larbi et al., 2010) and field-grown *P. communis* (López-Millán et al., 2001) using experimental concentrations of Fe, inorganic ions, carboxylates, sugars and amino acids measured from fluids isolated from Fe-sufficient and Fe-deficient plants. In both plant species, Fe was predicted to occur in the leaf apoplastic fluid as Fe-Cit complexes, with FeCitOH and $Fe(III)Cit_2$ being the major species. The effect of Fe deficiency altered the balance between these two Fe-Cit species and the contribution of $Fe(III)Cit_2$ increased with Fe deficiency in *B. vulgaris*, whereas in *P. communis* $Fe(III)Cit_2$ was lower in Fe-deficient trees.

SUMMARY AND CONCLUDING REMARKS

The new developments in MS techniques and the increased use of X-ray spectroscopy methods at synchrotron facilities have permitted the discovery of a number of natural metal species (*ca.* 19) in xylem and phloem saps (**Figure 1**; clear symbols). Moreover, evidence supporting the occurrence in such fluids of further putative metal species (*ca.* 15) has been provided by means of physiological studies, many of them applying molecular biology tools (**Figure 1**; faded symbols). Approximately 50% of the confirmed metal species and 27% of the putative ones have been reported in the xylem sap of plants (mostly hyper-accumulators) treated with high metal supply including Zn, Ni, and Cd. The second most abundant group of metal species has been described in the phloem sap of plants (including grasses) grown at low and adequate metal supply, and accounts for 37% of the confirmed metal species and 33% of those considered putative. This second (phloem) group includes mainly species containing Fe and Cu. Metal carboxylate complexes have always been found in xylem, whereas metals associated with proteins or high molecular weight compounds have been reported in phloem. Complexes with high affinity metal ligands (e.g., NA for Cu and Zn, PSs for Fe and PCs for Cd) have been commonly found in phloem sap, where complexation is needed to ensure metal solubility at the existing high pH as well as to avoid uncontrolled binding of metals in living cells, ensuring metal transport and delivery to sinks. Also, high affinity metal ligands have been found as metal carriers in the xylem sap when plants are grown with low or high metal supply. When metal availability is scarce, organic ligand-assisted xylem transport (e.g., Fe complexed by carboxylates or DMA) can increase transport efficiency, because complexation ensures metal delivery, while avoiding unwanted reactions and scavenging any metal pools occurring in the apoplast. Under conditions of high metal supply, organic ligand-assisted xylem transport (e.g., Ni-NA or Cd-PCs) may attenuate the toxicity derived of the exceptionally high metal concentrations as well as to ensure a correct delivery of other metals.

Most of the knowledge on metal complexes in xylem and phloem has been gained using plants (mostly hyper-accumulators) grown on hydroponics with either a short-time excess metal supply treatment or with a established metal deficiency followed by a short-time metal re-supply treatment (the latter in the case of Fe or Zn). Since these conditions are far from the natural ones, some of the reported metal species can differ from the actual complexes existing in plants in natural conditions (Centofanti et al., 2013). The reason to use such growth conditions is to force upwards the metal concentrations usually found in plant fluid samples (which rarely are $>50\,\mu M$; **Table 1**). These low concentrations make particularly challenging the speciation of metals in plant fluids in natural conditions. Also, plant fluids contain ions, sugars, proteins and other biomolecules along with the metal of interest and the rest of metals. This leads to a delicate balance among several metal species, which can include free metal ions and metal complexes having a great diversity of size, charge, and stability. Therefore, the direct analysis of the metal species in plant fluids requires of highly conservative (avoiding any alteration of sample that can damage metal species), sensitive and selective analytical techniques. Unfortunately, none of different techniques available comply with all of these characteristics.

X-ray spectroscopy methods are non-invasive and apparently conservative, although damage of the sample can occur, but they are much less sensitive than ICP-MS and much less selective than ESI-MS/MS. In contrast, MS-based techniques need to be combined with separation methodologies that are inherently invasive since they carry out the separation of the sample in fractions of different characteristics (e.g., molecular size in SEC), and this can significantly affect the distribution of metal chemical forms, particularly in the case of weak metal complexes specially sensitive to changes in pH and ligand-to-metal ratios. For these reasons, metal species found using MS techniques usually require confirmation using alternative separation methods to validate the actual existence of such metal-complexes in the samples, and sometimes alternative detection methods (e.g., NMR of isolated fractions) are needed to elucidate identity. Ultimately, the occurrence of the metal complexes identified *via* MS should be also confirmed in intact samples with XAS methods. On the other hand, the use of X-ray spectroscopy methods requires having pure standards of putative metal species, because data interpretation relies on linear combination fitting procedures where the sample spectra is fitted using those of standard compounds. Also, XAS techniques can hardly give any information on well-defined metal species when the sample contains several species with similar XANES spectra (e.g., metal complexes with carboxylates). Therefore, XAS also needs complementary techniques (e.g., ESI-MS/MS) to provide putative metal species as well as to confirm the correct identity of the metal species occurring in the samples.

The path of any given metal to its final destination (e.g., the chloroplast) involves transport across multiple membranes

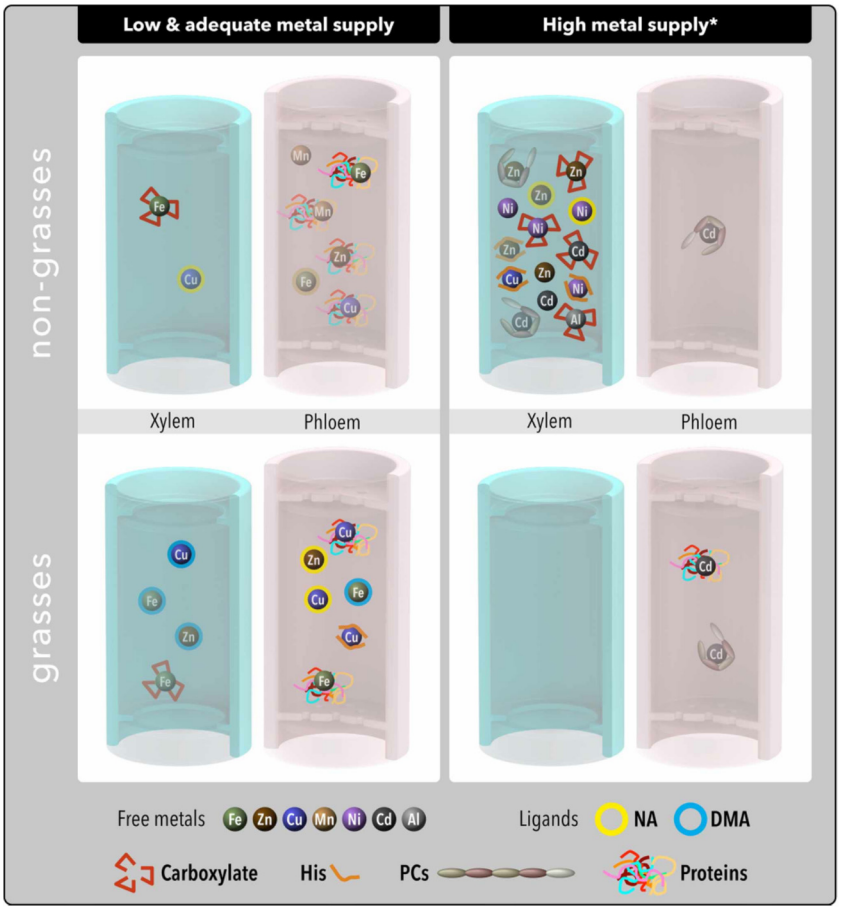

FIGURE 1 | Schematic representation showing the metal species found in the xylem and phloem saps of non-grass (upper panels) and grass plant species (lower panels) grown at low and adequate metal supply (left panels) or at high metal supply (right panels). Metals occurred in free ionic forms and in complexes with different ligands such as nicotianamine (NA), 2′-deoxymugineic acid (DMA), carboxylates (e.g., citrate), histidine (His), phytochelatins (PCs) and proteins. Putative metal species proposed to occur in plant fluids as supported by strong evidence from indirect approaches (e.g., molecular biology and others) are shown with faded symbols. *Most of the data with high metal supply have been described in metal hyper-accumulator plant species.

mediated by different transporter proteins and most likely metal complexation by different ligands in each compartment within the path. Although a complete picture of this complex process is still lacking even for one metal, an increasingly more complete and accurate knowledge of the metal species in plant fluids would be achieved performing studies that integrate molecular biology approaches, untargeted analyses of plant fluids using complementary MS-based and NMR techniques, and targeted XAS methods. The limits of detection and quantification of the techniques actually used are still far from ideal to analyze fluids coming from plants grown in natural conditions, and therefore more analytical efforts are required to completely decipher the metal species transported in plant fluids.

ACKNOWLEDGMENTS

We apologize to those authors whose work has not been cited owing to space constraints or possible oversight. This study was supported by the Spanish Ministry of Economy and Competitiveness (projects AGL2010-16515 and AGL2012-31988), and the Aragón Government (group A03). Pablo Díaz-Benito was supported by a MINECO-FPI grant. The authors thank J. Ascaso (Digital Works, Huesca, Spain) for art in **Figure 1**.

REFERENCES

Abadía, J., López-Millán, A. F., Rombolà, A. D., and Abadía, A. (2002). Organic acids and Fe deficiency: a review. *Plant Soil* 241, 75–86. doi: 10.1023/A:1016093317898

Agraval, B., Czymmek, K. J., Sparks, D. L., and Bais, H. P. (2013). Transient influx of nickel in root mitochondria modulates organic acid and reactive oxygen species production in nickel hyper-accumulator *Alysuum murale*. *J. Biol. Chem.* 288, 7351–7362. doi: 10.1074/jbc.M112.406645

Aki, T., Shigyo, M., Nakano, R., Yoneyama, T., and Yanagisawa, S. (2008). Nano scale proteomics revealed the presence of regulatory proteins including three FT-like proteins in phloem and xylem saps from rice. *Plant Cell Physiol.* 49, 767–790. doi: 10.1093/pcp/pcn049

Alam, S., Kamei, S., and Kawai, S. (2001). Effect of iron deficiency on the chemical composition of the xylem xap of barley. *Soil Sci. Plant Nutr.* 47, 643–649. doi: 10.1080/00380768.2001.10408428

Alexou, M., and Peuke, A. D. (2013). Methods for xylem sap collection. *Methods Mol Biol.* 953, 195–207. doi: 10.1007/978-1-62703-152-3_13

Alves, S., Navais, C., Simões Gonçalves, M. de L., and Correia Dos Santos, M. M. (2011). Nickel speciation in the xylem sap of the hiperaccumulator *Alyssum serpyllifolium* ssp. Lusitanicum growing on serpentine soils of northeast Portugal. *J. Plant Physiol.* 168, 1715–1722. doi: 10.1016/j.jplph.2011.04.004

Andaluz, S., López-Millán, A. F., Peleato, M. L., Abadía, J., and Abadía, A. (2002). Increases in phospho*enol*pyruvate carboxylase activity in iron-deficient sugar beet roots: analysis of spatial localization and post-translational modification. *Plant Soil* 241, 43–48. doi: 10.1023/A:1016000216252

Ando, Y., Nagata, S., Yanagisawa, S., and Yoneyama, T. (2013). Copper in xylem and phloem saps from rice (*Oryza sativa*): the effect of moderate copper concentrations in the growth medium on the accumulation of five essential metals and a speciation analysis of copper-containing compounds. *Funct. Plant Biol.* 40, 89–100. doi: 10.1071/FP12158

Atkins, C. A., Smith, P. M. C., and Rodríguez-Medina, C. (2011). Macro-molecules in phloem exudates-a review. *Protoplasma* 248, 165–172. doi: 10.1007/s00709-010-0236-3

Aucour, A. M., Pichat, S., Macnair, M. R., and Oger, P. (2011). Fractionation of stable zinc isotopes in the zinc hyperaccumulator *Arabidopsis halleri* and nonaccumulator *Arabidopsis petraea*. *Environ. Sci. Technol.* 45, 9212–9217. doi: 10.1021/es200874x

Barabasz, A., Wilkowska, A., Ruszczyñsk, A., Bulska, E., Hanikenne, M., Czarny, M., et al. (2012). Metal response of transgenic tomato plants expressing P1B-ATPase. *Physiol. Plant.* 145, 315–331. doi: 10.1111/j.1399-3054.2012.01584.x

Barnes, A., Bale, J., Constantinidou, C., Ashton, P., Jones, A., and Pritchard, J. (2004). Determining protein identity from sieve element sap in *Ricinus communis* L. by quadrupole time of flight (Q-TOF) mass spectrometry. *J. Exp. Bot.* 55, 1473–1481. doi: 10.1093/jxb/erh161

Baxter, I. R., Vitek, O., Lahner, B., Muthukumar, B., Borghi, M., Morrissey, J., et al. (2008). The leaf ionome as a multivariable system to detect a plant's physiological status. *Proc. Nat. Acad. Sci. U.S.A.* 105, 12081–12086. doi: 10.1073/pnas.0804175105

Benedicto, A., Hernández-Apaolaza, L., Rivas, I., and Lucena, J. J. (2011). Determination of ^{67}Zn distribution in navy bean (*Phaseolus vulgaris* L.) after foliar application of ^{67}Zn-lignosulfonates using isotope pattern deconvolution. *J. Agric. Food Chem.* 59, 8829–8838. doi: 10.1021/jf2002574

Bennett, J. H., Lee, E. H., Krizek, D. T., Olsen, R. A., and Brown, J. C. (1982). Photochemical reduction of iron. *II. Plant related factors. J. Plant Nutr.* 5, 335–344. doi: 10.1080/01904168209362962

Briat, J. F., Curie, C., and Gaymard, F. (2007). Iron utilization and metabolism in plants. *Curr. Opin. Plant Biol.* 10, 276–282. doi: 10.1016/j.pbi.2007.04.003

Cakmak, I., Welch, R. M., Erenoglu, B., Römheld, V., Norvell, W. A., and Kochian, L. V. (2000a). Influence of varied zinc supply on retranslocation of cadmium (^{109}Cd) and rubidium (^{86}Rb) applied on mature leaf of durum wheat seedlings. *Plant Soil* 219, 279–284. doi: 10.1023/A:1004777631452

Cakmak, I., Welch, R. M., Hart, J., Norvell, W. A., Oztürk, L., and Kochian, L. V. (2000b). Uptake and retranslocation of leaf—applied cadmium (^{109}Cd) in diploid, tetraploid and hexaploid wheats. *J. Exp. Bot.* 51, 221–226. doi: 10.1093/jexbot/51.343.221

Caldelas, C., Dong, S., Araus, J. L., and Weiss, D. J. (2011). Zinc isotopic fractionation in *Phragmites australis* in response to toxic levels of zinc. *J. Exp. Bot.* 62, 2169–2178. doi: 10.1093/jxb/erq414

Callahan, D. L., Baker, A. J. M., Kolev, S. D., and Wedd, A. G. (2006). Metal ion ligands in hyperaccumulating plants. *J. Biol. Inorg. Chem.* 11, 2–12. doi: 10.1007/s00775-005-0056-7

Callahan, D. L., Roessner, U., Dumontet, V., De Livera, A. M., Doronila, A., Baker, A. J. M., et al. (2012). Elemental and metabolite profiling of nickel hyperaccumulators from New Caledonia. *Phytochemistry* 81, 80–89. doi: 10.1016/j.phytochem.2012.06.010

Callahan, D. L., Roessner, U., Dumontet, V., Perrier, N., Wedd, A. G., O'Hair, R. A., et al. (2008). LC-MS and GC-MS metabolite profiling of nickel(II) complexes in the latex of the nickel-hyperaccumulating tree *Sebertia acuminata* and identification of methylated aldaric acid as new nickel(II) ligand. *Phytochemistry* 69, 240–251. doi: 10.1016/j.phytochem.2007.07.001

Carrasco-Gil, S., Álvarez-Fernández, A., Sobrino-Plata, J., Millán, R., Carpena-Ruiz, R. O., Leduc, D. L., et al. (2011). Complexation of Hg with phytochelatins is important for plant Hg tolerance. *Plant Cell Environ.* 34, 778–791. doi: 10.1111/j.1365-3040.2011.02281.x

Carrasco-Gil, S., Siebner, H., LeDuc, D. L., Webb, S. M., Millán, R., Andrews, J. C., et al. (2013). Mercury localization and speciation in plants grown hydroponically or in a natural environment. *Environ. Sci. Technol.* 47, 3082–3090. doi: 10.1021/es303310t

Centofanti, T., Sayers, Z., Cabello-Conejo, M. I., Kidd, P., Nishizawa, N., Kakei, Y., et al. (2013). Xylem exudate composition and root-to-shoot nickel translocation in *Alyssum* species. *Plant Soil* 373, 59–75. doi: 10.1007/s11104-013-1782-1

Chen, A., Komives, E. A., and Schroeder, J. I. (2006). An improved grafting technique for mature *Arabidopsis* plants demonstrates long-distance shoot-to-root transport of phytochelatins in *Arabidopsis*. *Plant Physiol.* 141, 108–120. doi: 10.1104/pp.105.072637

Chu, B. B., Luo, L. Q., Xu, T., Yuan, J., Sun, J. L., Zeng, Y., et al. (2012). XANES study of lead speciation in duckweed. *Spectrosc. Spect. Anal.* 32, 1975–1978. doi: 10.3964/j.issn.1000-0593(2012)07-1975-04

Clemens, S., Deinlein, U., Ahmadi, H., Höreth, S., and Uraguchi, S. (2013). Nicotianamine is a major player in plant Zn homeostasis. *Biometals* 26, 623–632. doi: 10.1007/s10534-013-9643-1

Clemens, S., Palmgren, M. G., and Krämer, U. (2002). A long way ahead: understanding and engineering plant metal accumulation. *Trends Plant Sci.* 7, 309–315. doi: 10.1016/S1360-1385(02)02295-1

Colangelo, E. P., and Guerinot, M. L. (2006). Put the metal to the petal: metal uptake and transport throughout plants. *Curr. Opin. Plant Biol.* 9, 322–330. doi: 10.1016/j.pbi.2006.03.015

Conte, S. S., and Walker, E. L. (2011). Transporters contributing to iron trafficking in plants. *Mol. Plant* 4, 464–476. doi: 10.1093/mp/ssr015

Curie, C., Cassin, G., Couch, D., Divol, F., Higuchi, K., Le Jean, M., et al. (2009). Metal movement within the plant: contribution of nicotianamine and yellow stripe 1-like transporters. *Ann. Bot.* 103, 1–11. doi: 10.1093/aob/mcn207

Deinlein, U., Weber, M., Schmidt, H., Rensch, S., Trampczynska, A., Hansen, T. H., et al. (2012). Elevated nicotianamine levels in *Arabidopsis halleri* roots play a key role in zinc hyperaccumulation. *Plant Cell* 24, 708–723. doi: 10.1105/tpc.111.095000

Dell'mour, M., Koellensperger, G., Quirino, J. P., Haddadm P. R., Stanetty, C., Oburger, E., et al. (2010). Complexation of metals by phytosiderophores revealed by CE-ESI-MS and CE-ICP-MS. *Electrophoresis* 31, 1201–1207. doi: 10.1002/elps.200900635

Deng, F., Yamaji, N., Xia, J., and Ma, J. F. (2013). A member of the heavy metal P-Type ATPase OsHMA5 is involved in xylem loading of copper in rice. *Plant Physiol.* 163, 1353–1362. doi: 10.1104/pp.113.226225

Dinant, S., and Kehr, J. (2013). Sampling and analysis of phloem sap. *Methods Mol Biol.* 953, 185–194. doi: 10.1007/978-1-62703-152-3_12

Donner, E., Punshon, T., Guerinot, M. L., and Lombi, E. (2012). Functional characterisation of metal(loid) processes in planta through the integration of synchrotron techniques and plant molecular biology. *Anal Bioanal. Chem.* 402, 3287–3298. doi: 10.1007/s00216-011-5624-9

Durrett, T. P., Gassmann, W. and Rogers, E. E. (2007). The FRD3-mediated efflux of citrate into the root vasculature is necessary for efficient iron translocation. *Plant Physiol.* 144, 197–205. doi: 10.1104/pp.107.097162

Erenoglu, B., Nikolic, M., Römheld, V., and Cakmak, I. (2002). Uptake and transport of foliar applied zinc (65Zn) in bread and durum wheat cultivars differing in zinc efficiency. *Plant Soil* 241, 251–257. doi: 10.1023/A:1016148925918

Fiehn, O. (2003). Metabolic networks of *Cucurbita maxima* phloem. *Phytochemistry* 62, 875–886. doi: 10.1016/S0031-9422(02)00715-X

Freisinger, E. (2011). Structural features specific to plant metallothioneins. *J. Biol. Inorg. Chem.* 16, 1035–1045. doi: 10.1007/s00775-011-0801-z

Führs, H., Behrens, C., Gallien, S., Heintz, D., Dorsselaer, A. V., Braun, H. P., et al. (2010). Physiological and proteomic characterization of manganese sensitivity

and tolerance in rice (*Oryza sativa*) in comparison with barley (*Hordeum vulgare*). *Ann. Bot.* 105, 1129–1140. doi: 10.1093/aob/mcq046

Fujimaki, S., Suzui, N., Ishioka, N. S., Kawachi, N., Ito, S., Chino, M., et al. (2010). Tracing cadmium from culture to spikelet: non-invasive imaging and quantitative characterization of absorption, transport, and accumulation of cadmium in an intact rice plant. *Plant Physiol.* 152, 1796–1806. doi: 10.1104/pp.109.151035

García-Hernández, M., Murphy, A. and Taiz, L. (1998). Metallothioneins 1 and 2 have distinct but overlapping expression patterns in *Arabidopsis*. *Plant Physiol.* 118, 387–397. doi: 10.1104/pp.118.2.387

Giavalisco, P., Kapitza, K., Kolasa, A., Buhtz, A., and Kehr J. (2006). Towards the proteome of *Brassica napus* phloem sap. *Proteomics* 6, 896–909. doi: 10.1002/pmic.200500155

Gogorcena, Y., Larbi, A., Andaluz, S., Carpena, R. O., Abadía, A., and Abadía, J. (2011). Effects of cadmium on cork oak (*Quercus suber* L.) plants grown in hydroponics. *Tree Physiol.* 31, 1401–1412. doi: 10.1093/treephys/tpr114

Gong, J. M., Lee, D. A., and Schroeder, J. I. (2003). Long distance root-to-shoot transport of phytochelatins and cadmium in *Arabidopsis*. *Proc. Natl. Acad. Sci. U.S.A.* 100, 10118–10123. doi: 10.1073/pnas.1734072100

Grillet, L., Ouerdane, L., Flis, P., Hoang, M. T. T., Isaure, M. P., Lobiński, R., et al. (2014). Ascorbate efflux as a new strategy for iron reduction and transport in plants. *J. Biol. Chem.* 289, 2515–2525. doi: 10.1074/jbc.M113.514828

Grusak, M. A. (1994). Iron transport to developing ovules of *Pisum sativum*. I. Seed import characteristics and phloem iron-loading capacity of source regions. *Plant Physiol.* 104, 649–655.

Guelke-Stelling, M., and von Blanckenburg, F. (2007). Fractionation of stable iron isotopes in higher plants. *Environ. Sci. Technol.* 41, 1896–1901. doi: 10.1021/es062288j

Guelke-Stelling, M., and von Blanckenburg, F. (2012). Fe isotope fractionation caused by translocation of iron during growth of bean and oat as models of strategy I and II plants. *Plant Soil* 352, 217–231. doi: 10.1007/s11104-011-0990-9

Han, D. G., Wang, L., Wang, Y., Yang, G. H., Gao, C., Yu, Z. Y., et al. (2013). Overexpression of Malus xiaojinensis CS1 gene in tobacco affects plant development and increases iron stress tolerance. *Sci. Hortic.* 150, 65–72. doi: 10.1016/j.scienta.2012.10.004

Han, D. G., Wang, Y., Zhang, L., Ma, L., Zhang, X. Z., Xu, X. F., et al. (2012). Isolation and functional characterization of *MxCS1*: a gene encoding a citrate synthase in *Malus xiaojinensis*. *Biol. Plantarum* 56, 50–56. doi: 10.1007/s10535-012-0015-4

Harris, N. S., and Taylor, G. J. (2001). Remobilization of cadmium in maturing shoots of near isogenic lines of durum wheat that differ in grain cadmium accumulation. *J. Exp. Bot.* 52, 1473–1481. doi: 10.1093/jexbot/52.360.1473

Harris, W. R., Sammons, D. R., and Grabiak, R. C. (2012). A speciation model of essential trace elements in phloem. *J. Inorg. Biochem.* 116, 140–150. doi: 10.1016/j.jinorgbio.2012.07.011

Haydon, M. J., and Cobbett, C. S. (2007). Transporters of ligands for essential metal ions in plants. *New Phytol.* 174, 499–506. doi: 10.1111/j.1469-8137.2007.02051.x

Haydon, M. J., Kawachi, M., Wirtz, M., Hillmer, S., Hell, R., and Krämer, U. (2012). Vacuolar nicotianamine has critical and distinct roles under iron deficiency and for zinc sequestration in *Arabidopsis*. *Plant Cell* 24, 724–737. doi: 10.1105/tpc.111.095042

Heise, J., Krejci, S., Miersch, J., Krauss, G. J., and Humbeck, K. (2007). Gene expression of metallothioneins in barley during senescence and heavy metal treatment. *Crop Sci.* 47, 1111–1118. doi: 10.2135/cropsci2006.03.0183

Hocking, P. J. (1980). The composition of phloem exudate and xylem sap from tree tobacco (*Nicotiana glauca* Grah.). *Ann. Bot.* 45, 633–643.

Hocking, P. J. (1983). The dynamics of growth and nutrient accumulation by fruits of *Grevillea leucopteris* Meissn., a proteaceous shrub, with special reference to the composition of xylem and phloem sap. *New Phytol.* 93, 511–529. doi: 10.1111/j.1469-8137.1983.tb02702.x

Huguet, S., Bert, V., Laboudigue, A., Barthes, V., Isaure, M. P., Llorens, I., et al. (2012). Cd speciation and localization in the hyperaccumulator *Arabidopsis halleri*. *Environ. Exp. Bot.* 82, 54–65. doi: 10.1016/j.envexpbot.2012.03.011

Husted, S., Persson, D. P., Laursen, K. H., Hansen, T. H., Pedas, P., Schiller, M., et al. (2011). Review: the role of atomic spectrometry in plant science. *J. Anal. At. Spectrom.* 26, 52–79. doi: 10.1039/c0ja00058b

Ingle, R. A., Mugford, S. T., Rees, J. D., Campbell, M. M., and Smith, J. C. (2005). Constitutively high expression of the histidine biosynthetic pathway contributes to nickel tolerance in hyperaccumulator plants. *Plant Cell* 17, 2089–2106. doi: 10.1105/tpc.104.030577

Irtelli, B., Petrucci, W. A., and Navari-Izzo, F. (2009). Nicotianamine and histidine/proline are, respectively, the most important copper chelators in xylem sap of *Brassica carinata* under conditions of copper deficiency and excess. *J. Exp. Bot.* 60, 269–277. doi: 10.1093/jxb/ern286

Ishikawa, S., Suzui, N., Ito-Tanabata, S., Ishii, S., Igura, M., Abe, T., et al. (2011). Real-time imaging and analysis of differences in cadmium dynamics in rice cultivars (*Oryza sativa*) using positron-emitting ^{107}Cd tracer. *BMC Plant Biol.* 11:172. doi: 10.1186/1471-2229-11-172

Ishimaru, Y., Kakei, Y., Shimo, H., Bashir, K., Sato, Y., Sato, Y., et al. (2011). A rice phenolic efflux transporter is essential for solubilizing precipitated apoplasmic iron in the plant stele. *J. Biol. Chem.* 286, 24649–24655. doi: 10.1074/jbc.M111.221168

Jelali, N., Wissal, M. S., Dell'orto, M., Abdelly, C., Gharsalli, M., and Zocchi, G. (2010). Changes of metabolic responses to direct and induced Fe deficiency of two *Pisum sativum* cultivars. *Environ. Exp. Bot.* 68, 238–246. doi: 10.1016/j.envexpbot.2009.12.003

Kakei, Y., Yamaguchi, I., Kobayashi, T., Takahashi, T., Nakanishi, H., Yamakawa, T., et al. (2009). A highly sensitive, quick and simple quantification method for nicotianamine and 2′-deoxymugineic acid from minimum samples using LC/ESI-TOF-MS achieves functional analysis of these components in plants. *Plant. Cell Physiol.* 50, 1988–1993. doi: 10.1093/pcp/pcp141

Kato, M., Ishikawa, S. Inagaki, K., Chiba, K., Hayashi, H., Yanagisa, S., and Yoneyama, T. (2010). Possible chemical forms of cadmium and varietal differences in cadmium concentrations in the phloem sap of rice plants (*Oryza sativa* L.). *Soil Sci. Plant Nutr.* 56, 839–847. doi: 10.1111/j.1747-0765.2010.00514.x

Kawai, S., Kamei, S., Matsuda, Y., Ando, R., Kondo, S., Ishizawa, A., et al. (2001). Concentrations of iron and phytosiderophores in xylem sap of iron-deficient barley plants. *Soil Sci. Plant Nutr.* 47, 265–272. doi: 10.1080/00380768.2001.10408390

Kerkeb, L., and Krämer, U. (2003). The role of free histidine in xylem loading of nickel in *Alyssum lesbiacum* and *Brassica juncea*. *Plant Physiol.* 131, 716–724. doi: 10.1104/pp102.010686

Khouzam, R. B., Szpunar, J., Holeman, M., and Lobiński, R. (2012). Trace element speciation in food: state of the art of analytical techniques and methods. *Pure Appl. Chem.* 84, 169–179. doi: 10.1351/PAC-CON-11-08-14

Kiczka, M., Wiederhold, J. G., Kraemer, S. M., Bourdon, B., and Kretzschmar, R. (2010). Iron isotope fractionation during Fe uptake and translocation in alpine plants. *Environ. Sci. Technol.* 44, 6144–6150. doi: 10.1021/es100863b

Kim, S. A., and Guerinot M. L. (2007). Mining iron: iron uptake and transport in plants. *FEBS Lett.* 581, 2273–2280. doi: 10.1016/j.febslet.2007.04.043

Klatte, M., Schuler, M., Wirtz, M., Fink-Straube, C., Hell, R., and Bauer, P. (2009). The analysis of Arabidopsis nicotianamine synthase mutants reveals functions for nicotianamine in seed iron loading and iron deficiency responses. *Plant Physiol.* 150, 251–271. doi: 10.1104/pp.109.136374

Kobayashi, N. I., Tanoi, K., Hirose, A., and Nakanishi, T. M. (2013). Characterization of rapid intervascular transport of cadmium in rice stem by radioisotope imaging. *J. Exp. Bot.* 64, 507–517. doi: 10.1093/jxb/ers344

Köster, J., Hayen, H., von Wirén, N., and Weber, G. (2011b). Isoelectric focusing of small non-covalent metal species from plants. *Electrophoresis* 32, 772–781. doi: 10.1002/elps.201000529

Köster, J., Shi, R., von Wirén, N., and Weber, G. (2011a). Evaluation of different column types for the hydrophilic interaction chromatographic separation of iron-citrate and copper-histidine species from plants. *J. Chromatogr. A* 1218, 4934–4943. doi: 10.1016/j.chroma.2011.03.036

Krämer, U. (2010). Metal hyperaccumulation in plants. *Annu. Rev. Plant. Biol.* 61, 517–534. doi: 10.1146/annurev-arplant-042809-112156

Krämer, U., Cotter-Howells, J. D., Charnock, J. M., Baker, A. J. M., and Smith, J. A. C. (1996). Free histidine as a metal chelator in plants that accumulate nickel. *Nature* 379, 635–638. doi: 10.1038/379635a0

Krämer, U., Talke, I. N., and Hanikenne, M. (2007). Transition metal transport. *FEBS Lett.* 581, 2263–2272. doi: 10.1016/j.febslet.2007.04.010

Krüger, C., Berkowitz, O., Stephan, U., and Hell, R. (2002). A metal-binding member of the late embryogenesis abundant protein family transports iron in the phloem of *Ricinus communis* L. *J. Biol. Chem.* 277, 25062–25069. doi: 10.1074/jbc.M201896200

Küpper, H., Goetz, B., Mijovilovich, A., Kupper, F. C., and Meyer-Klaucke, W. (2009). Complexation and toxicity of copper in higher plants. I.

Characterization of copper accumulation, speciation, and toxicity in *Crassula helmsii* as a new copper accumulator. *Plant Physiol.* 151, 702–714. doi: 10.1104/pp.109.139717

Küpper, H., Mijovilovich, A., Meyer-Klaucke, W., and Kroneck, P. M. (2004). Tissue- and age-dependent differences in the complexation of cadmium and zinc in the cadmium/zinc hyperaccumulator *Thlaspi caerulescens* (Ganges ecotype) revealed by x-ray absorption spectroscopy. *Plant Physiol.* 134, 748–757. doi: 10.1104/pp.103.032953

Larbi, A., Morales, F., Abadía, A., and Abadía, J. (2010). Changes in iron and organic acid concentrations in xylem sap and apoplastic fluid of iron-deficient *Beta vulgaris* plants in response to iron resupply. *J. Plant Physiol.* 167, 255–260. doi: 10.1016/j.jplph.2009.09.007

Larbi, A., Morales, F., Abadía, J., and Abadía, A. (2003). Effects of branch solid Fe sulphate implants on xylem sap composition in field-grown peach and pear: changes in Fe, organic anions and pH. *J. Plant Physiol.* 160, 1473–1481. doi: 10.1078/0176-1617-01010

Lasat, M. M., Baker, A. L. J. M., and Kochian, L. V. (1998). Altered Zn compartmentation in the root symplasm and stimulated Zn absorption into the leaf as mechanisms involved in Zn hyperaccumulation in *Thlaspi caerulescens*. *Plant Physiol.* 118, 875–883. doi: 10.1104/pp.118.3.875

Lattanzio, G., Andaluz, S., Andrea Matros, A., Calvete, J. J., Kehr, J., Abadía, A., et al. (2013). Protein profile of *Lupinus texensis* phloem sap exudates: searching for Fe and Zn containing proteins. *Proteomics* 13, 2283–2296. doi: 10.1002/pmic.201200515

Leitenmaier, B., and Küpper H. (2011). Cadmium uptake and sequestration kinetics in individual leaf cell protoplasts of the Cd/Zn hyperaccumulator *Thlaspi caerulescens*. *Plant Cell Environ.* 34, 208–219. doi: 10.1111/j.1365-3040.2010.02236.x

Leitenmaier, B., and Küpper, H. (2013). Compartmentation and complexation of metals in hyperaccumulator plants. *Front. Plant Sci.* 4:374. doi: 10.3389/fpls.2013.00374

Li, Y., Dankher, O. P., Carreira, L., Smith, A. P., and Meagher, R. B. (2006). The shoot-specific expression of γ-glutamylcysteine synthetase directs the long-distance transport of thiol-peptides to roots conferring tolerance to mercury and arsenic. *Plant Physiol.*141, 288–298. doi: 10.1104/pp.105.074815

Liao, M. T., Hedley, M. J., Woolley, D. J., Brooks, R. R., and Nichols, M. A. (2000). Copper uptake and translocation in chicory (*Cichorium intybus* L. cv. Grasslands Puna) and tomato (*Lycopersicon esculentum* Mill. cv. Rondy) plants grown in NFT system. I. Copper uptake and distribution in plants. *Plant Soil* 221, 135–142. doi: 10.1023/A:1004731415931

Lohaus, G., Pennewis, K., Sattelmacher, B., Hussman, M., and Muehling, K. H. (2001). Is the infiltration-centrifugation technique appropriate for the isolation of apoplastic fluid? *A critical evaluation with different plant species. Physiol. Plant.* 111, 457–465. doi: 10.1034/j.1399–3054.2001.1110405.x

Lombi, E., Scheckel, K. G., and Kempson, I. M. (2011). *In situ* analysis of metal(loid)s in plants: state of the art and artefacts. *Environ. Exp. Botany*. 72, 3–17. doi: 10.1016/j.envexpbot.2010.04.005

López-Millán, A. F., Grusak, M. A., and Abadía, J. (2012). Carboxylate metabolism changes induced by Fe deficiency in barley, a Strategy II plant species. *J. Plant Physiol.* 169, 1121–1124. doi: 10.1016/j.jplph.2012.04.010

López-Millán, A. F., Morales, F., Abadía, A., and Abadía, J. (2000). Effects of iron deficiency on the composition of the leaf apoplastic fluid and xylem sap in sugar beet. Implications for iron and carbon transport. *Plant Physiol.* 124, 873–884. doi: 10.1104/pp.124.2.873

López-Millán, A. F., Morales, F., Abadía, A., and Abadía, J. (2001). Iron deficiency-associated changes in the composition of the leaf apoplast fluid from field-grown pear (*Pyrus communis* L.) trees. *J. Exp. Bot.* 52, 1489–1498. doi: 10.1093/jexbot/52.360.1489

López-Millán, A. F., Morales, F., Gogorcena, Y., Abadía, A., and Abadía, J. (2009). Organic acid metabolism in iron deficient tomato plants. *J. Plant Physiol.* 166, 375–384. doi: 10.1016/j.jplph.2008.06.011

Lu, L., Tian, S., Zhang, J., Yang, X., Labavitch, J. M., Webb, S. M., et al. (2013). Efficient xylem transport and phloem remobilization of Zn in the hyperaccumulator plant species *Sedum alfredii*. *New Phytol.* 198, 721–731. doi: 10.1111/nph.12168

Ma, J. F., and Hiradate, S. (2000). Form of aluminium for uptake and translocation in buckwheat (*Fagopyrum esculentum* Moench). *Planta* 211, 355–360. doi: 10.1007/s004250000292

Marentes, E., and Grusak, M. A. (1998). Iron transport and storage within the seed coat of developing embryos of pea (*Pisum sativum* L). *Seed Sci. Res.* 8, 367–375. doi: 10.1017/S0960258500004293

Mari, S., Gendre, D., Pianelli, K., Ouerdane, L., Lobinski, R., Briat, J. F., et al. (2006). Root-to-shoot long-distance circulation of nicotianamine and nicotianamine-nickel chelates in the metal hyperaccumulator *Thlaspi caerulescens*. *J. Exp. Bot.* 57, 4111–4122. doi: 10.1093/jxb/erl184

Martínez-Cuenca, M. R., Iglesias, D. J., Talón, M., Abadía, J., López-Millán, A. F., Primo-Millo, E., et al. (2013). Metabolic responses to iron deficiency in roots of Carrizo citrange (*Citrus sinensis* (L.) Osb. x *Poncirus trifoliata* (L) Raf.). *Tree Physiol.* 33, 320–329. doi: 10.1093/treephys/tpt011

McNear, D. H., Afton, S. E., and Caruso, J. A. (2012). Exploring the structural basis for selenium/mercury antagonism in *Allium fistulosum*. *Metallomics* 4, 267–276. doi: 10.1039/c2mt00158f

McNear, D. H., Chaney, R. L., and Sparks, D. L. (2010). The metal hyperaccumulator *Alyssum murale* uses nitrogen and oxygen donor ligands for Ni transport and storage. *Phytochemistry* 71, 188–200. doi: 10.1016/j.phytochem.2009.10.023

Meija, J., Montes-Bayón, M., Caruso, J. A., and Sanz-Medel, A. (2006). Integrated mass spectrometry in (semi) metal speciation and its potential in phytochemistry. *Trends Anal. Chem.* 25, 44–51. doi: 10.1016/j.trac.2005.04.003

Mendoza-Cózatl, D. G., Butko, E., Springer, F., Torpey, J. W., Komives, E. A., Kehr, J., et al. (2008). Identification of high levels of phytochelatins, glutathione and cadmium in the phloem sap of *Brassica napus*. A role for thiol-peptides in the long-distance transport of cadmium and the effect of cadmium on iron translocation. *Plant J.* 54, 249–259. doi: 10.1111/j.1365-313X.2008.03410.x

Mendoza-Cózatl, D. G., Jobe, T. O., Hauser, F., and Schroeder, J. I. (2011). Long-distance transport, vacuolar sequestration, tolerance, and transcriptional responses induced by cadmium and arsenic. *Curr. Opin. Plant Biol.* 14, 554–562. doi: 10.1016/j.pbi.2011.07.004

Mesko, M. F., Hartwig, C. A., Bizzi, C. A., Pereira, J. S. F., Mello, P. A., and Flores, E. M. M. (2011). Sample preparation strategies for bioinorganic analysis by inductively coupled plasma mass spectrometry. *Int. J. Mass Spectrom.* 307, 123–136. doi: 10.1016/j.ijms.2011.03.002

Meyer, S., Angeli, A. D., Fernie, A. R., and Martinoia, E. (2010). Intra- and extra-cellular excretion of carboxylates. *Trends Plant Sci.* 15, 40–47. doi: 10.1016/j.tplants.2009.10.002

Mijovilovich, A., Leitenmaier, B., Mayer-Klaucke, W., Kroneck, P. M. H., Götz, B., and Küpper, H. (2009). Complexation and toxicity of copper in higher plants II. Different mechanisms for copper vs. cadmium detoxification in the copper-sensitive cadmium/zinc hyperaccumulator *Thlaspi caerulescens* (Ganges ecotype). *Plant Physiol.* 151, 715–731. doi: 10.1104/pp.109.144675

Milner, M. J., and Kochian, L. V. (2008). Investigating heavy-metal hyperaccumulation using *Thlaspi caerulescens* as a model system. *Ann. Bot.* 102, 3–13. doi: 10.1093/aob/mcn063

Monicou, S., Szpunar, J., and Lobinski, R. (2009). Metallomics: the concept and methodology. *Chem. Soc. Rev.* 38, 1119–1138. doi: 10.1039/b713633c

Monsant, A. C., Kappen, P., Wang, Y., Pigram, P. J., Baker, A. J. M., and Tang, C. (2011). *In vivo* speciation of zinc in *Noccaea caerulescens* in response to nitrogen form and zinc exposure. *Plant Soil.* 348, 167–183. doi: 10.1007/s11104-011-0887-7

Mori, S., Uraguchi, S., Ishikawa, S., and Arao, T. (2009). Xylem loading process is a critical factor in determining Cd accumulation in the shoots of *Solanum melongena* and *Solanum torvum*. *Environ. Exp. Bot.* 67, 127–132. doi: 10.1016/j.envexpbot.2009.05.006

Morita, A., Horie, H., Fujii, Y., Takatsu, S., Watanabe, N., Yagi, A., et al. (2004). Chemical forms of aluminum in xylem sap of tea plants (*Camellia sinensis* L.). *Phytochemistry* 65, 2775–2780. doi: 10.1016/j.phytochem.2004.08.043

Morrissey, J., and Guerinot, M. L. (2009). Iron uptake and transport in plants: the good, the bad and the ionome. *Chem. Rev.* 109, 4553–4567. doi: 10.1021/cr900112r

Moynier, F., Fujii, T.,Wang, K., and Foriel, J. (2013). Ab initio calculations of the Fe(II) and Fe(III) isotopic effects in citrates, nicotianamine, and phytosiderophore, and new Fe isotopic measurements in higher plants. *Comp. Rend. Geosci.* 345, 230–240. doi: 10.1016/j.crte.2013.05.003

Moynier, F., Pichat, S., Pons, M. L., Fike, D., Balter, V., and Albarède, F. (2009). Isotopic fractionation and transport mechanisms of Zn in plants. *Chem. Geol.* 267, 125–130. doi: 10.1016/j.chemgeo.2008.09.017

Mullins, G. L., Sommers, L. E., and Housley, T. L. (1986). Metal speciation in xylem and phloem exudates. *Plant Soil* 96, 377–391. doi: 10.1007/BF02375142

Murakami, T., Ise, K., Hayakawa, M., Kamei, S., and Takagi, S. (1989). Stabilities of metal complexes of mugineic acid and their specific affinities for iron(III). *Chem Lett. (Jpn.)* 18, 2137–2140. doi: 10.1246/cl.1989.2137

Nakamura, S., Akiyama, C., Sasaki, T., Hattori, H., and Chino, M. (2008). Effect of cadmium on the chemical composition of xylem exudates from oilseed rape plants (*Brassica napus* L.). *Soil Sci. Plant Nutr.* 54, 118–127. doi: 10.1111/j.1747-0765.2007.00214.x

Nishiyama, R., Kato, M., Nagata, S., Yanagisawa, S., and Yoneyama, T. (2012). Identification of Zn–nicotianamine and Fe–2′-deoxymugineic acid in the phloem sap from rice plants (*Oryza sativa* L.). *Plant Cell Physiol.* 53, 381–390. doi: 10.1093/pcp/pcr188

Orera, I., Rodríguez-Castrillón, J. A., Moldovan, M., García-Alonso, J. I., Abadía, A., Abadía, J., et al. (2010). Using a dual-stable isotope tracer method to study the uptake, xylem transport and distribution of Fe and its chelating agent from stereoisomers of an Fe(III)-chelate used as fertilizer in Fe-deficient Strategy I plants. *Metallomics* 2, 646–657. doi: 10.1039/c0mt00018c

Ouerdane, L., Mari, S., Czernic, P., Lebrun, M., and Lobiński, R. (2006). Speciation of non-covalent nickel species in plant tissue extracts by electrospray Q-TOFMS/MS after their isolation by 2D size exclusion-hydrophilic interaction LC (SEC-HILIC) monitored by ICP-MS. *J. Anal. At. Spectrom.* 21, 676–683. doi: 10.1039/b602689c

Pal, R., and Rai, J. P. N. (2010). Phytochelatins: peptides involved in heavy metal detoxification. *Appl. Biochem. Biotechnol.* 160, 945–963. doi: 10.1007/s12010-009-8565-4

Palmer, C. M., and Guerinot, M. L. (2009). Facing the challenges of Cu, Fe and Zn homeostasis in plants. *Nat. Chem. Biol.* 5, 333–340. doi: 10.1038/nchembio.166

Palmer, L. J., Palmer, L. T., Pritchard, J., Graham, R. D., and Stangoulis, J. C. R. (2013). Improved techniques for measurement of nanolitre volumes of phloem exudate from aphid stylectomy. *Plant Methods* 9, 18. doi: 10.1186/1746-4811-9-18

Persans, M. W., Yan, X., Patnoe, J. M. L., Krämer, U., and Salt, D. E. (1999). Molecular dissection of the role of histidine in nickel hyperaccumulation in *Thlaspi goesingense* (Haìlaìcsy). *Plant Physiol.* 121, 1117–1126. doi: 10.1104/pp.121.4.1117

Pich, A., and Scholz, G. (1996). Translocation of copper and other micronutrients in tomato plants (*Lycopersicon esculentum* Mill.): nicotianamine-stimulated copper transport in the xylem. *J. Exp. Bot.* 47, 41–47. doi: 10.1093/jxb/47.1.41

Pich, A., Scholz, G., and Stephan, U. (1994). Iron-dependent changes of heavy-metals, nicotianamine, and citrate in different plant organs and in the xylem exudate of two tomato genotypes- nicotianamine as a possible copper translocator. *Plant Soil* 165, 189–196. doi: 10.1007/BF00008061

Pittman, J. K. (2005). Managing the manganese: molecular mechanisms of manganese transport and homeostasis. *New Phytol.* 167, 733–742. doi: 10.1111/j.1469-8137.2005.01453.x

Puig, S., and Peñarrubia, L. (2009). Placing metal micronutrients in context: transport and distribution in plants. *Curr. Opin. Plant Biol.* 12, 299–306. doi: 10.1016/j.pbi.2009.04.008

Rellán-Álvarez, R., Abadía, J., and Álvarez-Fernández, A. (2008). Formation of metal-nicotianamine complexes as affected by pH, ligand exchange with citrate and metal exchange. A study by electrospray ionization time-of-flight mass spectrometry. *Rapid Commun. Mass Sp.*. 22, 1553–1562. doi: 10.1002/rcm.3523

Rellán-Álvarez, R., El-Jendoubi, H., Wohlgemuth, G., Abadía, A., Fiehn, O., Abadía, A., et al. (2011a). Metabolite profile changes in xylem sap and leaf extracts of strategy I plants in response to iron deficiency and resupply. *Front. Plant Sci.* 2:66. doi: 10.3389/fpls.2011.00066

Rellán-Álvarez, R., Giner-Martínez-Sierra, J., Orduna, J., Orera, I., Rodríguez-Castrillón, J. A., García-Alonso, J. I., et al. (2010). Identification of a tri-iron(III), tri-citrate complex in the xylem sap of iron-deficient tomato resupplied with iron: new insights into plant iron long-distance transport. *Plant Cell Physiol.* 51, 91–102. doi: 10.1093/pcp/pcp170

Rellán-Álvarez, R., López-Gomollón, S., Abadía, J., and Álvarez-Fernández, A. (2011b). Development of a new high-performance liquid chromatography-electrospray ionization Time-of-Flight mass spectrometry method for the determination of low molecular mass organic acids in plant tissue extracts. *J. Agric. Food Chem.* 59, 6864–6870. doi: 10.1021/jf200482a

Rodríguez-Castrillón, J. A., Moldovan, M., García-Alonso, J. I., Lucena, J. J., García-Tome, M. L., and Hernández-Apaolaza, L. (2008). Isotope pattern deconvolution as a tool to study iron metabolism in plants. *Anal. Bioanal. Chem.* 390, 579–590. doi: 10.1007/s00216-007-1716-y

Rodríguez-Medina, C., Atkins, C. A., Mann, A. J., Jordan, M. E., and Smith, P. M. C. (2011). Macromolecular composition of phloem exudate from white lupin (*Lupinus albus* L.). *BMC Plant Biol.* 11:36. doi: 10.1186/1471-2229-11-36

Rojas, C. L., Romera, F. J., Alcántara, E., Pérez-Vicente, R., Sariego, C., García-Alonso, J. I., et al. (2008). Efficacy of Fe(*o*,*o*-EDDHA) and Fe(*o*,*p*-EDDHA) isomers in supplying Fe to Strategy I plants differs in nutrient solution and calcareous soil. *J. Agric. Food Chem.* 56, 10774–10778. doi: 10.1021/jf80 22589

Rombolà, A. D., Brüggemann, W., López-Millán, A. F., Tagliavini, M., Abadía, J., Marangoni, B., et al. (2002). Biochemical responses to iron deficiency in kiwifruit (*Actinidia deliciosa*). *Tree Physiol.* 22, 869–875. doi: 10.1093/treephys/22.12.869

Roschzttardtz, H., Séguéla-Arnaud, M., Briat, J. F., Vert, G., and Curie, C. (2011). The FRD3 citrate effluxer promotes iron nutrition between symplastically disconnected tissues throughout Arabidopsis development. *Plant Cell* 23, 2725–2737. doi: 10.1105/tpc.111.088088

Ryan, B. M., Kirby, J. K., Degryse, F., Harris, H., McLaughlin, M. J., and Scheiderich, K. (2013). Copper speciation and isotopic fractionation in plants: uptake and translocation mechanisms. *New Phytol.* 199, 367–378. doi: 10.1111/nph.12276

Sagardoy, R. (2012). "Effects of Zn and Cd toxicity on metal concentrations in the xylem sap of *B. vulgaris* and *S. esculentum*," in *Study of Zn and Cd Homeostasis in Higher Plants*. Ph.D. Thesis, Zaragoza: University of Zaragoza.

Sagardoy, R., Morales, F., Rellán-Álvarez, R., Abadía, J., Abadía, A., and López-Millán, A. F. (2011). Carboxylate metabolism in sugar beet plants grown with excess Zn. *J. Plant Physiol.* 168, 730–733. doi: 10.1016/j.jplph.2010.10.012

Salt, D. E., Prince, R. C., Baker, A. J. M., Raskin, I., and Pickering, I. J. (1999). Zinc ligands in the metal hyperaccumulator *Thlaspi caerulescens* as determined using X-ray absorption spectroscopy. *Environ. Sci. Technol.* 33, 713–717. doi: 10.1021/es980825x

Salt, D. E., Prince, R. C., Pickering, I. J., and Raskin, I. (1995). Mechanisms of cadmium mobility and accumulation in indian mustard. *Plant Physiol.* 109, 1427–1433.

Sarret, G., Pilon Smits, E. A. H., Castillo Michel, H., Isaure, M. P., Zhao, F. J., and Tappero, R. (2013). Use of synchrotron-based techniques to elucidate metal uptake and metabolism in plants. *Adv. Agron.* 119, 1–82. doi: 10.1016/B978-0-12-407247-3.00001-9

Sasaki, A., Yamaji, N., Xia, J., and Ma, J. F. (2011). OsYSL6 Is involved in the detoxification of excess manganese in rice. *Plant Physiol.* 157, 1832–1840. doi: 10.1104/pp.111.186031

Sattelmacher, B. (2001). The apoplast and its significance for plant mineral nutrition. *New Phytol.* 149, 167–192. doi: 10.1046/j.1469-8137.2001.00034.x

Schaumlöffel, D., Ouerdane, L., Bouyssiere, B., and £obin, R. (2003). Speciation analysis of nickel in the latex of a hyperaccumulating tree *Sebertia acuminate* by HPLC and CZE with ICP MS and electrospray MS-MS detection. *J. Anal. At. Spectrom.* 18, 120–127. doi: 10.1039/b209819a

Schmidke, I., Krüger, C., Frömmichen, R., Scholz, G., and Stephan, U. W. (1999). Phloem loading and transport characteristics of iron in interaction with plant-endogenous ligands in castor bean seedlings. *Physiol. Plant.* 106, 82–89. doi: 10.1034/j.1399-3054.1999.106112.x

Schmidke, I., and Stephan, U. W. (1995). Transport of metal micronutrients in the phloem of castor bean (*Ricinus communis*) seedlings. *Physiol. Plant.* 95, 147–153. doi: 10.1111/j.1399-3054.1995.tb00821.x

Schmidt, H., Böttcher, C., Trampczynska, A., and Schuler, S. C. (2011). Use of recombinantly produced $^{15}N_3$-labelled nicotianamine for fast and sensitive stable isotope dilution ultra-performance liquid chromatography/electrospray ionization time-of-flight mass spectrometry. *Anal. Bioanal. Chem.* 399, 1355–1361. doi: 10.1007/s00216-010-4436-7

Schuler, M., Rellán-Álvarez, R., Fink-Straube, C., Abadía, J., and Bauer, P. (2012). Nicotianamine functions in the phloem-based transport of iron to sink organs, in pollen development and in pollen tube growth in *Arabidopsis*. *Plant Cell* 24, 2380–2400. doi: 10.1105/tpc.112.099077

Shelp, B. J. (1987). The composition of phloem exudate and xylem sap from Broccoli (*Brassica oleracea* var. italica) supplied with NH^{4+}, NO_3^- or NH_4NO_3. *J. Exp. Bot.* 38, 1619–1636. doi: 10.1093/jxb/38.10.1619

Silva, A. M., Kong, X., Parkin, M. C., Cammack, R., and Hider, R. C. (2009). Iron(III) citrate speciation in aqueous solution. *Dalton Trans.* 40, 8616–8625. doi: 10.1039/b910970f

Sinclair, S. A., and Krämer, U. (2012). The zinc homeostasis network of land plants. *Biochim. Biophys. Acta* 1823, 1553–1567. doi: 10.1016/j.bbamcr.2012.05.016

Singh, U. M., Sareen, P., Sengar, R. S., and Kumar, A. (2013). Plant ionomics: a newer approach to study mineral transport and its regulation. *Acta Physiol. Plant.* 35, 2641–2653. doi: 10.1007/s11738-013-1316-8

Song, J., Yang, Y. Q., Zhu, S. H., Chen, G. C., Yuan, X. F., Liu, T. T., et al. (2013). Spatial distribution and speciation of copper in root tips of cucumber revealed by μ-XRF and μ-XANES. *Biol. Plant.* 57, 581–586. doi: 10.1007/s10535-013-0317-1

Sperotto, R. A., Ricachenevsky, F. K., Waldow Vde A., and Fett, J. P. (2012). Iron biofortification in rice: it's a long way to the top. *Plant. Sci.* 190, 24–39. doi: 10.1016/j.plantsci.2012.03.004

Suzuki, M., Takahashi, M., Tsukamoto, T., Watanabe, S., Matsuhashi, S., Yazaki, J., et al. (2006). Biosynthesis and secretion of mugineic acid family phytosiderophores in zinc-deficient barley. *Plant J.* 48, 85–97. doi: 10.1111/j.1365-313X.2006.02853.x

Suzuki, M., Tsukamoto, T., Inoue, H., Watanabe, S., Matsuhashi, S., Takahashi, M., et al. (2008). Deoxymugineic acid increases Zn translocation in Zn-deficient rice plants. *Plant Mol. Biol.* 66, 609–617. doi: 10.1007/s11103-008-9292-x

Takahashi, M., Terada, Y., Nakai, I., Nakanishi, H., Yoshimura, E., Mori, S., et al. (2003). Role of nicotianamine in the intracellular delivery of metals and plant reproductive development. *Plant Cell* 15, 1263–1280. doi: 10.1105/tpc.010256

Tanaka, K., Fujimaki, S., Fujiwara, T., Yoneyama, T., and Hayashi, H. (2007). Quantitative estimation of the contribution of the phloem in cadmium transport to grains in rice plants (*Oryza sativa* L.). *Soil Sci. Plant Nutr.* 53, 72–77. doi: 10.1111/j.1747-0765.2007.00116.x

Tehseen, M., Cairns, N., Sherson, S., and Cobbett, C. S. (2010). Metallochaperone-like genes in *Arabidopsis thaliana*. *Metallomics* 2, 556–564. doi: 10.1039/c003484c

Terzano, R., Mimmo, T., Vekemans, B., Vincze, L., Falkenberg, G., Tomasi, N., et al. (2013). Iron (Fe) speciation in xylem sap by XANES at a high brilliant synchrotron X-ray source: opportunities and limitations. *Anal. Bioanal. Chem.* 405, 5411–5419. doi: 10.1007/s00216-013-6959-1

Thimm, O., Essigmann, B., Kloska, S., Altmann, T., and Buckhout, T. J. (2001). Response of *Arabidopsis* to iron deficiency stress as revealed by microarray analysis. *Plant Physiol.* 127, 1030–1043. doi: 10.1104/pp.010191

Thomine, S., and Vert, G. (2013). Iron transport in plants: better be safe than sorry. *Curr. Opin. Plant Biol.* 16, 322–327. doi: 10.1016/j.pbi.2013.01.003

Tian, S., Lu, L., Yang, X., Webb, S. M., Du, Y., and Brown, P. A. (2010). Spatial imaging and speciation of lead in the accumulator plant *Sedum alfredii* by microscopically focused synchrotron x-ray investigation. *Environ. Sci. Technol.* 44, 5920–5926. doi: 10.1021/es903921t

Tiffin, L. O. (1966). Iron translocation. I. Plant culture exudate sampling iron-citrate analysis. *Plant Physiol.* 41, 510–514. doi: 10.1104/pp.41.3.510

Trampczynska, A., Küpper, H., Meyer-Klaucke, W., Schmidt, H., and Clemens, S. (2010). Nicotianamine forms complexes with Zn(II) *in vivo*. *Metallomics* 2, 57–66. doi: 10.1039/b913299f

Tsednee, M., Mak, Y. W., Chen, Y. R., and Yeh, K. C. (2012). Sensitive LC-ESI-Q-TOF-MS method reveals novel phytosiderophores and phytosiderophore–iron complexes in barley. *New Phytol.* 195, 951–961. doi: 10.1111/j.1469-8137.2012.04206.x

Tsukamoto, T., Nakanishi, H., Kiyomiya, S., Watanabe, S., Matsuhashi, S., Nishizawa, N. K., et al. (2006). ^{52}Mn translocation in barley monitored using a positron-emitting tracer imaging system. *Soil Sci. Plant Nutr.* 52, 717–725. doi: 10.1111/j.1747-0765.2006.00096.x

Tsukamoto, T., Nakanishi, H., Uchida, H., Watanabe, S., Matsuhashi, S., Mori, S., et al. (2009). ^{52}Fe translocation in barley as monitored by a positron- emitting tracer imaging system (PETIS): evidence for the direct translocation of Fe from roots to young leaves via phloem. *Plant Cell Physiol.* 50, 48–57. doi: 10.1093/pcp/pcn192

Ueno, D., Iwashita, T., Zhao, F. J., and Ma, J. F. (2008). Characterization of Cd translocation and identification of the Cd form in xylem sap of the Cd-hyperaccumulator *Arabidopsis halleri*. *Plant Cell Physiol.* 49, 540–548. doi: 10.1093/pcp/pcn026

Uraguchi, S., Mori, S., Kuramata, M., Kawasaki, A., Arao, T., and Ishikawa, S. (2009). Root-to-shoot Cd translocation via the xylem is the major process determining shoot and grain cadmium accumulation in rice. *J. Exp. Bot.* 60, 2677–2688. doi: 10.1093/jxb/erp119

Vacchina, V., Mari, S., Czernic, P., Marques, L., Pianelli, K., Schaumloffel, D., et al. (2003). Speciation of nickel in a hyperaccumulating plant by high-performance liquid chromatography-inductively coupled plasma mass spectrometry and electrospray MS/MS assisted by cloning using yeast complementation. *Anal. Chem.* 75, 2740–2745. doi: 10.1021/ac020704m

van Belleghem, F., Cuypers, A., Semane, B., Smeets, K., Vangronsveld, J., d'Haen, J., et al. (2007). Subcellular localization of cadmium in roots and leaves of *Arabidopsis thaliana*. *New Phytol.* 173, 495–508. doi: 10.1111/j.1469-8137.2006.01940.x

van Goor, B. J., and Wiersma, D. (1976). Chemical forms of manganese and zinc in phloem exudate. *Physiol. Plant.* 36, 213–216. doi: 10.1111/j.1399-3054.1976.tb03938.x

Vilaine, F., Palauqui, J. C., Amselem, J., Kusiak, C., Lemoine, R., and Dinant, S. (2003). Towards deciphering phloem: a transcriptome analysis of the phloem of *Apium graveolens*. *Plant J.* 36, 67–81. doi: 10.1046/j.1365-313X.2003.01855.x

Vogel-Mikus, K., Arcon, I., and Kodre, A. (2010). Complexation of cadmium in seeds and vegetative tissues of the cadmium hyperaccumulator *Thlaspi praecox* as studied by X-ray absorption spectroscopy. *Plant Soil* 331, 439–451. doi: 10.1007/s11104-009-0264-y

von Blanckenburg, F., von Wirén, N., Guelke, M., Weiss, D. J., and Bullen, T. D. (2009). Fractionation of metal stable isotopes by higher plants. *Elements* 5, 375–380. doi: 10.2113/gselements.5.6.375

von Wirén, N., Khodr, H., and Hider, R. C. (2000). Hydroxylated phytosiderophore species possess an enhanced chelate stability and affinity for iron(III). *Plant Physiol.* 124, 1149–1157. doi: 10.1104/pp.124.3.1149

von Wirén, N., Klair, S., Bansal, S., Briat, J. F., Khodr, H., Shioiri, T., et al. (1999). Nicotianamine chelates both Fe-III and Fe-II. Implications for metal transport in plants. *Plant Physiol.* 119, 1107–1114. doi: 10.1104/pp.119.3.1107

Wada, Y., Yamaguchi, I., Takahashi, M., Nakanishi, H., Mori, S., and Nishizawa, N. K. (2007). Highly sensitive quantitative analysis of nicotianamine using LC/ESI-TOF-MS with an internal standard. *Biosci. Biotechnol. Biochem.* 71, 435–441. doi: 10.1271/bbb.60496

Watanabe, T., and Osaki, M. (2001). Influence of aluminum and phosphorus on growth and xylem sap composition in *Melastoma malabathricum* L. *Plant Soil* 237, 63–70. doi: 10.1023/A:1013395814958

Waters, B. M., and Sankaran, R. P. (2011). Moving micronutrients from the soil to the seeds: genes and physiological processes from a biofortification perspective. *Plant Sci.* 180, 562–574. doi: 10.1016/j.plantsci.2010.12.003

Watmough, S. A., Hutchinson, T. C., and Evans, R. D. (1999). The distribution of ^{67}Zn and ^{207}Pb applied to white spruce foliage at ambient concentrations under different pH regimes. *Environ. Exp. Bot.* 41, 83–92. doi: 10.1016/S0098-8472(98)00056-2

Weber, G., von Wirén, N., and Hayen, H. (2006). Analysis of iron(II)/iron(III) phytosiderophore complexes by nano-electrospray ionization Fourier transform ion cyclotron resonance mass spectrometry. *Rapid Commun. Mass* Spectrom. 20, 973–980. doi: 10.1002/rcm.2402

Wei, Z. G., Wong, J. W., Hong, F., Zhao, H. Y., Li, H. X., and Hu, F. (2007a). Determination of inorganic and organic anions in xylem saps of two contrasting oilseed rape (*Brassica juncea L.*) varieties: roles of anions in long-distance transport of cadmium. *Microchem. J.* 86, 53–59. doi: 10.1016/j.microc.2006.10.003

Wei, Z. G., Wong, J. W., Zhao, H. Y., Zhang, H. J., Li, H. X., and Hu, F. (2007b). Separation and determination of heavy metals associated with low molecular weight chelators in xylem xaps of Indian Mustard (*Brassica juncea*) by size exclusion chromatography and atomic absorption spectrometry. *Biol. Trace Elem. Res.* 118, 146–158. doi: 10.1007/s12011-007-0022-z

White, M. C., Decker, A. M., and Chaney, R. L. (1981). Metal complexation in xylem fluid. *Plant Physiol.* 67, 292–300. doi: 10.1104/pp.67.2.292

Wiersma, D., and van Goor, B. J. (1979). Chemical forms of nickel and cobalt in phloem of *Ricinus communis*. *Physiol. Plant.* 45, 440–442. doi: 10.1111/j.1399-3054.1979.tb02610.x

Wirth, J., Poletti, S., Aeschlimann, B., Yakandawala, N., Drosse, B., Osorio, S., et al. (2009). Rice endosperm iron biofortification by targeted and synergistic action of nicotianamine synthase and ferritin. *Plant Biotechnol. J.* 7, 631–644. doi: 10.1111/j.1467-7652.2009.00430.x

Wood, B. A., and Feldmann, J. (2012). Quantification of phytochelatins and their metal(loid) complexes: critical assessment of current. *Anal. Bioanal. Chem.* 402, 3299–3309. doi: 10.1007/s00216-011-5649-0

Wu, B., Chen, Y. X., and Becker, J. S. (2009). Study of essential element accumulation in the leaves of a Cu-tolerant plant *Elsholtzia splendens* after Cu treatment by imaging laser ablation inductively coupled plasma mass spectrometry (LA-ICP-MS). *Anal. Chimica Acta* 633, 165–172. doi: 10.1016/j.aca.2008.11.052

Wycisk, K., Kim, E. J., Schroeder, J. I., and Krämer, U. (2004). Enhancing the first enzymatic step in the histidine biosynthesis pathway increases the free histidine pool and nickel tolerance in *Arabidopsis thaliana*. *FEBS Lett.* 578, 128–134. doi: 10.1016/j.febslet.2004.10.086

Xuan, Y., Scheuermann, E. B., Meda, A. R., Hayen, H., von Wirén, N., and Weber, G. (2006). Separation and identification of phytosiderophores and their metal complexes in plants by zwitterionic hydrophilic interaction liquid chromatography coupled to electrospray ionization mass spectrometry. *J. Chromatogr. A* 1136, 73–81 doi: 10.1016/j.chroma.2006.09.060

Xuan, Y., Scheuermann, E. B., Meda, A. R., Jacob, P., von Wirén, N., and Weber, G. (2007). CE of phytosiderophores and related metal species in plants. *Electrophoresis* 28, 3507–3519. doi: 10.1002/elps.200700117

Yamaguchi, N., Ishikawa, S., Abe, T., Baba, K., Arao, T., and Terada, Y. (2012). Role of the node in controlling traffic of cadmium, zinc, and manganese in rice. *J. Exp. Bot.* 63, 2729–2737. doi: 10.1093/jxb/err455

Ye, W. L., Wood, B. A., Stroud, J. L., Andralojc, P. J., Raab, A., McGrath, S. P., et al. (2010). Arsenic speciation in phloem and xylem exudates of castor bean. *Plant Physiol.* 54, 1505–1513. doi: 10.1104/pp.110.163261

Yokosho, K., Yamaji, N., Ueno, D., Mitani, N., and Ma, J. F. (2009). OsFRDL1 is a citrate transporter required for efficient translocation of iron in rice. *Plant Physiol.* 149, 297–305. doi: 10.1104/pp.108.128132

Yoneyama, T. Gosho, T. Kato, M., Goto, S., and Hayashi, H. (2010). Xylem and phloem transport of Cd, Zn and Fe into the grains of rice plants (*Oryza sativa* L.) grown in continuously flooded Cd-contaminated soil. *Soil Sci. Plant Nutr.* 56, 445–453. doi: 10.1111/j.1747-0765.2010.00481.x

Yoshimura, E., Sakaguchi, T., Nakanishi, H., Nishizawa, N. K., Nakai, I., and Mori, S. (2000). Characterization of the chemical state of iron in the leaves of wild-type tomato and of a nicotianamine-free mutant chloronerva by X-ray Absorption Near-edge Structure (XANES). *Phytochem. Anal.* 11, 160–162. doi: 10.1002/(SICI)1099-1565(200005/06)11:3<160::AID-PCA500>3.0.CO;2-C

Yruela, I. (2009). Copper in plants: acquisition, transport and interactions. *Funct. Plant Biol.* 36, 409–430. doi: 10.1071/FP08288

Yun, W., Pratt, S. T., Miller, R. M., Cai, Z., Hunter, D. B., Jarstfer, A. G., et al. (1998). X-ray imaging and microspectroscopy of plants and fungi. *J. Synchrotron Radiat.* 5, 1390–1395. doi: 10.1107/S0909049598007225

Zhang, C., Yu, X., Ayre, B. G., and Turgeon, R. (2012). The origin and composition of curcubit "phloem" exudate. *Plant Physiol.* 158, 1873–1882. doi: 10.1104/pp.112.194431

Conflict of Interest Statement: The authors declare that the research was conducted in the absence of any commercial or financial relationships that could be construed as a potential conflict of interest.

Received: 22 January 2014; accepted: 04 March 2014; published online: 25 March 2014.
Citation: Álvarez-Fernández A, Díaz-Benito P, Abadía A, López-Millán A-F and Abadía J (2014) Metal species involved in long distance metal transport in plants. Front. Plant Sci. 5:105. doi: 10.3389/fpls.2014.00105
This article was submitted to Plant Nutrition, a section of the journal Frontiers in Plant Science.

Curriculum vitae

Personal information

Name: Pablo Díaz Benito de las Huertas Agüero

Nationality: Spain

Birth Date: May 30th 1985

Email: pablodiazbenito@hotmail.com

Studies

- Biology degree by the Autonomous University of Madrid. September 2009

  Project title: *Proteomic approach to study the changes produced by Benzothiadiazole elicitor in tomato plants*

- Master degree in Biophysics by the Autonomous University of Madrid. October 2010

  Project title: *Benzothiadiazole effects analysis in tomato plants using mass spectrometry*

Professional experience

- From 2011 August until present day. PhD student. Aula Dei Experimental Station, CSIC, Zaragoza, Spain
- May 2010 - October 2010. Master student at Proteomics Service at Biotechnology National Centre, CSIC, Madrid, Spain
- July 2008 - August 2009. Grade student in the Plant Physiology Departament of the Autonomous University of Madrid, Spain

Grants

- FPI contract from the Spanish Ministry of Economy, Industry and Competitiveness (Project AGL2010-16515, *Plant metallomics: an integrated mass spectrometry approach to study metal homeostasis in plants*). August 2011 - August 2015

Languages

- Spanish (native)
- English (TOEFL 2009) score 94/120

Courses

- "ISO 17025 Laboratory Certification". EuroInnova Formación. 200 h. January 2017
- "Good Clinical Practices (ICH)". Autonomous University of Madrid. 40 h. March 2016
- "Summer Elemental Biotechnology ". Autonomous University of Madrid. 24 h. July 2007

Participation in research projects

- Project title: *Plant metallomics: an integrated mass spectrometry approach to study metal homeostasis in plants* (AGL-2010-16515)
  - IP: Javier Abadía Bayona
  - Finnancial support: Spanish Ministry of Economy, Industry and Competitiveness
  - Period: January 2011 - December 2013
- Project title: *Towards an understanding of the roles of metabolites and proteins in plant metal homeostasis* (AGL2013-42175)
  - IP: Javier Abadía Bayona and Ana Flor López Millán
  - Finnancial support: Spanish Ministry of Economy, Industry and Competitiveness
  - Period: January 2014 - December 2016

Publications

- Álvarez-Fernández A, **Díaz-Benito P**, Abadía A, López-Millán AF, Abadía J. **2014**. Metal species involved in long distance metal transport in plants. *Frontiers in Plant Science* 5:105. DOI: 10.3389/fpls.2014.00105.
- Banakar R, Álvarez-Fernández A, **Díaz-Benito P**, Abadía J, Capell T, Christou P. Phytosiderophores levels of metals in rice endosperm by modulating expression of metal transporting genes. (*under review*)
- **Díaz-Benito P**, Abadía A, Abadía J, Álvarez-Fernández A. Levels of nicotianamine, organic acids and micronutrients in tomato (*Solanum lycopersicum*) plant fluids as affected by Fe deficiency and resupply. (*in preparation*)
- **Díaz-Benito P**, Fernández B, Banakar R, Rodríguez S, Christou P, García-Alonso JI, Pereiro R, Abadía J, Álvarez-Fernández A. Iron distribution between endosperm and embryo is assisted by 2'-deoxymugineic acid in rice seeds. (*in preparation*)

Symposia

2014

- *12th European Workshop on Laser Ablation. Egham, United Kingdom.*

  (**1**) Fernández B, Carrasco-Gil S, **Díaz-Benito P**, Banakar R, Álvarez-Fernández A, Abadía J, Christou P, García-Alonso JI, Pereiro R. Imaging studies of trace elements in biological samples by LA-ICP-MS: analysis of leaf and seed sections. (Comunication / panel)

- *17th International Symposium on Iron Nutrition and Interactions in Plants. Gatersleben, Germany.*

  (**2**) Abadía J, Sisó-Terraza P, **Díaz-Benito P**, Gutierrez-Carbonell E, Takahashi D, Abadía A, Uemura M, López-Millán AF, Álvarez-Fernández A. Advances in iron nutrition based on mass spectrometry approaches. (Opening talk)

2015

- *16th European Winter Conference on Plasma Spectrochemistry. Münster, Germany.*

  (**3**) Pereiro R, Rodríguez SM, Carrasco-Gil S, **Díaz-Benito P**, Álvarez-Fernández A, Abadía J, Christou P, Sanz-Medel A, García-Alonso JI & Fernández B. Imaging studies of trace elements in biological samples by LA-ICP-MS: analysis of leaf and seed sections. (Comunication / Panel)

- *XXI Reunión de la Sociedad Española de Fisiología Vegetal. XIV Congreso Hispano-Luso de Fisiología Vegetal. Toledo, Spain.* (Asistencia)

  (**4**) **Díaz-Benito P**, Banakar R, Fernández B, Abadía J, Morales F, Pereiro R, Christou P, Álvarez-Fernández A**.** Localization of metals and metal ligands in rice seeds. (Comunication / Panel)

- *6th Meeting of the International BioIron Society. Hangzhou, China.*

  (**5**) **Díaz-Benito P**, Abadía A, Abadía J, Álvarez-Fernández A. Nicotianamine in tomato plant fluids as affected by iron deficiency and iron resupply. (Comunication / Panel)

2016

- *17th International Symposium on Iron Nutrition and Interactions in Plants.* Madrid, Spain. (Asistencia)

  (**6**) **Díaz-Benito P**, Abadía A, Abadía J, Álvarez-Fernández A. Effects of Fe deficiency and Fe resupply in metal and metal ligand concentrations in xylem sap, apoplastic fluid and intracellular extracts of tomato plants (Panel) (**best poster award**)

(**7**) **Díaz-Benito P**, Fernández B, Banakar R, Rodríguez S, Christou P, Pereiro R, Abadía J, Álvarez-Fernández A. Localization of metals and metal ligands in rice seeds overexpressing Nicotianamine Synthase and/or barley Nicotianamine Amino Transferase (Panel)

Stays

- Applied Plant Biotechnology Laboratory, Department of Plant Production and Forestry Science, ETSEA, University of Lleida-Agrotecnio Center, Lleida, Spain. Obtention of plant tissues from rice plants overexpressing NAS and/or NAAT genes. Supervisor: Paul Christou.
- Mass Spectrometry Analytics Group, Department of Physical & Analytical Chemistry, University of Oviedo, Oviedo, Spain. Metal localization in rice seed sections by laser ablation inductively coupled mass spectrometry (LA-ICP-MS). Supervisor: Beatriz Fernández and Rosario Pereiro
- Insect Vectors of Plant Pathogens Group, Department of Crop Protection of the Institute of Agricultural Sciences, CSIC, Madrid. Obtention of phloem sap from rice plants by aphid stylectomy. Supervisor: Alberto Fereres and Elisa Garzo

Awards

- Best poster award in *17th International Symposium on Iron Nutrition and Interactions in Plants* (2016) Madrid, Spain.